
Indian Institute of Technology Guwahati
*Department of Physics*

---

# *Non-standard scalar field models of inflation and their reheating dynamics.*

A thesis submitted by:
**Pankaj Saha**

to

**Indian Institute of Technology Guwahati**
in partial fulfillment of the requirements
for the award of the degree of
Doctor of Philosophy in Physics

DECEMBER 2018

# Statement

The work contained in the thesis entitled "**Non-standard scalar field models of inflation and their reheating dynamics.**" has been carried out at the Department of Physics, Indian Institute of Technology Guwahati, India by me under the supervision of Dr. Debaprasad Maity. The material of this thesis is original and has not been submitted elsewhere for any other degree or diploma. Works presented in the thesis are all my own unless referenced to the contrary in the text.

Pankaj Saha
Department of Physics
Indian Institute of Technology Guwahati
Guwahati, Assam, India-781039
December 2018
Date:

# Disclaimer

The bibliography included in this thesis is, by no means, complete rather contains the one which are consulted thoroughly by me. I apologize for inadvertently missing out some of the research papers, review articles and other scientific documents pertaining to this thesis which also should have been cited. For illustration purpose some of the figures in this thesis are taken from other sources and properly cited.

# Certificate

It is certified that the work contained in the thesis entitled "**Non-standard scalar field models of inflation and their reheating dynamics.**" by Mr. Pankaj Saha (Roll no-136121001), a PhD student at the Department of Physics, Indian Institute of Technology Guwahati, India is carried under my supervision. The material of this thesis is original and has not been submitted elsewhere for any other degree or diploma.

Dr. Debaprasad Maity
Department of Physics
Indian Institute of Technology Guwahati
Guwahati, Assam, India-781039
December 2018
Date:

# Acknowledgments

I am particularly grateful to my supervisor Dr. Debaprasad Maity, for the unwavering patience and kindness with which he treated me throughout the entire period of my doctoral studies. He has was extremely supportive, offering patience and expertise while also allowed me to work in my own way and pace. Without him this thesis would certainly not have been completed. I have certainly learnt a lot from all the discussions with him. I would consider myself fortunate if I could have imbibed even a little of his passion for physics.

I would like to thank my doctoral committee members, Dr. Poulose Poulose, Dr. Arunansu Sil and Dr. Sayan Chakrabarti for valuable suggestions and critical comments. I would also like to thank faculty members and my teachers at Indian Institute of Technology Guwahati, Dr. Soumitra Nandi, Dr. Santabrata Das, Dr. Subhaditya Bhattacharya, Dr. Udit Raha, and Dr. Bibhas Ranjan Majhi from whom I have learn many topics in physics.

I would like to thank Department of Physics, Indian Institute of Technology Guwahati for the financial support and various helps.

I am thankful to Mr. Basab Bijoy Purokayastha for all the technical helps. I would like to convey my heartfelt regards to my seniors Abhijit Da, Sourav Da, Ramiz Da, Kallol Da, Shibananda Da, Ashmita Di, and Sujay Da for various helps and discussions. I would remember the help and company of my friends and colleagues Srikrishna, Pulak, Kajwal, Sanjib, Noor, Arun, Srimoy, Ram, Purusottam, Indu Kalpa, Jagan Mohan, Wadbor, Nawaz, Sumeet, Krishnakanta, Mousumi, Rajesh, Riajul, and Sourav.

I would like to thank my parents and my brother Pallab for all the emotional support and unconditional love. The expansion of universe starts and ends with them.

This thesis is dedicated to the memories of my loving grandmother whom I lost recently.

I am indebted to all the people with whom I have interacted or learned from. Especially to the organizers and teachers of various schools which I attended during the course. Those proved to really invaluable to my understanding of the subject. I would like to register my deepest regards to all of them through the words of some ancient poet

*For whom is the company of great people not benificial?*
*Even a water droplet when on lotus petal, shines like a pearl.*

Pankaj Saha
Guwahati
December 2018

*I have spent many days stringing and unstringing my instrument while the song I came to sing remains unsung.*

— *Rabindranath Tagore(GITANJALI-SONG OFFERINGS)*

*This is the way the world ends*
*Not with a bang but a whimper.*

— *T. S. Eliot(The Hollow Men)*

*It would not be much of a universe if it wasn't home to the people you love..*

— *Stephen Hawking*

**Abstract**

The inflationary paradigm, a period of exponential expansion of the universe prior to the radiation dominated phase, proposed in the 1980s to solve the so-called *homogeneity, flatness and monopole* problems of the big-bang theory is now an indispensable part of any study about the origin and evolution of our universe. Although a lot of progress has been made in the direction to have a model independent description of inflation from effective theory perspective, it is still largely a model dependent phenomena. A phase of exponential expansion can be easily achieved by a simple scalar field. An inflationary model is, as a result, usually synonymous with a scalar field potential $V(\phi)$. The list of inflationary models is practically inexhaustible. However, thanks to the remarkable advancements in observational cosmology, which provides several constraints on the model building. A large number of well-known inflationary models are found to be tightly constrained or disfavoured by the data. For instance, the simple power-law chaotic models $V(\phi) \propto \phi^n$ are now ruled out. This motivates us to consider some non-standard modifications to inflationary models. Another important aspect in the study of inflationary physics is the phase of reheating when the inflaton decays to other particles. Though lack of experimental observations make this phase largely unconstrained, there exists large number of attempts to constrain the reheating phase from data. In this thesis we have extended the existing analysis of reheating constraints considering more realistic scenario. Finally we also connect the reheating constraint analysis with the dark matter phenomenology in light of cosmic microwave background. In what follows, we will list a brief outline of the various issues mentioned above.

• **Inflation with plateau potential:** In this chapter, we analyze a class of phenomenological inflationary models with non-polynomial potential, and compare the model predictions with the currently favoured Starobinsky and its generalised $\alpha$-attractor models in $(n_s, r)$ plane constrained by PLANCK. Importantly for a wide range of parameter space, our model fits extremely well with the observation. We have performed a model independent analysis of reheating in terms of effective equation of state. In particular we consider two stages of reheating dynamics with generalised inflaton equation of state in the initial and relativistic equation of state in the later phase. We show how our generalised reheating analysis constrains the inflation models under consideration. We have also discussed the origin of the plateau potential from *supergravity* and a general *scalar-tensor theory*.

• **CMB constraints on reheating and dark matter phenomenology:** In this chapter, we have tried to understand the phenomenology of dark matter in light of very well understood properties of cosmic microwave background (CMB) anisotropy. To connect these two, inflation and the reheating phase play the important role. Following previous analysis, we first established one-to-one correspondence between the CMB power spectrum and the reheating temperature assuming the perturbative reheating scenario. Further by incorporating a possible dark matter candidate through the radiation annihilation process during reheating and the current value of dark matter abundance, we constrain the dark matter parameter space through the inflationary power spectrum for different inflationary models.

• **Preheating and thermalization after plateau inflation:** We have studied the preheating phase for a class of plateau inflationary model considering the four-legs interaction term $(1/2)g^2\phi^2\chi^2$ between the inflaton $(\phi)$ and reheating field $(\chi)$. We specifically focus on the effects of a parameter $\phi_*$ that controls inflationary dynamics and the shape of the inflaton potential. For $\phi_* < M_p$, the departure of the inflaton potential from the usual power-law behavior $\phi^n$ significantly modifies the microscopic behaviour of the preheating dynamics. We analyze and compare the efficiency of production, thermalization and the final equation of state of the system for different models under consideration with $n = 2, 4, 6$ for two different values of $\phi_*$. Most importantly as we increase $n$, or

decrease $\phi_*$, the preheating occurs very efficiently with the final equation of state to be that of the radiation, $w = 1/3$. Specially for $n = 2$, the final equation of state turned out to be $w \simeq 0.2$. However, a complete decay of inflaton could not be achieved with the four-legs interaction for any model under consideration. Therefore, in order to complete the reheating process, we perform the perturbative analysis for the second stage of the reheating phase. Taking the end product of the preheating phase as an initial condition we have solved the homogeneous Boltzmann equations for both the fields supplemented by the constraints coming from the subsequent entropy conservation. In so doing, we can calculate the reheating temperature which is otherwise ill-defined right after the end of preheating. The temperature can be uniquely fixed for a given inflaton decay constant and the CMB temperature. We also compare our results with the conventional reheating constraint analysis and discuss the limit of inflaton decay constant from the field theory perspective.

• **Galilean Modified Inflation** As we have mentioned, a large number of the well known canonical large field inflation models turned out to be strongly disfavored from recent Planck data. Axion inflation is one of such models which is becoming marginalized with the increasing precession of CMB data. In this chapter, we have shown that with a simple Galileon type modification to the marginally favored axion model (which we call the G-axion), we can turn them into one of the most favored models with its detectable prediction of $r$ and $n_s$ within its PLANCK $1\sigma$ range for a wide range of parameters. Interestingly it is this modification which plays the important role in turning the inflationary predictions to be independent of the explicit value of axion decay constant $f$. However, dynamics after the inflation turned out to have a non-trivial dependence on $f$. For each G-axion model there exists a critical value of $f_c$ such that for $f > f_c$ we have the oscillating phase after inflation and for $f < f_c$ we have non-oscillatory phase. Therefore, we obtained a range of sub-Planckian value of model parameters which give rise to consistent inflation. However for sub-Planckian axion decay constant the inflaton field configuration appeared to be singular after the end of inflation. To reheat the universe we, therefore, employ the instant preheating mechanism at the instant of first zero crossing of the inflaton. To our surprise, the instant preheating mechanism turned out to be inefficient as opposed to usual non-oscillatory quintessence model. For another class of G-axion model with super-Planckian axion decay constant, we performed in detail the reheating constraints analysis considering the latest PLANCK result.

## Publications and Preprints

This thesis is based on the following works:

1. *Modified natural inflation: A small single field model with a large tensor to scalar ratio*, Debaprasad Maity and Pankaj Saha, Phys. Rev. D 91, 023504 (2015), arXiv:1407.7692 [hep-th].

2. *Connecting CMB anisotropy and cold dark matter phenomenology via reheating*, Debaprasad Maity and Pankaj Saha, Phys. Rev. D 98, 103525 (2018) arXiv:1801.03059 [hep-ph].

3. *Studying G-axion Inflation model in light of PLANCK*, Debaprasad Maity and Pankaj Saha, JCAP 07 (2018) 065, arXiv:1801.08080 [hep-ph].

4. *CMB constraints on dark matter phenomenology via reheating in Minimal plateau inflation*, Debaprasad Maity and Pankaj Saha, arXiv:1804.10115 [hep-ph].
Accepted for Publication in Phys. Dark Univ.

5. *(P)reheating after minimal Plateau Inflation and constraints from CMB*,
Debaprasad Maity and Pankaj Saha,
arXiv:1811.11173 [astro-ph.CO], (Under Review).

6. *Minimal plateau inflationary cosmologies and constraints from reheating*, Debaprasad Maity and Pankaj Saha, 2019 Class. Quantum Grav. 36 045010, arXiv:1902.01895 [gr-qc].,

## Work Presented in Conferences

(a) Oral presentation on 'Modified natural inflation: a small single field model with large tensor to scalar ratio' in, 'XXI DAE-BRNS High Energy Physics Symposium 2014', at Indian Institute of Technology Guwahati, December $8^{th}$-$12^{th}$, 2014

(b) Oral presentation on 'Modified natural inflation: a small single field model with large tensor to scalar ratio' in, 'Saha Theory Workshop: Cosmology at the Interface', at Theory Division, Saha Institute of Nuclear Physics, January $28^{th}$-$30^{th}$, 2015

(c) Oral presentation on 'Inflation in the Early Universe' in, '100 Years of General Relativity: Where do we Stand?', at Indian Institute of Technology Guwahati, February 12, 2016

(d) Poster presentation on 'Minimal Inflationary Cosmologies and the production of Dark matter' in, 'Research Conclave'17', at Indian Institute of Technology Guwahati, March $16^{th}$-$19^{th}$, 2017

(e) Poster presentation on 'CMB Constrain on reheating and dark matter parameter space' during the, 'Summer School on Cosmology 2018', at the Abdus Salam International Centre for Theoretical Physics(ICTP), in Trieste, from $18^{th}$-$29^{th}$ June, 2018

---

## Confereces and Schools attended

(a) 'XXI SERC Preparatory School in THEP' at Indian Institute of Science Education and Research (IISER)- Bhopal, Bhopal during June $29^{th}$ - July $25^{th}$, 2015.

(b) 'XXX Main School in THEP' at Birla Institute of Technology & Science (BITS) - Pilani, Pilani during November $16^{th}$- December $5^{th}$, 2015.

(c) GIAN Course on 'Origin and Evolution of Perturbations During Inflation and Reheating' held at Indian Institute of Technology Madras during November $25^{th}$-$30^{th}$, 2016

(d) GIAN Course on 'Introduction to Cosmological Perturbation Theory' held at Jamia Millia Islamia, New Delhi during December $16^{th}$-$23^{th}$, 2016

(e) GIAN Course on 'Electroweak Symmetry breaking, Flavour Physics and BSM' held at Indian Institute of Technology Guwahati, March $18^{th}$-$22^{th}$, 2017

(f) ICTP Summer School on Cosmology 2018, held at The Abdus Salam International Center for Theoretical Physics, Trieste, Italy during June $18^{th}$-$29^{th}$, 2018

# Contents


Symbols and Conventions . . . . . xxiii

**I Overview of Standard Cosmology** **1**

**1 Introduction** **3**
1.1 Cosmology and Inflation . . . . . 3
1.1.1 A brief review of standard cosmology . . . . . 3
1.1.2 Basics of Inflation . . . . . 8
1.2 Inflation: A period of exponential expansion . . . . . 10
1.2.1 More on conditions for inflation: Slow roll parameters . . . . . 11
1.2.2 Scalar field as the source of inflation . . . . . 11
1.2.3 The slow-roll conditions . . . . . 12
1.3 Cosmological Perturbations . . . . . 13
1.3.1 Metric perturbation . . . . . 14
1.3.2 Matter Perturbations . . . . . 15
1.3.3 Gauge invariant variable and power spectrum: scalar mode . . . . . 16
1.3.4 Tensor Mode . . . . . 19
1.3.5 Observations and constraints . . . . . 20
1.4 Inflationary Models . . . . . 22
1.4.1 Large field models . . . . . 22
1.4.2 Small field models . . . . . 23
1.4.3 Hybrid Inflation Models . . . . . 24
1.5 Reheating after inflation: perturbative . . . . . 26
1.5.1 Non-Perturbative Reheating or Pre-heating . . . . . 28
1.6 Motivation of the thesis . . . . . 36

**II Non-standard scalar field models of inflation** **37**

**2 Inflation with plateau potential** **39**
2.1 The Model . . . . . 40
2.1.1 Background Equations . . . . . 41
2.1.2 Computation of $(n_s, r, dn_s^k)$ . . . . . 42
2.1.3 End of inflation and general equation of state . . . . . 45
2.2 Towards derivation of $V_{min}$ from non-minimal scalar-tensor theory . . . . . 46
2.3 Supergravity realization of our model potential . . . . . 47

2.3.1 The power-law plateau potential form Supergravity . . . 48
2.4 Model independent constraints from reheating predictions . . . 51
2.5 Summary and Conclusion . . . 56

**3 CMB constraints on reheating and dark matter phenomenology 57**
3.1 Introduction . . . 57
3.2 Inflationary observables and their connection with CMB . . . 59
3.3 Dark Matter during reheating . . . 60
3.3.1 Basic equations . . . 60
3.4 Constraints from CMB: dark matter phenomenology . . . 64
3.4.1 Connecting CMB and reheating via inflation . . . 64
3.4.2 Methodology: CMB to dark matter via reheating . . . 67
3.4.3 Chaotic inflation: General results . . . 69
3.4.4 Natural inflation . . . 73
3.4.5 Alpha attractor . . . 75
3.4.6 Minimal Plateau model . . . 77
3.5 Summary and outlook . . . 82

**4 Preheating and thermalization after plateau inflation 89**
4.1 Introduction . . . 89
4.2 A Brief Introduction to the Minimal Inflation Model . . . 91
4.3 Preheating: Parametric resonance . . . 91
4.3.1 The Model and equations . . . 91
4.3.2 Parametric resonance: Instability chart . . . 94
4.4 Preheating: Lattice Simulation . . . 96
4.4.1 The back-reaction and the emergence of non-linearity: Generalities . . . 96
4.4.2 Equation of state . . . 102
4.4.3 Occupation Numbers . . . 105
4.4.4 Perturbative reheating and constraints from CMB . . . 109
4.5 Conclusion and Outlook . . . 113

**5 Galilean Modified Inflation 117**
5.1 Introduction . . . 117
5.2 The most General Single-Field Inflation . . . 118
5.2.1 Potential-driven G-inflation . . . 119
5.2.2 Perturbations in Generalized G-inflation . . . 121
5.3 Potential driven G-inflation with a shift symmetric potential . . . 123
5.3.1 G-axion . . . 124
5.3.2 Cosmological quantities: $(n_s, r, dn_s^k)$ . . . 126
5.3.3 Number of e-folds and modified Lyth bound . . . 127
5.4 Simple choices of $M(\phi)$ and determination of cosmological parameters . . . 128
5.5 Evolution of the scalar field: sub-Planckian $(f, s)$ . . . 129
5.6 Non-oscillating axion: Instant preheating . . . 133
5.6.1 Conventional Shift Symmetry Breaking Coupling . . . 134
5.6.2 Shift Symmetric Coupling . . . 136
5.7 Conclusions . . . 137

**6 Conclusions** **139**
6.1 Summary of chapters . . . . . 139
6.2 Future perspectives . . . . . 141

**Appendices** **143**

**Background dependent unitarity for plateau potentials** **145**

**Boltzmann equations for out-of-equilibrium processes** **147**

**Bibliography** **149**

## Abbreviation List

**BAO** ..... Baryon Acoustic Oscillations

**BBN** ..... Big Bang Nucleosynthesis

**BK14** ..... BICEP2/Keck data through the end of the 2014

**CDM** ..... Cold Dark Matter

**CMB** ..... Cosmic Microwave Background

**DBI** ..... Dirac-Born-Infeld

**dof** ..... Degrees of Freedom

**FIMP** ..... Feebly Interacting Massive Particles

**FLRW** ..... Friedman-Leîmatre-Robertson-Walker

**GUT** ..... Grand Unification Theories

**IR** ..... InfraRed

**KGB** ..... Kinetic Gravity Braiding

**LSS** ..... Last Scattering Surface

**PNGB** ..... Pseudo Nambu Goldstone Boson

**SUGRA** ..... Supergravity

**UV** ..... UltraViolet

**VEV** ..... Vacuum Expectation Value

**WIMP** ..... Weakly Interacting Massive Particles

**WKB** ..... Wentzel-Kramers-Brillouin

**WMAP** ..... Wilkinson Microwave Anisotropy Probe

# Symbols and Conventions

## Symbols

Some of the frequently used symbols are listed below. Other symbols will be be defined at their places of occurring.

| | |
|---|---|
| $t$ | cosmic time |
| $\eta$ | conformal time |
| $\mathbf{x}$ | Position three-vector |
| $a,\ a(t)$ | Scale-factor of universe expansion |
| $H = \frac{\dot{a}(t)}{a(t)}$ | Hubble expansion rate |
| N, $\Delta$N | e-folding number |
| $c$ | Speed of light in vacuum |
| $G$ | Newton's constant |
| $\mathrm{m_{pl}} = \frac{1}{\sqrt{G}}$ | Planck constant |
| $\mathrm{M_p} = \frac{1}{\sqrt{8\pi G}}$ | reduced Planck constant |
| $H_0 = 100h\mathrm{km/sec/Mpc}$ | Current Value of H with $h = 0.70 \pm 0.0012$ |
| $T_0 = 2.725\mathrm{K} = 2.35 \times 10^{-13}\mathrm{GeV}$ | Present CMB temperature |
| $\Omega_R h^2 = 2.35 \times 10^{-5}$ | Present radiation abundance |
| $\mathbb{Z}^+$ | Set of positive integers. |

## Conventions

- We will use the natural units $G = \hbar = c = k_B = 1$ unless other wise stated
- In this unit $\mathrm{m_{pl}} = 1.22 \times 10^{19}\mathrm{GeV},\ \mathrm{M_p} = 2.43 \times 10^{18}\mathrm{GeV}$.
- Minkowski metric is given by $\eta_{\mu\nu} = \mathrm{diag}[1, -1, -1, -1]$
- Summation over repeated indices will be assumed unless otherwise stated.
- The Ricci tensor, defined in terms of the Christoffel symbol$\Gamma^\lambda_{\mu\nu}$ is

$$R_{\mu\nu} \equiv \partial_\lambda \Gamma^\lambda_{\mu\nu} - \partial_\nu \Gamma^\lambda_{\mu\lambda} + \Gamma^\lambda_{\lambda\rho}\Gamma^\rho_{\mu\nu} - \Gamma^\rho_{\mu\lambda}\Gamma^\lambda_{\nu\rho}$$

- And the Ricci scalar is

$$R = g^{\mu\nu} R_{\mu\nu}$$

# Part I

# Overview of Standard Cosmology

# Introduction 1

*..everything can be created from nothing, And "everything might include a lot more than what we can see. In the context of inflationary cosmology, it is fair to say that the universe is the ultimate free lunch."*

*Alan Guth in 'THE INFLATIONARY COSMOLOGY'*

## 1.1 Cosmology and Inflation

Cosmology is one of the oldest human endevour towards its quest to comprehend the universe, however, it is also one of the youngest branch of physics to be deemed as 'physical science'![1–4].The discovery of the expanding universe and the observation of cosmic microwave radiation at temperature $\sim$ 3K established the fact that our universe has originated from a hot and dense soup of matter at its very early stage called big-bang. The phenomenal success of big-bang theory in explaining the formation of primordial nucleus and consequently the correct abundance of light elements such as Hydrogen, Helium, Lithium etc supplanted other existing models such as the steady-state model, and established itself as the standard model of cosmology. In spite of the big-bang's phenomenal success it has its own limitations which are related to the so-called *'initial conditions'*. Soon after the formulation of the theory, it has been found that the big bang theory needs preciously curated initial conditions. There is no explanation for such fine-tuned pre big-bang universe within the theory itself, and it is realised that to have an answer we need a paradigm shift. It was found that a phase of exponential expansion, known as the inflation[5–9], prior to the standard big bang can naturally provide answers to many of those puzzles. Before embarking on our journey to explore the idea behind those initial condition problems, and how inflation cured them, we will look at the brief history of our universe to better appreciate the issues of big bang and why inflationary phase is thought to the most natural of remedies.

### 1.1.1 A brief review of standard cosmology

Cosmology is a branch of physics which deals with the evolution of our universe at large scales( $\sim$ 100Kpc $\simeq 3\times10^{21}m$). Even though what we see around us is a highly inhomogeneous

and anisotropic distribution of matter, a large number of cosmological observations over the years prove that our universe is spatially homogeneous and isotropic at large scales. Assuming these two observationally inferred principles of homogeneity and isotropy of space to be fundamental, theoretical cosmology begins it journey. Even though the study of cosmology is very old, the real progress in theoretical cosmology started with the discovery of general theory relativity by Albert Einstein. To make our journey short and to get to our main focus of the thesis, we will follow the path Einstein told us a century ago. Cosmology is essentially the study of evolution of spacetime geometry over large scales where the dynamics is controlled by the given matter energy distribution with appropriate initial conditions. Given the two aforementioned cosmological principles and Einstein's idea of geometric evolution, our universe can be accurately described by the Friedmann-Leîmatre-Robertson-Walker (FLRW) metric which is expressed as

$$\begin{aligned} ds^2 &= dt^2 - a^2(t)\gamma_{ij}dx^i dx^j \\ &= a^2(\eta)\left[d\eta^2 - \frac{dr^2}{1-\kappa r^2} - r^2(d\theta^2 + \sin^2\theta d\phi^2)\right], \end{aligned} \tag{1.1}$$

where, the three spatial co-ordinates $x^i$ are conventionally known as *comoving* co-ordinates. $t$ is the cosmic time measured by a *comoving* observer and $\eta$ is known as the conformal time defined as $\mathrm{d}\eta = \mathrm{d}t/a(t)$ with $a(t)$ being the scale factor. The spatial metric is written as $\gamma_{ij}$. The curvature parameter $\kappa = (1, 0, -1)$ corresponds to closed, flat, and open universe respectively. Throughout this thesis, we will consider spatially flat $\kappa = 0$ universe which is again an observational fact. The expansion of the universe is expressed by defining a quantity known as the Hubble parameter:

$$H(t) = \frac{1}{R_H} \equiv \frac{\dot{a}(t)}{a(t)}, \tag{1.2}$$

where, the *dot* represents the derivative with respect to the cosmic time. We have also defined a quantity known as the Hubble radius, $R_H$ which measures the size of a region of space being causally connected by any physical processes. As we have already mentioned, the dynamics of standard big-bang evolution of our universe is described in the framework of Einstein's theory of general relativity supplemented with the observational facts such as principle of spatial homogeneity and isotropy. Based on these principles one also expresses the distribution of matter in our universe by a perfect fluid with stress-energy tensor of the form

$$T_{00} = \rho(t); \quad T_{i0} = 0; \quad T_{ij} = -P(t)\gamma_{ij}(t, \vec{x}). \tag{1.3}$$

In a more familiar form with mixed tensor indices, it can be expressed as

$$T^{\mu}_{\nu} = g^{\mu\lambda}T_{\lambda\nu} = \begin{pmatrix} \rho & 0 & 0 & 0 \\ 0 & -P & 0 & 0 \\ 0 & 0 & -P & 0 \\ 0 & 0 & 0 & -P \end{pmatrix}. \tag{1.4}$$

Where $\rho$ is the energy density and $P$ is the thermodynamic pressure of the fluid in the rest-frame of the fluid. Due to homogeneity and isotropy, all these quantities, at the background level will naturally be function of time only.

The evolution equations of the spacetime geometry and the energy momentum distribution will be followed form the famous Einstein equation

$$G_{\mu\nu} = R_{\mu\nu} - \frac{1}{2}Rg_{\mu\nu} = 8\pi \mathrm{G} T_{\mu\nu}, \tag{1.5}$$

where $(g_{\mu\nu}, R_{\mu\nu}, R)$ are well known general spacetime metric and the associated Ricci curvature tensor, and $R = g_{\mu\nu}R^{\mu\nu}$ is the Ricci scalar of the given metric. Therefore, using the above Einstein's equation the dynamical equations for the cosmological scale factor $a(t)$, and the total matter density $\rho(t)$ of our universe are found to be

$$3M_{\mathrm{p}}^2 H^2 = \rho \tag{1.6}$$

$$6M_{\mathrm{p}}^2(H^2 + \dot{H}) = -\left(\rho + \frac{P}{3}\right), \tag{1.7}$$

where, $M_{\mathrm{p}} = 1/\sqrt{8\pi G}$ is the reduced Planck constant. Apart from this we have energy-momentum conservation,

$$\nabla_\mu T^\mu_\nu = 0. \tag{1.8}$$

From the above equation the evolution of the energy density can be written as the well known continuity equation

$$\dot{\rho} + 3\frac{\dot{a}}{a}(\rho + P) = 0. \tag{1.9}$$

Depending upon the type of matter component filling the universe, we can obtain the time evolution of the scale factor $a(t)$. For instance, if we consider the dominant energy component to be radiation(relativistic particles) with the characteristic equation of state $w = p/\rho = 1/3$, one obtains $\rho_{rad} \propto a^{-4}$, and consequently $a(t) \propto t^{1/2}$. If we consider the dominant energy component to be non-relativistic matter with the characteristic equation of state $w = 0$, one obtains $\rho_{mat} \propto a^{-3}$, and consequently $a(t) \propto t^{2/3}$. One can in principle consider any arbitrary dominant energy component in the universe with its associated equation of state, which solves the above set of Eq. (1.7) and gives the evolution of the scale factor. *Therefore, one of the important open problems in Einstein's description of our universe is the origin of matter fields.* So far, only way out to proceed further is to understand the nature of different form of the energy components from cosmological experiments. A Large volume of cosmological and astrophysical observations indicate that the total energy density of our present universe today comprises of completely unknown dark energy accounting for nearly 75% of total energy while rest are matter component. Even more surprising observation is that the matter energy density further comprises of two main components where the ordinary visible matter shares only 4% of the total matter and remaining 21% is occupied by an another unknown entity known as dark matter. There are also negligible contributions coming from neutrinos, electromagnetic radiation and gravity waves to the total energy density. Therefore, right at this point we can pause for a moment and little thought may completely overwhelm us for being completely ignorant of what constitutes our universe even after the centuries of endeavor towards understanding the cosmos. This fact not only left us a large void in our "knowns" but also gave us no clue of how to observe them. Until the discovery of some new breakthrough, we follow the conventional

approach to understand the unseen by the seen ones. A portion of our thesis will, therefore, be guided by the following important question: *Can the observed distribution of visible matter and/or radiation known as cosmic microwave background (CMB) shed light on the properties of dark matter/energy?* In this thesis, apart from inflationary model building we will focus on the possible connection between the observed CMB and unobserved dark matter.

The radiation component (CMB) that we see today is almost negligible compared to the other observed energy components of our universe. The contributions from radiation component however were significantly dominant in the past as the energy density of the radiation field evolves according to $\rho_{rad} \propto a^{-4}$ while that of the matter fields evolves as $\rho_{mat} \propto a^{-3}$ as mentioned earlier. The ratio of number density of matter to radiation per comoving volume is however constant and is given by[10, 11]

$$\eta_{BBN} = \frac{n_B}{n_\gamma} = (6.0 \pm 0.4) \times 10^{-10}. \tag{1.10}$$

$$\eta_{CMB} = \frac{n_B}{n_\gamma} = (6.05 \pm 0.07) \times 10^{-10}. \tag{1.11}$$

This ratio provides us the number of baryons per photon in our universe, which helps us to set an important initial condition for the standard big-bang theory.

Before we move on for setting up the stage of our thesis, let us briefly mention the chronological evolution of our universe as depicted in Fig.(1.1). However important point the reader should remember that, this chronological events were tabulated considering the present cosmological observations as well as our current theoretical understanding. Hence some facts specifically in the early time, may turn out to be incorrect if we have further observations or more theoretical understanding.

Let us read the timeline from the bottom. As mentioned earlier, the universe we see today is influenced by unknown dark energy. However most important breakthough that has set the very idea of big-bang cosmology into its firm footing is the observation of cosmic microwave background and its minute spatial fluctuations in temperature in one part of $10^5$. The present CMB temperature is estimated to be 2.726K. "Today" is attributed to the present time which is 13.6 billion years after the universe started from the big-bang, when universe is very hot. Observation of the current accelerated expansion of the universe parametrized by Hubble constant estimates the current age of the universe. The current estimated value of the Hubble constant is $H_0 = 67.3 \pm 1.2$ km/s/Mpc [11]. As emphasized, the present universe is dark energy dominated which apparently starts to dominate in the recent past. When the universe becomes around 1$\sim$13.7 million years old, the large scale structures are assumed to be formed which comprise of galaxies with full of stars, clusters of galaxies, super-clusters and so on. Those structures have been further proved to be originated from the gravitational instability due to spatial inhomogeneity of matter-energy distribution (imprinted on the CMB temperature anisotropies) in the early universe before the structure formation. We will see later how a period of accelerated expansion similar to present day dark energy dominated universe can naturally produce such a small inhomogeneity in the early universe. The age $t \sim 60,000$ years marks an important era of matter-radiation equality. The universe was radiation dominated prior to this time and after this era universe enters into the matter dominated phase. Going further backward in time, when the age of the universe is at around $t = 380,000$ years, it is the

TIMELINE 1: *Brief history of universe*

| | |
|---|---|
| $10^{-43}$s, $10^{19}$GeV | Planck scale - quantum gravity? |
| $\sim 10^{-25,-40}$s, $10^{10-18}$GeV | Inflation and reheating. |
| | Beginning of Hot Big Bang era... |
| $\sim 10^{-25,-38}$s, $10^{10-16}$GeV | Baryogenesis |
| $10^{-10}$s, 100GeV | Electroweak symmetry Breaking |
| $10^{-4}$s, $10^{13}$K, 100MeV | Quarks condense into hadrons |
| 10s, $10^{11}$K, 1MeV | Neutrino decoupling |
| | Era of Observational Cosmology begins... |
| $10^{2}$s, $10^{10}$K, 0.1MeV | Neucleosynthesis($n + \nu \leftrightarrow p + e^{-}$) |
| $10^{5}$yrs, $10^{4-5}$K | Matter domination( radiation-matter equality) |
| $3 \times 10^{5}$yrs, $10^{3-4}$K, 1eV | Photon decoupling ($p + e \leftrightarrow H$), CMB formed |
| $10^{9}$yrs | Structure formation. |
| $5 \times 10^{9}$yrs | Dark energy domination begins. |
| $13.6 \times 10^{9}$yrs, 2.7K | Today. |

FIGURE 1.1: Timeline

era of CMB. The CMB photons decouple from the baryon fluid as the mean photon energy of photon drops below the ionisation energy of hydrogen because of cosmological expansion. All the free electrons and protons recombine to form hydrogen. Before that Helium, which accounts for 25% of the total baryonic matter, is also recombined. Tiny inhomogeneities remaining after the recombination induces the small anisotropies in temperature of the photons which decouple at the Last Scattering Surface(LSS). These anisotropies will remain until the present day of CMB photons. At $t = 1 \sim 200$ seconds from big-bang, the nucleus are formed as the temperature drops below 1MeV. Protons and neutrons which were free streaming upto this point fuses to form Helium-4(mostly) as well as other lighter elements. Around 75% of the protons will remain free. The abundance of light elements resulting from synthesis of nuclear bound states are known as the Big Bang Nucleosythesis(BBN) show excellent agreement with observation and is one of the prime reasons why big bang theory supplanted its alternatives. When the age of our universe is of the order of one second corresponding to the temperature of the order 0.5 MeV, the electrons becomes almost massless. Therefore, the electron-positron pairs began to annihilate leaving only a tiny excess of matter which is of the order of one per billion photons. If we go further backward in time neutrino decouples from the cosmic

soup as their interaction fall out of equilibrium at around $t \sim 0.2$ second at a temperature $\sim 1MeV$. Quarks and gluons which were previously free at higher temperature, begin to get confined forming baryons and mesons at $t \sim 10^{-5}$ second at a temperature of 100MeV . At $10^{-10}$s we have electroweak symmetry breaking. The $W$ and $Z$ bosons acquire mass while photons remain massless. The present universe seems to be made entirely of the baryons. While the symmetries of the standard models predicts almost equal number of matter and antimatter in our universe. However, the process of generating this asymmetry in the number of baryonic matter is supposed to have occured at 1MeV $< T <$ $10^{16}$GeV via a process known as baryogenesis. A phase of exponential expansion known as inflation must precede all these phases. The inflationary phase explains the remarkable uniformity of the CMB and the flatness of the universe which we will describe in detail. In addition it also provides us with a mechanism of generating the primordial density fluctuations which eventually give rise to the large scale structure formation. The inflationary phase accompanies a phase of reheating when all the matter and radiation in some form is produced. Thus quantum processes during inflation and the accompanying phase of reheating is responsible for all the matter, radiation as well as large scale structure around us. In *INFLATIONARY UNIVERSE*, Alan Guth writes "...in the inflationary theory the universe evolves from essentially nothing at all, which is why I frequently refer to it as the ultimate free lunch". We do not have precise understanding of the state of the universe prior to the inflation. It has been generally agreed that a description of quantum gravity is necessary in this regime. In fact a complete theory of quantum gravity is also necessary for understanding the source of inflaton. Thus we may say that the inflationary period is actually the phase up-to which we have theoretical understanding backed by observational data about the origin of our universe. This phase standing between the borderline of knowns and unknowns is still in an active developmental stage.

After having a glimpse of the history of our universe, we will now introduce the idea of inflation in next couple of sections.

### 1.1.2 Basics of Inflation

Before developing the theory of inflation, in this section we will describe why at all a *period of exponential expansion* must be followed by the standard big bang model. The big bang cosmological model was very successful in describing the observable universe. A simple model of the expanding universe described based on the principle of homogeneous and isotropic FLRW spacetime propelled by mostly dark matter and dark energy so called ($\Lambda$CDM) is able to explain the current observed universe to a significant precession. However, the very idea of inflation originated from the fact that the big-band model has some inherent limitations. All of those limitations can be unified into one which is popularly known as *initial condition problem*. In the subsequent section we will briefly describe those problems.

#### 1.1.2.1 Homogeneity Problem

As we have already mentioned it is the cosmological observations which dictates us to consider our universe to be in the homogeneous and isotropic state. The observed temperature fluctuations in the cosmic microwave background (CMB) ($\delta T/T_0 \sim 10^{-5}$) put a solid foundation on those very assumptions. The prior assumptions of homogeneous and isotropic state in understanding the cosmological dynamics greatly simplifies the computational and analytical complexity of the actual problem. However this very principle turned out to be the origin

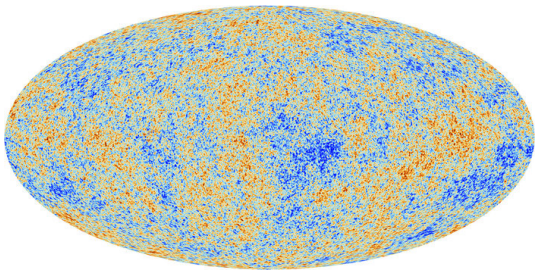

FIGURE 1.2: Fluctuations in the Cosmic Microwave Background (CMB) [Image courtesy: ESA website]

.

of all the limitations of the standard big-bang model. The CMB photons having the same average temperature $T_0 \simeq 2.73K$ across a large region on a spatial time slice of our universe poses the first question: *why our universe is homogeneous over such a large scale? Or in other words why the photons which are freely streaming to us from all possible directions from the last scattering surface have the same temperature?* Such a large degree of homogeneity can only be achieved if the whole region of scattering surface was causally connected. Therefore, the question of homogeneity can be translated into the question that how could such a vast region of space becomes homogeneous in spite of no causal connection inferred from the simple Hubble observation. This is known as the homogeneity problem or in other words horizon problem of hot big bang cosmology.

#### 1.1.2.2 Flatness Problem

In addition to the above one, we encounter another problems related to the critical energy density of our universe. If we consider the spatial curvature to be non-zero, the Friedman equation describing the dynamics of our universe with the curvature term $\kappa$ becomes,

$$H^2 = \frac{8\pi G}{3}\rho - \frac{\kappa}{a^2} \tag{1.12}$$

From the above equation one of the important dimensionless cosmological parameters defined as $\Omega = \rho/(3H^2/8\pi G)$ called density parameter becomes,

$$\Omega - 1 = \frac{\kappa}{a^2 H^2}. \tag{1.13}$$

The standards evolution of the scale factor and the associated energy density can be used to get the evolution of $\Omega - 1$ for different epoch of our universe dominated by

$$\text{Matter:} \quad a \propto t^{2/3}, \quad H \propto t^{-1} \implies \frac{1}{aH} \propto t^{1/3} \implies |1-\Omega| \propto t^{2/3}$$
$$\text{Radiation:} \quad a \propto t^{1/2}, \quad H \propto t^{-1} \implies \frac{1}{aH} \propto t^{1/2} \implies |1-\Omega| \propto t.$$

Further from the present observational estimate one gets $|\Omega(t_0) - 1| < 10^{-2}$. If we go backward in time following at the time of BBN, we will have $|\Omega(t_{BBN}) - 1| \leq 10^{-17}$. To maintain this value from the present to BBN, one needs do the extreme fine tuning of the value of spatial curvature $\kappa$ situated in the right hand side of the Eq. (1.13). However best solution will be to assume $\kappa = 0$, which means that the energy density of our universe is equal to the critical

energy density. The question then naturally arises is, how can one obtain such a unique critical state of the spatially flat universe at the very early stage. This is the well known *flatness problem* of standard big-bang.

In such a situation a new paradigm has emerged which is known as inflation in the field of early universe cosmology. In our following sections this will our main topic of discussions.

## 1.2 Inflation: A period of exponential expansion

We will now examine how inflation can solve the aforementioned problems of hot big-bang cosmology. We will also see how this new paradigm unexpectedly enter into a new realm of understanding the very fabrication our universe through large scale structure. The homogeneity problem as discussed has to do with the fact that the Hubble horizon always increases in the standard big-bang cosmology. This essentially suggests that as we go backward in time, more and more regions of space become causally disconnected. In other words two observers causally connected at the present epoch must have been causally disconnected in the distant past. Therefore, homogeneity at the time as early as the last scattering should be very difficult to maintain. As mentioned the observational fact of large scale homogeneity questions the very foundation of the 'bing-bang'. The simplest but elegant resolution of this problem has been proposed by introducing inflation in the early universe. This is the phase when the Hubble horizon is shrinking in time,

$$\frac{d}{dt}(aH)^{-1} < 0. \tag{1.14}$$

Hence, two points in the last scattering surface which were in causally disconnected regions can be in causal contact before the inflation. To further understand the above statement of horizon dynamics during inflation, the Eq. (1.14), can be expanded into

$$\frac{d}{dt}(aH)^{-1} = \frac{d}{dt}(\dot{a})^{-1} = -\frac{\ddot{a}}{(\dot{a})^2} < 0. \tag{1.15}$$

It is evident that a shrinking Hubble horizon also implies a period of accelerated expansion. Inflationary paradigm, assumed to be the perfect master stroke in the theory of cosmology, essentially solves all the aforementioned problems of hot big-bang. Moment one assumes a phase of accelerated expansion, it automatically leads to a spacetime with flat special geometry $\kappa = 0$. Therefore, solution of flatness problem is a natural consequence of inflationary universe. None the less let us use the above definition of horizon dynamics to inquire about the property of the source of energy-momentum which may result in an accelerated expansion of the spacetime. For that we first write Eq. (1.14) as

$$\frac{d}{dt}(aH)^{-1} = -\frac{\dot{a}H + a\dot{H}}{(aH)^2} = -\frac{1}{a}(1-\epsilon) < 0 \tag{1.16}$$

where, $\epsilon \equiv -\frac{\dot{H}}{H^2}$. For the above condition to be valid we must satisfy $\epsilon < 1$. Using one of the Friedmann Eq. (1.7)

$$\dot{H} + H^2 = -\frac{1}{6M_{\rm p}^2}(\rho + 3P) = -\frac{H^2}{2}\left(1 + \frac{3P}{\rho}\right), \tag{1.17}$$

and considering smallness of the parameter $\epsilon$ we get an important condition on the equation of state,$w \equiv P/\rho$,

$$\frac{3}{2}\left(1+\frac{P}{\rho}\right) < 1 \implies w < -\frac{1}{3} \tag{1.18}$$

This important restriction on the equation of state suggests that to have inflation, one needs unconventional matter content which contributes negative pressure with positive energy density $\rho$.

### 1.2.1 More on conditions for inflation: Slow roll parameters

Before we move on to discuss the explicit construction of matter field for inflation, let us elaborate more into the conditions for the inflation to understand the physical nature of the required matter field. As it is an accelerated expansion of spacetime, a natural measure of inflation can be defined by the well known quantity called *'e-folding number'*($N$) between two instants as

$$\mathrm{d}N \equiv \ln\left(\frac{a_f}{a_i}\right) = \mathrm{d}\ln a = H\,\mathrm{d}t\,. \tag{1.19}$$

Here, $i$ and $f$ are initial and final value of the scale factor respectively. Thus the condition for inflation in terms of e-folding number translates into,

$$\epsilon \equiv -\frac{\dot{H}}{H^2} = -\frac{\mathrm{d}\ln H}{\mathrm{d}N} < 1, \tag{1.20}$$

implying the change in the Hubble constant which must be very small with respect to change in $N$. The scale of homogeneity as is observed in the CMB or large scale structures, is quantified by the aforementioned inflationary parameter $N$. The present size of the observed homogeneous universe can be well explained by this e-folding number to be $\Delta N = 50 \sim 60$. Since the whole problem is dynamical in nature, and $N$ is essentially playing the role of time, one needs to keep the parameter $\epsilon$ small for longer period of time, which is parametrized by another quantity defined as

$$\eta \equiv \frac{\mathrm{d}\ln\epsilon}{\mathrm{d}N} = \frac{\dot{\epsilon}}{H\epsilon} \tag{1.21}$$

Therefore, smallness of both the parameters $|\eta|, |\epsilon| < 1$ will ensure the inflation for sufficient period of time such that one obtains $N = 50 \sim 60$. In the inflationary context those small parameters are called slow roll parameters. In next section we will consider a specific scalar field model of inflation and study in detail the important roles played by those parameters in defining important cosmological observables.

### 1.2.2 Scalar field as the source of inflation

By now it is understood that inflation is a period of exponential expansion which is in mathematical term known as quasi-de Sitter phase. Over the years large number of models have been constructed to realize this phase. However the simplest and the most successful inflationary model is the one where dynamics is driven by a real scalar field. The simplest action for the inflation in terms of scalar field called inflaton is written as

$$S_\phi = \int d^4x\sqrt{-g}\left[M_{\mathrm{p}}^2 R + \frac{1}{2}g^{\mu\nu}\partial_\mu\phi\partial_\nu\phi - V(\phi)\right], \tag{1.22}$$

where we have defined the reduced Planck mass $M_{\rm p} = 1/\sqrt{8\pi G}$ in natural unit. $V(\phi)$ is the potential energy. At this point let us mention that the significant part our thesis will be devoted to the construction of generalized scalar field model which can successfully explain the cosmological observation. Therefore, in this section our discussions will be mainly focused on the basic methodology of how to obtain inflation from the inflaton. None the less the stress-energy tensor associated with the inflaton comes out to be

$$T_{\mu\nu} = \partial_\mu\phi\partial_\nu\phi - g_{\mu\nu}\left(\frac{1}{2}g^{\sigma\rho}\partial_\sigma\phi\partial_\rho\phi - V(\phi)\right). \tag{1.23}$$

Because of background homogeneity considering the homogeneous inflaton namely, $\phi \equiv \phi(t)$, the expressions for the energy and pressure density of for inflaton turned out to be

$$\rho_\phi = \frac{1}{2}\dot{\phi}^2 + V(\phi) \tag{1.24}$$

$$P_\phi = \frac{1}{2}\dot{\phi}^2 - V(\phi) \tag{1.25}$$

With this expression of energy density and pressure, we readily obtain the equation of state parameter for the inflaton as,

$$w_\phi = \frac{P_\phi}{\rho_\phi} = \frac{\frac{1}{2}\dot{\phi}^2 - V(\phi)}{\frac{1}{2}\dot{\phi}^2 + V(\phi)} \tag{1.26}$$

The dynamics of the background inflationary phase is described by the following set of homogeneous equations for the inflaton and the scale factor derived from the action Eq. (1.22),

$$\ddot{\phi} + 3H\dot{\phi} + V'(\phi) = 0, \tag{1.27}$$

$$H^2 = \frac{8\pi G}{3}\rho_\phi = \frac{1}{3M_{\rm p}^2}\left[\frac{1}{2}\dot{\phi}^2 + V(\phi)\right]. \tag{1.28}$$

Where, the second is known as Friedmann equation. The above equation resembles the equation of a damped harmonic oscillator where the term $3H\dot{\phi}$ plays the role of a friction term. This very damping term will play the essential role in identifying the *'slow-roll'* parameters defined before in order to obtain the sufficient number of e-folding.

### 1.2.3 The slow-roll conditions

The slow roll parameters that have been previously discussed can now be expressed in terms of inflaton as follows,

$$2H\dot{H} = \frac{1}{3M_{\rm p}^2}\left[\dot{\phi}\ddot{\phi} + V'(\phi)\dot{\phi}\right]. \tag{1.29}$$

Using dynamical equation for the inflaton and the scale factor and Eq. (1.29), we get,

$$\dot{H} = -\frac{1}{2}\frac{\dot{\phi}}{M_{\rm p}^2}. \tag{1.30}$$

Hence, the slow roll parameters $(\epsilon, \eta)$ turned into the following form,

$$\epsilon = -\frac{\dot{H}}{H^2} = \frac{\frac{1}{2}\dot{\phi}^2}{M_{\rm p}^2 H^2} \tag{1.31}$$

$$\eta = \frac{\dot{\epsilon}}{H\epsilon} = 2\frac{\ddot{\phi}}{H\dot{\phi}} - 2\frac{\dot{H}}{H^2} = 2(\epsilon - \delta). \tag{1.32}$$

Therefore, slow roll conditions for inflation essentially means that the kinetic energy of inflaton should be negligible compared to the total energy during inflation. In other words, the inflationary period is dominated by the potential energy of the inflaton, and as a result acceleration of the field must be small for sufficient time. This second condition is defined by a dimensionless quantity which is the acceleration per Hubble time.

$$\delta \equiv -\frac{\ddot{\phi}}{H\dot{\phi}} \tag{1.33}$$

The physical significance for these slow-roll conditions will be more apparent when we will write them in terms of the scalar field potential. If we use above slow-roll conditions into Eq.(1.28), the dynamical equations for the inflation become

$$H^2 \approx \frac{V}{3M_{\rm p}^2} \quad ; \quad 3H\dot{\phi} \approx -V'. \tag{1.34}$$

Using these, the potential form of slow-roll conditions turned out to be

$$\epsilon_V = \frac{M_{\rm p}^2}{2}\left(\frac{V'}{V}\right)^2 ; \quad \eta_V = M_{\rm p}^2\left(\frac{V''}{V}\right) \tag{1.35}$$

For any canonical scalar field inflationary model, these equations can be taken as a starting point for further study. During the inflation these slow-roll parameters are smaller that unity, $|\epsilon_V|,\ |\eta_V| < 1$. Now we are in a position to express the e-folding number Eq. (1.19), between any two arbitrary instants during inflation in terms of inflaton as

$$\Delta N = \int_{\phi_i}^{\phi_f} \frac{1}{\sqrt{2\epsilon_V}} \frac{|\,{\rm d}\phi\,|}{M_{\rm p}}, \tag{1.36}$$

where, $\phi_i$, and $\phi_f$ are initial and final inflaton field values. So far all we have computed are at the background label, and choosing a particular form of the potential one can obtain the inflation. However, it would have been uninteresting if this is the end of the story. Inflation is not just a phase but a paradigm, which not only describes homogeneous and isotropic universe but also creates the tiny fluctuation we mentioned. It also brings various branches of physics namely particle phenomenology, non-equilibrium field theory to name a few, into a single fold. In this thesis we will touch upon all those aspects in some detail. In the subsequent section let us begin with the origin of the tiny fluctuation mentioned in terms of perturbation theory.

## 1.3 Cosmological Perturbations

The tiny fluctuations originating form the quantum effects during inflation is assumed to be the seed for the large scale structure of our observable universe. Until now we have considered the inflaton field as the homogeneous one $\phi(t)$ in the homogeneous FLRW background. However, the quantum fluctuations will lead to inhomogeneities. Assuming these inhomogeneities to be small such that the perturbation theory is applicable, we write the inflaton field as

$$\phi(\mathbf{x}, t) = \phi(t) + \delta\phi(\mathbf{x}, t). \tag{1.37}$$

Due to these small fluctuation of field value, the inflation will end at different time in different region of space. Therefore, different regions will inflate differently resulting in a small inhomogeneous distribution of energy density $\delta\rho(\mathbf{x})$. This small density fluctuation has been proved to be the origin of the observed temperature fluctuations in the CMB.

$$\delta\phi(\mathbf{x},t) \rightarrow \delta\rho(\mathbf{x},t) \rightarrow \Delta T(\mathbf{x}) \tag{1.38}$$

In the following sub-sections we will review[12–17], the dynamics of these perturbation in the inflationary background. The observed inhomogeneities in the CMB are very small $\Delta T/T \sim \mathcal{O}(10^{-5})$. This implies that the universe at the time of CMB decoupling was nearly homogeneous, and the inhomogeneities are small enough to be treated with linear order perturbation theory. The evolution of those perturbations are studied by expanding the Einstein equations to the first order

$$\delta G_{\mu\nu} = 8\pi \mathrm{G}\delta T_{\mu\nu} \tag{1.39}$$

As the above equation suggests, we can treat the perturbation of metric and matter field separately. In order to understand the basics of perturbation theory, will discuss the essential points as follows.

### 1.3.1 Metric perturbation

Since matter and energy is the ultimate source of curvature in the spacetime geometry. Any fluctuations in the matter field such as the field given in Eq. (1.37) will induce fluctuations in the metric. Thus it is necessary to calculate the action for those small fluctuations on the homogeneous background of Eq. (1.7). In this section we will first discuss about the general form of the perturbation and their important properties. General form of the metric perturbation is parametrized as

$$\mathrm{d}s^2 = (1+2\Phi)\,\mathrm{d}t^2 - 2a(t)B_i\,\mathrm{d}t\,\mathrm{d}x^i - a^2(\delta_{ij}+h_{ij})\,\mathrm{d}x^i\,\mathrm{d}x^j \tag{1.40}$$

The 10 degrees of freedom(d.o.f) of the perturbation $\delta g_{\mu\nu}(\mathbf{x})$ is decomposed into scalar, vector and tensor components according to their behavior under local spatial rotation group.

$$\delta g_{\mu\nu} \equiv \Big(\delta g_{00}, \delta g_{0i}, \delta g_{ij}\Big) \tag{1.41}$$

Which could be more explicitly written as

- 4 scalar d.o.f $\rightarrow \delta g_{00} \equiv \Phi$ and three other$(B, \Psi, E)$ which will be cleared below.
- 4 divergence-less vector d.o.f $\rightarrow (\widehat{B}_i, \widehat{E}_i)$. One of which is arising as follows,

$$\delta g_{0i} \equiv B_j = \underbrace{\partial_j B}_{scalar} + \underbrace{\widehat{B}_j}_{vector} \quad \text{where} \quad \partial_j \widehat{B}_j = 0.$$

- 2 trace-less and divergence-less tensor d.o.f $\rightarrow \delta g_{ij} \equiv h_{ij}$

$$h_{ij} = 2\Psi\delta_{ij} + 2\partial_i\partial_j E + \Big(\partial_i \widehat{E}_j + \partial_j \widehat{E}_i\Big) + 2\widehat{h}_{ij}$$

$$\text{where} \quad \partial^i \widehat{E}_i = 0, \quad \partial^i \widehat{h}_{ij} = 0, \quad \widehat{h}^i_i = 0.$$

The usefulness of such a decomposition is that, at linear level, we can study the evolution of those three class of perturbations independently of each other with the linearized Einstein equation. The scalar-vector-tensor(SVT) decomposition is most easily described in Fourier space. In all our future discussions the Fourier decomposition of a fluctuations will be defined as

$$X_{\mathbf{k}} = \int \mathrm{d}^3\mathbf{x} X(t,\mathbf{x}) e^{i\mathbf{k}\cdot\mathbf{x}} \quad \text{where,} \quad X \equiv (\delta\phi, \delta g_{\mu\nu}, \cdots) \tag{1.42}$$

It turned out that the vector perturbation has only a decaying mode under usual conditions of linear perturbation theory[12, 18]. This is also expected form the general coordinate invariance, as in the gravity sector, one only has two propagating degrees of freedom. Therefore, we will ignore vector mode through out our discussions. For our latter purpose let us express the transformation properties of fluctuation modes under the coordinate transformation $(t \to t+\alpha,\ x^i \to x^i + \beta^{,j})$ as

$$\begin{aligned}
\Phi &\to \Phi - \dot{\alpha}, \\
B &\to B + \frac{\dot{\beta}}{a} + \frac{1}{a}\alpha, \\
\Psi &\to \Psi + H\alpha, \\
E &\to E + \frac{\beta}{a^2}, \\
\widehat{h}_{ij} &\to \widehat{h}_{ij}.
\end{aligned} \tag{1.43}$$

From the transformations, one can understand the fact that all the perturbation variables are not physical, or we call them gauge dependent. For example $\widehat{h}_{ij}$ is clearly a gauge invariant perturbation. Never the less, these transformation properties will help us identifying the physical or gauge invariant perturbation variable which we finally identify as the curvature perturbation observed in CMB. Before we could define those physical perturbation let us discuss about the perturbation of energy momentum tensor specifically for inflaton.

### 1.3.2 Matter Perturbations

In the cosmological context the general form of the perfect energy momentum tensor takes the following form,

$$T_{\mu\nu} = \bar{T}_{\mu\nu} + \delta T_{\mu\nu} \tag{1.44}$$

At the background level, the energy momentum tensor takes the following homogeneous form $\bar{T}_{\mu\nu} = -\bar{p}\bar{g}_{\mu\nu} + (\bar{\rho}+\bar{p})\bar{u}_\mu\bar{u}_\nu$, with the co-moving 4-velocity $\bar{u}_\mu = (1,0)$. To write the perturbations of the stress energy tensor we first note the perturbations of the density and pressure as

$$\delta\rho(t,\mathbf{x}) \equiv \rho(t,\mathbf{x}) - \bar{\rho}(t) \tag{1.45}$$

$$\delta p(t,\mathbf{x}) \equiv p(t,\mathbf{x}) - \bar{p}(t) \tag{1.46}$$

While the perturbed 4-velocity with respect to the metric (1.40) is given as

$$u_\mu \equiv (1-\Phi, v_i), \quad u^\mu \equiv (1+\Phi, -\frac{1}{a^2}v^i - \frac{1}{a}B^i), \tag{1.47}$$

while, deriving this use has been mode on the normalization condition $u_\mu u^\mu = 1$. With these definitions,the perturbed components of the total stress-energy tensor is given as

$$T^0_0 = (\bar{\rho} + \delta\rho) \tag{1.48}$$
$$T^0_i = (\bar{\rho} + \bar{p})v_i \tag{1.49}$$
$$T^i_j = -\delta^i_j(\bar{p} + \delta p) + \Sigma^i_j \tag{1.50}$$
$$\tag{1.51}$$

where $\Sigma^i_j$ is the anisotropic stress which is a gauge-invariant quantity, while the density, pressure and momentum density are gauge dependent. In the similar manner under general coordinate transformations (gauge transformations) $(t \to t + \alpha,\ x^i \to x^i + \beta^{,j})$, above they transform as

$$\delta\rho \to \delta\rho - \dot{\bar{\rho}}\alpha \tag{1.52}$$
$$\delta p \to \delta p - \dot{\bar{p}}\alpha \tag{1.53}$$
$$\delta q_i \to \delta q_i + (\bar{\rho} + \bar{p})\alpha_{,i} \tag{1.54}$$

where, $\delta q_i \equiv (\bar{\rho} + \bar{p})v_i$ is momentum density. Now we have both the ingredients to track down the evolution of the perturbations via Eq. (1.39), namely the metric perturbations described in Section 1.3.1 and the perturbed matter in Section 1.3.2.

### 1.3.3 Gauge invariant variable and power spectrum: scalar mode

So far we have discussed about various perturbation variables and their transformation properties. In this section we consider a particular gauge invariant quantity [18], called comoving curvature perturbation ($\mathcal{R}$), which is defined as

$$\mathcal{R} = \Psi - \frac{H}{\bar{\rho} + \bar{p}}\delta q \tag{1.55}$$

where $\delta q$ is the scalar part of the 3-momentum density

$$T^0_i = \delta q_i = \partial_i \delta q + \widehat{\delta q}_i.$$

One can clear see that $\mathcal{R}$ is invariant under general coordinate transformation. If we consider the homogeneous inflaton field, the momentum density turned out to be $T^0_i = -\dot{\bar{\phi}}\partial_i\delta\phi$. Therefore, the co-moving curvature perturbation takes the following form,

$$\mathcal{R} = \Psi + \frac{H}{\dot{\bar{\phi}}}\delta\phi \tag{1.56}$$

In order further proceed, it is very convenient to consider a particular gauge as

$$\delta\phi = 0, \quad g_{ij} = a^2\Big[(1 - 2\mathcal{R})\delta_{ij} + h_{ij}\Big], \quad \partial_i h_{ij} = h^i_i = 0. \tag{1.57}$$

The utility of this choice is that as the inflaton field is unperturbed in this gauge, and since originally $\mathcal{R}$ behaves as a gauge invariant variable, all the other scalar perturbation $(\Phi, B)$ can be expressed in term of $\mathcal{R}(t, \mathbf{x})$ (for details see [15]). Most importantly $\Psi$ then measures

purely the three-curvature of the spatial section as $R^{(3)} = (1/3)\nabla^2\Psi$. Now in the gauge (1.57), the quadratic action for the comoving curvature perturbation $\mathcal{R}$ turned out to be

$$S_{(2)} = \frac{1}{2}\int \mathrm{d}^4x a^3 \frac{\dot{\phi}^2}{H^2}\Big[\dot{\mathcal{R}}^2 - \frac{1}{a^2}(\partial_i\mathcal{R})^2\Big]. \tag{1.58}$$

Using the following *Mukhanov variable*

$$v = z\mathcal{R} \quad \text{with} \quad z^2 = 2a^2\frac{\frac{1}{2}\dot{\phi}^2}{H^2} = 2a^2\epsilon, \tag{1.59}$$

where $\epsilon$ is the usual slow-roll parameter, the equation of motion for each individual mode takes the following form

$$v_k'' + \Big(k^2 - \frac{z''}{z}\Big)v_k = 0. \tag{1.60}$$

Where "prime" is taken with respect to the conformal time. The functions $z$ in the above equation depends on the background dynamics which makes the full general equation difficult to solve analytically. It is usually solved numerically. However, for inflationary background the above equation may be analysed in various limits to have an intuitive understanding of the solution.

In order compute the various correlation function for this fluctuation, one needs to quantize this with appropriate boundary condition. The steps are analogous to the usual free field quantization. We promote the mode functions $v_{\mathbf{k}}$ to quantum operator:

$$v_{\mathbf{k}} \to \widehat{v}_{\mathbf{k}} = v_{\mathbf{k}}(\eta)\widehat{a}_{\mathbf{k}} + v^*_{-\mathbf{k}}(\eta)\widehat{a}^\dagger_{-\mathbf{k}}, \tag{1.61}$$

where the creation and annihilation operators $\widehat{a}^\dagger_{-\mathbf{k}}$ and $\widehat{a}_{\mathbf{k}}$ respectively satisfy the usual canonical commutation relation.

$$\Big[\widehat{a}_{\mathbf{k}}, \widehat{a}^\dagger_{-\mathbf{k}}\Big] = (2\pi)^3\delta(\mathbf{k}-\mathbf{k}'), \tag{1.62}$$

provided that the modes functions are normalized as follows

$$\big\langle v_k, v_k'\big\rangle \equiv \frac{i}{\hbar}(v_k^* v_k' - v_k^* v_k). \tag{1.63}$$

The condition above provides us the appropriate boundary condition for the solution of Eq. (1.60). The ground state or the *vacuum* is defined as

$$\widehat{a}_{\mathbf{k}}\,|0\rangle = 0, \tag{1.64}$$

To explore the analytic solution, and understand the form of the spectrum, we consider the de Sitter limit $H = \text{const.}(\ \epsilon \to 0)$ when

$$\frac{z''}{z} = \frac{a''}{a} = \frac{2}{\eta^2}, \implies z \sim \frac{1}{\eta} \tag{1.65}$$

and the equation for the mode function in (1.60) reduces to

$$v_k'' + \Big(k^2 - \frac{2}{\eta^2}\Big)v_k = 0. \tag{1.66}$$

This has the exact solution as

$$v_k = \alpha \frac{e^{-ik\eta}}{\sqrt{2k}}\left(1 - \frac{i}{k\eta}\right) + \beta \frac{e^{ik\eta}}{\sqrt{2k}}\left(1 + \frac{i}{k\eta}\right) \tag{1.67}$$

The free parameters $\alpha$ and $\beta$ characterizing the non-uniqueness of the mode functions can be fixed uniquely by the condition Eq. (1.63) together with the subhorizon limit $|k\eta| \gg 1$. These set $\alpha = 1,\ \beta = 0$, leading to the unique Bunch-Davies vacuum with the mode function,

$$v_k = \frac{e^{-ik\eta}}{\sqrt{2k}}\left(1 - \frac{i}{k\eta}\right) \implies v_k \propto \frac{1}{\eta}, \tag{1.68}$$

where the last approximate solution is in the super-horizon limit. At this stage an important result one obtains for super-horizon modes $|k\eta| \to 0$, $\mathcal{R}_k = z^{-1}v_k \to constant$. Therefore, co-moving curvature perturbation freezes out once they become super-horizon modes during inflation. This fact will essentially gives rise to the physical observables related to various correlations of $\mathcal{R}_k$. One such observable is the power spectrum which is the two point correlation function in momentum space. For simplicity considering de Sitter limit, the two point correlation function of the curvature perturbation $\mathcal{R}_k = (Hv_k)/(\dot{\phi}a)$ at the horizon crossing $a(t_k)H(t_k) = k$ will take the following well known form,

$$\langle \mathcal{R}_{\mathbf{k}}(t)\mathcal{R}_{\mathbf{k}'}(t)\rangle = (2\pi)^3\delta(\mathbf{k}+\mathbf{k}')\frac{H_k^2}{(2k^3)}\frac{H_k^2}{\dot{\phi}_k^2} \tag{1.69}$$

$$= (2\pi)^3\delta(\mathbf{k}+\mathbf{k}')\mathcal{P}_{\mathcal{R}}(k). \tag{1.70}$$

While the dimensionless power spectrum $\Delta_{\mathcal{R}}(k)$ is defined as

$$\mathcal{P}_{\mathcal{R}}(k) = \frac{2\pi^2}{k^3}\Delta^2_{\mathcal{R}}, \tag{1.71}$$

yielding,

$$\Delta^2_{\mathcal{R}}(k) = \frac{H_k^2}{(2\pi)^2}\frac{H_k^2}{\dot{\phi}_k^2}. \tag{1.72}$$

We have calculated the power spectrum taking de Sitter limit. Now if we consider all the quantities to be slowly varying, then scale dependence of the power spectrum is quantified by well known spectral index $n_s$ as

$$n_s - 1 = \frac{\mathrm{d}\ln\Delta^2_{\mathcal{R}}}{\mathrm{d}\ln k} = -2\epsilon - \eta \simeq -6\epsilon_V + 2\eta_V. \tag{1.73}$$

Through out our thesis, we will be using the second relation for the spectral index. In a similar manner one also define the running of scalar spectral index, which can be expressed as

$$dn_s^k \equiv \frac{\mathrm{d}n_s}{\mathrm{d}\ln k} = -2\xi_V + 16\epsilon_V\eta_V - 24\epsilon_V^2, \tag{1.74}$$

where, $\xi_V = M_{\rm p}^4\left(V'_{min}V'''_{min}/V^2\right)$ is the second order inflationary slow roll parameter. We will describe how we will use this fact to relate the CMB temperature with the primordial perturbation in Section 1.3.5. In the following section let us briefly discuss about the tensor mode.

### 1.3.4 Tensor Mode

The discussion of tensor perturbation will be analogous to that of the scalar perturbations. The metric for the tensor perturbation in conformal coordinate is given by

$$\mathrm{d}s^2 = a(\eta)\Big[-\mathrm{d}\eta^2 + (1+\widehat{h}_{ij})\mathrm{d}x^i\mathrm{d}x^j\Big]. \tag{1.75}$$

We have already described before $\widehat{h}_{ij}$ is the gauge invariant transverse and traceless tensor perturbation. Therefore, it has only two independent component. The two independent degrees of freedom of the tensor perturbation are generally expressed as

$$\widehat{h}_{ij} \equiv \begin{pmatrix} h_+ & h_\times & 0 \\ h_\times & h_+ & 0 \\ 0 & 0 & 0 \end{pmatrix}. \tag{1.76}$$

Following the same methodology, the second order action for the tensor perturbation turns out to be

$$S^t_{(2)} = \frac{M_{\rm p}^2}{8}\int \mathrm{d}\eta\,\mathrm{d}x^3\,a^2\Big[(\widehat{h}'_{ij})^2 - (\partial_l\widehat{h}_{ij})\Big]. \tag{1.77}$$

This action is same for that of a massless scalar field(apart from a normalization factor of $M_{\rm p}/2$ in FLRW spacetime. We now expand the perturbation into Fourier modes as

$$\widehat{h}_{ij} = \int \frac{\mathrm{d}^3k}{(2\pi)^3}\sum_{s=+,\times}\epsilon^s_{ij}(k)h^s_{\mathbf{k}}(\eta)e^{i\mathbf{k}\cdot\mathbf{x}}, \tag{1.78}$$

where, transverse and traceless conditions $\partial^i\widehat{h}_{ij}=0,$ and $\widehat{h}^i_i=0$, turn into $\epsilon^i_i = k^i\epsilon_{ij}=0$, with the polarization sum $\epsilon^s_{ij}(k)\epsilon^{s'}_{ij}(k) = 2\delta ss'$. Using all these ingredients the action for the tensor perturbation modes turns out to be

$$S^t_{(2)} = \sum_s\int \mathrm{d}\eta\mathrm{d}\mathbf{k}\frac{a^2M_{\rm p}^2}{4}\Big[h^{s\prime}_{\mathbf{k}}h^{s\prime}_{\mathbf{k}} - k^2h^s_{\mathbf{k}}h^s_{\mathbf{k}}\Big] \tag{1.79}$$

Defining canonically normalized variable $v^s_{\mathbf{k}} = (a/2)M_{\rm p}h^s_{\mathbf{k}}$, we gets

$$S^t_{(2)} = \sum_s\frac{1}{2}\int \mathrm{d}\eta\mathrm{d}^3k\left[(v^{s\prime}_{\mathbf{k}})^2 - \Big(k^2 - \frac{a''}{a}\Big)(v^s_{\mathbf{k}})^2\right] \tag{1.80}$$

Following same de Sitter limit, the dimensionless tensor power spectrum turns becomes,

$$\Delta^2_t = \frac{2}{\pi^2}\frac{H_k^2}{M_p^2} \tag{1.81}$$

Analogously the tensor spectral index is

$$n_t \equiv \frac{\mathrm{d}\ln\Delta^2_t}{\mathrm{d}\ln k} = -2\epsilon \simeq -2\epsilon_V \tag{1.82}$$

Tensor fluctuations when normalized with respect to that of the scalar fluctuations is known as scalar to tensor ratio $r$ which is the quantity that is often quoted in cosmological observation. Therefore, one can express $r$ as follows,

$$r \equiv \frac{\Delta^2_t(k)}{\Delta^2_{\mathcal{R}}(k)} = 16\epsilon \simeq 16\epsilon_V \tag{1.83}$$

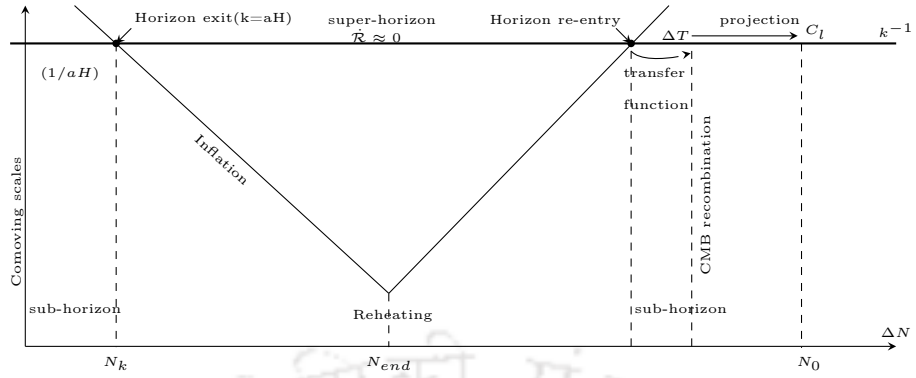


Figure 1.3: The curvature perturbations $\mathcal{R}$ generated during inflation do not evolve once they exit the horizon. The comoving horizon $(aH)^{-1}$ shrinks during inflation and grows in subsequent standard FLRW evolution. Hence the largest comoving scales $k^{-1}$ that exit during inflation re-enter the horizon only recently. As $\dot{\mathcal{R}} = 0$ on super-horizon scales, the correlation function $\langle|\mathcal{R}_k|^2\rangle$ at horizon exit is related to CMB observables at late times.

### 1.3.5 Observations and constraints

So far we have talked about the theoretical framework in which we can understand the dynamics of various matter fields and their fluctuations along with gravity. However, as emphasized already, goal is to understand the cosmological observations which can be fit with the predictions of the theory described above. In this section we will mainly emphasize on how can we connect the inflationary paradigm with the observed fluctuations in the CMB through some very specific observables. The properties of those fluctuations are determined by their evolution through the hot, dense plasma of tightly coupled baryons-photons fluid. However, as we have seen that those fluctuations were actually produced during the era of primordial inflation and most importantly various modes of those fluctuations exit the Hubble horizon when $k = aH$. On the other hand after the end of inflation the co-moving Hubble radius $1/aH$ increases with time, which suggests that the out going fluctuating modes during inflation will re-enter the horizon at the present time. This is clearly depicted in Fig. 1.3. Therefore, after re-entering the horizon those curvature perturbation modes will evolve into density perturbations on the matter components at all scales, which finally will be imprinted upon the CMB. These perturbations oscillate due to combined effects of gravity and thermodynamic pressure once they re-enter the horizon. This coherent oscillations are encoded in the CMB as various peaks in the temperature correlation functions. The presence of those peaks and troughs at different scales due to the difference in their horizon-exit/re-enter presents a remarkable evidence for the inflationary paradigm.

The temperature power spectrum that can be computed from the CMB fluctuations has been proved to be directly related to the primordial inflationary curvature power spectrum described before. The connection between these two power spectrum can be connected through appropriate transfer function which is related to the background evolution. The primordial power spectrum for the scalar curvature, $\Delta_{\mathcal{R}}$, and the tensor modes, $\Delta_t$, are parametrized by two important cosmological parameters related to the amplitudes of the their respective

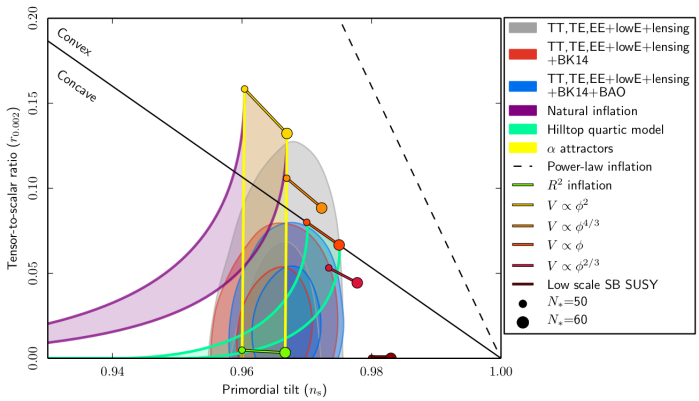


FIGURE 1.4: Marginalized joint 68 % and 95 % CL regions for $n_s$ and $r$ at $k = 0.002 Mpc^1$ from Planck alone and in combination with BK14 or BK14 plus BAO data, compared to the theoretical predictions of selected inflationary models. Figure is taken from Ref.[19]

fluctuations and spectral index as

$$\Delta^2_{\mathcal{R}} \equiv A_{\mathcal{R}} \left(\frac{k}{k_*}\right)^{n_s - 1}, \quad \Delta^2_t \equiv A_t \left(\frac{k}{k_*}\right)^{n_t}; \tag{1.84}$$

Where $k_*$ is reference scale of PLANCK which is called the *pivot* scale. Now from the CMB temperature fluctuation data, the amplitude of the curvature fluctuation is measured at the pivot scale of $k = 0.05$ Mpc$^{-1}$ form Planck 2018[19] as

$$A_{\mathcal{R}} = (2.196 \pm 0.060) \times 10^{-9}. \tag{1.85}$$

The value of the primordial spectral tilt and running are given as

$$n_s = 0.9649 \pm 0.0042 \quad \text{at} \quad ; \quad dn^k_s = 0.0045 \pm 0.0067 \qquad 68\% \text{ CL}. \tag{1.86}$$

While from CMB anisotropy tensor spectrum is bounded from above, which is given through the tensor to scalar ration as,

$$\frac{\Delta^2_t}{\Delta^2_{\mathcal{R}}} = r_{0.002} =< 0.10 \qquad 95\% \text{ CL}.$$

for $k_* = 0.002$ Mpc$^{-1}$. However, if one considers various other experimental observation such as from BICEP2/Keck Array BK14 date, value of $r$ is further tightened to

$$r_{0.002} < 0.064$$

In the Fig. 1.4 the latest constraints in the ($n_s$ *vs* $r$) plane is given along with some well known inflationary models from PLANCK paper. Details of the plots can be found in [19]. After discussing the phase of inflation and its observational signatures, let us introduce some special class of inflationary models and their viability in the context of PLANCK.

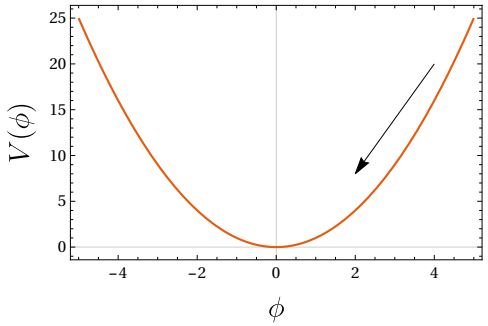


Figure 1.5: An Illustration of large field inflation potential.

## 1.4 Inflationary Models

So far we have seen the conditions for the successful inflation considering the generic scalar field model, and the associated observables. What we learned essentially is the form of the inflaton potential which plays the most important role. In this section we briefly summarize some well known form of the inflationary potentials which will appear in our thesis discussion in various forms. However, an encyclopedic list of inflationary scenario can be found in [20]. We will list here three large classes of models which include many prominent inflationary models in the literature. We categorize those models into three main classes, (a) Large field inflation, (b) Small field inflation (c) Hybrid inflation.

### 1.4.1 Large field models

For these type of models, as illustrated in Fig. 1.5, the inflation occurs for large field values, typically super-Planckian. The simplest power-law potentials [21] are the examples of large field inflation model.

Taking

$$V(\phi) = \frac{1}{n}\lambda\, m^{4-n}\phi^n$$

with $\lambda = 1$ when $n \neq 4$. The slow-roll conditions can be found to be

$$\epsilon_V = \frac{n^2}{2}\left(\frac{M_{\rm p}}{\phi}\right)^2, \quad \eta_V = n(n-1)\left(\frac{M_{\rm p}}{\phi}\right)^2, \quad \xi_V = 0. \tag{1.87}$$

The efolding number is

$$\Delta N \simeq \frac{1}{2n}\left(\frac{\phi_k}{M_{\rm p}}\right)^2 \tag{1.88}$$

As the name suggests, the typical inflationary initial condition are distributed randomly because of inherent quantum nature of the inflaton. Considering the observed scale of homogeneity, it can found that corresponding inflationary e-folding number $N$ will be be within $50 \sim 60$. For which one needs the super-Planckian initial field value $\phi_k > M_{\rm p}$. This is one of the reasons the

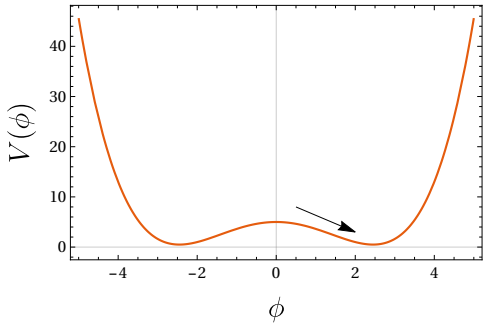


FIGURE 1.6: An Illustration of small field inflation potential.

chaotic model is said to be in the class of large field inflation. None the less the expression for the power spectrum reads,

$$\mathcal{P}_{\mathcal{R}}(k) = \lambda n^{\frac{n-4}{2}} \frac{2^{\frac{n-2}{2}}}{3\pi^2} \left(\frac{m}{M_{\rm p}}\right)^{4-n} N^{\frac{n+2}{2}}. \tag{1.89}$$

Therefore, for $N = 55$, and considering the value of $A_{\mathcal{R}}$ given in Eq. (1.85) the value of the model parameter $m = 1.6 \times 10^{13}$GeV for $n = 2$ and $\lambda = 8 \times 10^{-13}$ for $n = 4$. Once we have fixed the value of the model parameter, the spectral index and the scalar-to-tensor ratio can be predicted as

$$n_s = 1 - \left(\frac{n+2}{2}\right)\frac{1}{N}, \qquad r = \frac{4n}{N}, \tag{1.90}$$

which implies,

$$n_s = 0.964, \quad r = 0.15 \quad \text{for} \quad n = 2 \tag{1.91}$$

$$n_s = 0.945, \quad r = 0.30 \quad \text{for} \quad n = 4 \tag{1.92}$$

From the value of $r$, therefore, we can conclude that simple chaotic model is strongly disfavored by PLANCK.

### 1.4.2 Small field models

In these class of models, inflation occurs near the origin of the field space rendering $\phi \ll M_{\rm p}$. This is the reason we call it small field inflation. A particularly simple model potential is given as

$$V(\phi) = \frac{\lambda}{4}(\phi^2 - v^2)^2 \tag{1.93}$$

These type of potential, illustrated in Fig. 1.6 may arise in the model of spontaneous symmetry breaking phenomena such as in Higgs mechanism. It is obvious that at the origin inflaton is unstable. Therefore, inflation is just evolution of the field near the maximum towards the global minimum. The slow-roll parameters in this case read as

$$\epsilon_V = \frac{8M_{\rm p}^2\phi^2}{(\phi^2 - v^2)^2}, \quad \eta_V = \frac{4M_{\rm p}^2(3\phi^2 - v^2)}{(\phi^2 - v^2)^2}, \tag{1.94}$$

The parameter $\epsilon(\phi)$ is small for both $\phi \gg v$ as well as $\phi \to 0$. The latter limit corresponds to small field inflation. We find the field value at the end of inflation from the condition $\epsilon_V(\phi_e) = 1$ as

$$\phi_e^2 = v^2 + 4M_{\rm p}^2 - \sqrt{(v^2+2)8M_{\rm p}^2} \approx (x^2 - 2\sqrt{2}x)M_{\rm p}^2, \tag{1.95}$$

where we have set $x \equiv M_{\rm p}/v$ and the last approximate is valid when $x \gtrsim 1$. The number of e-folding $N$ from the beginning of inflation at $\phi_k$ to the end of inflation $\phi_e$ is expressed as

$$N = \int_{\phi_k}^{\phi_e} \frac{H}{\dot\phi} {\rm d}\phi = \frac{x^2}{4} \ln\frac{\phi_e}{\phi_k} - \frac{1}{8M_{\rm p}^2}(\phi_e^2 - \phi_k^2) \simeq \frac{x^2}{4}\Big(\ln\frac{\phi_e}{\phi_k} - \frac{1}{2}\Big). \tag{1.96}$$

The amplitude of curvature perturbation takes the following from,

$$\mathcal{P}_{\mathcal{R}} = \frac{\lambda(\phi_k^2 - v^2)^4}{768\pi^2 M_{\rm p}^2 \phi_k^2} \simeq \frac{\lambda x^8}{768\pi^2}\Big(\frac{M_{\rm p}}{\phi_k}\Big)^2 \simeq \frac{\lambda x^8}{768\pi^2(x-\sqrt{2})^2}\exp\Big(\frac{8N}{x^2} + 1\Big), \tag{1.97}$$

where the second and third approximation is made for small field $\phi_k \ll v$ and $\phi_e \sim (x - \sqrt{2})M_{\rm p}$ respectively. The spectral index and the scalar-to-tensor ratio become

$$n_s = 1 - \frac{8(3\phi_k^2 + v^2)M_{\rm p}^2}{(\phi_k^2 - v62)} \simeq 1 - \frac{8}{x^2}$$
$$r = \frac{144 M_{\rm p}^2 \phi_k^2}{(\phi_k^2 - v^2)^2} \simeq \frac{8}{x^2}\Big(\frac{\phi_k}{M_{\rm p}}\Big)^2$$

setting the pivot scale at $N = 55$ and taking $x = 15$, we find $n_s = 0.964$, $r \sim 0.04$ and amplitude of power spectrum set the value of self-coupling $\lambda \simeq 7 \times 10^{-14}$. The small field models predicting small values of scalar-to-tensor ratio are thus favored by data.

### 1.4.3 Hybrid Inflation Models

Our previous two models were single field inflation models. For the case of hybrid inflation [22–25] there are more than one scalar fields. The inflation in hybrid models starts at large values of the inflaton field and moves towards the minimum until it reaches a bifurcation point, where it becomes unstable and the inflation ends as depicted in Fig. 1.7.

A particular form of hybrid potential is given by[22]

$$V(\phi, \chi) = \frac{\lambda}{4}\left(\chi^2 - \frac{M^2}{\lambda}\right)^2 + \frac{1}{2}g^2\phi^2\chi^2 + \frac{1}{2}m^2\phi^2. \tag{1.98}$$

The effective mass of the waterfall field $\chi$ can be expressed as

$$m_\chi^2 = -M^2 + g^2\phi^2, \tag{1.99}$$

For large values of the inflaton field $\phi > \phi_c \equiv M/g$, the field $\chi$ is stabilized around its minimum $\chi = 0$, as is clear from the figure. This phase of evolution can be effectively described by single field $\phi$ with mass $m$, which is identified as inflaton. However, when the value of the inflaton reaches $\phi = \phi_c$, the $\phi$ field develops tachyonic instability which is responsible for ending the

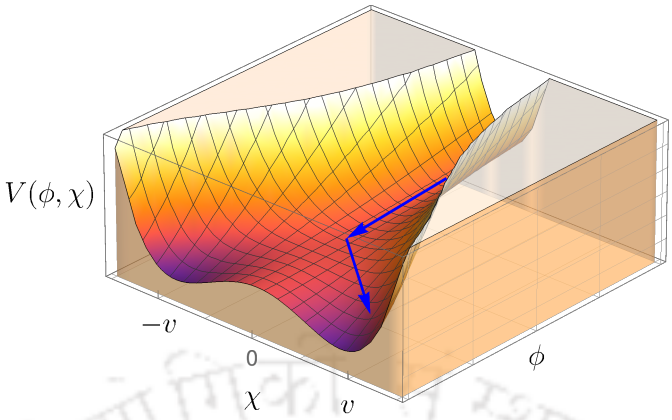


FIGURE 1.7: Hybrid inflation model

inflation. As in this case inflation is driven by vacuum energy, to make analytic estimates can done based on inflation potential as

$$V(\phi) = V_0 + \frac{1}{2}m^2\phi^2, \tag{1.100}$$

where, $V_0 = M^4/(4\lambda)$. The slow-roll parameters in this case is given by

$$\epsilon_V = \frac{1}{18}\Big(\frac{m}{H}\Big)^4\Big(\frac{\phi}{M_{\rm p}}\Big)^2, \quad \eta_V = \frac{m^3}{3h^2}. \tag{1.101}$$

In this case the energy scale of inflation can not be set from the amplitude of power spectrum alone. The spectral index and scalar-to-tensor ratio is given as

$$n_s - 1 \simeq 2\eta_V = \frac{2m^2}{3H^2} > 1; \quad r = (n_s-1)^2\Big(\frac{\phi}{M_{\rm p}}\Big)^2. \tag{1.102}$$

This prediction of spectral index is inconsistent with the current data. However, if the second term in Eq. (1.100) dominates over the vacuum energy, the prediction becomes closer to that of a large-field models.

With all these necessary ingredients for inflation and their predictions, let us illustrate through the Fig. 1.8, another important aspect of this paradigm. This will be our main focus in the subsequent sections. It is clear from the figure that the inflation itself is not the end of the story. Even though we successfully inflate the universe to create large number of causally disconnected regions which were other wise causally connected before the inflation, the question remains: *How can one connect the inflationary phase with the standard big-bang phase?*. This is where the story starts to become even more non-trivial. The inflation inflates the space and it becomes completely empty except the homogeneous distribution of inflaton energy. The natural mechanism would be to end the inflation and transfer the inflaton energy to the matter energy we see today. Therefore, in order to set the perfect initial condition for the standard big-bang, on needs to first end the inflation which has already been defined before at $\phi_{end}$ with $\epsilon_V(\phi_{end}) = 1$. After this the only successful scenario which is known to connect between the two phases are called reheating depicted in the Fig. 1.8. A significant part of our thesis is devoted to understand this particular reheating phase and its observable effects for some

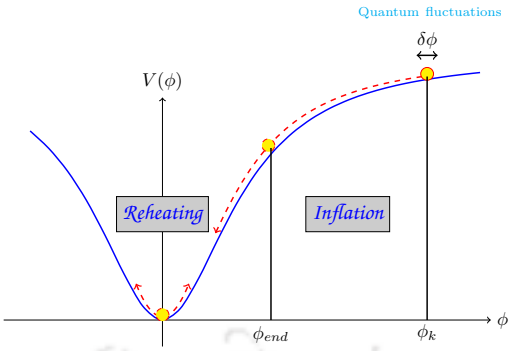


FIGURE 1.8: Illustration of a slow-roll inflation and reheating

special classes of inflationary models. The usual picture is that after the end of inflation, the inflaton oscillates around the minimum of the potential as shown in the figure. Depending upon the couplings to other fields, inflaton decays into daughter fields, thereby, setting the stage for a radiation dominated universe, which is the beginning of the big-bang. In next section, we will discuss the reheating at some lengths.

## 1.5 Reheating after inflation: perturbative

As we already described, essential idea will be to understand the mechanism through which the inflaton field transfers its energy into our visible matter field. The real problem of this energy transfer is non-trivial. Therefore, simple model of reheating needs to be constructed to understand this. The original idea of particle production after inflation was studied with the following phenomenological equation of motion for the inflaton $\phi$[26–29]

$$\ddot{\phi} + 3H\dot{\phi} + V'(\phi) = -\Gamma_\phi \dot{\phi} \tag{1.103}$$

where the phenomenological decay term accounts for the decay of inflaton field into daughter fields. After the complete decay of inlaton, the daughter field will thermalize and the reheating will be completed. The coupling with the daughter fields will be such that they should not spoil the flatness condition during inflation namely $\Gamma_\phi \ll H$. After the end of inflation, however, this term comes into play as an effective dissipative term for inflaton. In terms of inflaton energy density density $\rho_\phi$, the Eq. (1.103) will be transformed into one of the Boltzmann equations as

$$\dot{\rho}_\phi + 3H(\rho_\phi + P_\phi) = -\Gamma_\phi(\rho_\phi + P_\phi). \tag{1.104}$$

Using the definition of equation of state defined in Eq. (1.26), we may write the above equation as

$$\dot{\rho}_\phi + 3H(1 + w_\phi)\rho_\phi = -\Gamma_\phi(1 + w_\phi)\rho_\phi \tag{1.105}$$

In our discussion, we will consider the simplest situation where the daughter fields behaves like radiation. Hence the second Boltzmann equation will be,

$$\dot{\rho}_{\rm R} + 4H\rho_{\rm R} = \Gamma_\phi(1 + w_\phi)\rho_\phi. \tag{1.106}$$

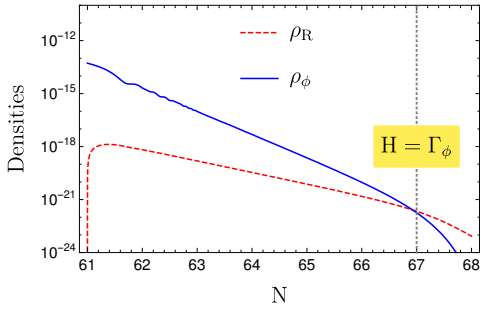


FIGURE 1.9: The evolution of inflaton energy density and radiation energy density.

$\rho_R$ is the radiation energy density. Finally, the Hubble expansion is given by $H^2 = (\rho_\phi + \rho_{\rm R})/3M_{\rm p}^2$. Assuming the radiation component to be thermal, we can always assign the associated temperature $T$ through the following standard relation,

$$\rho_{\rm R} = \left(\frac{\pi^2}{30}\right) g_* T^4. \tag{1.107}$$

Where $g_*$ represents the effective number of relativistic degrees of freedom at the end of reheating. Now for qualitative understanding, assuming $\Gamma_\phi$ is constant, and the inflation equation of state $w_\phi = 0$, the time evolution of equation for inflaton energy density reduces to

$$\rho_\phi(t) = \rho_e \left(\frac{a}{a_e}\right)^{-3} e^{\Gamma_\phi (t - t_e)}, \tag{1.108}$$

where $\rho_e (= V(\phi_e))$ is the inflaton energy density at the end of inflation which is also the onset of reheating phase. During this matter dominated phase the scale factor grows as $a(t) \propto t^{2/3}$ and $H(t) = 2/3t$. Using these relations, the evolution of the radiation component has been found to be

$$\rho_{\rm R}(t) \simeq \frac{3}{5}\rho_e \left(\frac{t}{\tau_\phi}\right)\left[1 - \left(\frac{t_e}{t}\right)^{\frac{5}{3}}\right], \tag{1.109}$$

where $\tau_\phi \equiv \Gamma_\phi^{-1}$ is the inflaton decay time. We have taken $\rho_{\rm R} = 0$ as the initial condition for radiation. The evolution of the inflaton and the radiation energy density are shown schematically in the Fig. 1.9. Starting from zero, the radiation component quickly gets to a maximum value and then decreases due to the expansion of the universe. The definition of the temperature given in Eq. (1.107), then implies the existence of the maximum possible temperature during reheating epoch as

$$T_{\rm MAX} \sim g_*^{-\frac{1}{4}} V(\phi_e)^{\frac{1}{8}} (M_{\rm p}\Gamma_\phi)^{\frac{1}{4}} \tag{1.110}$$

It is also evident from the figure that the inflaton decay will be complete at the instant $t = 1/\Gamma_\phi$, when $H \sim \Gamma_\phi, a = a_{re}$. Hence, one can define an important parameters called reheating temperature $T_{re}$ at this instant as

$$H = \Gamma_\phi \simeq \rho_{\rm R}^{\frac{1}{2}} \simeq \left(\frac{\pi}{90^{\frac{1}{2}}}\right)\frac{T_{\rm re^2}}{M_{\rm p}}, \tag{1.111}$$

from the well known expression for the *reheating* temperature is

$$T_{\rm re} = \left(\frac{90}{g_*\pi^2}\right)^{\frac{1}{4}} \sqrt{\Gamma_\phi M_{\rm p}}. \tag{1.112}$$

Similarly another important reheating parameter called reheating e-folding number $N_{re}$, which measures the duration of reheating, is expressed as

$$N_{re} = \log\left(\frac{a_{re}}{a_e}\right) \tag{1.113}$$

This is the temperature and the reheating e-folding number with which the radiation dominated phase of the hot big-bang starts to evolve. We can put a bound on the possible values of $T_{re}$ as

$$10\text{TeV} \lesssim T_{\rm re} \lesssim V(\phi_e)^{\frac{1}{4}}, \tag{1.114}$$

where, lower bound is coming from the constraint on BBN. Till now we do not have any direct cosmological observables which can directly constrain this phase. Therefore, we have to rely on the indirect measurements. Understanding this phase by indirect means such as CMB, dark matter is one of main goals of the thesis.

All we have discussed so far will be incomplete if we do not talk about the interpretation of the inflaton decay constant $\Gamma_\phi$. In order to qualitatively understand the origin of this term we can take help of perturbative quantum field theory. Assuming the following interaction term of inflaton with another scalar $\chi$ and a fermion field $\psi$

$$\mathcal{L}_{int} \supset -\sigma\phi\chi^2 - h\phi\bar{\psi}\psi, \tag{1.115}$$

one can obtain the leading order decay constant to be [30]

$$\Gamma_{\phi\to\chi\chi} = \frac{\sigma^2}{8\pi m_\phi}; \qquad \Gamma_{\phi\to\bar{\psi}\psi} = \frac{h^2 m_\phi}{8\pi}. \tag{1.116}$$

Therefore, effectively we can identify those decay constant and consider in the Boltzmann equation described above depending upon the type of reheating fields. However, this identification can not be derived from the first principle. Let us not discuss about this any further. Instead let us point out that this elementary treatment of perturbative reheating has several shortcomings. At the end of inflation, most of the inflaton energy is stored in $k = 0$ mode. Hence the oscillating homogeneous inflaton can be thought of as a condensation of large number of zero momentum inflaton particles. This makes the perturbative treatment of decaying inflaton rather inappropriate. Therefore, one surely needs to take into account the non-perturbative effects. This turned out to be true for a wide range of coupling parameters among the inflaton and the daughter particles. Parametric resonance is an important phenomena in this regime. However, the perturbative treatment will be responsible for the completion of reheating phase after the non-perturbative effects ceases to exist. The elementary reheating treatment will be useful when connecting the reheating phase with the CMB anisotropy described in Chapter 3.

### 1.5.1 Non-Perturbative Reheating or Pre-heating

In their seminal work, Kofman, Linde and Starobinsky[31, 32](see also[33]), first introduced and worked out the idea of non-perturbative production of particles after inflation based on

the idea of parametric resonance in classical mechanics[34]. Though the full non-linear theory of preheating is still not well understood but a significant advancement in this field has been made and it is one of the most active field of research in inflationary cosmology[35–37]. Let us introduce the basic idea of parametric resonance considering simplest chaotic inflation model with inflaton coupled to another scalar field.

#### 1.5.1.1 Parametric resonance after inflation

In order to understand the basic mechanism, we consider the interaction term between the inflaton ($\phi$) and another scalar field $\chi$. * The interacting Lagrangian for $\chi$ filed is

$$\mathcal{L}_\chi = \frac{1}{2}\partial_\mu\chi\partial^\mu\chi - \frac{1}{2}m_\chi^2\chi^2 - \frac{1}{2}g^2\phi^2\chi^2. \tag{1.117}$$

Where, $m_\chi$ is the mass of the $\chi$ particle. The matter field $\chi$ satisfies the following equation,

$$\ddot{\chi} + 3H\dot{\chi} - \frac{1}{a^2}\nabla^2\chi + (m_\chi^2 + g^2\phi^2)\theta = 0. \tag{1.118}$$

Decomposing the scalar field into its Fourier components,

$$\chi(t,x) = \int \frac{d^3k}{(2\pi)^{2/3}}[a_k\ \chi_k(t)e^{ik\cdot x} + h.c.], \tag{1.119}$$

the mode equation for $\chi_k(t)$ then takes the following from

$$\ddot{\chi}_k + 3H\dot{\chi}_k + \left(\frac{k^2}{a^2} + m_\chi^2 + g^2\phi^2\right)\chi_k = 0. \tag{1.120}$$

with this mode function one can define the particle number density with momentum $k$ as [32]

$$n_k = \frac{\omega_k}{2}\left(\frac{|\dot{\chi}_k|^2}{\omega_k^2} + |\chi_k|^2\right) - \frac{1}{2} \tag{1.121}$$

Where, $\omega_k^2 = k^2 + a^2m_\chi^2$. The analytic theory of parametric resonance has been studied extensively in the literature for simple potentials viz the power-law chaotic potentials[31, 38]. Before we go into detail, let us first analyze the parametric resonance phenomena with the help of stability-instability diagram from the well known method of Floquet analysis[39, 40].

#### 1.5.1.2 Preheating: Analytic Treatment

To study the parametric resonance phenomena we define $X_k(t) \equiv a^{3/2}(t)\chi_k(t)$ to re-scale Eq. (4.5) as

$$\ddot{X}_k + \omega_k^2 X_k = 0, \tag{1.122}$$

where, time dependent frequency parameter is,

$$\omega_k^2 \equiv \frac{k^2}{a^2} + g^2\phi^2(t) + \Delta, \qquad \Delta \equiv -\frac{3}{4}(3H^2 + 2H). \tag{1.123}$$

*for preheating with fermions see,P. B. Greene and L. Kofman Phys. Lett B 448, 6 1999. [arXiv:hep-ph/9807339], P. B. Greene and L. Kofman Phys. Rev. D 62, 123516 2000. [arXiv:hep-ph/0003018]. we will here only consider the bosonic case

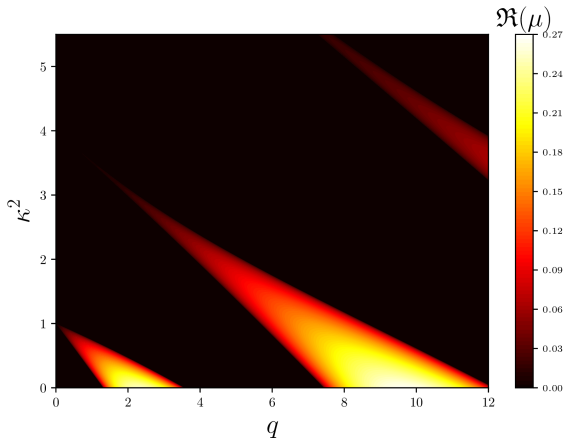


FIGURE 1.10: instability bands of Mathieu/Hill type equations. For parameters $(q, \kappa)$ value within a instability band, the equation will show exponential growth.

To understand the analytic behavior let us set $\Delta = 0$, which can also be justified by the fact that during reheating evolution of scalar factor is negligible within the few oscillation time. To study the resonance phenomenon in the context of Floquet theory[39, 40], therefore, we further switch off the expansion. Then Eq.(4.14) can be identified as Hill's differential equation,

$$\ddot{X}_k + \left(\kappa + q\varphi^2(t)\right) X_k = 0, \tag{1.124}$$

with $a = 1$. The new parameters are given as $\kappa = k^2/a^2$ and $q = (g^2\Phi^2)$ which are assumed to be time-independent. While the homogeneous oscillatory background solution has been written as $\phi(t) = \Phi\varphi(t)$. In reality, the amplitude is also decaying with time i.e., $\Phi \equiv \Phi(t)$. We will introduce the time dependence quantitatively later. The solution of Eq. (4.15) is of the form $X_k \propto exp(\mu_k t)$. Depending upon the values of the parameters $(\kappa, q)$, this solution will be exponentially growing when $\Re(\mu_{\kappa,q}) > 0$, which is identified as the particle production. This is the reason we call it parametric resonance. The contours of $\Re(\mu_{\kappa,q}) = 0$ in the $(\kappa, q)$ space, known as the instability bands, Fig. 1.10, helps us understanding the parameter regions as well as the resonance structure during preheating.

#### 1.5.1.3 Narrow Resonance

From the stability/instability chart given in the Fig. 1.10, it can be seen that for small values of the resonance parameter $q \ll 1$, the resonance occurs for a very narrow range of $k$ which renders its name the narrow resonance. The phenomenon of narrow resonance can qualitatively understood in terms of Bose enhancement mechanism [41], which is essentially a quantum statistical mechanical effect. Considering the interaction $\mathcal{L}_{int} \supset (1/2)g^2\phi^2\chi^2$ mentioned above, the $\phi$ field can decay into two $\chi$ field in the oscillating inflaton background with an effective coupling parameter $g^2\phi(t)$. It is well known that the Bose condensate effect will enhance the $\chi$ production if the states in the phase space of $\chi$ are already occupied. Therefore, the effective decay rate of the $\phi$ particle $\Gamma_\phi$ can be expressed in terms of $\chi$-decay constant $\Gamma_\chi$ as

$$\Gamma_\phi \simeq \Gamma_\chi(1 + 2\mathrm{n}_k). \tag{1.125}$$

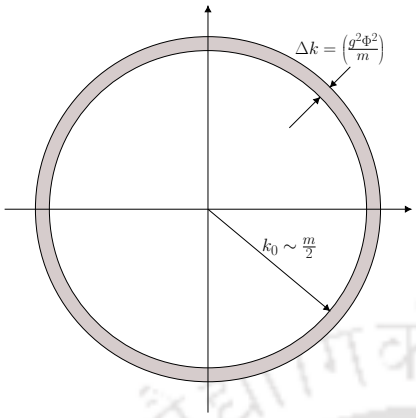


FIGURE 1.11: Momentum range for narrow-resonance

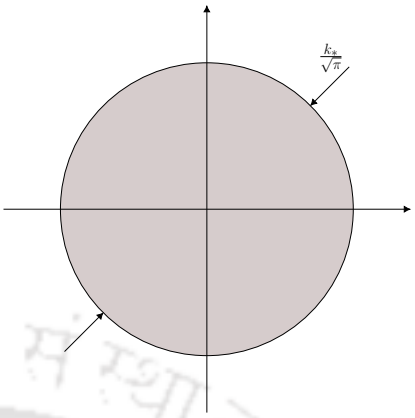


FIGURE 1.12: Momentum bound for broad-resonance

Where we can clearly see the presence of $\chi$-particle number density. Now our task is to find $\mathrm{n}_k$ for the given number density $n_\chi$.[†] The $\phi$-particle at its rest frame decays into two $\chi$ particles of energy $m/2$. The effective squared mass of $\chi$ particle depends on the value of the inflaton field and is given by $m_\chi^2 + g^2\phi^2$. Assuming $m_\chi^2 + g^2\phi^2 \ll m^2$, the corresponding 3-momentum of the produced $\chi$ particle is

$$k = \left[\left(\frac{m}{2}\right)^2 - m_\chi^2 - 2g^2\phi^2\right]^{\frac{1}{2}} \tag{1.126}$$

Assuming $m_\chi$ being negligible, all the created particles will be withing a thin momentum shell of width

$$\Delta k \simeq m\left(\frac{2g^2\Phi^2}{m^2}\right) \ll m, \tag{1.127}$$

centred around $k_0 \simeq \frac{1}{2}m$ as illustrated in Fig. 1.11. Hence,

$$\mathrm{n}_{k=m/2} \simeq \frac{n_\chi}{(4\pi k_0^2\Delta k)/(2\pi)^3} \simeq \frac{\pi^2 n_\chi}{mg^2\Phi^2} = \frac{\pi^2}{g^2}\frac{n_\chi}{n_\phi}. \tag{1.128}$$

Thus the Bose condensation effect will be essential when $\mathrm{n}_k \gg 1$ or,

$$n_\chi > \frac{g^2}{\pi^2} n_\phi \tag{1.129}$$

Around the end of inflation, taking $\Phi \sim M_\mathrm{p}$, the occupation number therefore exceeds unity as soon as the inflaton converts a fraction $g^2$ of its energy into $\chi$. The above derivation is valid in the limit when $g^2\Phi^2 \ll m^2/8$. For instance, in chaotic inflation we have $m \sim 10^{-6}M_\mathrm{p}$ and $\Phi \sim 1$ at the end of inflation, then the maximum fraction of inflaton energy that can be transferred to the decay product is $g^2 \sim m^2 \sim 10^{-12}$ in the regime where $\mathrm{n}_k < 1$. It is evident that the perturbative treatment of reheating which is applicable when $\mathrm{n}_k \ll 1$, fails very soon after reheating sets off. The effective decay width given in Eq. (1.125) will be given by

$$\Gamma_\phi \simeq \frac{g^2\Phi}{8\pi m}\left(1 + \frac{\pi^2}{g^2}\frac{n_\chi}{n_\phi}\right). \tag{1.130}$$

[†]We have used n to denote occupation number and $n$ for number density.

Considering this effective decay constant we can solve for the Boltzmann equation for $\chi$-particle density.

$$\frac{1}{a^3}\frac{\mathrm{d}(a^3 n_\chi)}{\mathrm{d}dN} = \frac{g^4\Phi^2}{2m^2}\left(1+\frac{\pi^2}{g^2}\frac{n_\chi}{n_\phi}\right)n_\phi, \tag{1.131}$$

where $N \equiv mt/2\pi$ accounts for the number of inflaton oscillations. Neglecting the expansion of the universe as well as decrease of infaton amplitude die to particle production for simplicity, in the regime $n_\chi \gg 1$, the above differential equation approximately yields

$$n_\chi \propto exp\left(\frac{\pi g^2\Phi^2}{4m^2}N\right) \propto exp(2\pi\mu N), \tag{1.132}$$

where, $\mu \equiv \pi\Phi^2/(2m)^2$ is the instability parameter defined before. The narrow resonance will be commencing when $g\Phi \ll m$ while the width of the first resonance band can be estimated to find as $\Delta l \sim m(g^2\Phi^2/m^2)$.

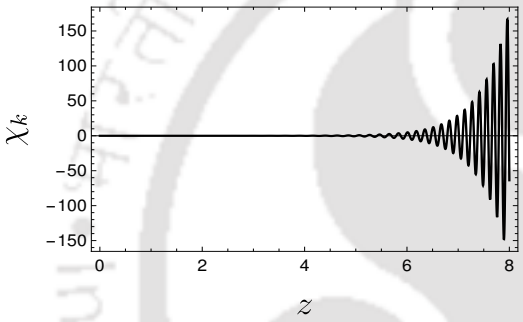


Figure 1.13: $\chi_k$

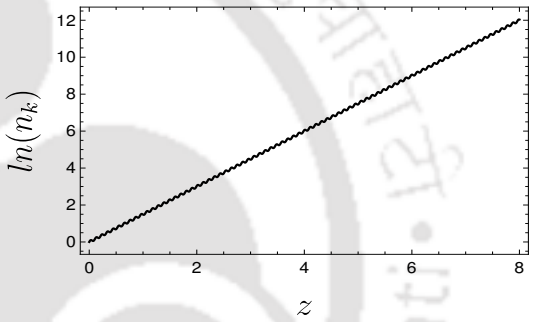


Figure 1.14: $ln(n_k)$

It is thus evident that for smaller coupling constant the perturbative treatment is needed to be supplemented with the Bose effect to describe the reheating phenomenon. So far we have not included the effects of expansion of the universe, the back-reaction of the created particles and their re-scatterings. The expansion will shift the momenta of the produced particles out of the layer of resonance( shown as the shaded region in Fig. 1.11. This result in smaller occupation number that might be needed for Bose condensation. If the rate of supply of newly produced particles in the resonance layer is fewer that their rate of escape, we get $n_k < 1$ and in that case the perturbative treatment can be used. Another important effect which goes against the efficiency of narrow resonance is the decrease of the inflaton amplitude with time. As the width of resonance layer is proportional to $\Phi^2$(or, $\Phi$ in case of three-legs interaction), the width will get narrower with time. Thus the particle will eventually escape the resonance regime more easily and will fail to get resonate. The effect of re-scattering also decrease the resonance by eliminating the particles from the resonance layer. Hence all these effects will work in suppressing the efficiency of the narrow resonance. The narrow resonance is thus very sensitive to a number of different complicated phenomena which presently can only be tracked with full numerical simulation. The analytic treatment above indicates that the in real situation the inflaton decay with some intermediate pace between the perturbative reheating and the narrow resonance.

In Fig. 1.13 and Fig. 1.14 we have shown the result of a numerical simulation for the narrow resonance regime. The first figure shows the growth of the mode $\chi_k$ while the second figure

shows the growth of the occupation number of the mode. It can be seen that the number of particles grows exponentially, and the logarithmic growth of $n_k$ is almost a straight line with constant slope. The value of the resonance parameter $\mu$ described in Eq. (1.132) can be found by dividing the slope of $ln(n_k)$ by $4\pi$. In the next segment of resonance phenomenon, we will consider the effect of having larger coupling constants.

#### 1.5.1.4 Broad Resonance

In this section we briefly discuss about broad parametric resonance. From the stability diagram it is evident that for $q \gg 1$, the resonance will occur for very broad momentum range. The perturbative method is not applicable for this case as particles will be produced from the homogeneous condensate. One particularly notices the time dependent effective mass for $\chi$ Eq. (4.15). For solving such type of equation with time dependent parameters WKB method is very useful provided, $\omega_k \equiv (k^2/a^2 + g^2\phi^2(t))^{1/2}$ varies slowly with time compared to a mode under consideration, which is known as *adiabatic* regime. Using the quasi-classical (WKB) approximation, the solution is written as,

$$\chi_k \propto \frac{1}{\sqrt{\omega_k}} exp\left(\pm i \int \omega_k dt\right). \tag{1.133}$$

If there is no violation of adiabaticity, the number of particles, $n_\chi \sim \epsilon_\chi/\omega$ remains adiabatically invariant. However, if the effective mass changes rapidly the WKB method breaks down and we are in the *non-adiabatic* regime. Hence, particle number will no longer be conserved. The measure of adiabaticity is naturally defined by

$$R_a \equiv \frac{\dot{\omega}_k}{\omega_k^2} \tag{1.134}$$

The solution in the regime $|R_a| \gg 1$ grows exponentially which is interpreted as particle production. For interaction given in Eq. (1.115), and for long wave-lenghts $k/aH \ll 1$, the ratio $R_a$ reduces to

$$R_a = \frac{\dot{\phi}}{g\phi^2} \sim \frac{m}{g\phi}, \tag{1.135}$$

It is evident from the above relation that the ratio $R_a$ diverges as $\phi \to 0$. Therefore, whenever the background oscillating field (inflaton) crosses zero, the adiabatic condition breaks down, and explosive particle production will occur. For a finite value of $k$, the adiabatic condition is violated if

$$R_a = \frac{g^2\phi\dot{\phi}}{(k^2 + g^2\phi^2)^{\frac{3}{2}}} \sim \frac{g^2 m\phi^2}{(k^2 + g^2\phi^2)^{\frac{3}{2}}} > 1. \tag{1.136}$$

In the above equation we use $\dot{\phi} \simeq m\phi$ where, $m$ is related to the inflaton mass with which it is oscillating. From the above relation we have,

$$k^2 \lesssim (g^2 m\phi^2)^{\frac{2}{3}} - g^2\phi^2 \equiv f(\phi). \tag{1.137}$$

Considering a small time interval $\Delta t \ll m^{-1}$ in the vicinity of $t_0$ where $\phi(t_0) = 0$, we may rewrite Eq. (4.44)

$$\frac{\Delta t/\Delta t_*}{(k^2\Delta t_*^2 + (\Delta t/\Delta t_*)^2)^{\frac{3}{2}}} \geq 1, \tag{1.138}$$

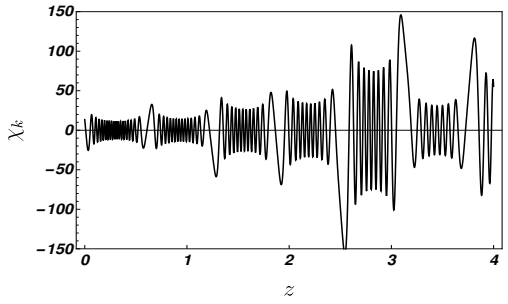


Figure 1.15: Growth of mode $\chi_k$ in the broad resonance.

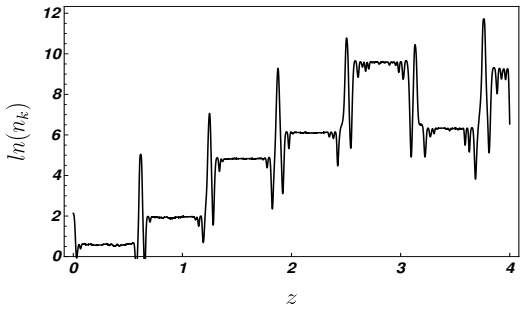


Figure 1.16: The stochastic change of $ln(n_k)$ in the broad resonance.

where,

$$\Delta t_* \simeq (g\phi m)^{-\frac{1}{2}} = \frac{1}{m}\left(\frac{g\phi}{m}\right)^{-\frac{1}{2}}. \tag{1.139}$$

Thus the adiabatic condition is violated only within a very short interval of $\Delta t \sim \Delta t_*$ around the zero crossing. Using the uncertainty principle we find the maximum value of the mode up-to which the resonance occurs as(see Fig. 1.12)

$$k < k_* \simeq \Delta t_*^{-1} \simeq m\left(\frac{g\phi}{m}\right)^{\frac{1}{2}}. \tag{1.140}$$

In case of expanding universe the above condition modifies to

$$\frac{k}{a(t)} < k_*(gm\phi(t))^{\frac{1}{2}} \tag{1.141}$$

We see that the expansion, contrary to the narrow resonance case, make the broad resonance *more* efficient, as more $k$-modes are red-shifted towards the instability bands with time.

In Fig. 1.15 we have shown the a typical result of numerical calculation for the chaotic inflation in an expanding universe. While Fig. 1.16 shows the growth of number for $\chi$ quanta. It is evident that $n_k$ increases with time, however may be occasionally decrease. This is a feature of *stochastic resonance* typical in an expanding universe.

#### 1.5.1.5 Backreaction and termination of preheating

Until now we have neglected the effects of back-reaction of the created particles on preheating dynamics. However the backreaction effect is very important in preheating which eventually terminates the preheating. The full effect of back-reaction presently can only be incorporated with numerical simulation. A full study of preheating is done with the help of numerical simulations[42–48]. Below we will estimate the back-reaction and time of termination of preheating. However a full analysis has to be done with the help of above mentioned numerical codes. In our thesis, we have done the detail analysis of this phenomena for a class of inflationary models.

Writing the quantum expectation value of $\chi$ as

$$\langle\chi^2\rangle = \frac{1}{2\pi^2 a^3}\int k^2 dk |X_k(t)|^2, \tag{1.142}$$

where, $X_k(t) = a^{3/2}\chi_k(t)$

The back-reaction effect on the inflaton mass can be estimated as

$$\Delta m^2 = g^2 \langle \chi^2 \rangle , \tag{1.143}$$

Now inserting the mode expansion of $X_k$, we obtain

$$\Delta m^2(t) \approx \frac{g n_\chi(t)}{\phi(t)}. \tag{1.144}$$

The above expression diverges when $\phi = 0$. However as the equation of motion is well behaved we can make an estimate of the back-reaction by replacing $\phi$ by its amplitude $\Phi$. Hence, the backreaction becomes important when

$$\begin{aligned} &\Delta m^2 > m^2 \\ \implies & n_\chi(t_{br}) > \frac{m^2 \Phi(t_{br})}{g}. \end{aligned} \tag{1.145}$$

This will be the time $t > t_{br}$ when broad resonance is destroyed and preheating is terminated and we enter in a regime of turbulence.

In our discussion of parametric resonance we have seen that the main idea behind such an explosive particle production was the violation of adabatic condition. One of necessary condition for such a change is the oscillatory inflation background. However in some inflationary models such a oscillatory solution is not possible for this we need to resort to alternative mechanism of particle production. One such mechanism is the so-called *instant preheating* when, with appropriate couplings, a single oscillation may be sufficient to extract most of the energy from inflaton. In the next section we will briefly describe the instant preheating mechanism.

#### 1.5.1.6 Instant preheating

Finally we will discuss a variation of preheating phenomenon proposed by Felder and Linde[49] devised especially for the inflationary models when the inflaton does not oscillate after the end of inflation. As we have seen that the basic idea of resonance phenomenon is the changing effective mass. Let consider an interaction Lagrangian of the form

$$\mathcal{L}_{int} \subset -\frac{1}{2} g \phi^2 \chi^2 + h \chi \bar{\psi} \psi \tag{1.146}$$

where the scalar $\chi$ is coupled to infaton and the field $\chi$ may decay into a pair of fermions $\psi$. As we have seen that for a large resonance parameter $q \gg 1$, the violation of adabatic condition occurs for short period around time when inflaton crosses zero. An explosive production of $\chi$ quanta will result in this time interval. Now due to the coupling of $\chi$ to a fermion, the produced particles will instantly decay via an single-body decay process with a decay rate

$$\Gamma_{\chi \to \bar{\psi}\psi} \simeq \frac{h^2 g |\phi|}{8\pi} \tag{1.147}$$

Thus first there will be a massive resonant production of $\chi$ particles due to violation of adiabatic condition, as in the broad resonance case, when $\phi \simeq 0$(during which $\Gamma_{\chi \to \bar{\psi}\psi} \sim 0$). After that the inflaton rolls up to its maximum value resulting in a maximum effective mass for $\chi$. This

heavy $\chi$ then will decay into pair of fermions. The produced fermion mass could be half of that of the effective $\chi$ mass. As an estimate, consider the chaotic inflation model where in the first couple of oscillations $|\phi| \sim 0.5 M_{\rm p}$ and hence it is possible to have fermions pair of mass upto $\sim g|\phi| \simeq g M_{\rm p}/2 \sim 10^{18} GeV$ for $g \sim 1$.

For the production of massive fermions in instant preheating we need the explosive production of $\chi$ and often *just one instant* of such production is sufficient. This mechanism thus suitable for inflationary models when the inflation do not oscillate after inflation as in the case of quintessential inflation[50, 51]. We have used the instant preheating after inflation driven by higher derivative kinetic terms in Chapter 5 when the usual oscillatory solution does not exist.

## 1.6 Motivation of the thesis

Throughout this chapter we have discussed some of the outstanding problems of big bang cosmology and how inflation can solve them. We have discussed how the CMB observables are generated during inflation and how those observables act as a probe for inflationary models. We have also seen how the post-inflationary phase, known as the reheating, is responsible for setting the stage for standard hot big bang evolution. However, we have also noticed various issues with the inflationary model building as well as the reheating phase. The inflation which is a model independent mechanism is usually described in terms of a scalar field potential. The most prominent inflationary models are now disfavored from observation. Hence finding a suitable inflationary model that will not only reproduce the observed data but will do so within sub-Planckian values of its parameters is of prime importance from the inflationary model building perspective. We will discuss it in Chapter 2. The reheating phase which has no direct observable is still not very well constrained. We will take on this issue in Chapter 3 and also check how to relate the dark matter parameter space with CMB data assuming that the dark matter is produced during reheating. We will also inquire about the preheating phase taking a specific inflationary model in Chapter 4. Finally, we will study the effects of higher derivative kinetic terms on inflationary dynamics and reheating in Chapter 5.

# Part II

# Non-standard scalar field models of inflation

*"There is an often made statement that if the government drops lots of money from a helicopter, this may cause inflation. Of course, there is always a possibility that the money will be lost on its way. In our case, if we consider a theory with a plateau potential, and the scalar field $\phi$ drops in an expanding universe down from the state with the Planck energy density, then it is very difficult for it to end up in a narrow minimum of the potential and miss an infinite plateau. And if it falls to the plateau, then, just as in the situation with a positive cosmological constant background, it is difficult to avoid inflation."*

*Andrei Linde in[52]*

In this chapter we will start our discussion with a class of supergravity inspired inflationary mode. As we already seen that the inflation [5–9] is a model independent mechanism proposed to solve some of the outstanding problems in standard Big-Bang cosmology. We have also seen that the most simple way one can have a phase of exponential expansion in the early universe is by considering a scalar field. The scalar field potential has to be very flat so that we have sufficient amount of inflation. The inflation model is thus specified by a suitable scalar field potential. Over the years a large number of models have been introduced to realize this mechanism [20], as well as to reproduce the cosmological observations [11, 19, 53, 54]. Out of these large number of models, a particularly interesting class of models that has recently gained a significant interest is known as the $\alpha$ attractor [55–58]. One of the interesting properties of this class of model is that it unifies a large number of existing inflationary models within a single framework. In this chapter, we will introduce a new class inflationary scenario generalizing the model proposed in [59]. The goal here is to study the inflationary dynamics for a plateau potential which is flat at large field value and near the minimum it behaves like simple chaotic power law potentials. We will provide a derivation of our potential starting from simple power-law scalar field potentials in general scalar-tensor theory. We also discuss a supergravity realization of our model in a specific limit and compare the results with the well know Starobinsky model in $(n_s, r)$ plane[19]. The main motivation of our study could be

stated as follows: The general power law canonical potentials of the form $V(\phi) \sim |\phi|^n$ has already been disfavored from data due to their large predictions of tensor to scalar ratio. In addition, because of super-Planckian initial value of the scalar field, the effective field theory description of those inflationary models may not be robust. One of our goals in this work is to circumvent the above mentioned problems in the framework of canonical scalar field theory. To this end, we generalize the power law form of the potential to non-polynomial form such that it can match well with the observation while the inflaton field assumes sub-Plankian initial conditions. After the end of inflation, the production of radiation and other particles occur during the phase of reheating which sets in the stage for standard radiation domination. To the best of our knowledge a detailed analysis of this phase for arbitrary power law inflaton potential is still missing. Therefore, in this chapter we have generalized the existing reheating constraint analysis [60, 61] by considering the general equation of state, $w = (n-2)/(n+2)$, of inflaton for power law form $V(\phi) \sim \phi^n$ near the minimum of our potential. However detail study of the perturbative and non-perturbative issues of reheating phase for the model will be reported in subsequent chapters.
The plan of the chapter is as follows: we will introduce the model in Section 2.1, and study the model predictions for important cosmological parameters such as scalar spectral index ($n_s$), the tensor to scalar ratio ($r$), and the spectral running ($dn_s^k$) in light of the experimental observations. From those cosmological observations, we constrain the parameters of our model. In Section 2.3, we constructed the supergravity realization of our model and compared the predictions with respect to the PLANCK result. After the end of inflation, the inflaton, in general, starts to have coherent oscillation around the minimum of the potential. We have shown how the energy density scales for different models during the coherent oscillation and found the effective equation of state of the oscillating inflaton for use in our subsequent studies. In Section 2.4, we have done the model independent analysis for possible range of reheating temperature ($T_{re}$), and e-folding number ($N_{re}$) during reheating phase considering the background expansion and the evolution of entropy density. Subsequently, we have considered the evolution of scales and entropy density to constrain further the parameter space of our model. Finally, we concluded in Section 2.5.

## 2.1 The Model

Our starting point in this section is the phenomenological non-polynomial plateau potential

$$V_{min}(\phi) = \lambda \frac{m^{4-n}\phi^n}{1 + \left(\frac{\phi}{\phi_*}\right)^n} \tag{2.1}$$

This potential behaves as has simple power-law potentials around its minimum. A construction of this model from general non-minimal scalar-tensor theory has been presented in the Section 2.2. In Section 2.3, we will also describe a possible realization of this type of plateau potential in the supergravity framework specifically in the sub-Planckian limit of $\phi_*$. In the above form of the potentials, we have introduced two free parameters ($n, m$ *or* $\lambda$). Where, $n \in 2\mathbb{Z}^+$ while the parameter $\lambda$ is defined for $n = 4$, which has been studied as minimal Higgs inflation in [59]. For $n \neq 4$, we set $\lambda = 1$. For large value of $\phi_*$ the potential is plateau like and the associated inflationary scale is $\Lambda = \lambda m^{4-n}\phi_*^n$. One can further generalize the model by considering the potential to be dependent only upon the modulus of the inflaton field. In that case all the integer values of $n$ can be included. For the sake of simplicity we will stick to

only even values of $n$. Another simple generalization of our model can be done by defining $V(\phi)^q$ as a new potential. Where, $q \in \mathbb{Z}^+$ would a new parameter.

### 2.1.1 Background Equations

In this section we will study in detail the background dynamics using the above form of the potentials. We will start with the following action,

$$S = \int d^4x\sqrt{-g}\left[\frac{M_p^2}{2}R + \frac{1}{2}\partial_\mu\phi\partial^\mu\phi - V_{min}(\phi)\right] \tag{2.2}$$

Where $M_p = \frac{1}{\sqrt{8\pi G}}$ is the reduced Planck mass. Assuming the usual Friedmann-Lemaître-Robertson-Walker(FLRW) background ansatz for the space-time

$$ds^2 = dt^2 - a(t)^2(dx^2 + dy^2 + dz^2), \tag{2.3}$$

the system of equations governing the dynamics of the inflaton and the scale factor are

$$3M_p^2H^2 = \frac{1}{2}\dot{\phi}^2 + V_{min}(\phi) \tag{2.4}$$

$$2M_p^2\dot{H} = -\dot{\phi}^2 \tag{2.5}$$

$$\ddot{\phi} + 3H\dot{\phi} + V'_{min}(\phi) = 0. \tag{2.6}$$

Where, the usual definition of Hubble constant is $H = \dot{a}/a$. As we have seen, our potential is asymptotically flat for large field value compared to $\phi_*$. Thus the flatness condition for the potential is automatically met. The slow-roll parameters for the model is

$$\begin{aligned}\epsilon \equiv \frac{M_p^2}{2}\left(\frac{V'_{min}}{V_{min}}\right)^2 &= \frac{n^2M_p^2\phi_*^{2n}}{2\phi^2\left(\phi_*^n + \phi^n\right)^2} \\ \eta \equiv M_p^2\left(\frac{V''_{min}}{V_{min}}\right) &= \frac{nM_p^2\phi_*^n\left((n-1)\phi_*^n - (n+1)\phi^n\right)}{\phi^2\left(\phi_*^n + \phi^n\right)^2}\end{aligned} \tag{2.7}$$

The end of inflation, as we have seen, is usually set by the condition $\epsilon = 1$. Let us also define a higher order slow-roll parameter related to the third derivative of the potential for spectral running. The expression for the higher order slow-roll parameter is as follows:

$$\begin{aligned}\xi &\equiv M_p^4\left(\frac{V'_{min}V'''_{min}}{V^2}\right) \\ &= \frac{n^2M_p^4\phi_*^{2n}\left(\left(n^2-3n+2\right)\phi_*^{2n} - 4\left(n^2-1\right)\phi_*^n\phi^n + \left(n^2+3n+2\right)\phi^{2n}\right)}{\phi^4\left(\phi_*^n + \phi^n\right)^4}\end{aligned} \tag{2.8}$$

In addition to provide the successful inflation, all the aforementioned slow-roll parameters play very important role in controlling the dynamics of cosmological perturbation during inflation. The e-folding number ($N$) is found to be

$$N = ln\left(\frac{a_{end}}{a_{in}}\right) = \int_{a_{in}}^{a_{end}} d\,lna = \int_{t_{in}}^{t_{end}} Hdt \simeq \int_{\phi_{in}}^{\phi_{end}} \frac{1}{\sqrt{2\epsilon}}\frac{|d\phi|}{M_p}. \tag{2.9}$$

As we have mentioned the inflation ends when $\epsilon = 1$, and one can use Eq.(5.69) to find the value of the inflaton at the beginning of the inflation. By solving the aforementioned condition, we can express the e-folding number $N$ into the following form,

$$N = \frac{\phi_*^2}{nM_p^2}\left[\frac{1}{(n+2)}(\tilde{\phi}^{(n+2)} - \tilde{\phi}_{end}^{(n+2)}) + \frac{1}{2}(\tilde{\phi}^2 - \tilde{\phi}_{end}^2)\right] \simeq \frac{\phi_*^2}{nM_p^2}\frac{1}{(n+2)}\tilde{\phi}^{(n+2)} \tag{2.10}$$

Where we have defined, $\tilde{\phi} = \phi/\phi_*$. In the above expressions for $N$, we have ignored the contribution coming from $\phi_{end}$, and also the squared term. We have numerically checked the validity of those expressions for a wide range of value of $\phi* \leq \mathcal{O}(M_p)$. From cosmological observations one needs $N \simeq 50 - 60$, such that the scales of our interest in CMB were in causal contact before the inflation. By using the above mentioned boundary conditions for the inflaton we have solved for the homogeneous part of inflaton $\phi(t)$ and the scale factor $a(t)$. Next we study the perturbation around inflationary background and derive the relevant cosmological parameters associated the various correlation functions of fluctuation for this model.

### 2.1.2 Computation of $(n_s, r, dn_s^k)$

As we have already discussed in Chapter 1, all the relevant inflationary observables are identified with various correlation functions of those primordial fluctuations calculated in the framework of quantum field theory.

We have curvature and tensor perturbation. The two and higher point correlation functions of those fluctuation are parametrized by power spectrum. The scalar curvature power spectrum is given by

$$\Delta_s^2 = \frac{1}{8\pi^2}\frac{1}{\epsilon}\frac{H^2}{M_p^2}\bigg|_{k=aH} = \frac{1}{12\pi^2}\frac{V_{min}^3}{M_p^6(V'_{min})^2}. \tag{2.11}$$

Once, we know the power spectrum, cosmological quantity of our interests are the spectral tilt and its running. During inflation a particular inflaton field value corresponds to a particular momentum mode exiting the horizon. Hence by using the following relation to the leading order in slow-roll parameters, $\frac{d}{d\,lnk} = \frac{\dot{\phi}}{H}\frac{d}{d\phi}$, one obtains the following inflationary observables,

$$n_s - 1 \equiv \frac{\mathrm{d}\ln\Delta_s^2}{\mathrm{d}\ln k} = -6\epsilon + 2\eta \tag{2.12}$$

$$dn_s^k \equiv \frac{\mathrm{d}n_s}{\mathrm{d}\ln k} = -2\xi + 16\epsilon\eta - 24\epsilon^2. \tag{2.13}$$

Similarly we can compute the tensor power spectrum $\Delta_t^2$ for the gauge invariant tenor perturbation $h_{ij}$. To quantify this, standard practice is to define tensor-to-scalar ratio

$$r = \frac{\Delta_t^2}{\Delta_s^2} = 16\epsilon. \tag{2.14}$$

Once we have all the expression for cosmological quantities in terms of slow roll parameters, by using Eqs.(2.7,2.10), and considering $\phi_* \leq \mathcal{O}(1)$ in unit of $M_p$, we express $(n_s, r, dn_s^k)$ in terms of $n$,$N$ and $\phi_*$, as

$$\begin{aligned} 1 - n_s &= \frac{2(n+1)}{(n+2)}\frac{1}{N} \quad ; \quad dn_s^k = -\frac{(2+3n+n^2)}{(n+2)^2}\frac{1}{N^2} \\ r &= 8n^2\left(\frac{\phi_*}{M_p}\right)^{\frac{2n}{(n+2)}}\frac{1}{[n(n+2)]^{\frac{2(n+1)}{(n+2)}}N^{\frac{2(n+1)}{(n+2)}}} \end{aligned} \tag{2.15}$$

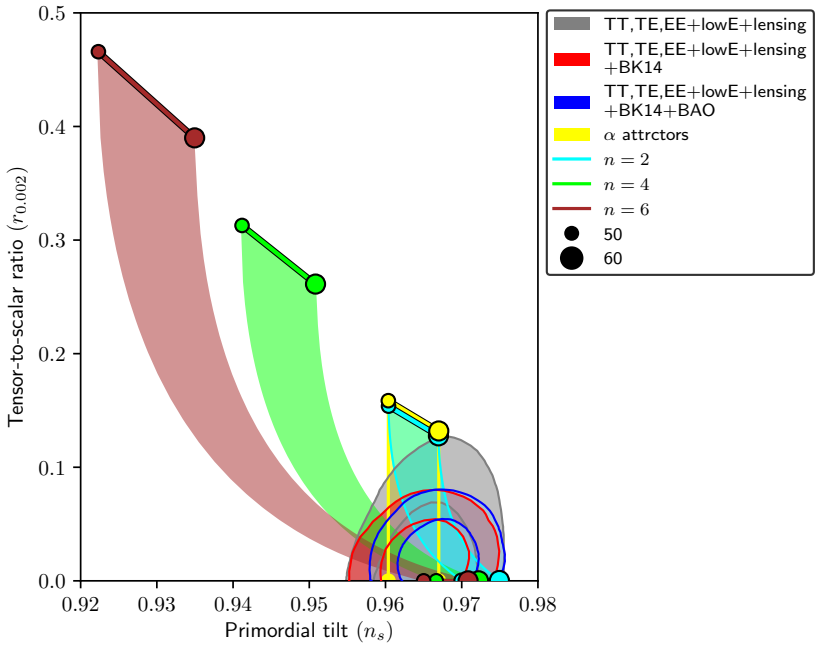


FIGURE 2.1: The $n_s$-$r$ plot of the model on the marginalized joint 68% and 95% CL regions at $k = 0.002 Mpc^{-1}$ from Planck alone and in combination with BK14 or BK14 plus BAO data[19].

The numerical results for inflationary predictions of this model is shown in Fig. 2.1 on the latest Planck data[19] data.

It is evident that the above analytic expressions for the inflationary observables derived in Eq.(2.15) are valid for subplanckian values of the scale $\phi_*$. For large values of this scale, the potentials reduce to the simple power-law form $V(\phi) \propto \phi^n$ and the observables are given by well-known results

$$1 - n_s = \frac{(2+n)}{2N}, \quad r = \frac{4n}{N}, \quad \mathrm{d}n_s^k = -\frac{2}{N^2}, \quad . \tag{2.16}$$

At this point let us point out an important difference between our models and the $\alpha$-attractor models. For large $N$, with $\alpha \ll N$, the spectral data for the $\alpha$-attarctor models are[62]

$$1 - n_s = \frac{2}{N}, \quad r = \frac{12\alpha}{N^2}. \tag{2.17}$$

This is in sharp contrast with that of our models given in Eq.(2.15). Therefore, as emphasized before, our model will not fall in the class of $\alpha$-attractor models. An important feature of the $\alpha$-attractor models is that the cosmological parameters do not depend upon the details of the potentials specifically on the power of the potential. We will do the detailed comparison on this in section 2.3.

So far all we have discussed is directly related to the cosmological observation made by PLANCK. Another important quantity from theoretical point of view is the Lyth bound [63] $\Delta\phi$. This quantity measures the difference of field values which is traversed by the inflaton field during inflation. Inflation is a semi-classical phenomena. It is believed that natural cut off scale for any theory minimally or non-minimally coupled with gravity is Planck scale $M_p$. Therefore, value of field excursion can naturally be a good measure to tell us the validity of a

| $\frac{\phi_*}{M_p}$ | $n$ | $n_s$ | $r$ | $dn_s^k$ | $\Delta\phi$ |
|---|---|---|---|---|---|
| 0.01 | 2 | 0.969 | $4 \times 10^{-5}$ | -0.00066 | 0.39 |
| | 4 | 0.966 | $2 \times 10^{-6}$ | -0.00066 | 0.12 |
| | 6 | 0.965 | $3 \times 10^{-7}$ | -0.00069 | 0.06 |
| 1.00 | 2 | 0.969 | $4 \times 10^{-3}$ | -0.0006 | 3.53 |
| | 4 | 0.966 | $9.6 \times 10^{-4}$ | -0.0007 | 2.13 |
| | 6 | 0.964 | $3.5 \times 10^{-4}$ | -0.0007 | 1.47 |

Table 2.1: The spectral quantities for different values of $n$ for 50 efolding. The two values of $\phi_*$ are chosen to illustrate that we can have both small field and large field inflation depending on the value of $\phi_*$. For large values of $\phi_*$, the model reproduce the results of chaotic $\phi^n$ models

model under study within parlance of the effective field theory. Hence the calculated expression for the field excursion in terms of $N$ and $\phi_*$ is:

$$\Delta\phi \gtrsim M_p N \sqrt{\frac{r}{8}} = M_p \left(\frac{n}{n+2}\right) \frac{1}{[n(n+2)]^{\left(\frac{n+1}{n+2}\right)}} N^{\frac{1}{(n+2)}} \tag{2.18}$$

All the quantities we have discussed so far is independent of $m$ or $\lambda$. (At this point let us again remind the reader that for $n \neq 4$, $\lambda$ is a dimensionless quartic coupling parameter. While for $n \neq 4$, $m$ is dimensionful parameter, and we set $\lambda = 1$). However, comparing the inflationary power spectrum with the PLANCK normalization we will determine the value of $m$ or $\lambda$ and then calculate all the other quantities of our interest. The expression for the power spectrum of the curvature perturbation is

$$\Delta_s^2 = \frac{\lambda}{12\pi^2 n^2} \left(\frac{m}{M_p}\right)^{4-n} \left(\frac{\phi_*}{M_p}\right)^{\frac{n^2}{n+2}} [n(n+2)N]^{\frac{2(n+1)}{(n+2)}} = 2.4 \times 10^{-9}. \tag{2.19}$$

Here we considered the PLANCK normalization: $\Delta_s^2$ at the pivot scale $k/a_0 = 0.05 Mpc^{-1}$, and corresponding estimated scalar spectral index is $n_s = 0.9682 \pm 0.0062$.

After having all our necessary expressions for all the cosmological quantities, we have plotted our main results in $(n_s, r)$ space and compared with the experimental values $n_s = 0.968 \pm 0.006$ and upper limit on $r < 0.11$ in Fig. 2.1. In Table 2.1, we have given some sample values of all the cosmologically relevant quantities for different values of the model parameters. As we have mentioned already, we found infinitely many model potentials with a universal shape. Most interesting case would probably be for $n = 4$. In a recent paper [59], it has been identified as a minimal Higgs inflation. Of course this identification is not straight forward. However for small field value, we can certainly Taylor expand the potential, and identify the coupling $\lambda$ as Higgs quartic coupling which can be set to its electroweak value. Renormalization group analysis needs to be performed from inflation scale to the electroweak scale to make this identification precise. Nonetheless like for the usual Higgs inflation scenario, question needs to be asked regarding the unitarity scale of the model under consideration and compare with the $\phi_*$. For completeness, in the appendix-6.2 we provide a short discussion on this issue.

| $n$ | $w = \frac{n-2}{n+2}$ | $p = 3(1+w)$ | $p$ from fitting |
|---|---|---|---|
| 2 | 0 | 3 | 3.12 |
| 4 | $\frac{1}{3}$ | 4 | 3.99 |
| 6 | $\frac{1}{2}$ | 4.5 | 4.56 |
| 8 | $\frac{3}{5}$ | 4.8 | 4.83 |

Table 2.2: The variation of inflation energy density with scale factor for different potentials

### 2.1.3 End of inflation and general equation of state

In this section we will be interested in the dynamics of the inflaton field after the inflation. During this phase the inflaton field oscillates coherently around the minimum of the potential. At the beginning the oscillation dynamics will naturally be dependent upon the inflation scale $\phi_*$ because of the large amplitude. This is the stage during which non-perturbative particle production will be effective. Therefore, resonant particle production will take place and conversion of energy from the inflaton to matter particles will be highly efficient. This phenomena is usually known as preheating of the universe. In this section we will discuss about the late time behavior of the inflaton, specifically focusing on the dynamics of the energy density of the inflaton field. After the many oscillations, when the amplitude of the inflaton decreases much below the $\phi_*$, the dynamics will be controlled by usual power law potential. As we have emphasized the coherent oscillation is very important in standard treatment of reheating. For any models of inflation this is thought to be an important criteria to have successful reheating. In this section, we will first discuss the evolution of inflaton and its energy density in full generality for all classes of potentials. As mentioned before, at late time the potential can be approximated as

$$\lim_{\frac{\phi}{\phi_*}<1} V_{min}(\phi) = \lambda m^{4-n}\phi^n. \tag{2.20}$$

In cosmology for any dynamical field such as inflaton, one usually defines the equation of state parameter $w$. For the oscillating inflaton, when the time scale of oscillation about the minimum of a potential is small enough compared to the background expansion time scale, by using virial theorem effective equation of state for a potential of the form $V(\phi) \propto \phi^n$ can be expressed as[41, 64]

$$w \equiv \frac{P_\phi}{\rho_\phi} \simeq \frac{\langle \phi V'(\phi)\rangle - \langle 2V\rangle}{\langle \phi V'(\phi)\rangle + \langle 2V\rangle} = \frac{n-2}{n+2}. \tag{2.21}$$

Therefore, in an expanding background, the evolution of energy density $\rho_\phi$ of the inflaton averaged over many oscillation will follow,

$$\dot{\rho}_\phi + 3H(1+w)\rho_\phi = 0. \tag{2.22}$$

At late time we relate the energy density($\rho_\phi$) of the universe (assuming that the universe is dominated by a single component) and the scale factor ($a$) as

$$\rho_\phi \propto a^{-3(1+w)} = a^{-p}. \tag{2.23}$$

In Table 2.2, we compare the numerical values of the exponent of energy density $p = 3(1+w)$ of the inflaton for our models potentials with that of the theoretical values corresponding to

the $\phi^n$ potentials. It can seen that the model potential around the minimum is given by their power-law behavior. It is therefore clear that the usual study of the preheating and reheating phase is applicable for this model. We will discuss the CMB constrain on the reheating phase in this chapter while the preheating and perturbatve reheating for the model will be studied in the subsequent chapters. In the next section we describe a possible realization of our model potential from general scalar-tensor theory and in the following section we will also provide a realization of our model in $\mathcal{N} = 1$ supergravity.

## 2.2 Towards derivation of $V_{min}$ from non-minimal scalar-tensor theory

In this section starting from non-minimal scalar-tensor theory, we will try to construct our model potentials which were a priori ad hoc in nature. As is well known, inflationary models based on power law potential $V(\phi) \sim \phi^n$ are simple but have been ruled out in general because of their large prediction of tensor to scalar ratio. Moreover, the models with large plateaus (Starobinsky or $\alpha$-attractors) are found to be most favored form the PLANCK observation. While most of these plateau models can be cast into exponential potential, plateau potentials with power-law form have also been discussed in super gravity[65, 66] and non-minimal coupling to gravity[67, 68]. In this section we will try to construct our model based on this non-minimally coupled scalar-tensor theory. We will see, how simple power-law potentials in the Jordan frame can give rise to the plateau potentials of desired form in the Einstein frame. However, this transformed models coincide with our minimal models only in a limiting regime (weak conformal coupling). At this point let us point out that equivalence between the Einstein frame and Jordon frame is an important question to ask. This issue has been discussed [69–73], from theoretical as well as cosmological point of views.

Nevertheless, our motivation in this section is to construct our desired form of the potentials which we have shown to be in different class of models rather tan $\alpha$ attractor model. We start with the following non-minimally coupled scalar-tensor theory,

$$S_J = \int d^4x\sqrt{-g}\left[\frac{\Omega(\varphi)}{2}M_p^2 R - \frac{\omega(\varphi)}{2}g^{\mu\nu}\partial_\mu\varphi\partial_\nu\varphi - V(\varphi)\right], \tag{2.24}$$

where, $\Omega(\varphi), \omega(\varphi)$ are arbitrary function of a scalar field $\varphi$. We will chose a specific form of those function for our later purpose. To get the action in the Einstein frame, one performs the following conformal transformation as,

$$\tilde{g}_{\mu\nu} = \Omega(\varphi)g_{\mu\nu}, \tag{2.25}$$

The action in the Einstein frame can be written as[74]

$$S_E = \int d^4x\sqrt{-\tilde{g}}\left[\frac{M_p^2}{2}\tilde{R} - \frac{1}{2}F^2(\varphi)\tilde{g}^{\mu\nu}\partial_\mu\varphi\partial_\nu\varphi - \tilde{V}(\varphi)\right] \tag{2.26}$$

Where, we have assumed that $\omega(\varphi) = \Omega(\varphi)$ and $F$ and the new potential can be found to be,

$$F^2(\varphi) = \frac{3M_p^2}{2}\frac{\Omega'^2(\varphi)}{\Omega^2(\varphi)} + 1 \quad ; \quad \tilde{V}(\varphi) = \frac{V(\varphi)}{\Omega^2(\varphi)} \tag{2.27}$$

Now, we choose the following non-minimal coupling function [62, 75], for $\Omega^2(\varphi)$,

$$\Omega^2(\varphi) = 1 + \xi(\frac{\varphi}{M_p})^n. \tag{2.28}$$

Therefore, applying (2.28), we find F and $\tilde{V}$ as,

$$F^2(\varphi) = \frac{3n^2\xi^2\left(\frac{\varphi}{M_p}\right)^{2(n-1)}}{8\left[1+\xi\left(\frac{\varphi}{M_p}\right)^n\right]^2} + 1 \quad ; \quad \tilde{V}(\varphi) = \frac{V(\varphi)}{1+\xi\left(\frac{\varphi}{M_p}\right)^n} \tag{2.29}$$

We use the following field redefinition

$$\frac{d\phi}{d\varphi} = F(\varphi) \tag{2.30}$$

to transform the non-minimal into the action of a minimally coupled scalar field with canonical kinetic term,

$$S_E = \int d^4x\sqrt{-\tilde{g}}\left[\frac{M_p^2}{2}\tilde{R} - \tilde{g}^{\mu\nu}\partial_\mu\phi\partial_\nu\phi - \tilde{V}(\phi)\right] \tag{2.31}$$

At this point we can integrate Eq.(2.30), to find the new field in terms of the old field, and construct the modified potential as a function of new field. It is clear from the above set of transformations that for entire range of parameter $\xi$, it is very difficult to reproduce our model. However, in the regime of weak coupling $\xi << 1$, $F \sim 1$, hence we can approximately write, using Eq.(2.30); $\varphi \sim \phi_0\phi$ ($\phi_0$ is some integration constant). Considering Jordan frame potential as power-law: $V(\varphi) \approx \varphi^n$, one gets plateau potential as

$$\tilde{V}(\phi) = \frac{\lambda\, m^{4-n}\phi^n}{1+\left(\frac{\phi}{\phi_*}\right)^n} \tag{2.32}$$

where, we identify $\phi_*$ as $M_p/\xi^{\frac{1}{n}}$. Therefore, in the weak coupling regime, $\xi \ll 1$ or $\phi_* > 1$, the non-minimal scalar tensor theory can give rise to a large class of minimal cosmologies such as ours which do not belong the $\alpha$-attractor model.

## 2.3 Supergravity realization of our model potential

For any inflationary model, it is important to understand its ultraviolet origin if any. One usual procedure is to embed the model under consideration in the well known supergravity framework. Therefore, a large amount of works have been devoted to construct the supergravity inflation. In order to achieve our goal we will generalize the construction given in [66] for $n = 2$. Let us first briefly review the scalar field inflation from supergravity[76–78]. For supergravity model of inflation, the usual approach is to consider the Kähler potential $K(\Phi_i, \Phi_{\bar{i}}^*)$, the superpotential $W(\Phi_i)$ in terms of scalar superfields $\{\Phi_i\}$ with the associated Lagrangian in the Einstein frame

$$\mathcal{L} = K_{i\bar{j}}(\partial^\mu\Phi_i)(\partial_\mu\Phi_{\bar{j}}^*) - V. \tag{2.33}$$

However for our present purpose, we also need to consider gauge kinetic function $f(\Phi_i)$, which couples with the gauge field kinetic term. Considering all those terms in the supergravity

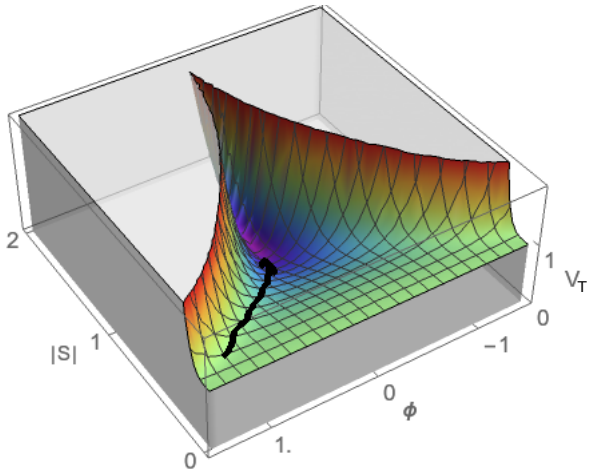


Figure 2.2: Total supergravity potential $V_T$ has been plotted. All the field are plotted in unit of Planck unit with $\phi_* = M = M_p$. The black curve corresponds to a possible inflationary trajectory around the minimum direction of $|S|$ which is the scalar field potential $V_{sugra}$.

Lagrangian, one obtains $F$-term and the $D$-term potential for the inflaton and other associated moduli fields from superpotential and gauge kinetic function respectively,

$$V = V_F + V_D, \tag{2.34}$$

$$V_F = e^{K/M_p^2}\left[K^{i\bar{j}}(D_iW)(D_{\bar{j}}\bar{W}) - 3\frac{|W|^2}{M_p^2}\right], \tag{2.35}$$

$$V_D = \frac{g^2}{2}\Re(f)^{-1}(iK_iX_i)^2, \tag{2.36}$$

where $K^{i\bar{j}}(= K_{i\bar{j}}^{-1})$ is the inverse matrix of the Kähler metric $K_{i\bar{j}}$, $D_iW = W_i + K_iW/M_p^2$ is the Kähler covariant derivative, and $X_i$ is the Killing vector of the Kähler manifold, and $g$ is the gauge coupling constant. For a linearly tranforming fields under the $U(1)$ symmetry we have $X_i = iq_i\Phi_i$ with $q_i$ being the $U(1)$ charge of $\Phi_i$. The D-term potential in this case reduces to

$$V_D = \frac{1}{2\Re(f)}\left(\sum_i q_iK_i\Phi_i + \xi_i\right)^2 \tag{2.37}$$

where $\xi_i$ is the as Fayel-Iliopoulos (FI) term which is non-zero only when the gauge symmetry is Abelian.

### 2.3.1 The power-law plateau potential form Supergravity

Let us consider a general superpotential with two chiral superfields $S$ and $\{\Phi_i\}$

$$W(S,\Phi_i) = \frac{\phi_*^{3-n}S^n}{n}F(\Phi_i) \tag{2.38}$$

Where, $\phi_*$ mass scale and $F$ is a dimensionless holomorphic function of the superfields $\Phi_i$. We will take the canonical Kähler potential to be given by

$$K = |S|^2 + \sum_i |\Phi_i|^2. \tag{2.39}$$

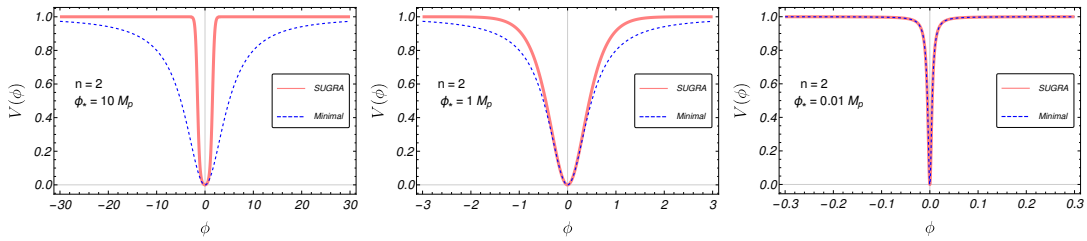


(a) (b) (c)

FIGURE 2.3: Comparison of the shape of the two potentials for three different values the scale $\phi_*$. It can be seen that for sub-Planckian values of $\phi_*$ the two potentials are identical.

With the above ingredient we can straightforwardly compute the $F$-term potential which is computed as,

$$V_F = \phi_*^{2(3-n)} e^{K/M_p^2} \left\{ |F|^2 |S|^{2(n-1)} \left(1 + \frac{|S|^2}{nM_p^2}\right) + \frac{|S|^{2n}}{n^2} \left| \frac{\partial F}{\partial \Phi_i} + \frac{\Phi_i^* F}{M_p^2} \right|^2 - 3\frac{|W|^2}{M_p^2} \right\} \tag{2.40}$$

Let us now take the specific form of the super potential with $n = 2$ and two additional superfields,

$$\begin{aligned} W(S, \Phi_1, \Phi_2) =& \frac{\phi_* S^2}{2} F(\Phi_1, \Phi_2) \\ \text{with,} \quad F(\Phi_1, \Phi_2) =& F_1(\Phi_1) - F_2(\Phi_2) \end{aligned} \tag{2.41}$$

As a first simplification we will assume that the functional form of the holomorphic functions $F_1$ and $F_2$ are same, i.e., $F_1 \equiv F_2$. The $D$-term potential for a suitable gauge coupling function and charge we will take from the reference [66, 79], and the expression is given as

$$V_D = \frac{1}{2}\left(|S|^2 - \sqrt{2}M^2\right)^2 \tag{2.42}$$

where $M$ is the scale of a grand unified theory(GUT)
A point is to be noted about the D-term potential is that we may generate such a term in the case of an anomalous $U(1)$ symmetry[80, 81]. These type of symmetries usually appears in the realm of string theories[82–84]. The anomaly cancellation requires the Green-Schwarz (GS) mechanism[85] which now set the value of the Fayet-Illiopoulos term as

$$\xi_{GS} = \frac{Tr[Q_A]}{192\pi} g^2 M^2 \tag{2.43}$$

where $Q_A$ is the charge of the fields under the anomalous $U(1)$ group and the trace is taken over fields. Now let us assign the charges of the fields following the discussion in[81]. The charge of the fields $\Phi_1$ and $\Phi_2$ (whose modulus will be identified as the inflaton) must vanish. The charges of $S$, taken to be $-1$, can be non-zero as long as it is opposite of $Tr[Q_A]$.(This will make it necessary to consider the existence of another field charged under the anomalous $U(1)$ with zero VEV.) With the above considerations, the total potential for inflaton $\phi$ and the moduli $S$ will be $V_T = V_D + V_F$. Given the simple form of the superpotential, the minimization along $\Phi_i$ leads to the $\Phi_1 = \Phi_2$. Now assuming a suitable R-symmetry we will take $|\Phi_1| = |\Phi_2| = \phi$ ($\phi$

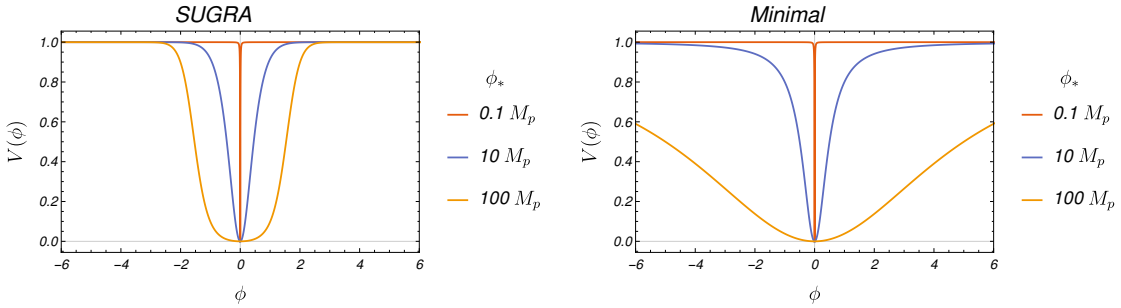


(a) Increase (b) Increase

Figure 2.4: The variation of the shape of the two potentials with scale $\phi_*$. The width of the potential vary slowly with $\phi_*$ for the plateau potential compared to the minimal potential.

being a canonically normalised, real scalar field), the total scalar potential for sub-Planckian value of $|S|$ simplifies to

$$V_T = e^{\frac{\phi}{M_p^2}}\phi_*^2|S|^4\left|F'(\phi)\right|^2 + \frac{1}{2}\left(|S|^2 - \sqrt{2}M^2\right)^2 \tag{2.44}$$

In Fig. 2.2, we have given simple illustration of our supergravity potential in $(|S|, \phi)$ space and the inflationary trajectory. In order to obtain an effective potential in term of inflaton $\phi$, we minimize $V_T$ along the $S$ direction and plug it back into the total potential which takes the following simple form

$$V_T(\phi) = M^4\left[\frac{e^{\left(\frac{\phi}{M_p}\right)^2}\phi_*^2\left|F'(\phi)\right|^2}{1 + e^{\left(\frac{\phi}{M_p}\right)^2}\phi_*^2\left|F'(\phi)\right|^2}\right] \tag{2.45}$$

It is now easy to check that for $F(\varphi) \propto (\phi/\phi_*)^p$ ($\{p \in \mathbb{Z} \mid p > 1\}$ ) we get a potential of the form

$$V_{sugra}(\phi) = \frac{m^{4-n}\phi^n}{exp(-\frac{\phi^2}{2M_p^2}) + \left(\frac{\phi}{\phi_*}\right)^n} \tag{2.46}$$

Where $n = 2(p-1)$ and the scale $m$ is defined by combining the scale $M$ with $\phi_*$ as $m = (M^4\phi_*^{-n})^{1/(4-n)}$. In the limit $\phi_* < M_p$, this potential reduces to the minimal plateau model given as,

$$V_{min}(\phi) = \frac{m^{4-n}\phi^n}{1 + \left(\frac{\phi}{\phi_*}\right)^n} \tag{2.47}$$

In our subsequent discussions, we will try to compare both aforementioned potentials as a separate entity. In Fig. 2.3, we plotted them for illustrations corresponding to different values of the parameters. It is apparent that the supergravity potential $V_{sugra}$ and our minimal plateau potential $V_{min}$ are identical for the sub-Planckian values of the scale $\phi_*$. Therefore, for our subsequent analysis, we will mostly concentrate in the sub-Planckian region of $\phi_*$. At this point we also would like to point out that we can arrive at the same form of our minimal potential if we start from the non-minimal scalar filed theory as discussed in the appendix. However, point to be noted that in such case $\phi_*$ needs to be super-Planckian.

Nevertheless in Fig. 2.4 we illustrate the change of the shape of the two potentials with the scale $\phi_*$. The $V_{sugra}$ is extremely flat even for large vales of the scale $\phi_*$, while the minimal potential reduces to the simple power law potentials for large values of the scale. This fact significantly controls the prediction of inflationary observables for both the models. In Fig. 2.5, we have plotted the dependence of the $n_s$ and $r$ on the scale $\phi_*$. We clearly notice that the two models predictions are identical as we go towards sub-Planckian value of $\phi_*$. In the Fig.(2.6), we have plotted predictions of our different models in $n_s$-$r$ plane. For explicit comparison, we have also plotted the predictions of the $\alpha$ attractor $T$ model($V = \Lambda^4[1 - exp(-\sqrt{2/3\alpha}\ \phi/\mathrm{M_p})]^n$) for different $n$ with increasing values of the parameter $\alpha$ with $(n = 2, \alpha = 1)$ being the Starobinsky model. Interestingly, the super-gravity model turned out to be well within the $2\sigma$ region of $n_s$ at all scales. Even at large field value of the inflaton the prediction of $r$ is always small. On the other hand as discussed before, our minimal potential mimics the usual chaotic inflation at large field value. Another interesting point that is worth mentioning is the absence of attarctor behavior in terms of cosmological predictions for the minimal plateau models. As can be seen from the Fig.(2.6), for our supergravity potential and the $\alpha$-attractor potential the value of $(n_s, r)$ going towards their respective unique attractor value with increasing $\phi_*$ and $\alpha$ respectively irrespective of any other parameter values. For $\alpha$-attractor this unique value is that of Starobinsky model with $(n_s = 0.9667, r = 3 \times 10^{-3})$, and for our supergravity potential the unique attractor value turned out to be $(n_s = 0.9667, r = 1 \times 10^{-5})$. It would be interesting to find that specific theory for this particular prediction. For the $\alpha$-attractor models, these attractor behavior is due to the pole in the kinetic term[62]. As we have considered only the canonical kinetic term in our Lagrangian, the attractor behavior is absent for our minimal plateau models(see also sec-2.2 for the region when this approximation is valid). However, the emergence of attractor behavior for the original supergravity potential given in (2.45) is indeed an interesting phenomena. The detailed theoretical implications of this supergravity potential will be important which we leave for future study. On the other hand as discussed above, our minimal potential mimics the usual chaotic inflation model at large field value.

After discussing the origin of the model potentials we will now turn to post-inflationary phases. In the following sections, we will consider the equation of state parameters for our models and study their role in the subsequent cosmological evolution. We will first discuss about the constraints on reheating phenomena by taking a model independent approach. We will not consider the explicit dynamics during reheating phase here.

## 2.4 Model independent constraints from reheating predictions

After inflation, reheating is the most important phase where all the visible matter and energy will be produced due to inflaton decay. In this section, we will try to constrain our model parameters without any specific mechanism of reheating. The background evolution of the cosmological scales from inflation to the present day and the conservation of entropy density provide us important constraints on reheating as well as our model parameters. Reheating is supposed to be the integral part of the inflationary paradigm. However, due to lack of direct observables in this phase, it is very difficult to constrain the phase. Thermalization process erases all the information about the initial conditions which is the most important part of this phase. To understand this phase an indirect attempt has been made in the recent

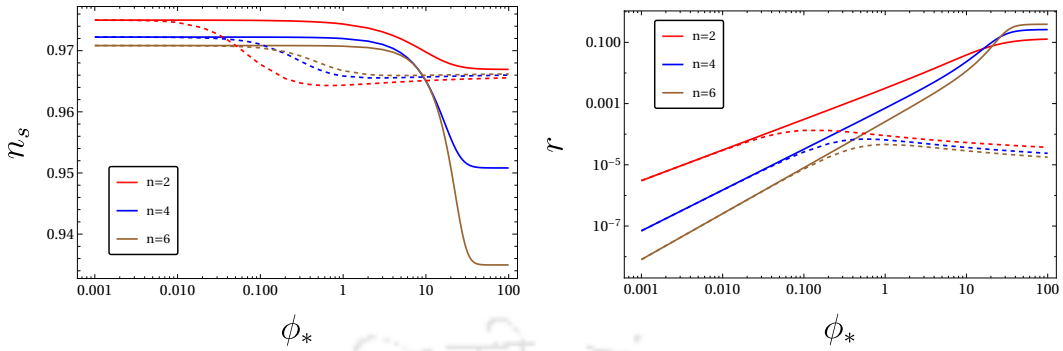


(a) Increase (b) Increase

Figure 2.5: variation of the spectral index ($n_s$) and scalar-to-tensor ratio with the scale $\phi_*$ for the two potentials. The solid lines corresponds to the minimal model while the dotted lines are for the SUGRA model. For smaller values of $\phi_*$ the two model predictions are identical.

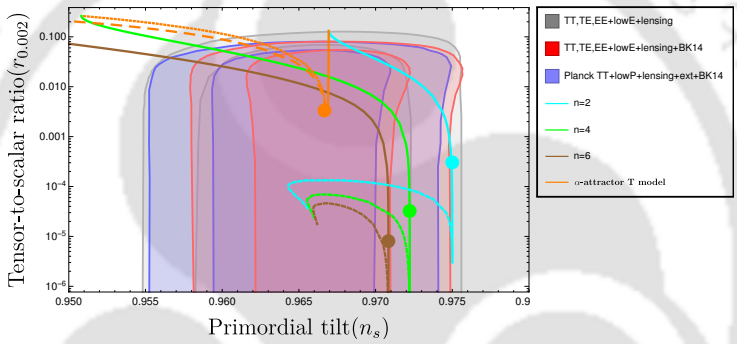


Figure 2.6: The $n_s$-$r$ plot for 60 e-folding number of the two models plotted on the Planck data[19]. The solid lines corresponds to the minimal model while the dotted lines are for the SUGRA model. The dots are the theoretical prediction from Eq.(2.15) for $\phi_* = 0.1M_p$. The orange dot corresponds to the Starobinsky model prediction for the same e-folding number.

past [60, 61, 86, 87] through the evolution of cosmological scales and the entropy density by parameterizing it by reheating temperature ($T_{re}$), equation of state ($w_{re}$), and efolding number ($N_{re}$). In this section we follow the reference [88] by taking into account the two stage reheating phase generalizing the formalism of [86]. Our main goal is to understand the possible constraint on our minimal plateau inflationary models. As we have seen from previous analysis, all the cosmological quantities during inflation can be expressed in terms of two main parameters ($m$ *or* $\lambda, \phi_*$) for a particular model. Because of two stage reheating process, the suitable reheating parameters are as follows, ($N_{re} = N^1_{re} + N^2_{re}, T_{re}, w^1_{re}, w^2_{re}$). Where, $N^1_{re}, N^2_{re}$ are efolding number during the first and second stage of the reheating phase with the equation of state $w^1_{re}, w^2_{re}$ respectively. At the initial stage the oscillating inflaton will be the dominant component, and at the end radiation must be the dominant component. Therefore, instead of taking the equation of state as free parameters, we will be considering only the following particular case

$$w^1_{re} = \frac{n-2}{n+2} \quad ; \quad w^2_{re} = \frac{1}{3}. \tag{2.48}$$

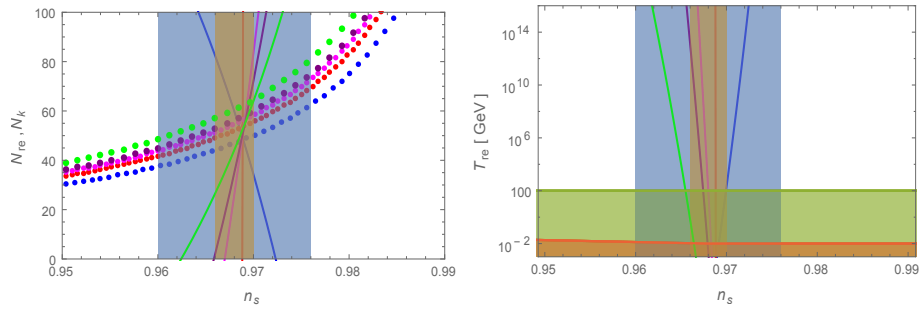


FIGURE 2.7: Variation of $(N_{re}(\text{solid}), N_k(\text{dotted}), T_{re})$ as a function of $n_s$ have been plotted for $\phi_* = 0.01 M_p$. This is the plot for our model potential. (Blue, red, magenta, brown, green) curves correspond to $n = (2, 4, 6, 8, 30)$. Each curve corresponds to a specific set of equation of state parameters $(w^1_{re}, w^2_{re}) = ((n-2)/(n+2), 1/3)$ during reheating. We also consider $N^1_{re} = N^2_{re}$. The light blue shaded region corresponds to the $1\sigma$ bounds on $n_s$ from Planck. The brown shaded region corresponds to the $1\sigma$ bounds of a further CMB experiment with sensitivity $\pm 10^{-3}$ [89–91], using the same central $n_s$ value as Planck. Temperatures below the horizontal red line is ruled out by BBN. The deep green shaded region is below the electroweak scale, assumed 100 GeV for reference.

We also assumed the change of reheating phase from the first to the second stage as instantaneous. A particular scale $k$ going out of the horizon during inflation will re-enter the horizon during usual cosmological evolution. This fact will provide us an important relation among different phases of expansion parameterized by e-folding number as follows

$$\ln\left(\frac{k}{a_0 H_0}\right) = \ln\left(\frac{a_k H_k}{a_0 H_0}\right) = -N_k - \sum_{i=1}^{2} N^i_{re} - \ln\left(\frac{a_{re} H_k}{a_0 H_0}\right), \tag{2.49}$$

In the above expressions, we have used $k = a_0 H_0 = a_k H_k$. Where, $(a_{re}, a_0)$ are the cosmological scale factor at the end of the reheating phase and at the present time respectively. $(N_k, H_k)$ are the efolding number and the Hubble parameter respectively for a particular scale $k$ which exits the horizon during inflation. Therefore, the following relations will be used in the final numerical calculation,

$$H_k = \sqrt{\frac{V(\phi_k)}{3M_p^2}} = \begin{cases} \left(\frac{\lambda \phi_*^n}{3M_p^2}\right)^{\frac{1}{2}} \frac{m^{\frac{4-n}{2}} \tilde{\phi}_k^{\frac{n}{2}}}{\left(1+\tilde{\phi}_k^n\right)^{\frac{1}{2}}} \\ \left(\frac{\lambda \phi_*^n}{3M_p^2}\right)^{\frac{1}{2}} \frac{m^{\frac{4-n}{2}} \tilde{\phi}_k^{\frac{n}{2}}}{\left(1+\tilde{\phi}_k^2\right)^{\frac{n}{4}}}, \end{cases} \tag{2.50}$$

$$N_k = \frac{1}{M_p} \int_{\phi_{end}}^{\phi_k} \frac{1}{\sqrt{2\epsilon}} d\phi \simeq \begin{cases} \frac{\phi_*^2}{n M_p^2} \left[\frac{1}{(n+2)} \tilde{\phi}_k^{(n+2)} + \frac{1}{2} \tilde{\phi}_k^2\right] \\ \frac{\phi_*^2}{n M_p^2} \left[\frac{1}{4} \tilde{\phi}_k^4 + \frac{1}{2} \tilde{\phi}_k^2\right] \end{cases} \tag{2.51}$$

$\phi_k$ and $\phi_{\text{end}}$ are the inflaton field values corresponding to a particular scale $k$ crossing the inflationary horizon, and at the end of inflation respectively. In the above expressions, we have ignored the contribution coming from the inflaton field value $\phi_{\text{end}}$. It is important to note that, in principle we can write the field value at a particular scale $k$ in terms of $n_s, r$, by inverting those relations. Because of non-linear form, we will numerically solve those. The above unknown efolding numbers during reheating will certainly be dependent upon the energy densities $(\rho_{end}, \rho_{re})$, at the end of inflaton (beginning of reheating phase) and at the end of

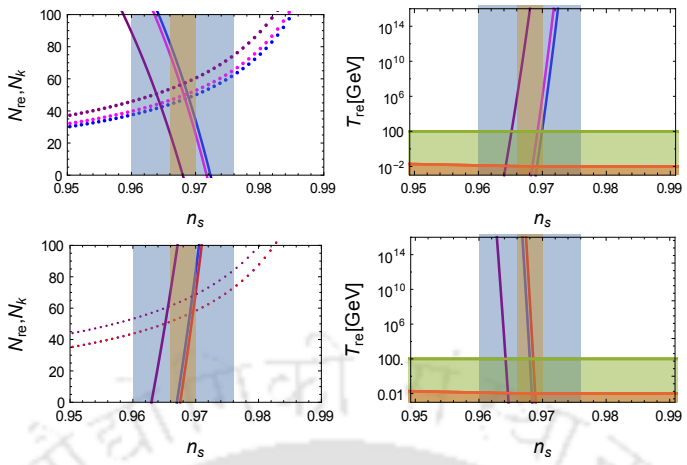


FIGURE 2.8: Variations of $(N_{re}(\text{solid}), N_k(\text{dotted}), T_{re})$ as a function of $n_s$ have been plotted for for three different values of $\phi_*$. (Blue, magenta, purple) curves are for $\phi_* = (0.01, 0.1, 10)M_p$ respectively. The left two figures are for $n = 2$, and tight two figures are for $n = 6$.

the reheating phase( beginning of the standard radiation dominated phase);

$$\ln\left(\frac{\rho_{end}}{\rho_{re}}\right) = 3(1+w_{re}^1)N_{re}^1 + 3(1+w_{re}^2)N_{re}^2 = 3\sum_{i=1}^{2}(1+w_{re}^i)N_{re}^i. \tag{2.52}$$

Above two Eqs.(2.49,2.52), can be easily generalized for multi-stage inflation with different equation of state parameters. As has been mentioned, after the end of reheating standard evolution of our universe is precisely known in terms of energy density and the equilibrium temperature of the relativistic degrees of freedom such as photon and the neutrinos. Therefore, the equilibrium temperature after the end of reheating phase, $T_{re}$, is related to temperature $(T_0, T_{\nu 0})$ of the CMB photon and neutrino background at the present day respectively, as follows

$$g_{re}T_{re}^3 = \left(\frac{a_0}{a_{re}}\right)^3 \left(2T_0^3 + 6\frac{7}{8}T_{\nu 0}^3\right). \tag{2.53}$$

The basic underlying assumption of the above equation is the conservation of reheating entropy during the evolution from the radiation dominated phase to the current phase. $g_{re}$ is the number of relativistic degrees of freedom after the end of reheating phase. We also use the following relation between the two temperatures, $T_{\nu 0} = (4/11)^{1/3}T_0$. For further calculation, we define a quantity, $\gamma = N_{re}^2/N_{re}^1$. If we identify the scale of cosmological importance $k$ as the pivot scale of PLANCK, so that $k/a_0 = 0.05Mpc^{-1}$, and the corresponding estimated scalar spectral index $n_s = 0.9682 \pm 0.0062$, we arrive at the following equation for the e-folding number during reheating period and the reheating temperature,

$$N_{re} = \frac{4(1+\gamma)}{(1-3w_{re1}) + \gamma(1-3w_{re2})}\left[61.6 - \ln\left(\frac{V_{end}^{\frac{1}{4}}}{H_k}\right) - N_k\right] \tag{2.54}$$

$$T_{re} = \left[\left(\frac{43}{11g_{re}}\right)^{\frac{1}{3}}\frac{a_0T_0}{k}H_k e^{-N_k}\right]^{\frac{3[(1+w_{re1})+\gamma(1+w_{re2})]}{(3w_{re1}-1)+\gamma(3w_{re2}-1)}}\left[\frac{3^2.5V_{end}}{\pi^2 g_{re}}\right]^{\frac{1+\gamma}{(1-3w_{re1})+\gamma(1-3w_{re2})}} \tag{2.55}$$

| n | $n_s$ | $T_{re}$(GeV) | $N_{re}$ | $N_k$ |
|---|---|---|---|---|
| 2 | 0.9723 | $1 \times 10^{15}$ | 0.4 | 54 |
| | 0.9702 | $1 \times 10^{3}$ | 32 | 50 |
| 6 | 0.9670 | $1 \times 10^{14}$ | 00 | 53 |
| | 0.9679 | $2 \times 10^{3}$ | 23 | 55 |
| 8 | 0.9659 | $7 \times 10^{13}$ | 0.6 | 53 |
| | 0.9673 | $1 \times 10^{3}$ | 23 | 55 |
| 30 | 0.9625 | $6 \times 10^{13}$ | 00 | 52 |
| | 0.9653 | $1 \times 10^{3}$ | 21 | 56 |

Table 2.3: Some sample values of $(n_s, T_{re}, N_{re}, N_k)$ are give for two different models for $n = (2, 6, 8, 30)$. As we have mentioned, for $n = 4$, $(T_{re}, N_{re})$ become indeterministic. All these prediction are for $\phi_* = 0.01 M_p$.

In the above derivation, we have used $g_{re} = 100$. Before discussing any further, let us provide the general descriptions of the figures we have drawn in this section. As has been mentioned before, we have considered specific values of equation of state parameter $(w^1_{re}, w^2_{re}) = ((n-2)/(n+2), 1/3)$ in compatible with our model discussed in the previous section. Important to mention regarding a special point in the aforementioned state space is $(1/3, 1/3)$ which is realized for $n = 4$. Analytically one can check that at this special point both $(T_{re}, N_{re})$ become indeterminate as seen in Eq.(2.55). This fact corresponds to all the vertical solid red lines in $(n_s \; vs \; T_{re})$ and $(n_s \; vs \; N_{re})$ plots. We have considered $\gamma = 1$ as our arbitrary choice. Each curve corresponds to different values of $n$. On the same plot of $(n_s \; vs \; N_{re})$, we also plotted $(n_s \; vs \; N_k)$ corresponding to the dotted curves for different models. At this stage, we would like to remind the reader again that for a wide range of $\phi_*$, all the models predict very small value of tensor to scalar ratio $r$. Therefore, we will be discussing all the constraints without explicitly mentioning $r$. Given the overall description of all the plots, we now set to discuss the prediction and constraints for two different models. In Table 2.3, we provide the values for reheating temperature and the e-folding number. We provided only the limiting values of $T_{re}$ which are still allowed from the cosmological observation.

From the figure we see that for a very small change in $n_s$, the variation of reheating temperature is very high. Therefore, reheating temperature provides tight constraints on the possible values of e-folding number $N_{re}$ during reheating phase. Except for $n = 4$, if we restrict the value of $T_{re} \gtrsim 10^3$ GeV, the e-folding number turned out to be $N_{re} \lesssim 35$ during reheating. As an example, for $n = 2$, we find spectral index lies within $0.9723 \lesssim n_s \lesssim 0.9702$. Within this range of spectral index, the reheating temperature has to be within $1 \times 10^{15} \gtrsim T_{re} \gtrsim 1 \times 10^3$ in unit of GeV. This restriction in turn fixed the possible range of e-folding number within a very narrow range $50 < N < 54$ for $n = 2$. For other value of $n$, the ranges are provided in the Table 2.3. What we can infer from our analysis in this section is that reheating constraint does not allow $n$ to be vary large specifically for our model. With increasing value of the equation of state, e-folding number during reheating $N_{re}$, decreases for a fixed value of reheating temperature. This essentially means that as one increases the value of inflationary equation of state $w$, faster will be the thermalization process, therefore, earlier will be the radiation dominated phase. To complete the discussion, in the Fig. 2.8, we have also plotted the dependence of reheating parameters for different values of $\phi_*$. We have plotted for $n = 2, 6$. For all the other

models qualitative behaviors of those plots will be same, except $n = 4$. Qualitative behavior of $(N_{re}, T_{re}, N_k)$ remain same for different $\phi_*$

## 2.5 Summary and Conclusion

Before we conclude, let us summarize the main results of this chapter. We studied in detail a specific class of supergravity inspired inflationary models. Most importantly to best fit the experimental data all the important scales $(\phi_*, m)$ which control the inflationary as well as reheating dynamics turned out to be sub-Planckian. Therefore, our model prediction can be trusted from the effective field theory point of view. As a result, we also have sub-Planckian field excursion during inflation, which is thought to be important in order to avoid any unwanted quantum gravity effects. However, depending upon the choice of scale $\phi_*$ we can realize both large field as well as small field inflation. Even for large field cases the scalar-to-tensor ratio $(r)$ turned out to be significantly smaller compared to the usual chaotic models. This fact can be attributed to the extreme flatness of the potential. Another important point we would like to mention is that this model belongs to a different class as compared to recently proposed $\alpha$-attractor models.

At this point let us point out that a detailed statistical analysis on inflationary models is done in [20] to select the *best fit* models out of a large number of models. Similar analysis is beyond the scope of the present work. However, an important conclusion of their work is that there exist a common feature among all the best fit models. They found that all these best fit model potentials have a large plateau region, i.e., $V'(\phi) \to 0$ as $\phi \to \infty$. Thus it can be inferred that our power-law plateau model as well as the full supergravity model will also be among the best fit models of inflation.

Near the minimum inflaton potential behaves like a power law $V \propto \phi^n$. Therefore, after the end of inflation coherently oscillating inflaton can be well approximated as an effective fluid with the equation of state parameter, $w = (n-2)/(n+2)$ at least at the initial stage of reheating. With the usual power law potential, one finds it very difficult to fit the cosmological observation for even $n \geq 2$. Because of this detailed studies have not been done for general power law potential specifically in the context of reheating. However, as we have seen in this chapter, with the non-polynomial generalization we can easily have power law form specifically at the minimum of the potential. This fact leads us to generalize the work of reheating constraint analysis proposed in [61, 86] for general effective inflaton equation of state $w$. Main outcome of this analysis can be seen in the Table 2.3.

After studying the PLANCK constraints it would be very much important to study in detail the reheating dynamics. Reheating is the stage during which all the matter fields are produced. Usual strategy would be to consider the effective coupling among the inflaton and various other matter fields we see today. Considering perturbative reheating phenomena we discuss important issue related to dark matter in the next chapter and we will deal with the non-perturbative effects in Chapter 4.

# CMB constraints on reheating and dark matter phenomenology 3

*"The most important thing accomplished by the ultimate discovery of the $3^{\circ}K$ radiation background (Penzias and Wilson, 1965) was to force all of us to take seriously the idea that there was an early universe"*

*Steven Weinberg, in The First Three Minutes: A Modern View of the Origin of the Universe*

## 3.1 Introduction

In the previous chapter we constructed a specific class of plateau inflationary model. We have seen that our model fit very well with the current CMB observation. In this chapter we will be specifically focusing on the aftermath. It has been observed that associated with the inflation, the generic inflation energy scale assumes the value $\geq 10^{10}$GeV. On the other hand, successful big bang nucleosynthesis(BBN) predicting the current light elements abundance requires our universe to be radiation dominated with the minimum temperature to be $T_{\rm BBN} \sim 1$ MeV[10, 92–94]. Therefore, the evolution of our universe from the inflation to BBN needs highly nontrivial dynamics that not only produces all the matter particles we see today but also connects these widely separated energy scales though complex nonlinear process and thermalization.

The signature of the inflationary evolution can be extracted from the cosmic microwave background(CMB) measurements[11, 19, 53, 54]. On the other hand, the BBN is very successful in explaining the light element abundance in the present universe. However, until now the period between the aforementioned two cosmological eras is poorly understood. The reasons behind this lack of understanding are our observational limitations to directly probe this phase and most importantly the dynamics during this phase, are expected to be highly nonlinear in nature as just noted above. This phase, which has been dubbed as the reheating era [26, 27, 29, 95], is, in general, parameterized by the reheating temperature $T_{re}$ which is defined at the instant when the inflaton decay rate to radiation becomes equal to the expansion rate

of the universe. After the reheating period is over, the reheating temperature can be directly connected to the current CMB temperature through background expansion. Therefore, it is possible to constrain the inflationary models and the subsequent reheating phase with CMB anisotropy[61, 96, 97]. This idea of the reheating constraint on inflation dynamics has recently been studied extensively for various inflationary models[87, 98–103].

One of the important assumptions of the aforementioned reheating constraint analysis is that during the reheating phase, the inflaton decays only into the radiation component. Therefore, it has an inherent limitation to extend the analysis beyond radiation. In this paper, our main goal is to extend and generalize the existing analysis of reheating constraints considering the effect of dark matter production during the reheating phase. In the current epoch, apart from the cosmological constant, dark matter and CMB are the two main components of our universe. From the current observational point of view CMB is the most powerful probe to understand the evolution of the universe. Through CMB, we not only understand the background expansion of our universe but also understand various physical processes acting during the formation of a large-scale structure that we see today. Dark matter is believed to play one of the important roles in the aforementioned processes of structure formation. However, because of the perceived very weak interaction with the visible matter field, the direct detection of dark matter has been found to be difficult. From the background evolution, we know that our universe to be 23% dark matter dominant out of the total energy budget of the universe. This fact motivates us to understand the following question: *does the CMB have any role to play in understanding the dark matter phenomenology?*

To answer this question, we think it is the reheating phase that has the potential to shed some light on the possible connection between the CMB and the current dark matter abundance. With this in mind and following our previous work [104], we assume decaying dynamics of the inflaton to be perturbative during reheating and dark matter is produced through annihilation of the radiation component. Inflation decaying into various fields and their observable effects has already been extensively studied before [105–111]. However, as already emphasized, our main goal is to connect the dark matter phenomenology and CMB anisotropy via inflation and reheating. Therefore our analysis will be an important generalization of the previous work [61].

Since inflaton is decaying through a perturbative process, the assumption of a complete conversion of inflation into radiation at the instant of reheating will not hold which has been extensively considered before. This assumption is applicable if the reheating is instantaneous. But in general, this is not the case. Therefore, we will see that there will be a significant correction in the reheating temperature as only a fraction of total inflaton energy is converted into radiation at the time [106] when $\Gamma_\phi = H$. For simplicity, we will assume that the dark matter is produced only through annihilation channel from the radiation component. We believe our study can also help us gain more insight into the production mechanism of dark matter intimately tied with the inflationary and reheating dynamics. We leave explicit model construction for our future studies.

To this end let us point out an important observation we made through our analysis. The production of dark matter particle in an expanding universe such as ours generally can be of two types. Depending upon the initial energy density and the rate of background expansion, if the annihilation cross section to dark matter is large, the produced particle will reach thermal equilibrium before freeze-out to current abundance [112–121], which is the well known “freeze-out" mechanism. On the other hand, if the annihilation cross section is small enough, the comoving dark matter particle density becomes constant much before it can reach thermal equilibrium with the background radiation. This production mechanism is known as

the "freeze-in" mechanism. In the particle physics context, the existing model of this type is known as feebly interacting dark matter [122–125]. Interestingly, if we consider the reheating process to be perturbative, our analysis shows that for dark matter mass much larger than the reheating temperature, the current dark matter abundance can be produced only via the freeze-in mechanism. The reason is the unique boundary conditions set by the inflation. However, for dark matter mass smaller than the reheating temperature, both mechanisms will work. For the present purpose, we have explicitly considered the freeze-in mechanism. A detailed analysis of different mechanisms will be studied elsewhere.

The remainder of this chapter is organized as follows. In the first two sections, we essentially review the well-known results to set the stage for our current analysis. In Section 3.2, we will discuss the inflationary observables and its connection with CMB. In Section 3.3, we describe the set of Boltzmann equations that describes the dynamics of the reheating phase. As has been mentioned in the Introduction, we will calculate the reheating temperature and corresponding e-folding number considering the explicit decay of inflaton. For this, we solve the system of Boltzmann equations numerically and identify the individual components during reheating with their current abundance. With this identification, we are able to shed light on the dark matter through CMB anisotropy. We study different inflationary models and their constraints on the dark matter phenomenology in Section 3.4. Finally, we conclude in Section 3.5

## 3.2 Inflationary observables and their connection with CMB

One of the important observable in CMB is the correlation of temperature fluctuations which is directly related to the inflationary observable is the scalar spectral index $n_s$. The equations governing the dynamics of the inflaton $\phi$ with a potential $V(\phi)$ is

$$\ddot{\phi} + (3H + \Gamma_\phi)\dot{\phi} + V'(\phi) = 0, \tag{3.1}$$

$$H^2 = \left(\frac{\dot{a}}{a}\right)^2 = \frac{1}{3M_{\rm p}^2}\rho_t, \tag{3.2}$$

where, we consider the following FLRW spacetime background $ds^2 = dt^2 - a(t)^2(dx^2+dy^2+dz^2)$. $H$ is the Hubble expansion rate and $M_{\rm p}(= 1/\sqrt{8\pi G})$ is the reduced Planck mass. The decay term $\Gamma_\phi\dot{\phi}$ in the above equation is assumed to be negligible during inflation, however, it will become important during the reheating period. Therefore, during inflation total energy density of the universe will be dominated by the inflaton energy $\rho_t = \rho_\phi$. As is well known that almost homogeneous temperature $T_0 \simeq 2.7$K of the CMB can be shown to be intimately tied with the slow-roll nature of inflaton dynamics, and it is parameterized in terms of potential $V(\phi)$ as follows,

$$\epsilon = \frac{1}{2}M_{\rm p}^2\left[\frac{V'(\phi)}{V(\phi)}\right]^2 \quad \eta = M_{\rm p}^2\left[\frac{V''(\phi)}{V(\phi)}\right]. \tag{3.3}$$

Once we define the background inflationary dynamics, the main quantities of interest are the amplitude of the inflaton fluctuation $A_s$, the spectral index, $n_s$, and the tensor-to-scalar ratio $r$, which in terms of the slow-roll parameters are

$$n_s = 1 - 6\epsilon_k + 2\eta; \qquad r = 16\epsilon. \tag{3.4}$$

The CMB normalization and the temperature correlation are in one-to-one correspondence with $A_s$ and $n_s$ respectively. Therefore, those observables are directly used to constrain the

inflationary models. Tensor to scalar ratio $r$, which is related to the inflationary energy scale has its signature in the polarization $B$ mode of CMB, which has not yet been observed. All those quantities are defined for a particular cosmological scale $k$ which is the pivot scale of CMB, $k/a_0 = 0.05\text{Mpc}^{-1}$. The latest bound on the scalar spectral index is [19] given as $n_s = 0.9659 \pm 0.0082$ for $\Lambda$CDM + r model from Planck data alone or $n_s = 0.9670 \pm 0.0074$ from Planck and BK14 and BAO data. In our subsequent analysis, we will assign all the inflationary parameters at the aforementioned CMB scale at the time of its horizon crossing during inflation.

Further, important inflationary quantities that will be considered are the Hubble parameter $H_k$ and e-folding number $N_k$ for a particular scale $k$ (CMB pivot scale) at its horizon crossing. Those quantities will be described in the appropriate places, but before that in the next section, we will review the Boltzmann equation for three different energy components namely inflaton, radiation, and dark matter.

## 3.3 Dark Matter during reheating

### 3.3.1 Basic equations

As has been emphasized in our previous discussions, the information of CMB has the potential to shed light on the dark matter sector through the reheating phase. Production of dark matter like particles considering different models and its phenomenology has already been worked out in detail in the literature considering the decaying inflaton during reheating[105, 107–109, 123, 126–133]. Also, how a nonzero Higgs VEV during inflation can impact the standard reheating history of the universe has been discussed in[134–136]. However the direct connection of the aforementioned analysis with the CMB has never been carefully looked into. Therefore, combining the analysis mentioned in the previous section with the existing reheating analysis, in the subsequent sections, we will uncover a surprising connection between the CMB and dark matter phenomenology. Our study opens up a new avenue toward understanding the detail properties of the dark matter though CMB observations.

It is well known that after the end of inflation the universe becomes extremely homogeneous. Therefore, to set in the subsequent evolution, the inflaton field has to go through the reheating phase when it decays into other fields and radiation. Depending upon the coupling with the inflaton field, the reheating field can have either perturbative or nonperturbative production. For our current analysis, we will consider the purely perturbative reheating process. Therefore, we essentially follow the existing analysis by considering the evolution of Boltzmann equations for three different energy components consisting of the inflation energy density $\rho_\phi$, the radiation energy density $\rho_\phi$ and the dark matter particle number density $n_X$[106, 137].

$$\frac{d\rho_\phi}{dt} = -3H(1+w_\phi)\rho_\phi - \Gamma_\phi(1+w_\phi)\rho_\phi \tag{3.5}$$

$$\frac{d\rho_R}{dt} = -4H\rho_R + \Gamma_\phi\rho_\phi + \langle\sigma v\rangle 2\langle E_X\rangle \left[n_X^2 - (n_{X,eq})^2\right] \tag{3.6}$$

$$\frac{dn_X}{dt} = -3Hn_X - \langle\sigma v\rangle \left[n_X^2 - (n_{X,eq})^2\right], \tag{3.7}$$

and the background expansion is given by

$$H^2 = \frac{8\pi}{3\text{m}_{\text{pl}}^2}(\rho_\phi + \rho_R + \rho_X)\ . \tag{3.8}$$

where, $\langle E_X \rangle = \rho_X / n_X \simeq \sqrt{M_X^2 + (3T)^2}$ is the average energy density of a single component dark matter X particle and $n_X^{eq}$ is the equilibrium number density of the matter particle of mass $M_X$ at the equilibrium background temperature $T$. $\Gamma_\phi$ is the inflaton decay constant. As has been mentioned, the dark matter particles create and annihilate into radiation with a thermal-averaged cross section $\langle \sigma v \rangle$. $w_\phi$ is the average equation of state for an oscillating scalar field (inflaton)[41],

$$w_\phi = \frac{p_\phi}{\rho_\phi} \simeq \frac{\langle \phi V'(\phi) - 2V(\phi) \rangle}{\langle \phi V'(\phi) + 2V(\phi) \rangle} \tag{3.9}$$

For an inflaton potential $V(\phi) \propto \phi^n$, it is found to be $w_\phi = (n-2)/(n+2)$. At this point let us state an important difference of our work and that of [61, 103]. In those works, the equation of state parameters for the reheating period is expressed as that of an effective single fluid( comprising inflaton and its decay products) equation of state. This is taken to be constant during the entire reheating period. In the present work, as we are explicitly solving the Boltzmann equations for different components of the universe during reheating, we need not consider the single field equation of the state parameter rather the quantity that is important here is the equation of state parameter for the homogeneous component of inflaton during oscillation. At this stage let us emphasize the fact that, nonperturbative decay could have a potential impact on our conclusion which we leave for our future studies.

Our goal of this chapter is to look into a wide range of dark matter mass, $M_X$ which can be greater as well as less than the reheating temperature. We also assume the dark matter to follow the fermionic distribution having the internal degree of freedom $g$. Therefore, in thermal equilibrium the number density at temperature $T$ can be expressed as,

$$n_{X,eq} = \frac{g}{2\pi^2} \int_{m_X}^{\infty} \frac{\sqrt{E^2 - M_X^2}}{e^{E/T} + 1} E dE \simeq \frac{gT^3}{2\pi^2} \left(\frac{M_X}{T}\right)^2 K_2 \left(\frac{M_X}{T}\right), \tag{3.10}$$

where, $K_2$ is the modified Bessel function of second kind [106]. Now, in order to solve the equations numerically, it is convenient to work in terms of the following dimensionless quantities,

$$\Phi = \frac{\rho_\phi a^{3(1+w_\phi)}}{m_\phi^{(1-3w_\phi)}}; \qquad R = \rho_R a^4; \qquad X = n_X a^3. \tag{3.11}$$

The Boltzmann equations[106, 138] in the re-scaled variables with the time variable $A = a/a_I$ reduces to,

$$\begin{aligned}
\frac{d\Phi}{dA} &= -c_1(1+w_\phi)\frac{A^{1/2}\Phi}{\mathbb{H}}; \\
\frac{dR}{dA} &= c_1(1+w_\phi)\frac{A^{3(1-2w_\phi)/2}}{\mathbb{H}}\Phi + c_2\frac{A^{-3/2} 2 \langle E_X \rangle \langle \sigma v \rangle \mathrm{m_{pl}}}{\mathbb{H}} \left(X^2 - X_{eq}^2\right); \\
\frac{dX}{dA} &= -c_2\frac{A^{-5/2} 2 \langle E_X \rangle \langle \sigma v \rangle \mathrm{m_{pl}}}{\mathbb{H}} \left(X^2 - X_{eq}^2\right);
\end{aligned} \tag{3.12}$$

where, $\mathbb{H} = \left(\Phi/A^{3w_\phi} + R/A + X \langle E_X \rangle / m_\phi\right)^{1/2}$ is the Hubble expansion rate and the constants $c_1$ and $c_2$ are given by

$$c_1 = \sqrt{\frac{\pi^2 g_*}{30}} \left(\frac{T_\Gamma}{m_\phi}\right)^2, \qquad c_2 = \sqrt{\frac{3}{8\pi}} \tag{3.13}$$

Here, $m_{pl}(=\sqrt{8\pi}M_p)$ is the Planck mass. The initial conditions for solving the above set of Boltzmann equations are,

$$\Phi(1) = \frac{3}{8\pi}\frac{m_{pl}^2 H_I^2}{m_\phi^4}; \qquad R(1) = X(1) = 0, \tag{3.14}$$

where, the initial Hubble expansion rate is expressed as $H_I^2 = (8\pi/3{m_{pl}}^2)\rho_\phi^{end}$. The set of Boltzmann equations can be solved for a given inflaton decay constant $\Gamma_\phi$ which, for notational convenience, has been parameterized as,

$$\Gamma_\phi = \sqrt{\frac{4\pi^3 g_*}{45}}\frac{T_\Gamma^2}{m_{pl}}\,, \tag{3.15}$$

Notice that $T_\Gamma$ here is just a parameter related to the decay rate of inflation. Usually, $T_\Gamma$ is identified as the reheating temperature by assuming an instantaneous conversion of inflaton energy into radiation at the instant of reheating [i.e., when $H(t) = \Gamma_\phi$]. We will define the temperature during reheating period in terms of radiation energy density as $T \equiv T_{rad} = \left[30/\pi^2 g_*(T)\right]^{1/4}\rho_R^{1/4}$ . Hence, as we have mentioned in the Introduction, the reheating temperature $T_{re}$ is measured from the radiation temperature $T_{rad}$ at the instant of maximum transfer of inflation energy into radiation when $H(t) = \Gamma_\phi$. Another, important bit of information we must keep in mind while connecting reheating with CMB is the existence of maximum radiation temperature during the reheating era[105, 106, 139]. The maximum temperature depends upon the reheating temperature as well as the initial condition of reheating. Depending upon the initial value of Hubble rate, the maximum temperature can be many order of magnitude higher than the reheating temperature. Hence, for any physically acceptable model, this temperature must be less than the inflationary energy scale at the end of inflation. The significance of this maximum temperature is that when producing a particle of mass greater than the reheating temperature, the abundance will not be exponentially suppressed by the reheating temperature[105]. In the next section we will derive a analytic expression for this quantity.

#### 3.3.1.1 The early time solution and the maximum temperature for general $\omega_\phi = (n-2)/(n+2)$

Before we resort to the numerical solution to find the connection among the CMB anisotropy and the dark matter abundance, let us compute an analytic expression for the maximum possible temperature during reheating phase for general equation of state of the inflaton field. In the early phase of the reheating stage ($H \gg \Gamma_\phi$), considering the initial condition $R(A_I) \simeq X(A_I) \simeq 0$ Eq.(3.12) can be solved as

$$\frac{dR}{dA} \simeq c_1(1+w_\phi)\Phi_I^{\frac{1}{2}} A^{\frac{3}{2}(1-w_\phi)} \implies R \simeq 2c_1\left(\frac{1+w_\phi}{5-3w_\phi}\right)\left[A^{\frac{5-3w_\phi}{2}} - A_I^{\frac{5-3w_\phi}{2}}\right]. \tag{3.16}$$

Therefore, by using the above solution and using the definition of temperature in terms of the radiation density, one arrive at the following expression

$$T = \left[\frac{60c_1}{g_*\pi^2}\,\frac{1+w_\phi}{5-3w_\phi}\right]^{\frac{1}{4}} m_\phi \left(\frac{\Phi_I}{A_I^{3(1+w_\phi)}}\right)^{\frac{1}{8}}\left[\left(\frac{A}{A_I}\right)^{-\frac{3}{2}(1+w_\phi)} - \left(\frac{A}{A_I}\right)^{-4}\right]^{\frac{1}{4}} \tag{3.17}$$

By using the Eq.(3.14), the maximum temperature can be found as

$$T_{\rm max} = \left[\frac{60c_1}{g_*\pi^2}\,\frac{1+w_\phi}{5-3w_\phi}\right]^{\frac{1}{4}} m_\phi^{\frac{1}{2}} \left(\frac{3}{8\pi}\frac{{\rm m}_{\rm pl}^2 H_I^2}{A_I^{3(1+w_\phi)}}\right)^{\frac{1}{8}} \times \left[\left(\frac{8}{3(1+w_\phi)}\right)^{-\frac{3(1+w_\phi)}{5-3w_\phi}} - \left(\frac{8}{3(1+w_\phi)}\right)^{-\frac{8}{5-3w_\phi}}\right] \tag{3.18}$$

For $w_\phi = 0$, the expression for maximum temperature reduces to

$$T_{\rm max} \equiv \left(\frac{3}{8}\right)^{2/5}\left(\frac{40}{\pi^2}\right)^{1/8}\frac{g_*^{1/8}(T_{\rm re})}{g_*^{1/4}(T_{\rm max})} M_p^{1/4} H_I^{1/4} T_{re}^{1/2}. \tag{3.19}$$

In the following numerical analysis for the dark matter abundance, we will find maximum temperature plays an important role in constraining the dark matter parameter space. The essential idea behind this temperature is that as the reheating temperature is measured at a later stage of reheating, the radiation production commences at the very early stage. As one can clearly see the non-trivial dependence of the temperature on the inflaton equation of state parameter ($\omega_\phi$) and the inflaton decay constant $\Gamma_\phi$. Depending upon the initial value of the Hubble rate which has a direct connection with the CMB anisotropy, the maximum temperature can be many orders higher than the reheating temperature[105, 106, 139]. Therefore, this maximum temperature will play as an intermediate scale between the inflationary energy scale and the reheating temperature. Subsequently we show how this will effect the dark matter production mechanism during depending upon the dark matter mass.

#### 3.3.1.2 Dark matter relic abundance and its $(T_{\rm re}, T_{\rm max})$ dependence

As we have emphasized already, we will describe how the present dark matter abundance is controlled by the CMB anisotropy through the inflationary model and its subsequent reheating phase. The present dark matter abundance parameterized by the normalized density parameter $\Omega_X$ can be expressed in terms of present day radiation abundance $\Omega_{\rm R}$ ($\Omega_{\rm R}h^2 = 4.3\times10^{-5}$), as follows

$$\Omega_X h^2 = \langle E_X\rangle \frac{X(T_{\rm F})}{R(T_{\rm F})}\frac{T_{\rm F}}{T_{\rm now}}\frac{A_{\rm F}}{m_\phi}\Omega_{\rm R}h^2 \tag{3.20}$$

where, $T_{\rm F}$ is the temperature at very late time when dark matter and radiation comoving energy densities became constant. The current CMB temperature is given by $T_{\rm now} = 2.35\times10^{-13}$GeV. For our subsequent discussions, it is important to know the behavior of the dark matter abundance in terms of reheating parameters $(T_{re}, M_X, \langle\sigma v\rangle)$. The analytic expressions for the dark matter abundance for different dark matter mass $M_X$ can be calculated following the references [106](see also[107, 108] for an alternative derivation). As we have considered a generic equation of state parameter for the inflaton, we are interested in the generalized expression for dark matter abundance for arbitrary $w_\phi$. The dependence of relic abundance on reheating temperature, the dark matter mass, and annihilation cross section can be expressed

as

$$\Omega_X h^2 \propto \langle\sigma|v|\rangle\, M_X^4 Exp\left[-\frac{E(w_\phi)M_X}{T_{\rm max}}\right] \quad \text{for } M_X \gtrsim T_{\rm max} \tag{3.21}$$

$$\Omega_X h^2 \propto \langle\sigma v\rangle \frac{T_{re}^{\frac{7+3w_\phi}{1+w_\phi}}}{M_X^{\frac{9-7w_\phi}{2(1+w_\phi)}}} \quad \text{for } T_{\rm max} > M_X > T_{\rm re}. \tag{3.22}$$

One can particularly notice the non-trivial dependence of $w_\phi$ for two different dark matter mass range with respect to the $T_{\rm max}$ as derived before. The proportionality factors for the above expressions and $E(w_\phi)$ has a complicated dependence on $w_\phi$, which are important for our subsequent discussions. Furthermore, if we consider the dark matter mass to be less than the reheating temperature, the *freeze-in* happens after the reheating is over. For that case the relic abundance can be expressed as [140]

$$\Omega_X h^2 \propto \langle\sigma v\rangle\, M_X\, T_{re} \qquad \text{when } M_X < T_{\rm re}, \tag{3.23}$$

For all the above three expressions for the dark matter abundance, we have considered the freeze-in mechanism. This essentially means that dark matter will never reach the equilibrium with the thermal bath. In the literature, these dark matter is known as feebly interacting dark matter(FIMP)[122–125]. In the next section, we will briefly outline the steps to connect CMB, reheating and dark matter abundance.

## 3.4 Constraints from CMB: dark matter phenomenology

In this section, we explicitly show how the CMB anisotropy can shed light on the dark matter sector considering the present value of its abundance. As emphasized before we will not consider any specific model of dark matter. The main ingredient of our analysis will be a specific model of inflation and its perturbative decay to radiation and then radiation to dark matter during the reheating phase. Considering a specific model of dark matter would be interesting to analyze. However, an important point one should remember when constructing a particle physics model is that all our analyses are at an energy of the order of inflation scale. Therefore, proper high energy modification should be taken into account for any particle physics model of dark matter. Anyway, for the present purpose, we will consider the simplest case as described before. In the subsequent subsections, we will first illustrate the general procedure to compute the dark matter abundance in terms of the CMB parameters for a chaotic inflation and then will apply the mechanism to study other observationally viable models and discuss the constraints.

### 3.4.1 Connecting CMB and reheating via inflation

In this section, we will discuss, in detail, the deep connection between the reheating phase and the CMB[61]. During inflation, the perturbation modes that became comparable to the horizon are the ones which we observe today. The PLANCK set the pivot scale $k = 0.05{\rm Mpc}^{-1}$ for determining the spectral index $n_s$. In Fig. 3.1 we depicted how various scales and phased are correlated in the inflationary-big-bang scenario. For this we considered a specific value of the inflaton equation of state. The comoving Hubble scales $a_k H_k = k$ at $(A)$ and $(D)$ in Fig. 3.1 are connected through the reheating period through the following equation

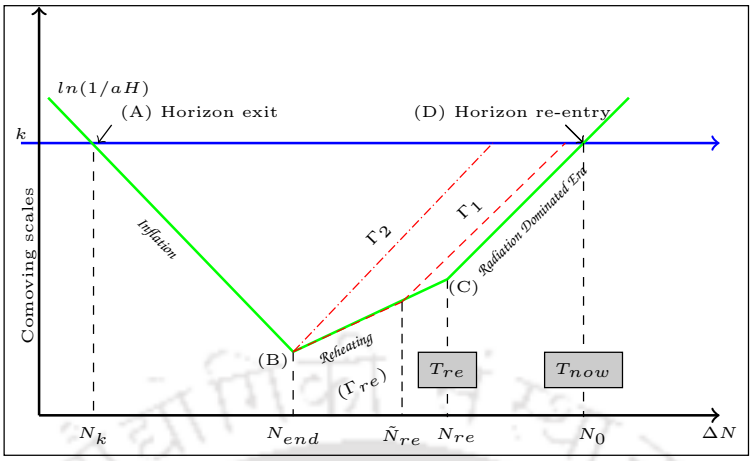


FIGURE 3.1: The comoving scales connect the inflationary phase with the CMB. The solution of Boltzmann equations for inflaton decay will connect the end of inflation denoted by the point $B$ and beginning of radiation domination denoted by the point $C$, and the consistent solution exists only for a specific inflaton decay constant $\Gamma_{\rm re}$. All other decay constants $(\Gamma_1, \Gamma_2)$ shown as red lines will not give the correct CMB temperature. Given a particular inflation model, the Boltzmann equations are solved considering three unknown parameters $(\Gamma_\phi, \langle\sigma v\rangle, M_X)$. However, imposing two other constraints Eq.(3.33) for our physical universe, we uniquely fix the value of $(\Gamma_\phi = \Gamma_{\rm re}, \langle\sigma v\rangle)$ and consequently the reheating parameters $(N_{re}, T_{\rm re})$ for a given dark matter mass $M_X$. One of the aforementioned constraint equations essentially sets the correct initial condition for the radiation domination at (C) which evolves to the currently observed CMB through standard big-bang evolution. In the conventional approach the expansion of the universe during the reheating phase is parameterized by a time-independent effective equation of state $w_{re}$. Therefore, decay of inflaton cannot be directly constrained. Here, however, we have considered the dynamical situation.

$$\ln\left(\frac{a_{\rm k}H_{\rm k}}{a_0H_0}\right) = -N_k - N_{\rm re} - ln\left(\frac{a_{\rm re}H_{\rm k}}{a_0H_0}\right). \tag{3.24}$$

As we will discuss about general inflaton equation of state, in the Fig. 3.2 we plotted the evolution of scales and phases considering different values of the effective equation state $w_{eff}$ which will be relate to $w_\phi$ non-trivially. However, from our perturbative analysis we show that behavior in terms of $w_{eff}$ depicted in the Fig. 3.2 will qualitatively be same as that in terms of $w_\phi$. In order to proceed further specifically from the radiation dominated era to the present time, one important assumption we need to make is that there is no extra entropy production in primordial plasma after reheating. More specifically the entropy is conserved. This assumption is necessary if we want to compute the reheating temperature from CMB otherwise we will only be able to give a bound on the reheating temperature through CMB. With this assumption that the reheating entropy is preserved in the CMB and the neutrino background one can arrive at the following relation,

$$a(t)^3 s = \text{const} \implies g_{re}T_{re}^3 = \left(\frac{a_0}{a_{re}}\right)^3\left(2T_0^3 + 6\times\frac{7}{8}T_{\nu 0}^3\right). \tag{3.25}$$

where, $s$ is the entropy density. $T_0 = 2.725$K is the present CMB temperature, and $T_{\nu 0} = (4/11)^{1/3}T_0$ the neutrino temperature and $g_{\rm re}$ is the effective number of light species. $H_0$ is the present value of the Hubble parameter. Therefore, combining the above two equations, one arrives at the following important equation

$$T_{\rm re} = \left(\frac{43}{11g_{\rm re}}\right)^{\frac{1}{3}}\left(\frac{a_0T_0}{k}\right)H_k e^{-N_k}e^{-N_{\rm re}}. \tag{3.26}$$

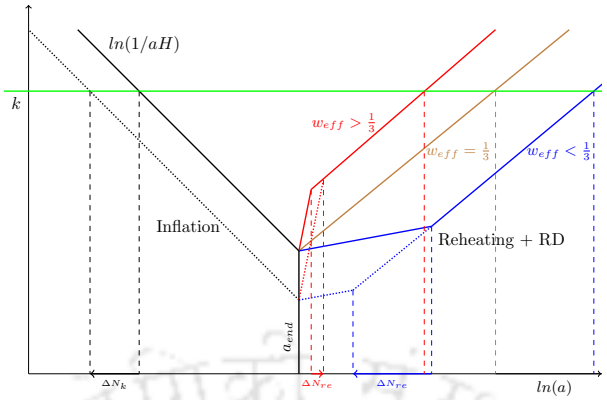


FIGURE 3.2: Evolution of the comoving Hubble horizon starting from inflation (left side black lines), reheating (intermediate lines), radiation domination up to the present time(the shorter period of matter domination and the current dark energy domination is not shown as they don't affect the qualitative conclusion). During the reheating phase when the effective equation of state $w_{eff} = 1/3$, the evolution is indistinguishable from radiation dominated phase as shown in solid brown line. This fact makes reheating parameters $(N_{re}, T_{re})$ indeterministic as observed in [61]. The evolution with $w_{eff} < 1/3$ is shown in blue intermediate lines while that of $w_{eff} > 1/3$ is shown in red intermediate lines. Increase in $n_s$ implies going from solid black line to dotted black line adding extra e-folding number $\Delta N_k$ for horizon crossing of a particular CMB mode $k$. It is clear from the figure for $w_{eff} < 1/3$, increasing $n_s$ will result in decreasing reheating e-folding number $N_{re}$, and thereby increasing reheating temperature $T_{re}$. While for $w_\phi > 1/3$ it will just be the opposite. Hence, one can clearly expect an upper bound on $n_s$ for a particular inflation model with $w_\phi < 1/3$ where the intermediate line closes indicating an instantaneous reheating with maximum possible reheating temperature. On the other hand for models with $w_\phi > 1/3$, one expects a lower bound on $n_s$. The bound on the other end of $n_s$ for both the cases will be from the condition of minimum reheating temperature for a successful BBN.

This equation thus establishes the connection between the CMB anisotropy with the reheating temperature once we know the e-folding number during reheating $N_{\rm re}$.

Now, we can have two ways to determine $N_{\rm re}$: (i), solve the scale factor and the evolution equation for the total energy density during reheating by using an effective equation of state parameter($w_{\rm eff}$) [61] of the fluid comprising inflaton and radiation during reheating, or, (ii) explicitly solve the Boltzmann equation for decaying inflaton during reheating. The first method has been widely studied in the literature. For the convenience of the reader, let us note the expression of $N_{re}$ in terms of inflationary observable and reheating parameters following the references [61, 103],

$$N_{\rm re} = \frac{4}{3w_{\rm eff}-1}\left[N_k + \ln\left(\frac{k}{a_0T_0}\right) + \frac{1}{4}\ln\left(\frac{40}{\pi^2 g_*}\right) + \frac{1}{3}\ln\left(\frac{11g_*}{43}\right) - \frac{1}{2}ln\left(\frac{\pi^2 M_{\rm p}^2\, rA_s}{2V_{\rm end}^{\frac{1}{2}}}\right)\right]. \tag{3.27}$$

where $N_k$, $r$, $A_s$, etc. are known for a specific inflationary models in terms of the spectral index $n_s$. $w_{\rm re}$ is assumed to be an effective time-independent equation of state of during reheating. The main disadvantage of this method is that it does not shed light on the microphysics of the reheating phase and its effect on the subsequent evaluation. We propose the second method [104] with added advantages that we have largely exploited in this paper. We have also stated the limitations of our approach and possible extensions. For both the cases the initial conditions will be at point "B" in Fig. 3.1 which is set by slow roll inflation constrained by the CMB observation. This connection is clearly depicted in Fig. 3.1. From the figure, it is clear that a particular inflationary model with a scalar spectral index $n_s$ sets unique initial conditions for the Boltzmann equations for decaying inflaton and its decay products during reheating. And in this phase, one of the important parameters is the inflaton decay constant

$\Gamma_\phi$ that controls the dynamics with a strong constraint that the dominant energy component will be the inflaton and the radiation. This requirement fixes a specific value of $\Gamma_\phi = \Gamma_{\rm re}$ for which Boltzmann equations predict a particular reheating e-folding number $N_{\rm re}$ and reheating temperature $T_{re}$ which finally evolves to the current value of the CMB temperature $T_0 = 2.7$K. Hence, the first part of our calculation is to figure out $\Gamma_{\rm re}$, Finally solving the Boltzmann equations has added advantages as opposed to the conventional effective equation of state method. As mentioned earlier, because of considering the explicit decay of inflaton, apart from radiation we can easily consider an addition component such as dark matter in our analysis. Because of the constraint of dark matter abundance in the present universe, we can establish a direct connection between the CMB anisotropy and the dark matter phenomenology. Therefore, this approach will lead us to establish a direct connection between the CMB and the dark matter through the inflation and reheating.

### 3.4.2 Methodology: CMB to dark matter via reheating

Let us now summarize again the connection between the CMB and dark matter phenomenology via reheating. CMB power spectrum provides the initial conditions for reheating phase through inflationary observables. While the CMB temperature is intimately connected to the reheating temperature, the reheating phase links the end of inflation and the beginning of the radiation phase parametrized by the reheating temperature. All the particles including dark matter in the universe were created during the phase of reheating through inflaton decay. Therefore, we can clearly understand the deep connection between the CMB and dark matter we see today via the reheating phase. In this section, we will discuss the methodology toward establishing this connection between the CMB anisotropy and the dark matter phenomenology we just mentioned. For any general canonical inflation model, we first identify the inflation model dependent input parameters such as $(N_k, H_k, V_{\rm end}(\phi_k))$ for a particular CMB scale $k$ (CMB pivot scale) at its horizon crossing. As has been pointed out before, given a canonical inflaton potential $V(\phi)$, the inflationary e-folding number $N_k$ and Hubble constant $H_k$ can be expressed as

$$H_k = \frac{\pi M_{\rm p}\sqrt{rA_s}}{\sqrt{2}} \quad ; \quad N_k = \ln\left(\frac{a_{\rm end}}{a_k}\right) = \int_{\phi_k}^{\phi_{\rm end}} \frac{H}{\dot{\phi}} d\phi = \int_{\phi_k}^{\phi_{\rm end}} \frac{1}{\sqrt{2\epsilon_V}} \frac{|d\phi|}{\rm M_p}. \tag{3.28}$$

In order to define above quantities, we use the following slow-roll approximated equations

$$3H\dot{\phi} = -V'(\phi) \quad ; \quad H_k^2 = \frac{V(\phi_k)}{3M_{\rm p}^2}. \tag{3.29}$$

where the field value $\phi_{\rm end}$ is computed form the condition of the end of inflation,

$$\epsilon(\phi_{end}) = \frac{1}{2M_{\rm p}^2}\left(\frac{V'(\phi_{end})}{V(\phi_{end})}\right)^2 = 1, \tag{3.30}$$

while the field $\phi_k$ at the horizon crossing in terms of the scalar spectral index $n_s^k$ can be found by inverting the following equation:

$$n_s^k = 1 - 6\epsilon(\phi_k) + 2\eta(\phi_k). \tag{3.31}$$

Once we identify all the required parameters from the inflation, the subsequent reheating phase will be described by the appropriate Boltzmann equations(3.5-3.7) and also the background

dynamics for the scale factor $a$. As emphasized earlier we will consider all the decay process to be perturbative. During the reheating phase, one of the important parameters is the reheating e-folding number $N_{\rm re}$. It connects the scale factor between the end of inflation $a_{\rm end}$ and the end of reheating $a_{\rm re}$ with following definition $N_{\rm re} = \ln(a_{\rm re}/a_{\rm end})$. In order to establish the relation between the reheating temperature $T_{\rm re}$, the inflationary index $n_s$, and dark matter parameters $(M_X, \sigma)$ we simultaneously solve the set of Boltzmann equations in the re-scaled variables given in Eq.(3.12)for numerical stability. For solving the those equation while keeping the inflation deay term $\Gamma_\phi$ and the dark matter annihilation cross section as a free parameter, we have used a Built-in Function called `PametricNDSolve` in `Mathematica`®. The code can be made available if requested. We have also verified the results of the codes in other numerical languages. The initial conditions for three components of energy density are given as,

$$\Phi(1) = \frac{3}{8\pi}\frac{\mathrm{m}_{\rm pl}^2 H_I (n_s^k)^2}{m_\phi^4}; \qquad R(1) = X(1) = 0. \tag{3.32}$$

While solving Boltzmann equations we simultaneously satisfy the following two constraint equations

$$\Omega_X h^2 = 0.12 \;\; ; \;\; T_{re} = \left(\frac{43}{11 g_{re}}\right)^{\frac{1}{3}} \left(\frac{a_0 T_0}{k}\right) H_k e^{-N_k} e^{-N_{re}}, \tag{3.33}$$

which are related to current dark matter abundance, and evolution of $T_{\rm re}$ to current CMB temperature $T_0 = 2.7$K. Therefore, we essentially solve the Boltzmann Eq.(3.12) starting from the end of inflation till the dark matter freezes out considering constraints Eq.(3.33). Following the relations given in Eqs.(3.21,3.22,3.23), the aforementioned connection are expressed as follows,

$$\begin{aligned}
&\Omega_X h^2 \propto \langle\sigma|v|\rangle\, M_X^4 Exp\left[-\frac{E(w_\phi) M_X}{T_{\rm max}}\right] \quad \text{for } M_X \gtrsim T_{\rm max} \\
&\Omega_X h^2 \propto \langle\sigma v\rangle \frac{T_{re}^{\frac{7+3w_\phi}{1+w_\phi}}}{M_X^{\frac{9-7w_\phi}{2(1+w_\phi)}}} \propto \frac{\langle\sigma v\rangle}{M_X^{\frac{9-7w_\phi}{2(1+w_\phi)}}} \left[\left(\frac{a_0 T_0}{k}\right) H_k e^{-N_k} e^{-N_{re}}\right]^{\frac{7+3w_\phi}{1+w_\phi}} \quad \text{for } T_{\rm max} > M_X > T_{re} \\
&\Omega_X h^2 \propto \langle\sigma v\rangle\, M_X\; T_{re} \propto \langle\sigma v\rangle\, M_X \left(\frac{a_0 T_0}{k}\right) H_k e^{-N_k} e^{-N_{re}} \quad \text{for } M_X < T_{re}.
\end{aligned} \tag{3.34}$$

Depending upon the mass of the dark matter we can clearly see the behavior of the dark matter parameter space intimately connected to the CMB scale and the associated temperature. Once the dark matter freezes out to the current value of dark matter abundance, one of the dark matter parameters, for instance, the cross-section $\langle\sigma v\rangle$ can be fixed for a given set of values of $(\Gamma_\phi, M_X)$. By using further condition on the end of reheating with the e-folding number $N_{\rm re} = \ln(a_{\rm re}/a_{\rm end})$,

$$H(a_{re})^2 = \frac{\dot{a}_{re}}{a_{re}} = \frac{8\pi}{3\mathrm{m}_{\rm Pl}^2}\left[\rho_\phi(\Gamma_\phi, M_X) + \rho_R(\Gamma_\phi, M_X) + \rho_X(\Gamma_\phi, M_X)\right] = \Gamma_\phi^2, \tag{3.35}$$

we fix the value of $\Gamma_\phi$ in terms of scalar spectral index $n_s$ and the dark matter mass $M_X$. In the above expression all the energy densities are written as function of $(\Gamma_\phi, M_X)$ at the end of

reheating. Upon getting the solution for all the energy components we express the reheating temperature as

$$T_{re} \equiv T_{rad}^{end} = \left[30/\pi^2 g_*(T)\right]^{1/4} \rho_R(\Gamma_\phi, n_s, M_X)^{1/4}. \tag{3.36}$$

where, radiation energy density is computed at the end of reheating

$$\rho_R(\Gamma_\phi, n_s, M_X) = \frac{R\, m_\phi^4}{A^4}\Big|_{H=\Gamma_\phi} \tag{3.37}$$

This is the temperature of the radiation component at the end of reheating. In our numerical analysis, we will feed this definition of reheating temperature into Eq.(3.33). Hence for a given dark matter mass, the reheating temperature will be fixed by the spectral index $n_s$. As mentioned earlier the connection between the reheating temperature and the inflation scalar spectral index was first pointed out in [61]. After solving all the above equations we are left with one free parameter that is the mass of the dark matter $M_X$.

With this strategy in hand, we will numerically solve the Boltzmann equations starting from the end of inflation and show how for a specific dark matter mass $M_X$ one can constrain the dark matter annihilation cross-section through the CMB anisotropy. For this, we will consider some specific inflationary models. As we have mentioned, we will use the CMB pivot scale of PLANCK, $k/a_0 = 0.05\text{Mpc}^{-1}$. All the quantities of our interest such as $(T_{\rm re}, N_{\rm re}, \langle\sigma v\rangle)$ will be studied at the aforementioned scale with respect to the inflationary power spectrum $n_s = 0.9659 \pm 0.0082$ for $\Lambda$CDM+r model from Planck data.

At this point we must mention that the production of dark matter prior to the nucleosynthesis era may have important consequences on the subhorizon perturbations of the radiation and the dark matter[141] and may also affect the annihilation rate of the dark matter[142]. A detailed study of these effects is done by following the evolution equations for perturbations of the above three components and the appropriate transfer function. These studies are beyond the scope of the present work and will be interesting study in the future.

### 3.4.3 Chaotic inflation: General results

To elucidate our method and discuss the general results, in this section we would discuss the chaotic inflationary model in detail. For all the other models we will see the qualitative behavior will be the same. The chaotic type models are represented by the power-law potentials of the form

$$V(\phi) = \frac{1}{2} m^{4-n} \phi^n. \tag{3.38}$$

where $m$ is the mass scale associated with the inflation. The initial conditions for Boltzmann equations are provided by the inflation energy density at the beginning of the reheating, which in turn will depend on the inflationary power spectrum $n_s$. To establish such a connection, and its effect on the subsequent evolution we compute the field value at the end of inflation $\phi_{\rm end} = \mathrm{M_p}\frac{n}{\sqrt{2}}$ using the condition for the end of slow roll inflation $\epsilon(\phi) = 1$. Therefore, using this we get the initial condition for the reheating phase as defined in Eq.(3.14)

$$\Phi(1) = \frac{3}{8\pi}\frac{\mathrm{m_{pl}^2} H_I^2}{m_\phi^4} \simeq \frac{4V_{\rm end}}{3m_\phi^4} = \frac{2}{3}\frac{m^{4-n}}{m_\phi^4}\left(\frac{n M_{\rm p}}{\sqrt{2}}\right)^n; \quad R(1) = X(1) = 0. \tag{3.39}$$

Other important quantities that are directly connected with the CMB anisotropy through the relations Eq. (3.24) are

$$H_k = \frac{\pi M_{\rm p}\sqrt{r_k A_s}}{\sqrt{2}} = \frac{\pi M_{\rm p}\sqrt{\frac{8n}{n+2}(1-n_s^k)A_s}}{\sqrt{2}} \quad ; \quad N_k = \ln\left(\frac{a_{\rm end}}{a_k}\right) = \left[\frac{n+2}{2(1-n_s^k)} - \frac{n}{4}\right], \tag{3.40}$$

where, the scalar spectral index $n_s^k$ and consequently the tensor to scalar ratio $r_k$, for a particular CMB scale $k$ are expressed in terms of the inflaton field as

$$n_s^k = 1 - \frac{2n(1-n)M_{\rm p}^2}{\phi_k^2} - \frac{3n^2 M_{\rm p}^2}{\phi_k^2} \quad ; \quad r_k = \frac{8n}{n+2}(1-n_s^k). \tag{3.41}$$

$\phi_k$ is the inflaton field value for a particular scale $k$. And finally, using Eqs.(3.28, 3.29, 3.40 and 3.41)the parameter $m$ in terms of the spectral index is found to be

$$m = M_{\rm p}(3\pi^2 r A_s)^{\frac{1}{4-n}}\left[\frac{1-n_s}{n(n+2)}\right]^{\frac{n}{2(4-n)}}. \tag{3.42}$$

Another important quantity before solving the Boltzmann equations is to know the equation of state parameter, which for the power-law potential is given in Eq.(4.36). For, $n = 2$, the homogeneous inflaton field will behave as pressureless dust with equation of state $w_\phi = 0$.

Now, in order to establish the relation between the reheating temperature $T_{re}$ and the inflationary index $n_s$, we follow the methodology explained before. The numerical procedure would be to first solve the set of Boltzmann Eqs.(3.12) considering inflaton decay constant, $\Gamma_\phi$ and annihilation cross-section $\langle\sigma v\rangle$ as free parameters. The initial condition for the inflaton energy density is fixed by the spectral index as discussed earlier. Once the solution for the radiation energy density during reheating is known, we simultaneously solve Eq.(3.35) and Eq.(3.26) relating the reheating temperature with the current CMB temperature in a self-consistent manner.

For any other model, we will follow the same procedure discussed above. As we have already mentioned and elaborated in the introduction, in the usual reheating constraint analysis [61], the connection between the inflationary parameters $(n_s^k, N_k)$, the reheating parameters $(T_{re}, N_{re})$ and the CMB temperature $T_0$ are established based on two important assumptions. First one is the effective single fluid description of the reheating phase with a time independent equation of state. The second assumption is that the inflaton energy is completely transferred into radiation at an instant $H = \Gamma_\phi$. We have already stressed earlier that all those two assumptions are obviously not correct. In addition, we also have considered additional dark matter field into the picture. Therefore, we compare our result with the usual formalism and the difference will be displayed in various plot. Including the dark matter component in the reheating constraint analysis and generalizing the formalism given in [104], we will solve the system of Boltzmann equation in (3.12) taking inflaton decay rate $\Gamma_\phi$ as a free parameter. For this, the initial condition is set by CMB power spectrum via inflation as given in Eq.(3.39). From our analysis, we will see that one of the free parameters $\Gamma_\phi$ will be fixed by $n_s$ through reheating temperature Eq.(3.26). At this point, there are several important questions we will ask such as a) Does the dark matter mass has any effect on the reheating temperature? As we have already stated in the introduction, b) Does the CMB play any role in understanding the properties of dark matter and its production mechanisms?

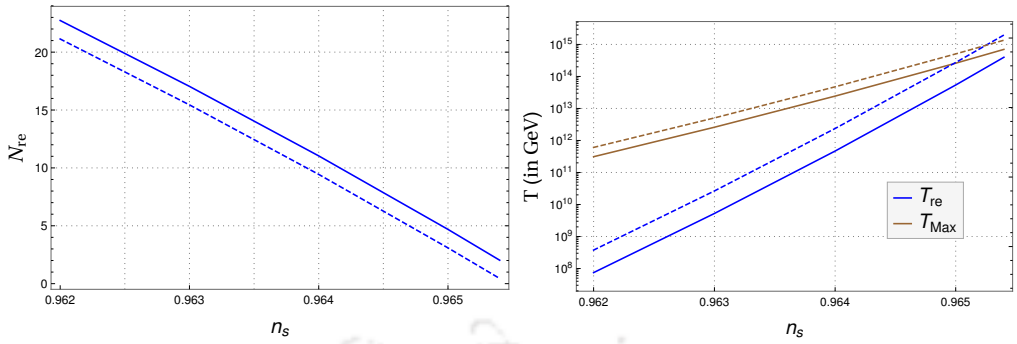


(a) (b)

FIGURE 3.3: Variation of (a) reheating e-folding number $N_{\rm re}$ and (b)the reheating temperature $T_{\rm re}$ and the maximum radiation temperature $T_{\rm max}$ with respect to $n_s$ have been plotted. For comparison, dashed lines are shown from the Ref.[61] where the complete conversion from inflaton to radiation has been assumed. We clearly see the order of magnitude difference in the temperature at the moment we include the explicit decay of inflaton in the reheating analysis [104]. These two plots are independent of dark matter masses for a set of given initial conditions.

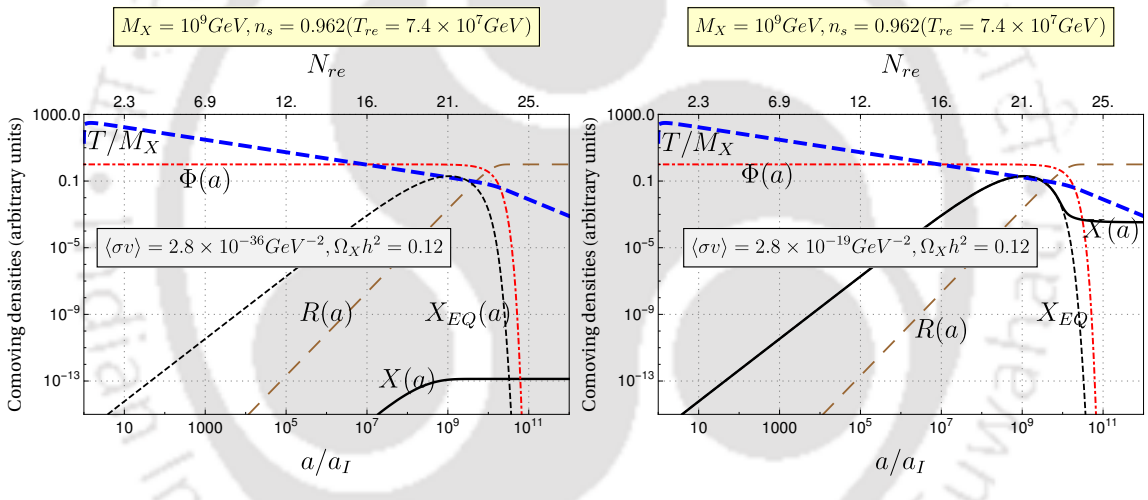


(a) (b)

FIGURE 3.4: We have two different dark matter production mechanisms as described in the text: (a) Freeze-in and (b) Freeze-out as discussed. Choosing the same dark matter mass and reheating temperature, we can realize these two production mechanisms depending upon its annihilation cross section $\langle\sigma v\rangle$. The figures here show the evolution of different components(in some suitable units) the inflaton(red dot dashed), the radiation(brown dashed line) and the temperature(thick blue dashed line) with the normalized scale factor( alternatively, the e-folding number after the end of inflation). Black dashed lines show the evolution of equilibrium dark matter distribution while the black solid line is for the dark matter. In this work we will exclusively assume the dark matter production via freeze-in mechanism when connecting the current relic abundance with CMB.

Throughout the subsequent discussions, we will try to answer the aforementioned questions. Even though the dark matter will play important role after reheating we have not found any significant effect of it's mass or the annihilation cross-section on $(T_{\rm re}, N_{\rm re})$ provided the produced dark matter relic abundance is within the current dark matter relic abundance. In Fig. 3.3, we have plotted $(N_{re}, T_{re})$ with respect to $n_s$. An important observation is the existence of a maximum reheating temperature where two radiation temperature $T_{\rm max}$ and $T_{\rm re}$ meet at around $(n_s^{\rm max} \simeq 0.9656, T_{\rm re}^{\rm max} \simeq 10^{15}{\rm GeV})$. This is the point where the reheating

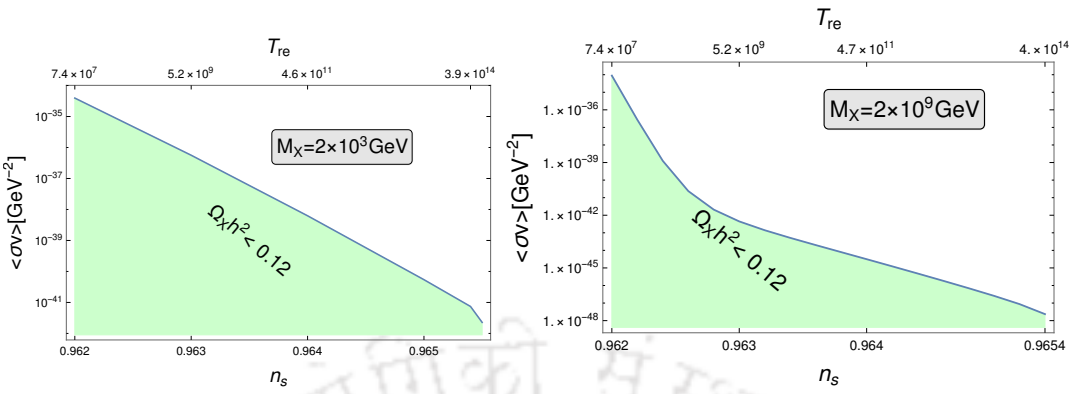


FIGURE 3.5: For fixed dark matter mass, we have plotted the contour of $\Omega_X h^2 = 0.12$ in the $n_s$-$\langle\sigma v\rangle$ plane. The reheating temperature which is fixed once we know the spectral index is also plotted on the upper axis. The shaded region below the contour line is the parameter space allowed by current dark matter abundance. Here, we have considered the dark matter masses (a)$10^9 GeV$ and (b)$10^3 GeV$ for the chaotic $m^2\phi^2$ model.

process is almost instantaneous. If we consider $1\sigma$ range of $n_s$ from PLANCK, one also gets minimum reheating temperature $T_{\rm re}^{\rm min} \simeq 6 \times 10^7$ GeV for $n_s \simeq 0.962$. At this point let us emphasize the difference between the result of our analysis(solid line) and the usual reheating constraint analysis(dashed line) following the reference [61]. It clearly shows one order of magnitude difference in reheating temperature. The source of this difference is coming from the incomplete decay of inflaton to radiation field. Finally, we numerically fitting the data, and the relation between the reheating temperature $T_{re}$ and spectral index $n_s$ is found as,

$$log\,(T_{re}) \simeq Q_p\left[A + B(n_s - 0.962) + C(n_s - 0.962)^2\right]. \tag{3.43}$$

where, the dimensionless constants $A = 8$, $B = 1.8 \times 10^3$ and $C = 5.5 \times 10^4$, turned out to be almost model independent. The reason may have its origin in the same mechanism that is responsible for the inflaton decay into the radiation. Model dependence in the above expression for reheating temperature comes only through the parameter $Q_p$. To complete the discussion, let us mention here that for a chaotic and $\alpha-$attractor model with $\alpha = 1$, the value of $Q_p$ turned out to be unity. Also, our numerical fitting shows that for different $\alpha$ values, $Q_p \sim log_{10}(\alpha)/\alpha^{1/2}$ and for natural inflation $Q_p \propto 1/f_b$. Let us now turn to question-b, which is the main purpose of this work. In the previous section, we have established one-to-one correspondence between $n_s$ and $T_{\rm re}$. This fact provides us a way to figure out the direct connection between the CMB anisotropy and the dark matter via reheating. Before we discuss the constraints, we emphasize again the fact that dark matter production mechanism can be either freeze-in or freeze-out depending upon the couplings as has been discussed in the introduction. However, we will consider the dark matter production via freeze-in mechanism in this work. However, let emphasize the fact that for $M_X \gg T_{\rm re}$, freeze-in is the only mechanism that satisfies correct dark matter abundance namely $\Omega_X h^2 \leq 0.12$. This is also clearly seen for a specific case shown in the Fig. 3.4. For $M_X < T_{re}$, we have only considered the dark matter production via the freeze-in mechanism. We will study other mechanisms in more detail in our future work. Given a specific mechanism, we constrain the dark matter parameter space depending upon a specific inflationary model. In the Fig. 3.5, we have plotted annihilation cross-section $(\langle\sigma v\rangle, n_s)$ for different dark matter masses considering specific chaotic

model $n = 2$. The important point one infers from those plots is that the CMB temperature correlation can directly constrain the dark matter parameter space $(M_X, \langle\sigma v\rangle)$ through the inflationary power spectrum $n_s$. For a given value of $n_s$, one can precisely predict the value of annihilation cross-section once the dark matter mass is fixed. As an example given a dark matter mass $M_X = 2\times10^3$ GeV, CMB anisotropy restricts the annihilation cross-section within $10^{-35}\text{GeV}^{-2} > \langle\sigma v\rangle > 10^{-41}\text{GeV}^{-2}$ for $2\sigma$-region of $n_s$.

Depending upon the value of dark matter mass our main results of the current paper are the following important relations: i) If $M_X > T_{\rm re}$, the dark matter freezes in before the reheating and the relic abundance for a fixed dark matter mass behaves as $\Omega_X h^2 \propto \langle\sigma v\rangle\, T_{re}^7$ [105, 106]. Therefore, we established an important relation between the annihilation cross-section $\langle\sigma v\rangle$ and the scalar spectral index $n_s$ considering the current value of the dark matter relic abundance as

$$\langle\sigma v\rangle\Big|_{M_X>T_{\rm re}} \propto 10^{-7A-7B(n_s-0.962)-7C(n_s-0.962)^2}. \tag{3.44}$$

ii) In a similar manner, for $M_X < T_{\rm re}$, the dark matter freezes in during the radiation dominated phase following the relation $\Omega_X h^2 \propto \langle\sigma v\rangle\, T_{\rm re}$[140]. In this case also we will have following important relation in different dark matter mass regime,

$$\langle\sigma v\rangle\Big|_{M_X<T_{re}} \propto 10^{-A-B(n_s-0.962)-C(n_s-0.962)^2}. \tag{3.45}$$

So far, all our important findings were based on the chaotic inflation. In the subsequent sections we will consider various other prominent inflationary models.

### 3.4.4 Natural inflation

The natural inflation model[143, 144] proposed in the early 1990s is one of the best theoretically motivated models of inflation. The prediction of this model is marginally consistent with the recent observations.* The inflationary potential in this case is given by

$$V(\phi) = \Lambda^4\left[1-\cos\left(\frac{\phi}{f}\right)\right]. \tag{3.46}$$

where $\Lambda$ is the height of the potential setting the inflationary energy scale, and $f$ is the width of the potential known as the axion decay constant in particle physics. To be consistent with the CMB data this model needs a super-Planckian value of axion decay constant. We have taken $f = 10\text{M}_\text{p}$ and $f = 50\text{M}_\text{p}$ for illustration. During reheating, the potential may be approximated as a power-law potential by expanding it around the minimum as long as $\phi < f$

$$V(\phi) \simeq \frac{1}{2}\frac{\Lambda^4}{f^2}\phi^2 \tag{3.47}$$

From, this expression of potential it is easy to identify the inflaton mass by tree-level expression

$$m_\phi = \frac{\Lambda^2}{f} \tag{3.48}$$

while the inflation equation of state from Eq.(4.36), is found to be $w_\phi = 0$. The CMB

*It has been shown in[145] that by considering the neutrino properties in calculating $n_s$, this model may comply well with observation.

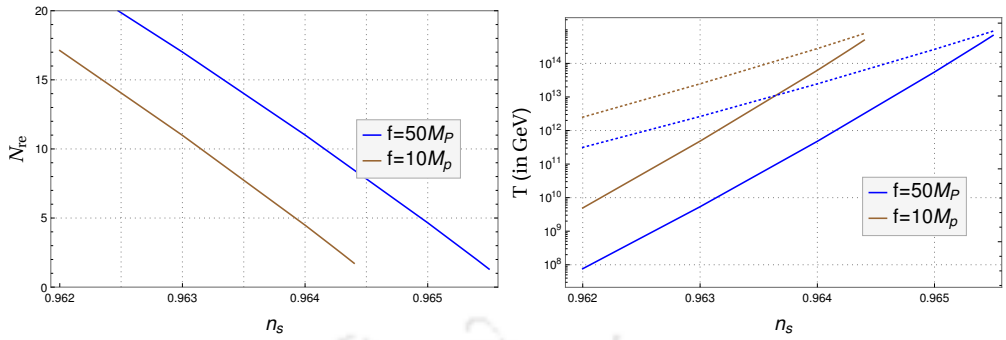


(a) (b)

FIGURE 3.6: Variation of (a) $N_{\rm re}$ and (b) $(T_{\rm re}, T_{\rm max})$ with respect in $n_s$ have been plotted for for axion decay constant $f = (10, 50)$ $\rm M_p$. The duration of reheating increases with $f$ as a result the reheating temperature decreases with increasing $f$

normalization defined as $A_s$ fixes the value of $\Lambda \simeq 10^{16}$ GeV. Therefore, by tuning the value of the axion decay constant $f$ we can fit model with respect to the observation. For the usual quadratic axion potential near its minimum, we consider effective equation state $w = 0$ during reheating. From Fig. 3.6 the behavior of the $(N_{\rm re}, T_{\rm rad})$ in terms of $n_s$ can be summarized as follows: with decreasing $f$, the model becomes increasingly disfavored as it is going out of the $1\sigma$ range of $n_s = 0.9682 \pm 0.0062$. This conclusion is anyway true just from the $(n_s, r)$ curve for the axion inflation. It is also interesting to notice that for a particular $n_s$, with decreasing $f$, the reheating temperature increases in accord with the decreasing reheating e-folding number $N_{\rm re}$. Within the $1\sigma$ range our numerical computation shows that $f = 6\rm M_p$ is disfavored as it predicts the maximum value of $n_s^{\rm max} \simeq 0.957$ which outside the $1\sigma$ range of $n_s$ from PLANCK. However for $f = (10, 50M_{\rm p})$, we found $n_s^{\rm max} \simeq (0.9644, 0.9655)$ at which $N_{\rm re} = (1.72, 1.3)$. For both the cases, the lowest $n_s \simeq 0.962$ corresponds to the minimum reheating temperature $T_{\rm re}^{\rm min} \simeq (4.9 \times 10^9, 7.6 \times 10^7)$ in GeV units. Now we are in a position

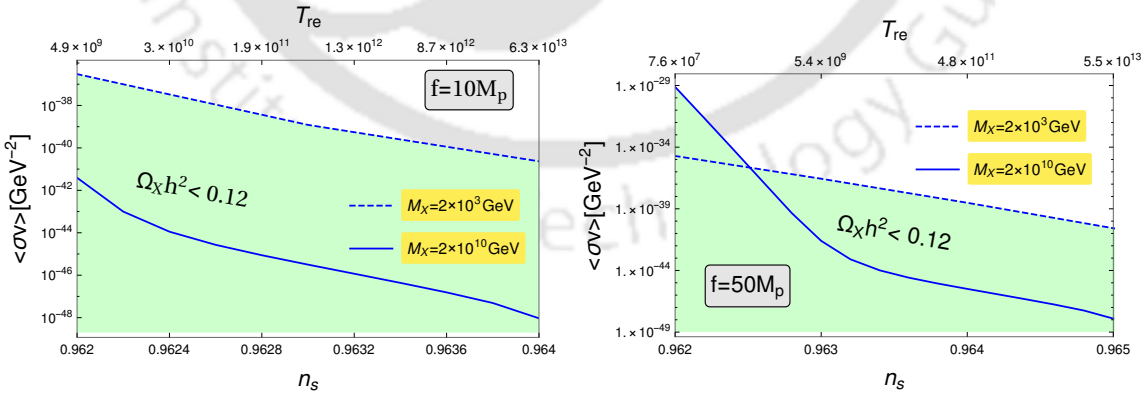


(a) (b)

FIGURE 3.7: The same plot as in Fig. 3.5 for the natural inflation model. Axion decay constant for Fig.(a) is $f = 10\rm M_p$ and for (b) $f = 50\rm M_p$.

to figure out the effect of the axion inflation model in the dark matter phenomenology. In

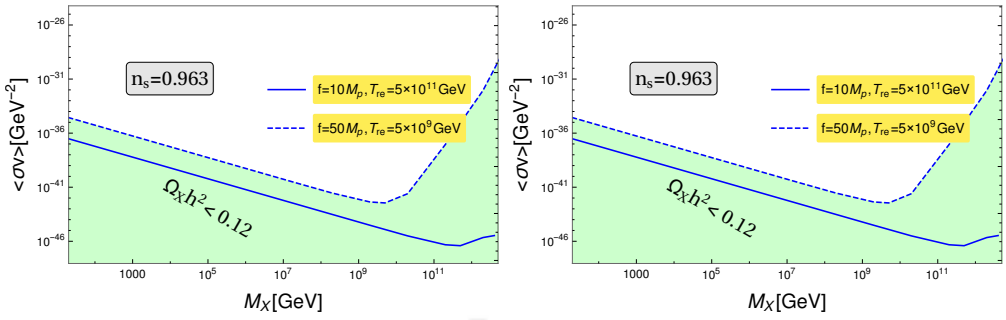


(a) (b)

FIGURE 3.8: The same contour plot as in Fig. 3.5 in the $M_X$-$\langle\sigma v\rangle$ space for the natural inflation model. Axion decay constant for Fig.(a) is for to $f = 10\mathrm{M_p}$ and for (b) $f = 50\mathrm{M_p}$.

Fig. 3.7, and Fig. 3.8, we have displayed the allowed regions of parameter space for a single component dark matter based on the constraints from CMB observation. The allowed region in ($n_s$ Vs $\langle\sigma v\rangle$) space from the current dark matter relic abundance is shown in Fig. 3.7 for two sample values of dark matter mass $M_X = (2 \times 10^3, 2 \times 10^9)$ GeV. For $f = 10M_\mathrm{p}$, the reheating temperatures for all the spectral indexes are higher than both the masses and they freeze-in in the radiation dominated era. However, for $f = 50M_\mathrm{p}$ and the dark matter mass $10^9$ GeV, we will have two distinct behaviors given in Eqs.(3.44-3.45), which are also reflected in the change of slopes of the contour plots Fig. 3.7 for $\Omega_X h^2 = 0.12$. The analytic expression for the relic abundance in the different regions can be found in [106, 108]. In Fig. 3.8 we present the allowed region in parameter space of ($M_X$ $Vs$ $\langle\sigma v\rangle$) for a fixed value of $n_s$ corresponding to two different reheating temperatures $T_\mathrm{re} \simeq (5 \times 10^{11}, 5 \times 10^9)$ GeV for two different vales $f = (10, 50)$ $M_\mathrm{p}$. From the physical point of view as expected for a particular value of $n_s = 0.963$, there exists a minimum value of the annihilation cross-section $\langle\sigma v\rangle \simeq (5 \times 10^{-47}, 5 \times 10^{-43})$ for $f = (10, 50)$ $M_\mathrm{p}$ and $M_X = (5 \times 10^{11}, 5 \times 10^9)$ GeV which are of same order as the reheating temperature. From the physical point of view, this fact can be understood as follows: for dark matter mass $M_X > T_\mathrm{re}$, the freeze-in temperature $T_\mathrm{freeze} > T_\mathrm{re}$, during which the radiation density is very small as most of the energy is in the form of oscillating inflaton field. Therefore, in order to achieve the current dark matter abundance $\Omega_X h^2 \simeq 0.12$ one needs to increase the annihilation cross-section as we increase the value of dark matter mass. However, for $M_X < T_\mathrm{re}$, the freeze-in temperature is obviously $T_\mathrm{freeze} < T_\mathrm{re}$, which is in the radiation dominated phase, and most importantly the radiation temperature $T_{rad}$ becomes inversely proportional to the cosmological scale factor. Therefore, dark matter abundance crucially depends upon the freeze-in time or freeze-in temperature. With the decreasing $M_X$ the freeze-in happens at a late time or, in other words, at a lower value of the freeze-in temperature. This late time freeze-in will naturally reduce the dark matter abundance. Hence below the reheating temperature, with decreasing $M_X$, one needs to increase cross-section $\langle\sigma v\rangle$ in order to produce correct dark matter abundance.

### 3.4.5 Alpha attractor

In this section will consider a class of models called $\alpha$-*attractor* model[55–57, 75, 146, 147] which has recently been proposed to unify different inflationary models parametrized by parameter $\alpha$. The uniqueness of this class of models is its conformal property which leads to a universal

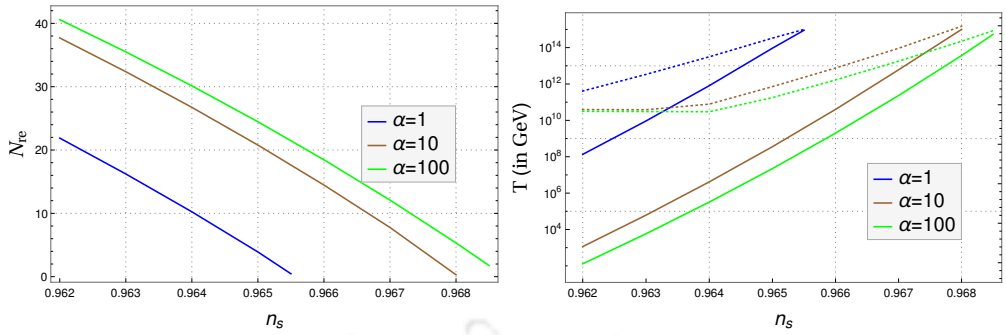


(a) (b)

FIGURE 3.9: Variations of (a) $N_{\rm re}$ and (b) $(T_{\rm re}, T_{\rm max})$ with respect to $n_s$ have been plotted for $\alpha$-attractor model. We have considered three sample values of $\alpha = (1, 10, 100)$.

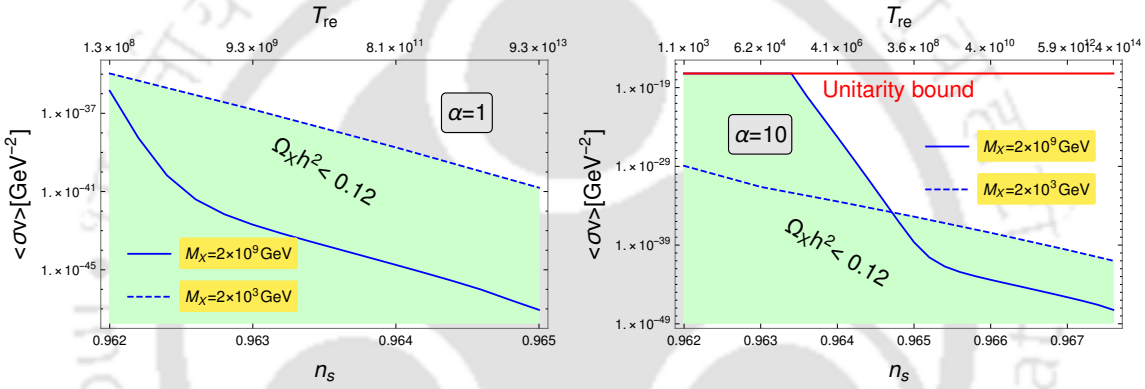


(a) (b)

FIGURE 3.10: The shaded region shows the region in the parameter space allowed by current dark matter abundance for two dark matter masses in the $\alpha$-attractor $E$ model. (a) Corresponds to $\alpha = 1$, while (b) is for $\alpha = 10$.

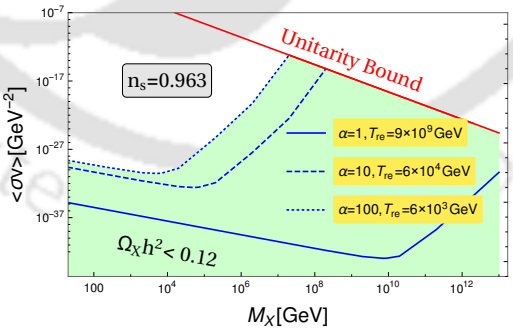


FIGURE 3.11: Considering a sample value of $n_s$ or equivalently $T_{re}$ as given, we plotted $(\langle\sigma v\rangle vs M_X)$ for $\alpha$-attractor $E$-model, for $\alpha = (1, 10, 100)$. Solid red line corresponds the unitarity limit $\langle\sigma v\rangle \propto 1/MX$.

prediction for the inflationary observables $(n_s, r)$ in favor of Planck observation [53]. After the conformal transformation of a large class of originally noncanonical inflaton field Lagrangian, one generically gets canonically normalized inflaton field with an exponential potential of the following form

$$V(\phi) = \Lambda^4 \left[1 - e^{-\sqrt{\frac{2}{3\alpha}}\frac{\phi}{M_{\rm p}}}\right]^{2n} \tag{3.49}$$

In the literature, this model is known as $E$ model. The quantities that we will need for solving the Boltzmann equation is the inflaton equation of state parameter and the inflaton mass, which we will get by expanding the potential around the minimum when $\sqrt{\frac{2}{3\alpha}}\phi_{\rm end} < M_{\rm p}$ which is equivalent to choosing $\alpha > 0.5n^2$.

$$V(\phi) \simeq \Lambda^4 \left(\frac{2}{3\alpha}\right)^n \left(\frac{\phi}{M_{\rm p}}\right)^n \tag{3.50}$$

Now, it is easy to identify the inflaton mass with the tree-level expression as

$$m_\phi = \frac{2\Lambda^2}{\sqrt{3\alpha}M_{\rm p}} \tag{3.51}$$

and the equation of state parameter, as noted before, is given by $w_\phi = 0$.

As has been discussed for natural inflation, in this case also we found $\Lambda \simeq 10^{16}$ GeV. The new parameter $\alpha$ determines the shape of the canonically normalized inflaton potential near the minimum. The qualitative behavior of all the plots will be the same as for the other models we have discussed so far. However, the reheating temperature in this class of models can be very small depending on the value of the $\alpha$ parameter. For the purpose of our current study, we have taken $n = 1$ and $\alpha = (1, 10, 100)$ for illustration. It is important to note that $\alpha = 1$ encodes two important well studied inflationary models, namely Starobinsky[6] and Higgs[148] inflation. Nonetheless, some important facts can be observed from the Fig. 3.9 as follows: we clearly see that as one increases the value of $\alpha$, the reheating temperature decreases for a fixed value of $n_s$. For example at $n_s = 0.962$ which is the lowest of $1\sigma$ range from PLANCK, we found $T_{\rm re}^{\rm min} \simeq (10^8, 10^3, 10^2)$ GeV for $\alpha = (1, 10, 100)$ respectively. The qualitative behavior on the constraints on the dark matter parameter space appeared to be the same as that of the chaotic and natural inflation cases discussed in the previous sections. Specifically, let us emphasize again one of the important results of our analysis shown in Eq.(3.44) Eq.(3.45), which will be satisfied for the $\alpha$-attractor model as well. However, from fig.Fig. 3.10,Fig. 3.11, we point out that with increasing $\alpha$, the annihilation cross-section increases for a fixed value of the dark matter mass. This fact could be an interesting point to further understand from the theoretical point of view. From our naive numerical solution of Boltzmann equations one finds that for higher value of $\alpha$, the annihilation cross could be arbitrarily large depending upon the value of $n_s$ or equivalently the reheating temperature $T_{\rm re}$. However, this should not hold true as the unitarity limit on $\langle\sigma v\rangle_{\rm max} = 8\pi/M_X^2$ restrict the allowed region of $n_s$. Therefore, one gets a lower limit on the value of $n_s$ which is coming from the dark matter sector. For example, from Fig. 3.10 if one considers $\alpha = 10, M_X = 2 \times 10^9$ GeV, the lowest possible value is $n_s = 0.9634$ set by the unitarity limit(red line). On the other hand, the highest value of the $n_s^{\rm max} \simeq 0.968$ does not depend upon the dark matter parameters as has already been pointed out. This important constraint on the $n_s$ coming from dark matter sector could be very important to understand and needs further study.

### 3.4.6 Minimal Plateau model

In this section we will study the predictions for minimal plateau model introduced in Chapter 2. The simplest chaotic inflationary models $V(\phi) \propto \phi^n$ are now ruled out from observational data.

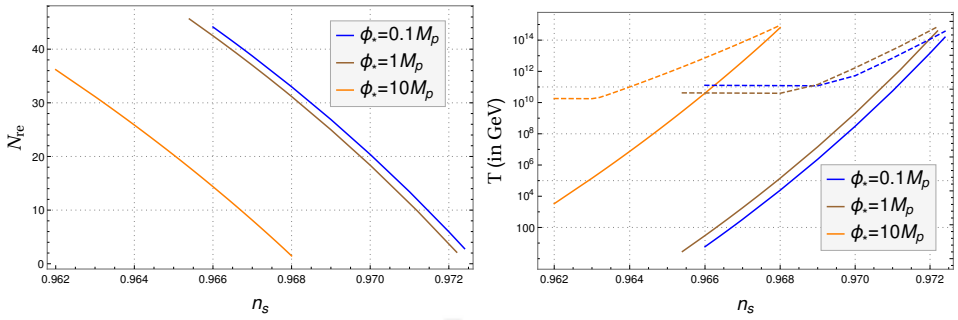


(a) (b)

FIGURE 3.12: Evolution of (a) Reheating e-folding number $N_{\rm re}$ during reheating and (b) the reheating temperature $T_{re}$(solid lines) and the maximum temperature $T_{\rm max}$(dotted lines) with respect to $n_s$ for $n = 2$ for three different values of $\phi_*$. If one extrapolates the solid and dotted lines, one will have maximum reheating temperature $T_{\rm re}^{\rm max} \simeq 10^{15}$ GeV. All the plots are independent of dark matter masses for a set of given initial condition.

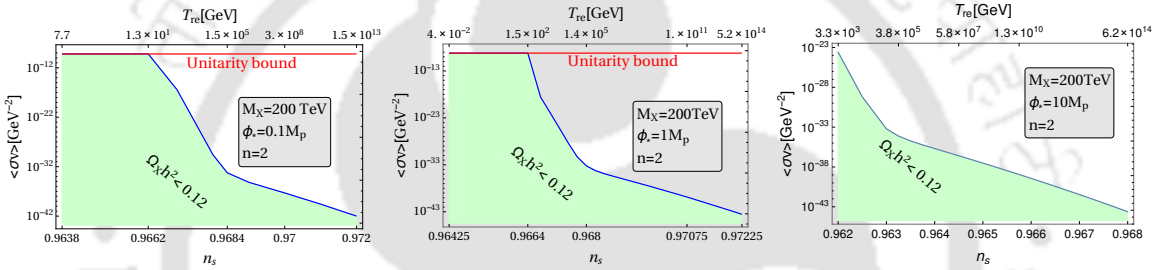


(a) (b) (c)

FIGURE 3.13: ($\langle\sigma v\rangle$ *vs* $n_s$) were plotted for three values of $\phi_*$ and $n = 2$. The blue line with green shaded region corresponds to dark matter abundance $\Omega_X h^2 \leq 0.12$. We consider three possible values of $\phi_*$. For all the cases we have chosen a dark matter mass $M_X = 200TeV$. Red horizontal line corresponds unitarity bound described in the main text.

However, as we have seen that the plateau type inflationary models when the potential during reheating can be well represented by the above from of chaotic power-law potentials. This help us to study the effects of effects of general equation of state parameters for different models related by the equation $w_\phi = (n-2)/(n+2)$ on the reheating phase. Below we will study the reheating and dark matter production with the mechanism developed in this chapter for general equation of state parameter.

#### 3.4.6.1 Results and constraints: Model n=2

This is similar to the usual quadratic chaotic model. However, as we have seen before the new parameter $\phi_*$ controls the behavior of cosmological parameters in a significant way. From the Fig.(3.12.a-b) we see the behavior of $N_{\rm re}$ and $(T_{\rm re}, T_{\rm max})$ in terms of $n_s$. It is evident that the allowed region of $n_s$ shifts towards lower values as we increase $\phi_*$, which in fact resembles the usual chaotic inflation. For $\phi_* < M_{\rm p}$ we have small field inflation and the values of $(n_s, r)$ are in agreement with the observation.

For these small field models, therefore, within the $1\sigma$ range of $n_s$, very small reheating temperature can be achieved. For example at the central value of $n_s = 0.968$, reheating temperature turned out to be $10^4 \sim 10^5$ GeV for $\phi_* = (1, 0.1)M_{\rm p}$, whereas for $\phi_* = 10M_{\rm p}$,

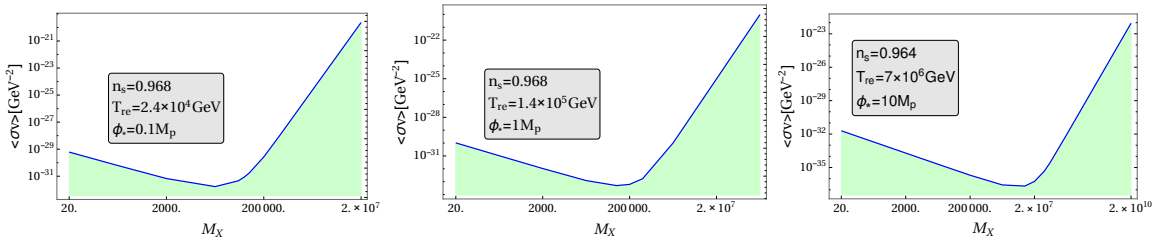


(a) (b) (c)

FIGURE 3.14: ($\langle\sigma v\rangle$ *vs* $M_X$) were plotted for three values of $\phi_*$ and $n = 2$. Depending upon the available ranges of temperature within the $1\sigma$ range of $n_S$, we have considered three possible values of $n_s$. Minimum of the blue curve corresponds to the equality $M_X = T_{re}$. It is obvious that at this point the required value of the cross-section is minimum for a given abundance $\Omega_X h^2 = 0.12$.

Table 3.1: Model parameters and associated constrains on dark matter parameters for $n = 2$, $M_X = 200$GeV

$\phi_* = 0.1M_{\rm p}$

| $n_s$ | $N_{\rm re}$ | $T_{\rm re}$(GeV) | $\langle\sigma v\rangle$GeV$^2$ |
|---|---|---|---|
| 0.966 | 44 | 5.8 | *unitarity* |
| 0.968 | 33 | $2.4\times10^{4}$ | $3\times10^{-30}$ |
| 0.970 | 20 | $3\times10^{8}$ | $5\times10^{-38}$ |
| 0.972 | 6 | $1.5\times10^{13}$ | $1\times10^{-42}$ |

$\phi_* = 1M_{\rm p}$

| $n_s$ | $N_{\rm re}$ | $T_{\rm re}$(GeV) | $\langle\sigma v\rangle$GeV$^2$ |
|---|---|---|---|
| 0.966 | 42.5 | 30.1 | *unitarity* |
| 0.968 | 31 | $1.4\times10^{5}$ | $6\times10^{-34}$ |
| 0.970 | 18 | $2\times10^{9}$ | $2\times10^{-40}$ |
| 0.9722 | 2 | $3.8\times10^{14}$ | $3\times10^{-44}$ |

$\phi_* = 10M_{\rm p}$

| $n_s$ | $N_{\rm re}$ | $T_{\rm re}$(GeV) | $\langle\sigma v\rangle$GeV$^2$ |
|---|---|---|---|
| 0.962 | 36 | $3.3\times10^{3}$ | $3\times10^{-24}$ |
| 0.964 | 26 | $7.4\times10^{6}$ | $2\times10^{-36}$ |
| 0.966 | 14 | $4\times10^{10}$ | $4\times10^{-40}$ |
| 0.968 | 1.5 | $6\times10^{14}$ | $3\times10^{-44}$ |

reheating temperature is very high $\sim 10^{14}$ GeV. These fact can be seen from sample values given in the Table 3.1 and also from the fig.(3.12.a-b). The lower limit of the value of $n_s$ is set from BBN constraints[10, 92–94], which is $T_{\rm re} \sim 0.1$GeV. On the other hand, we can see from the all the plots as well as from the data tables, there exists a maximum temperature(corresponding to the instantaneous reheating) irrespective of the value of the scale $\phi_*$.

In addition to the one to one correspondence between $n_s$ and $T_{re}$, we simultaneously get constraints on the dark matter parameter space as shown in Fig. 3.13, and Fig. 3.14. We have chosen a sample dark matter mass $M_X = 200TeV$. It is clear that once $n_s$ is fixed, for a given $(\phi_*, M_X)$, the scattering cross-section is also fixed. Therefore, within the $1\sigma$ range of $n_s$, the dark matter cross-section $\langle\sigma v\rangle$ is bounded given the value of dark matter abundance $\Omega_X h^2 = 0.12$. More importantly depending upon the values of $(M_X, n_s)$ the freeze-in will occur in three different regimes as we have already described in detail and also can be observed in the change of slopes of blue curves as a function of $n_s$ as shown in Figs.(3.13-3.14). From our analysis, we see that for a fixed dark matter mass, annihilation cross-section increases with decreasing $n_s$. However, as the cross section can not be arbitrarily large, the unitarity limit on $\langle\sigma v\rangle_{\rm max} = 8\pi/M_X^2$ restricts the allowed region of $n_s$ at its lowest value. From Figs.(3.13.a-b) when, $\phi_* = 0.1M_{\rm p},\ 1M_{\rm p}$ the production of dark matter particle of mass $200TeV$ for lower $n_s$ regime is forbidden due to the unitarity bound(shown as red line). The lowest possible value of $n_s$ turns out to be around 0.9664 and the highest value $n_s^{\rm max} \simeq 0.968$ for $\phi_* = 10{\rm M_p}$. For $\phi_* = (0.1, 1){\rm M_p}$, it turned out that $n_s^{\rm max} \simeq 0.972$ as has already been noted before, depend upon the maximum attainable temperature for the model. This important constraint on the

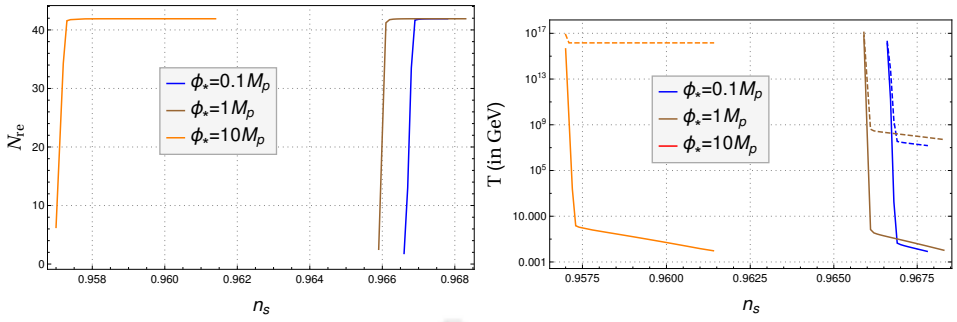


(a) (b)

FIGURE 3.15: Evolution of (a) Reheating e-folding number $N_{\rm re}$ during reheating and (b) the reheating temperature $T_{re}$(solid lines) and the maximum temperature $T_{\rm max}$(dotted lines) with respect to $n_s$ for $n = 4$ for three different values of $\phi_*$. We have will same $T_{\rm re}^{\rm max} \simeq 10^{15}$ GeV.

value of $n_s$ coming from dark matter sector could be very important to understand and needs further study. Figs.(3.14.d-f) illustrates the conventional behavior of annihilation cross-section in terms of dark matter mass. However, an important point we would like to make again is that depending upon the value of inflationary power spectrum $n_s$ or CMB anisotropy, we can shed light on the possible production mechanism given the value of dark matter mass.

#### 3.4.6.2 Results and constraints: Model n=4

This is a very special case out of all the models. One of the main reasons is that for $n = 4$, the inflaton behaves like radiation during reheating with the equation of state parameter $\omega_\phi = 1/3$. It is known that during reheating if we consider the effective equation of state to be radiation like, then distinguishing the reheating period and the radiation dominated period becomes very difficult as can be seen from the schematic diagram Fig. 3.2. This very fact makes the reheating parameters $(N_{re}, T_{re})$ indeterministic which has been observed in [61]. However, in our analysis, we managed to resolve this fact by considering the explicit decay of inflaton into the analysis. Therefore, even though the inflaton equation of state is radiation like, the effective single fluid equation of state during reheating will not be exactly radiation like rather it has complicated time dependence, expressed as

$$w_{eff} = \left\langle \frac{3p_\phi + \rho_{rad}}{3(\rho_\phi + \rho_{rad} + \rho_X)} \right\rangle . \tag{3.52}$$

However, in deriving the above equation of state we assumed the perturbative decay of inflation. Keeping this fact in mind, our result for $n = 4$ is given in the Fig. 3.15. It clearly shows the stiffness of the curve which can be attributed to the fact that effective equation of state varies very close to 1/3. There exist some flat regions as we lower the value of $n_s$, which we think should be our numerical artifact. Therefore, if we discard that flat region, $n = 4$ model predicts a precise value of scalar spectral index $n_s$, however, $N_{re}, T_{re}$ become very sensitive to slight variation of it. As we can see from the Fig. 3.15, the scalar spectral index assumes $n_s \simeq (0.9575, 0.966, 0.967)$ values for $\phi_* = (10, 1, 0.1)M_{\rm p}$. Therefore, an important conclusion we can arrive from our analysis that super-Planckian values of $\phi_* > 1M_{\rm p}$ are disfavored as long as $n_s$ measurement is concerned.

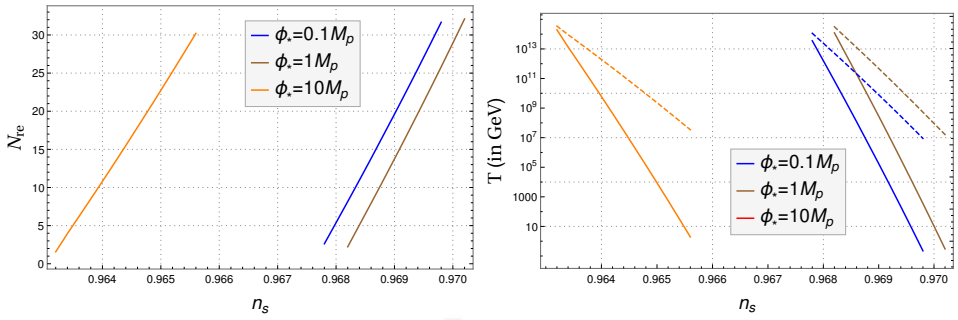


(a) (b)

FIGURE 3.16: Evolution of (a) Reheating e-folding number $N_{\rm re}$ during reheating and (b) the reheating temperature $T_{\rm re}$(solid lines) and the maximum temperature $T_{\rm max}$(dotted lines) with respect to $n_s$ for $n = 6$ for three different values of $\phi_*$. One clearly see the change of slop in compared to $n < 4$ models. However, we observed maximum reheating temperature to the same $T_{\rm re}^{\rm max} \simeq 10^{15}$ GeV.

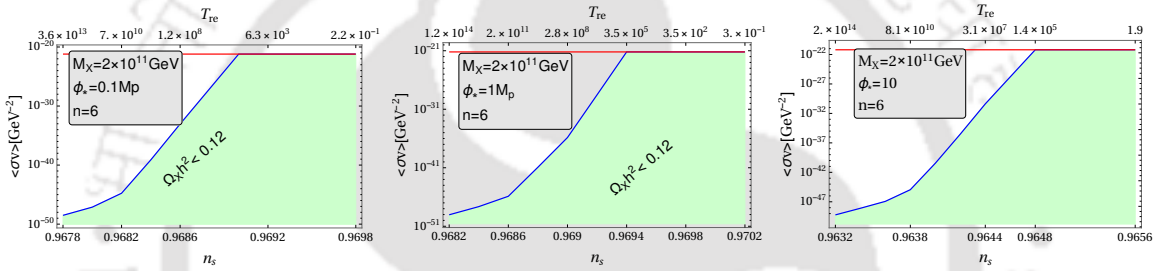


(a) (b) (c)

FIGURE 3.17: ($\langle\sigma v\rangle$ *vs* $n_s$) were plotted for three values of $\phi_*$ and $n = 6$. For all the cases we have chosen a dark matter mass $M_X = 2 \times 10^{11} GeV$.

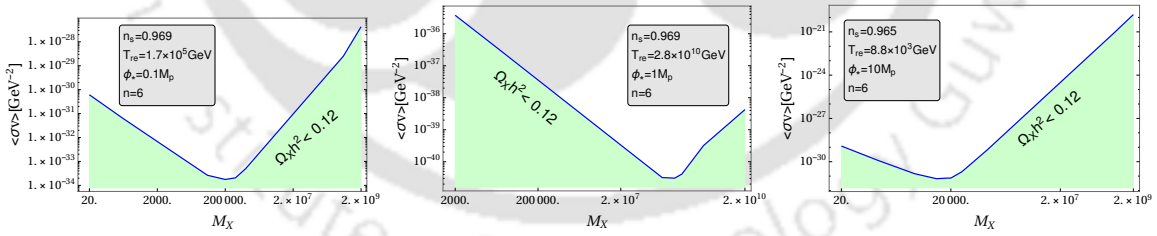


(a) (b) (c)

FIGURE 3.18: ($\langle\sigma v\rangle$ *vs* $M_X$) were plotted for three values of $\phi_*$ and $n = 6$. General descriptions of the plots are same as before.

#### 3.4.6.3 Results and constraints: Model n=6

As we know all the usual power law inflationary models are large field and consequently predicts large $r$ value. However, because of new scale $\phi_*$, we were able to make our model perfectly compatible with the observation for even stiffer model such as $n = 6$ and $n = 8$. In this sub-section we summarized all our analysis in the Figs.(3.16,3.17,3.18) and the following Table 3.2 for $n = 6$.

Table 3.2: Model parameters and associated constraints on dark matter parameters for $n = 6$, $M_X = 10^{11}$GeV

$\phi_* = 0.1M_{\rm p}$

| $n_s$ | $N_{\rm re}$ | $T_{\rm re}$(GeV) | $\langle\sigma v\rangle$GeV$^2$ |
|---|---|---|---|
| 0.9678 | 3 | $4 \times 10^{13}$ | $3 \times 10^{-49}$ |
| 0.968 | 5 | $2 \times 10^{12}$ | $7 \times 10^{-48}$ |
| 0.969 | 20 | $2 \times 10^{5}$ | $9 \times 10^{-34}$ |
| 0.9698 | 32 | 0.2 | $6 \times 10^{-22}$ |

$\phi_* = 1M_{\rm p}$

| $n_s$ | $N_{\rm re}$ | $T_{\rm re}$(GeV) | $\langle\sigma v\rangle$GeV$^2$ |
|---|---|---|---|
| 0.9682 | 2 | $1 \times 10^{14}$ | $9 \times 10^{-50}$ |
| 0.969 | 14 | $3 \times 10^{8}$ | $1 \times 10^{-36}$ |
| 0.970 | 29 | 10.58 | *unitarity* |
| 0.972 | 32 | 0.3 | *unitairty* |

$\phi_* = 10M_{\rm p}$

| $n_s$ | $N_{\rm re}$ | $T_{\rm re}$(GeV) | $\langle\sigma v\rangle$GeV$^2$ |
|---|---|---|---|
| 0.9632 | 2 | $1.9 \times 10^{14}$ | $6 \times 10^{-50}$ |
| 0.964 | 11 | $6 \times 10^{9}$ | $4 \times 10^{-41}$ |
| 0.965 | 23 | $8.8 \times 10^{3}$ | *unitarity* |
| 0.9656 | 30 | 2 | *unitarity* |

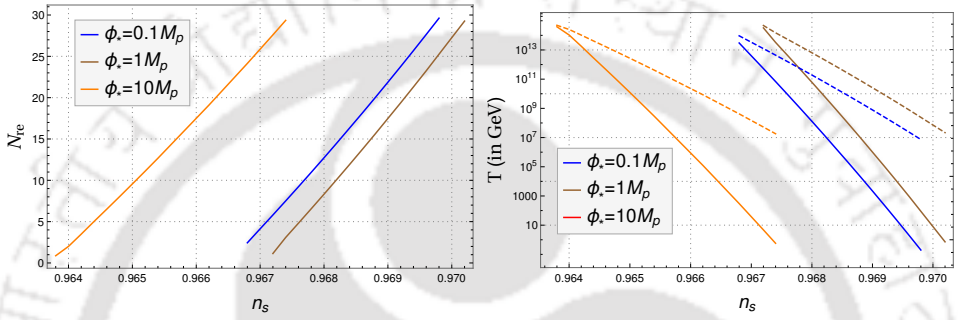


FIGURE 3.19: Evolution of (a) Reheating e-folding number $N_{\rm re}$ during reheating and (b) the reheating temperature $T_{re}$(solid lines) and the maximum temperature $T_{\rm max}$(dotted lines) with respect to $n_s$ for $n = 8$ with the same behavior as $n = 6$..

Important difference with $n < 4$ models turned out to be the slope of ($n_s$ *vs* $T_{re}$) and ($n_s$ *vs* $N_{re}$) curve. This has also been explained in the schematic diagram Fig. 3.2. This is coming from the stiff equation of state of the oscillating inflaton $w_\phi = (n-2)/(n+2) = 1/2 > 1/3$. The duration of reheating period ($N_{re}$) increases with increasing $n_s$. Therefore, unlike $n < 4$ models, corresponding to the maximum reheating temperature we have minimum possible values of $n_s$.

#### 3.4.6.4 Results and constraints: Model n=8

For $n = 8$, the qualitative behavior of all the plots will be same as $n = 6$. Therefore we summarize all our results in the Table 3.3 and the respective plots. Important to see that very small reheating temperature can be reached in this model. At the central value of $n_s = 0.968 \pm 0.006$, we see reheating temperature could be $10^4 \sim 10^5$ GeV given in the Table 3.3. The lowest value of $n_s$ can be set from the minimum possible reheating temperature coming from BBN constraints[10, 92–94], which is $T_{re} \sim 0.1GeV$.

## 3.5 Summary and outlook

Through our present work the first and foremost point we wanted to bring to the reader's notice is that it is an important generalization of the work proposed in [61] by considering explicit decay of inflaton into radiation and dark matter into the reheating constraint analysis. At

Table 3.3: Model parameters and associated constraints on dark matter parameters for $n = 8$, $M_X = 10^{11}$GeV

$\phi_* = 0.1M_{\rm p}$

| $n_s$ | $N_{\rm re}$ | $T_{\rm re}$(GeV) | $\langle\sigma v\rangle$GeV$^2$ |
|---|---|---|---|
| 0.9668 | 2 | $3\times10^{13}$ | $4\times10^{-49}$ |
| 0.968 | 13 | $1\times10^{8}$ | $7\times10^{-35}$ |
| 0.969 | 22 | $2\times10^{3}$ | *unitairty* |
| 0.9698 | 30 | 0.2 | *unitarity* |

$\phi_* = 1M_{\rm p}$

| $n_s$ | $N_{\rm re}$ | $T_{\rm re}$(GeV) | $\langle\sigma v\rangle$GeV$^2$ |
|---|---|---|---|
| 0.9672 | 1 | $3\times10^{14}$ | $4\times10^{-50}$ |
| 0.968 | 8 | $6\times10^{10}$ | $2\times10^{-45}$ |
| 0.9692 | 19 | $1\times10^{5}$ | *unitarity* |
| 0.9702 | 29 | 0.72 | *unitarity* |

$\phi_* = 10M_{\rm p}$

| $n_s$ | $N_{\rm re}$ | $T_{\rm re}$(GeV) | $\langle\sigma v\rangle$GeV$^2$ |
|---|---|---|---|
| 0.9638 | 1 | $4\times10^{14}$ | $3\times10^{-50}$ |
| 0.964 | 2 | $1\times10^{14}$ | $1\times10^{-49}$ |
| 0.965 | 10 | $1\times10^{10}$ | $3\times10^{-43}$ |
| 0.9674 | 29 | 1 | *unitarity* |

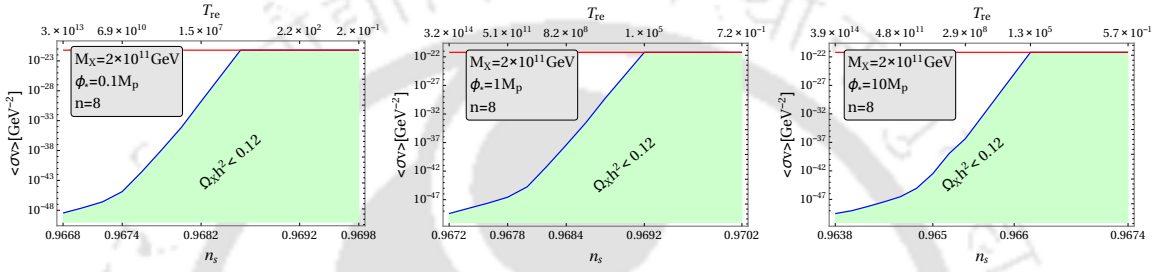


FIGURE 3.20: ($\langle\sigma v\rangle$ *vs* $n_s$) were plotted for $n = 8$. Descriptions are same as previous plots. For all the plots we have chosen dark matter mass $M_X = 2\times10^{11}GeV$.

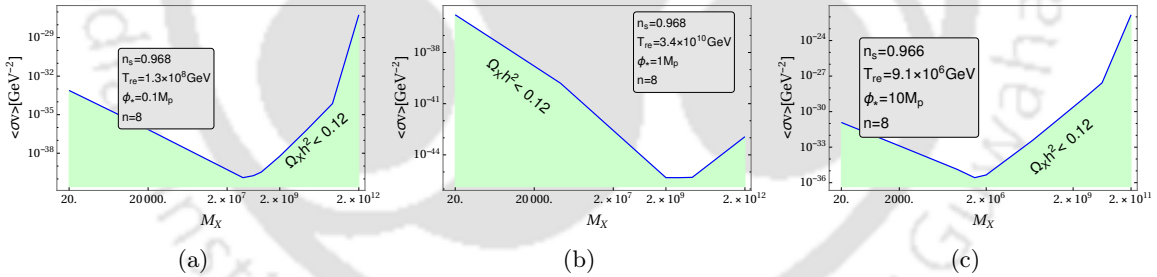


FIGURE 3.21: ($\langle\sigma v\rangle$ *vs* $M_X$) were plotted for $n = 8$.

this point let us also remind the reader that in all the PLANCK analysis [53] on constraining the inflationary models, an effective time independent equation of state $w_{\rm eff}$ during reheating is assumed. One of the important messages we try to convey through the present analysis is that those assumptions have limited applicability. After the inflation, every inflationary model has its own characteristic oscillatory period that contributes to the equation of state during reheating. Therefore, considering $w_{\rm eff}$ as a free parameter loses some of the fundamental characteristic properties of the inflaton potential itself. Furthermore if reheating occurs for a longer period of time, the time dependent $w_{\rm eff}$ should also be very important to get a precise constraint on any inflationary model. This is where our analysis not only can play an important role in better understanding the inflationary models but also opens up the possibility of understanding the microphysics of reheating process through CMB physics. To further clarify

Table 3.4: Summary of two methods for reheating constraints

| | **Standard approach[61, 97]** | **Our approach** |
|---|---|---|
| Assumptions | - During the reheating period time-independent effective equation of state $w_{\rm re}$ is assumed to be a free parameter that parametrizes the expansion of the universe. No microphysics of inflaton decay is considered.<br>- Instantaneous conversion of inflaton energy into radiation. | - Reheating phase is described by perturbative inflaton decay into various other fields. Hence $\Gamma_\phi$ is free parameter.<br>- The inflaton equation state is that of the homogeneous inflaton condensate. Hence, total effective equation of state $w_{\rm eff}$ is time-dependent Fig. 3.22. |
| Components of the Universe | - Assumes two component universe comprising inflaton and radiation | - In principle we can accommodate any number of energy components, such as dark matter and dark radiation and do the analysis. |
| Methodology | - Find out the inflationary quantities $N_k, r, V_{\rm end}$, etc. in terms of $n_s, A_s$ for a specific inflation model.<br>- Calculate $N_{\rm re}$ in terms of $w_{\rm re}$ using (3.27).<br>- Finally one obtains the relation among $T_{\rm re}, n_s$ and $w_{\rm re}$ using (3.26)<br>- The inflaton decay constant is indirectly defined through the reheating temperature. | - Find out the inflationary quantities $N_k, r, V_{\rm end}$, etc. in terms of $n_s, A_s$ for a specific inflation model.<br>- Solve the Boltzmann equation considering $(\Gamma_\phi, \langle\sigma v\rangle, M_X)$ as a free parameters.<br>- The "right" $(\Gamma_\phi, \langle\sigma v\rangle)$ are uniquely determined by the condition (3.33) for given $(M_X, n_s)$, which are combination of entropy conservation and background evolution, and dark matter abundance. Inflation fixes the value of $n_s$. Therefore, we only have dark matter mass as a free parameter $M_X$. |
| Relations with CMB and primordial density fluctuation | - With the conventional transfer function connect the primordial spectral tilt with the CMB anisotropy. | - In our present analysis we assumed the conventional relation.<br>- However our analysis connects dark matter phenomenology with the inflationary observables through reheating. Hence dark matter observation can constrain the inflationary dynamics.<br>- Therefore, to connect the primordial spectral tilt with the CMB anisotropy appropriate transfer function needs to be derived which explicitly includes the dynamics of reheating. |

in Table 3.4 we summarize and compare our analysis with that of the existing analysis. As we can clearly see, the CMB power spectrum constrains the value of inflation-radiation coupling parametrized by $\Gamma_\phi$ through reheating temperature $T_{\rm re}$, which we found to be expressed in terms of spectral index $n_s$ as,

$$log\,(T_{re}) \propto \left[A + B(n_s - 0.962) + C(n_s - 0.962)^2\right]. \tag{3.53}$$

The usual relation $T_{\rm re} \propto \sqrt{\Gamma_\phi}$ will not be exactly correct any more once we consider inflaton decaying into various matter fields. Further, in all the previous theoretical as well as in PLANCK analysis, complete decay of inflaton is assumed at the beginning of the radiation era. This also can not be true because of perturbative part of the reheating. Another interesting point is that irrespective of the model under consideration, our analysis indicates the existence

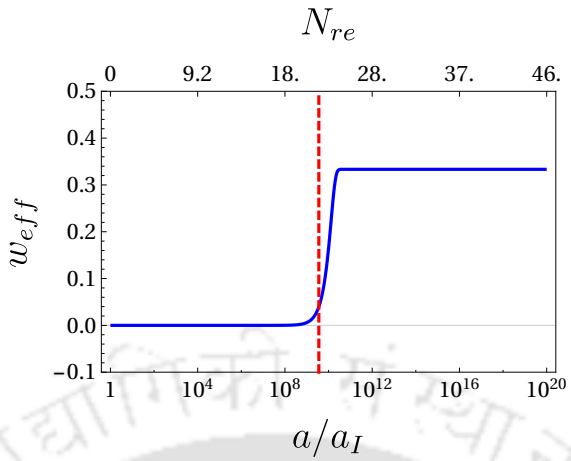


FIGURE 3.22: Variation of effective equation of state $w_{eff} = \langle(3p_\phi + \rho_R)/3(\rho_\phi + \rho_R + \rho_X)\rangle$ during reheating phase. Vertical red dotted line corresponds to the end of reheating.

of a universal value of the maximum reheating temperature $T_{\rm re}^{\rm max} \simeq 10^{15}$ GeV and maximum of value of inflationary e-folding number $N_{\rm max} \simeq 56$ [104].

In this work, our main goal was to understand the connection between the CMB anisotropy and the properties of dark matter. Till now the only known quantity related to the dark matter is the dark matter density parametrized by the density parameter $\Omega_X h^2 \simeq 0.12$, which can be extracted from the CMB power spectrum. However in this paper for the first time to our knowledge, we managed to establish the fact that CMB anisotropy not only provides the background value but also can shed light on the microscopic detail of dark matter. In this regard thanks to the Ref. [61], a beautiful connection between the CMB power spectrum and the reheating temperature via the inflation has been established. Here we have extended their formalism by including the effect of explicit decay of inflaton into the reheating study [104]. The main assumption of our analysis was the perturbative decay of inflation. In any inflationary model, the inflaton energy is supposed to be the only source of energy of the current universe. Therefore, in addition to the standard radiation field, we have included the production of a stable dark matter particle species during the reheating period. As has been mentioned in the Introduction, detailed analysis on this has been done in the literature [105, 107–109, 123, 126–133] without any constraint from the CMB. However, let us emphasize again that we reanalyzed the dark matter production considering the important constraints coming from observed CMB anisotropy.

Other important conclusions of our analysis are that for a particular inflation model, the inflationary scalar spectral index that is directly connected with the CMB power spectrum can uniquely fix the dark matter parameter space $(M_X, \langle\sigma v\rangle)$, through the following important relations for different dark matter mass ranges:

$$\begin{aligned}\langle\sigma v\rangle\Big|_{M_X>T_{\rm re}} &\propto 10^{-7A-7B(n_s-0.962)-7C(n_s-0.962)^2}.\\ \langle\sigma v\rangle\Big|_{M_X<T_{\rm re}} &\propto 10^{-A-B(n_s-0.962)-C(n_s-0.962)^2}.\end{aligned} \tag{3.54}$$

As is clear from the above expressions for the dark matter annihilation cross-section, which turned out to be very sensitive to the inflationary scalar spectral index because of the power-law

form, it is very important to pinpoint the value of $n_s$ in the future CMB experiments. It is clear from the expression that for a given dark matter mass and the inflationary model, the dark matter scattering cross-section will be within the bound coming from the $2\sigma$ error bar on $n_s = 0.9670 \pm 0.0074$ from Planck and BK14 and BAO data. For marginally relevant axion inflation models, we found for axion decay constant $f = 10\mathrm{M_p}$ and the dark matter mass, $M_X = 10^3$GeV, the dark matter cross-section should be with $10^{-39} > \langle\sigma v\rangle > 10^{-41}\mathrm{GeV}^{-2}$ which is very narrow within the $2\sigma$-error of $n_s$ mentioned before. If we consider one of the observationally favorable models of $\alpha$ attractor with $\alpha = 10$, we get a large range of annihilation cross-section $10^{-29} > \langle\sigma v\rangle > 10^{-42}$ GeV$^{-2}$ possible for dark matter mass $M_X = 10^3$ GeV. More detail of this bound on the allowed range of $\langle\sigma\rangle$ for different mass ranges has already been discussed in the main text considering various models of inflation.

Explicit model building in the dark matter sector during the reheating period could be an important research direction. In addition to the connection we have been discussing, we also found that to satisfy the bound on the current dark matter abundance, freeze-in is the only mechanism through which dark matter with $M_X \gg T_{re}$ can be produced. Our numerical analysis also showed that dark matter production during reheating does not significantly affect the determination of reheating temperature.

In the present analysis, we have only considered the homogeneous evolution. It would be of utmost importance to analyze the evolution of perturbations of radiation and dark matter components and study their spectral properties which can give further constraints on our parameters. Most importantly in our analysis inflation and the subsequent reheating control the dynamics of all the energy components such as radiation and dark matter of our universe. Reheating is effective in the subhorizon scale. Therefore any small-scale observables related to CMB and matter distribution could play an important role in constraining inflationary models though our analysis. One of the important such set of observables could be the well-known small-scale $\mu$-type and $y$-type spectral distortions of CMB. The standard $\Lambda$CDM cosmology already predicts those spectral distortions through standard photon-charge particle interaction [149, 150] at different redshift values. However, at present those distortion parameters are tightly constrained by COBE and FIRAS experiments, $|\mu| < 9 \times 10^5$ and $y < 1.5 \times 10^5$ [151]. However, future projected sensitivity of those quantities in new experiments like PIXIE [152] and PRISM [90] are within $10^{-8} - 10^{-9}$. Therefore, it would be important to understand various physical processes that can give rise to any deviation from a blackbody spectrum. In our present analysis, we consider the scenario where the energy is being extracted out of the radiation to dark matter and depending upon the dark matter mass and the inflationary scalar spectral index, the freezing out of dark matter happens in a large range of cosmological red shift values. Therefore, this energy extraction process can leave its footprint in the CMB spectral distortion parameters [150, 153–155], which can further constrain the inflationary models. We leave these important topics for our future studies.

An important assumption in our analysis that needs further investigation is the assumption of the perturbative decay of inflaton during reheating. The perturbative decay of inflaton [27, 95] has been parametrized by an effective phenomenological friction term with inflaton decay constant $\Gamma_\phi$. However, from the action principle, this is very difficult to generate. Therefore, as has been mentioned before, one should construct an explicit dark matter model. Most importantly it has long been argued that the nonperturbative decay of inflaton will be very important and efficient at the initial stage of the reheating phase. In the literature this phase is known as preheating [31, 32, 35, 37]. However, once the amplitude of the oscillating inflaton is small after preheating, the perturbative decay will automatically come into play. Hence, it

would be more appropriate to understand the non-perturbative dynamics and how it sets the initial conditions for the perturbative reheating where our analysis will be important. This subject is beyond the scope of our present work and will be addressed in a future publication. Nonetheless, as long as the coupling parameters are such that perturbative decay is the only way to reheat the universe, all our conclusions will be qualitatively correct.

To the end let us elaborate one more issue which we have already mentioned in the last point of the Table 3.4. The issue is related to the relation between the CMB anisotropy and primordial anisotropy originated from the quantum fluctuation of the inflaton field. The evolution of the primary power spectrum of the CMB is generally determined through transfer function. This transfer function, which is intimately related to the Sachs-Wolfe effect [156] entails a simple geometrical scaling relation. Furthermore, there exists an inherent connection between this aforementioned scaling relation and the wellknown geometrical parameter degeneracy in determining the CMB spectra ([157], *and references therein*). The parameter degeneracy states that the same anisotropy spectrum can be produced even if cosmological constant and spatial curvature is varied keeping the size of the last scattering surface constant. In the usual analysis of this transfer function, the initial condition for the perturbation is set at the BBN. However, the initial spectral density distribution at the BBN for various matter components should originate from the primordial spectrum through the evolution during the intermediate reheating phase. In our present analysis we solved the homogeneous Boltzmann equations for all the important energy components of our universe starting from the end of inflation, and we tried to understand the constraints on inflation supplemented by not only CMB but also the dark matter abundance. By this we can establish a direct connection among the inflationary dynamics, CMB anisotropy and dark matter phenomenology via the reheating phase. Therefore, to have a complete correspondence between the CMB and the primordial anisotropy, we need to have an additional transfer function that can connect the anisotropy at the end of inflation and the end of reheating. In order to find out that additional transfer function one needs to solve inhomogeneous Boltzmann equations for various components during the reheating phase. Importantly for those equations to be solved, inflationary dynamics provides us precise initial conditions at the end of inflation. In this additional phase a new parameter degeneracy may appear or if we include the dynamical generation of cosmological constant from the inflaton during reheating, it may lift some amount of degeneracy in the transfer function. All these important questions will constitute a very interesting future study.

*"...we could conceive the beginning of the universe in the form of a unique atom, the atomic weight of which is the total mass of the universe. This highly unstable atom would divide in smaller and smaller atoms by a kind of super-radioactive process."*

*Georges Leîmatre In 'The Beginning of the World from the Point of View of Quantum Theory', Nature (1931)*

## 4.1 Introduction

From the discussions of the last two chapters, we have seen that the plateau type inflationary models are favored in terms of cosmological observation. In Chapter 2 we have introduced and studied a class of supergravity inspired inflationary model which we call minimal plateau inflation. Depending upon the choice of the controlling parameter $\phi_*$ we have seen that those model fit very well with the cosmological observations. We have also studied the reheating constraints on those models supplemented with the CMB anisotropy and the present dark matter abundance considering the perturbative decay of inflaton in Chapter 3. The study of perturbative reheating with a phenomenological inflaton decay constant $\Gamma_\phi$ is simple and convenient to understand several important aspects of the reheating phase. However, this treatment relies on several assumptions on the nature of the reheating processes: (i) The first assumption is the absence of non-perturbative phenomena such as parametric resonance during reheating phase. Although the parametric resonance can be ignored depending upon the chose of coupling parameter among the inflaton and the reheating field, in the large occupation number limit it may not hold true in general. Therefore, it will be more appropriate to consider the perturbative reheating as a final stage of the whole reheating process with the initial conditions set by the non-perturbative stage. In this chapter this is exactly what we will be studying. (ii) The second assumption is that we have also ignored the phenomena of inflaton fragmentation and the growth of inhomogeneities in the inflaton sector. For potential of form $V(\phi) \sim \phi^n$ near the minimum, using the virial theorem, the average equation of state

are found to be $w_\phi = (n-2)/(n+2)$. It is needless to say that in any realistic reheating scenario the above assumptions have limited applicability. As mentioned we will study the full non-perturbative reheating phenomena which naturally leads to inflaton fragmentation and inhomogeneity in distribution of energy. However, while studying the perturbative reheating, we will still consider the evolution of homogeneous energy density. Full inhomogeneous evolution we left for our future studies. The effects of parametric resonance is well studied in classical mechanics[34]. The importance of resonant particle production at the initial stage of reheating has been recognized and studied extensively for the first time in the seminal works of Kofman, Linde, and Starobinsky[31, 32]. The structure of resonance in the class of conformally invariant theories such as $(\lambda/4)\phi^4 + (g^2/2)\phi^2\chi^2$ has been developed in [38]. It has been understood that the analytic study of preheating does not capture the full non-linear dynamics of this phase. A full non-linear study of non-perturbative field theory is needed for. However, if the occupation number of the different species is much larger than one we may study the system by ignoring their quantum nature[158–161] and solving the appropriate classical wave equations. This fact serves as the basis for studying the preheating phase in $3+1$ dimensional lattice. With the advent of different lattice codes[42, 44, 46, 47], lattice simulation study of preheating becomes quite frequent in the literature (see refs.([36, 37, 162]) and references therein). Another import aspect of preheating is the study of self resonance after inflation. In this case the inflaton quanta may became unstable due to small spatial perturbations even without the couplings to other fields. The self-resonance is found to be inefficient for the case of chaotic models[38], however they can be efficient for multifield inflation[163, 164] or in the case of plateau type potentials[165, 166].

In this work we have studied the preheating and subsequent thermalization after minimal plateau inflation introduced in our earlier work[167]. These class of models are parameterized by the power $n$ of the inflaton field $\phi$ and most importantly a scale $\phi_*$ that controls the energy scale of inflation, similar to the $\alpha$ parameter for $\alpha$-attractor models. The study of self-resonance phenomena with $\alpha$-attractor type potentials has been performed in [165, 166]. However, in any realistic model of preheating the inflaton coupled with other matter fields must be incorporated. The study of preheating for the archetypal plateau inflation model viz the Starobinsky-Higgs inflation has been done in[168, 169]. However, the study of preheating when other matter fields are coupled has not been done in the literature for general plateau type of potentials with a controlling parameter such as $\phi_*$. Therefore, in this paper we will consider the class of minimal plateau inflation models mentioned before. We will study, in detail, how the particle production and the subsequent thermalization process depend on the scale $\phi_*$ and the power of the potential $n$. The end of preheating can be identified around the scale factor where average value of all the energy components tend to become stationary. Interestingly for $n > 2$, all the models lead to effective equation of state equal to that of the radiation $w = 1/3$.

It is well known that the inflaton decay is not complete with a four-legs interaction[170]. It has been found here that this situation prevails even if we change the parameter $\phi_*$ for all the models considered. Therefore, as a logical next step we study the perturbative reheating process considering a phenomenological inflaton decay term into the Boltzmann equations for the inflaton and the radiation component. The phase of perturbative reheating enables us to connect the reheating phase with the current CMB date in terms of the primordial spectral index of the inflaton fluctuation. For a particular inflation model, the preheating dynamics turned out to be insensitive to the inflationary e-folding number which is a function of scalar spectral index. As a consequence in determining the reheating temperature the effect of preheating appears only though its e-folding number. Finally we have commented on the

range of value of the coupling parameter that will set the value of the above perturbative inflaton decay term. Although, this work concerns with the above plateau potentials, the general conclusions in this work will be applicable to any other class of plateau potential having a controlling scale similar to $\phi_*$ or $\alpha$.

We have structured this chapter as follows. After briefly describing the minimal plateau inflationary models in Section 4.2, we have described the requisite equations and introduced various quantities of interest in Section 4.3. In Section 4.3.2 we have studied the analytic behavior of parametric resonance with the help of instability chart associated with the Mathieu/Hill type differential equations. Section 4.4 describes the results of the lattice simulation. The perturbative reheating and CMB constrains on reheating phase has been described in Section 4.4.4. Finally we conclude in Section 4.5.

We will consider $\hbar = c = 1$ unless otherwise stated. We have denoted $m_p(= 1/\sqrt{G})$ as the Planck constant and $M_p(= 1/\sqrt{8\pi G})$ as the reduced Planck constant. We will take the usual Friedmann-Leîmatre-Roberson-Walker (FLRW) metric as our background metric $\mathrm{d}s^2 = \mathrm{d}t^2 - a^2(t)(\mathrm{d}x^2 + \mathrm{d}y^2 + \mathrm{d}z^2)$ for deriving our equations. With $a(t)$ is the scale factor and $t$ representing the cosmic time.

## 4.2 A Brief Introduction to the Minimal Inflation Model

In this section we will briefly describe the minimal plateau inflationary model and its characteristics introduced in[167]. We have already explained in our previous work, considering a simple power-law potential $\phi^n$, we can obtain our general class of non-polynomial form of the potential given as

$$V(\phi) = \frac{1}{n}\frac{\lambda\, m^{4-n}\phi^n}{1 + \left(\frac{\phi}{\phi_*}\right)^n} \tag{4.1}$$

either by using a conformal transformation in a certain class of non-minimal scalar-tensor theory, or from a supergravity construction. The scale $\phi_*$ can be identified with the non-minimal coupling in scalar-tensor theory, and inflationary energy scale in the supergravity potential. We take $\lambda = 1$ for $n \neq 4$ and the values of $\lambda$ or, $m$ is fixed from WMAP normalization. The inflationary predictions of this model has been studied extensively in the original work, here we present the $n_s$ and $r$ plot in fig.(5.1) on the latest Planck data[19]. After introducing the scalar potential, next we will introduce the parametric resonance after the end of inflation.

## 4.3 Preheating: Parametric resonance

### 4.3.1 The Model and equations

In this subsection we will first describe the main equations and methodology for our subsequent discussions. The exponential growth of a dynamical field coupled with an oscillating classical background for certain ranges of parameters is known as the parametric resonance[34]. In their seminal work, Kofman, Linde and Starobinsky[31, 32](see also[33]), introduced and work out the idea of non-perturbative resonance production of particles after inflation based on the idea of parametric resonance. The fields under consideration could be the fluctuations of the inflaton or any other daughter field or both, which will experience the homogeneous oscillating background inflaton for the present case. The daughter fields coupled with the inflaton could

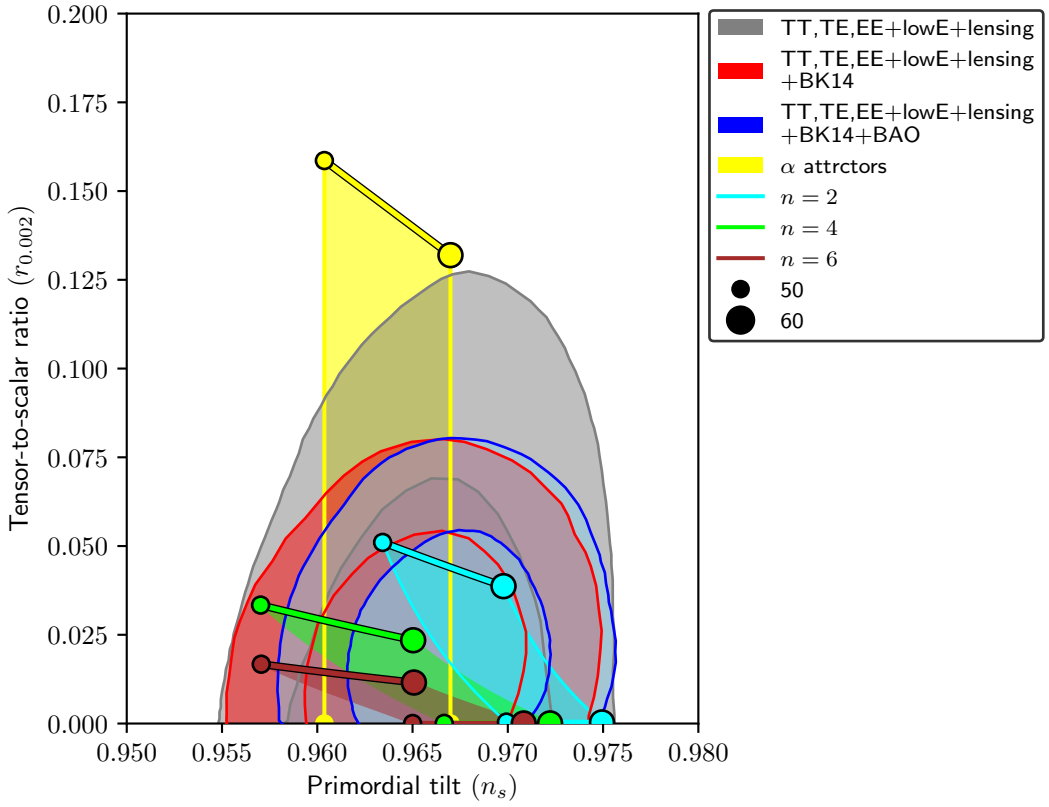


Figure 4.1: The $n_s$ and $r$ plot of the model on the marginalized joint 68% and 95% CL regions for $n_s$ and $r$ at $k = 0.002Mpc^1$ from Planck alone and in combination with BK14 or BK14 plus BAO data. Dotted line corresponds to $\phi_* = 10M_p$ and the solid line is for $\phi_* = 0.1M_p$

be any other scalar fields or usual standard model particles(usually bosons *). The energy density of the universe just after the inflation is in the form of the homogeneous inflaton field. This energy starts decaying into fluctuations of the inflaton and other fields at the onset of preheating. The initial stage of preheating is marked by exponential growth of decay product due to resonance effects. The analysis of this initial stage could be treated analytically. However, the expeditious draining of energy due to exponential particle production affects the dynamics of the inflaton field. This back-reaction of the produced particle leads to a fragmentation of the homogeneous inflaton and eventually shuts down the particle production. The rich dynamical nature of the combined inflaton and the produced fields call for a numerical simulation of the system on a lattice. The decay of inflaton by studying the classical field equation can be faithfully done as long as the occupation number of the fields are much larger that unity[158]. In the alter part of this work we will do the simulation with the heavy-duty `LATTICEEASY`[42] and its parallelized version `CLUSTEREASY`[43]. The inflaton potential for the model is given in (4.1). Throughout this work we will work exclusively with the four-legged

*the presence of bosons are important for parametric resonance, for preheating with fermions see,P. B. Greene and L. Kofman Phys. Lett B 448, 6 1999. [arXiv:hep-ph/9807339], P. B. Greene and L. Kofman Phys. Rev. D 62, 123516 2000. [arXiv:hep-ph/0003018]. we will here only consider the bosonic case

interaction given as

$$\mathcal{L}_{int} = -\frac{1}{2}g^2\phi^2\chi^2 \tag{4.2}$$

It has been noted that this four-legged interaction term will be dominant over the three-legged interaction viz $g^2\sigma\phi\chi^2$ for the initial stages of preheating when the amplitude of the homogeneous inflaton oscillation is large[170]. This interaction does not lead to any tree level decay of the inflaton and particle production will solely due to non-perturbatives processes. The four-legged interaction is usually not able to complete the decay of inflaton for general chaotic inflationary scenario[170]. Therefore, after the preheating three-legged interaction will be dominating in the perturbative decay process and may complete the reheating dynamics. In this work we will exclusively consider the aforementioned interaction for the preheating stage. At the end we will discuss about the perturbative reheating and connection with CMB. Nevertheless, the full potential for our lattice simulation is

$$V(\phi,\chi) = \frac{1}{n}\frac{\lambda\, m^{4-n}\,\phi^n}{\left[1+\left(\frac{\phi}{\phi_*}\right)^n\right]} + \frac{1}{2}g^2\phi^2\chi^2. \tag{4.3}$$

With this potential `LATTICEEASY` will solve the following classical scalar field equations

$$\ddot{\phi} + 3H\dot{\phi} - \frac{1}{a^2}\nabla^2\phi + \frac{\partial}{\partial\phi}V(\phi,\chi) = 0, \tag{4.4}$$

$$\ddot{\chi} + 3H\dot{\chi} - \frac{1}{a^2}\nabla^2\chi + \frac{\partial}{\partial\chi}V(\phi,\chi) = 0. \tag{4.5}$$

While the Hubble parameter $H$ is calculated self-consistently from the Friedmann equations. The redundancy of the Friedmann equations is used in `LATTICEEASY` to monitor the energy conservation. In all of our results we have kept the energy conservation at the $\mathcal{O}(10^{-4}-10^{-2})$ level. Denoting the preheating fields as by a generic symbol $f(t,\vec{x})$ and its Fourier transform as $f_k(t)$, the (comoving) occupation number of the particles are with this generic symbol $f$ are given by[42, 171]

$$n_k(t) \equiv \frac{1}{\omega_k}|\dot{f}_k|^2 + \frac{\omega_k}{2}|f_k|^2, \quad \text{with,} \quad \omega_k \equiv \sqrt{k^2+m_{eff}^2}, \quad \text{and,} \quad m_{eff}^2 \equiv \frac{\partial^2 V}{\partial f^2} \tag{4.6}$$

The evolution of various energy components such as kinetic, gradient and interaction part contain important information about the thermalization process and the growth of inhomogeneities. We will study in detail the evolution of those individual components defined below

$$\rho \equiv E_t = (E_\phi^K + E_\chi^K + E_\phi^G + E_\chi^G + E_\phi^P + E_{\phi\leftrightarrow\chi}^I) \tag{4.7}$$

Where,

$$E_\phi^K = \frac{1}{2}\dot{\phi}^2; \qquad E_\chi^K = \frac{1}{2}\dot{\chi}^2; \tag{4.8}$$

$$E_\phi^G = \frac{1}{2a^2}(\nabla\phi)^2, \quad E_\chi^G = \frac{1}{2a^2}(\nabla\phi)^2; \tag{4.9}$$

$$E_\phi^P = V(\phi), \qquad E_{\phi\leftrightarrow\chi}^I = \frac{1}{2}g^2\phi^2\chi^2. \tag{4.10}$$

Where, the subscript $(K,G,P,I)$ stand for kinetic, gradient, potential and interaction component of the total energy respectively. However, for evolution of the scale factor it is the

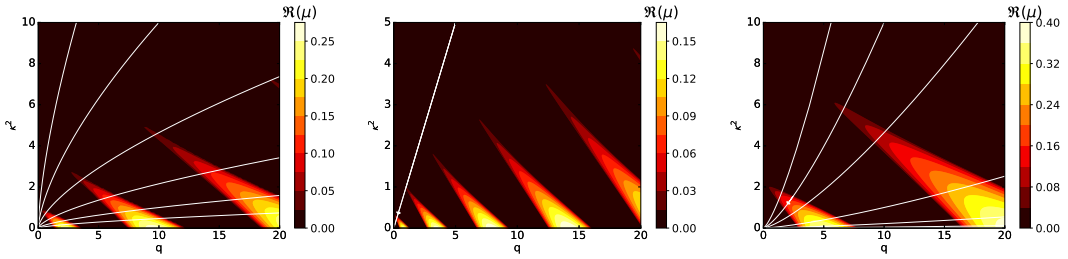

(a) $n = 2$ (b) $n = 4$ (c) $n = 6$

Figure 4.2: Instability regions for the models

total energy density $\rho$ that plays the important role. The energy total energy density may be expressed as

$$\rho \approx \frac{1}{(2\pi)^3 a^4} \int d^3k \omega_k n_k, \tag{4.11}$$

and the total (comoving) number density of the $f$ field is expressed as

$$n_f(t) \equiv \frac{1}{2\pi^2} \int d^3k \; n_k(t). \tag{4.12}$$

Before describing the numerical results, we will analyze the resonance structure analytically by studying the stability-instability diagram of the above equation with the well known method of Floquet theory[39, 40].

### 4.3.2 Parametric resonance: Instability chart

The instability of a mode is intimately tied with the violation of adiabatic condition that controls the particle production measured in terms of its growth over time. However this growth of a mode depends upon the coupling parameter and the value of the momentum. The exponential growth of a mode function depending upon the parameter values is termed as parametric resonance. Ignoring the gradient term during the initial linear regime, we can study this parametric resonance with the help of Mathieu/Hill equation. To this end, we first do the following re-scaling $X_k(t) \equiv a^{3/2}(t)\chi_k(t)$ to the $\chi$ field Eq.(4.5) as

$$\ddot{X}_k + \omega_k^2 X_k = 0, \tag{4.13}$$

where

$$\omega_k^2 \equiv \frac{k^2}{a^2} + g^2\phi^2(t) + \Delta, \qquad \Delta \equiv -\frac{3}{4}(3H^2 + 2H). \tag{4.14}$$

During preheating, we will set $\Delta = 0$. To study the resonance phenomenon in the context of Floquet theory, we will first ignore the expansion of the universe. In that case eq.(4.14) can be identified as a form of Hill's differential equation[40]

$$X_k'' + \left(\kappa + q\varphi^2(t)\right) X_k = 0, \tag{4.15}$$

with $a = 1$ for no expansion, the coefficients $\kappa$ and $q$ given by $\kappa = k^2/a^2$ and $q = (g^2\Phi^2)/\mathcal{B}^2$ are time-independent. The time will be measured in unit of $\mathcal{B}$ with $\mathcal{B} = \phi_0^{n/2-1}\sqrt{\lambda m^{4-n}}$( $\phi_0$

being the initial inflaton amplitude) set the natural time scale of the systems. Writing the homogeneous oscillatory background solution as $\phi(t) = \Phi\varphi(t)$. $\Phi$ is the amplitude of oscillation. In reality, the amplitude is also decaying with time i.e., $\Phi \equiv \Phi(t)$. However, without expansion, for the present discussion we can take it to be constant. We will introduce the time dependence quantitatively later. The solution of the eq.(4.15) is of the form $X_k \propto exp(\mu_k t)$. Where $\mu_k$ is known as the Floquet exponent in the field of differential equations that set the nature of the solution. If $\Re(\mu_{\kappa,q}) > 0$ for certain values of the parameters $(\kappa, q)$, the solution shows exponential growth which is identified as the particle production. The contours of $\Re(\mu_{\kappa,q}) = 0$ in the $(\kappa, q)$ plane, known as the instability bands, help us to understand qualitatively the region of parameter space as well as the strength of the resonance during preheating. In figs.(4.2), we present the stability-instability chart for three different values of $n = (2, 4, 6)$ for $\phi_* = 10M_p$. The shaded regions are the instability regions while the color-code value shows the strength of resonance. The effect of decreasing $\phi_*$ for a particular $n$(not shown in the figure) is to shift the instability regions towards higher values of $q$. This is expected as decreasing $\phi_*$ will result in reducing the initial amplitude of inflaton field. Hence, we will naturally need a higher value of the coupling constant $g$ to get the resonance. Also for a particular $q$(or, $g$), decreasing $\phi_*$ will lead to resonance only for the higher momentum modes. We will describe other important effects of the scale on preheating and thermalization as we go along. Till now, we have ignored the effect of expansion on the resonance phenomena. A striking difference between the parametric resonance in an expanding universe with the normal resonance is that the parameters $(\kappa, q)$ in an expanding universe are not constants. They depend on time via the scale factor and the time-dependent amplitude $\Phi(t)$ of the inflaton oscillation. As a result of the expanding universe all the momentum modes will be red-shifted while the back reaction of produced particles will eventually shut-down the resonance. Nonetheless, we may incorporate the effect of expansion in the instability analysis by noting including the fact that the amplitude of the inflaton oscillation will decay as $\Phi \propto a^{-6/(n+2)}$. Hence, a particular mode residing in an instability band in an expanding universe will not have indefinite growth rather it will travel through different instability and stability regions(when the solution is oscillatory indicating an absence of particle production) with time. The white flow-lines with the arrow direction shows the trajectory of a mode through different bands. We will close this section with an estimate of the maximum allowed momenta range that can be produced during broad parametric resonance. This maximum value has important consequence on setting up the lattice parameters as we will discuss later. To this end, we first note that due to large effective mass(most of the time interval during inflaton oscillation we have $m^{\chi}_{\rm eff} \sim g\phi \simeq g\Phi \gg m_\phi$), the preheating field mode $\chi_k$ will oscillate much faster than the inflaton. This implies that the oscillation frequency $\omega_k$ mostly changes adiabatically. As a result the occupation number $n_k$ with variables frequency $\omega_k$ can be treated as an adiabatic invariant.

$$n_k \sim \frac{1}{2}\omega_k^2 \frac{|\chi_k^2|}{\omega_k} \simeq \text{constant}. \tag{4.16}$$

$$\implies |\chi_k| \sim \omega_k^{-1/2} \tag{4.17}$$

The violation of adiabatic condition signals particle production i.e.,

$$\dot{\omega} \gtrsim \omega^2 \quad \implies \text{Particle production} \tag{4.18}$$

Now, we will approximate $\dot{\phi} \sim \mathcal{B}\phi_0$. Where $\mathcal{B}$ sets, as mentioned before, the natural time scale of inflaton oscillation. With $\omega^2 = k^2 + g^2\phi^2$ and $\dot{\omega} \simeq g^2\phi_0\mathcal{B}\phi$, the adiabatic condition in (4.18)

provides the range of excited momenta $k$ as

$$0 \leq k^2 \lesssim (g^2\phi_0\mathcal{B}\phi)^{2/3} - g^2\phi^2 \tag{4.19}$$

Momentum will be maximum when

$$\phi \equiv \tilde{\phi} \simeq \frac{1}{2}\left(\frac{\mathcal{B}\phi_0}{g}\right)^{1/2} \tag{4.20}$$

This estimate the range of typical momenta $k$ of the particles that are produced in the broad resonance regime as

$$0 \leq 2k \lesssim k_{\rm max} \equiv (g\mathcal{B}\phi_0)^{1/2} \tag{4.21}$$

Where $k_{\rm max}$ gives the maximum momentum scale that can be reached during preheating. The above estimation of $k_{\rm max}$ for particular cases can be found in [32, 162] for $n = 2$ and in [38, 162] for $n = 4$. With these results, we will describe the results of our lattice simulations in the next Section.

## 4.4 Preheating: Lattice Simulation

In this section we will describe the results of our lattice simulation for three particular class of models from the potential given in 4.1. The details of specific model and its parameters as well as variaous lattice specification will be mentions in their respective places. However, before diving into details of the specific models we will first mention some general features of the study which is almost universal across all the class of models.

### 4.4.1 The back-reaction and the emergence of non-linearity: Generalities

The preheating phase, in general, is episodic with at least three distinct phases. The first phase of preheating is marked by the linear growth of produced field(s) via parametric resonance. The comoving amplitude of the inflaton field remains almost constant throughout this phase while most of the energy of the system is contained in the inflaton field oscillating mostly in the form of kinetic and potential energies. While all other energies are sub-dominant. The characteristic scale marking the end of this phase will be denoted, following the terminology used in[162], by the instant $z_{br}$ where *'br'* stands for back-reaction. In practice, we will measure $z_{br}$ as an instant when the comoving inflaton amplitude drops to 95% of its initial value. The second phase is the non-linear regime when the back-reaction of the produced field quanta became appreciable on the dynamics of the inflaton field. As a result, the comoving amplitude of the field starts decreasing appreciably. Inflaton kinetic and potential energies start to decrease resulting in the increase of other energy components. The gradient energy of the inflaton field which represents the growth of the inhomogeneities will also start to increase. This phase ends when the inflaton decay stops. We will denote the end of this phase as $z_{dec}$. Where *'dec'* represents the instant when the inflaton decay ends[162] and it enters into a stationary regime.

Other interesting aspect of preheating is observed by observing the virialization of the system. The inflaton with a potential $V(\phi) \propto \phi^n$ and the produced field satisfy the following

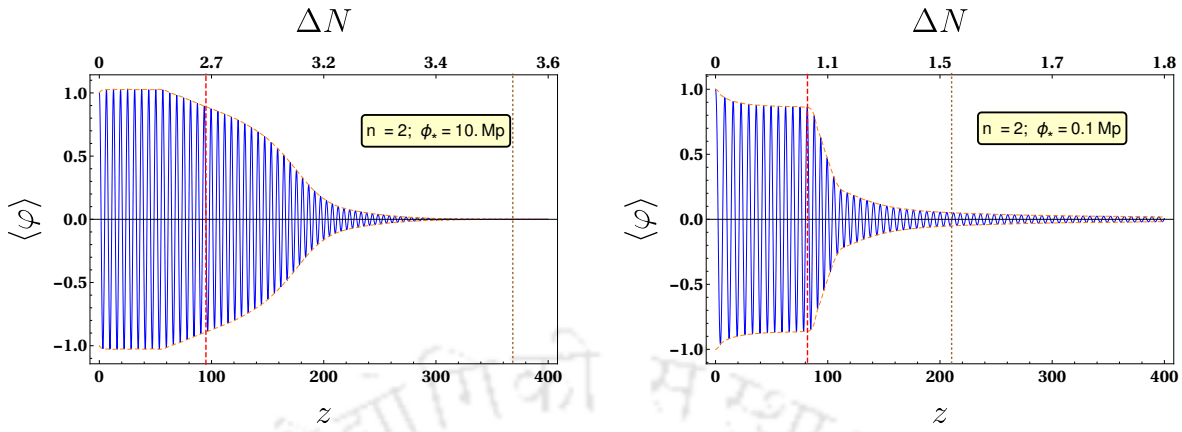


FIGURE 4.3: Evolution of volume averaged comoving inflation amplitude $\varphi = (a/a_i)^{3/2}(\phi/\phi_0)$ for the model potential $n = 2$ for $\phi_* = 10M_p$ and $0.1M_p$. The red dashed line shows the instant of back-reaction initiation while the brown dotted line is for the instant of decoupling.

virialization relation.

$$\frac{1}{2}\left\langle\dot{\phi}^2\right\rangle = \frac{1}{2}\left\langle\left(\frac{\nabla\phi}{a}\right)^2\right\rangle + \frac{n}{2}\left\langle V(\phi)\right\rangle + \frac{1}{2}\left\langle g^2\phi^2\chi^2\right\rangle \tag{4.22}$$

$$\frac{1}{2}\left\langle\dot{\chi}^2\right\rangle = \frac{1}{2}\left\langle\left(\frac{\nabla\chi}{a}\right)^2\right\rangle + \frac{1}{2}\left\langle g^2\phi^2\chi^2\right\rangle \tag{4.23}$$

Where the average is over space and time. We will discuss the virialization of each system separately below. Through out our study we will compare models under consideration for mainly two different value of $\phi_*$: one super-Planckian value when the models predictions are similar to their respective power-law chaotic models and one sub-Planckian value when the effects of the scale $\phi_*$ are important.

#### 4.4.1.1 $n = 2$

Since we will be considering different inflationary models where different kind of parameterization will be needed for the our lattice simulation. We will describe those in detail for each models. For $n = 2$ model, using the default re-scaling scheme of `LATTICEEASY`, we define the following quantities that will be used for simulation

$$\varphi \equiv \frac{\phi}{\phi_0}a^{\frac{3}{2}}, \quad X \equiv \frac{\chi}{\phi_0}a^{\frac{3}{2}}, \quad z \equiv mt, \quad \vec{z} \equiv m\vec{x}. \tag{4.24}$$

where $x^\mu \equiv (t, \vec{x})$ is the cosmic time and comoving coordinate. The field equations described in Eqs.(4.4) and (4.5) now reduces to

$$\varphi'' - \frac{1}{a^2}\nabla^2\varphi - \left[\frac{3}{4}\left(\frac{a'}{a}\right)^2 - \frac{3}{2}\frac{a''}{a}\right]\varphi + \frac{\mathcal{Q}}{a^3}\varphi X^2 + \frac{\partial}{\partial\varphi}V(\varphi) = 0 \tag{4.25}$$

$$X'' - \frac{1}{a^2}\nabla^2 X - \left[\frac{3}{4}\left(\frac{a'}{a}\right)^2 - \frac{3}{2}\frac{a''}{a}\right]X + \frac{\mathcal{Q}}{a^3}\varphi^2 X = 0. \tag{4.26}$$

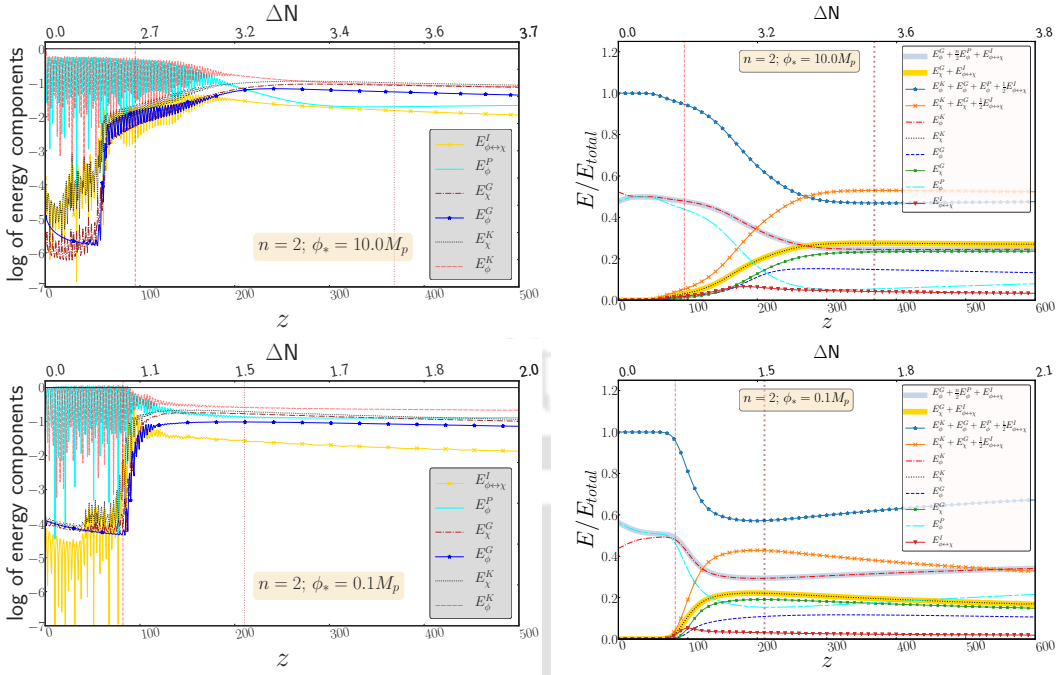


Figure 4.4: The variation of energy components normalized by the initial energy with time and the e-folding number is shown. The plot in the right is oscillation average.

Where *prime*($\prime$) denotes derivative with respect to $z$ and $\mathcal{Q}$ is the resonance parameter defined as

$$\mathcal{Q} \equiv \frac{g^2}{m^2}\phi_0^2$$

We chose the two values of $\phi_* = (10M_p, 0.1M_p)$. To felicitate comparison with previous works, in all our lattice simulation we have set $\mathrm{m_p} = 1$. PLANCK normalization set the values of the scale $m$ as $(m_{10}, m_{0.1}) = (1.38 \times 10^{-6},\ 9.38 \times 10^{-6})$ in unit of $\mathrm{m_p}$. We have started our simulation when $\varphi'(z_0) = 0$ with the initial field values at $(0.191\mathrm{m_p},\ 0.0157\mathrm{m_p})$. The coupling parameter for both values of $\phi_*$ is taken to be $g^2 = 2.2 \times 10^{-5}$. We have used a $256^3$ lattice with a comoving edge size $L = (10/m_{10}, 70/m_{0.1})$ respectively for the two values of $\phi_*$. The grid spacing corresponding to the above set of parameters are $dx \sim (0.04/m_{10}, 0.3/m_{0.1})$. Different choices of $L$ are made so that the grid spacing which set the limit to capture the momenta ranges in the simulation is nearly the same in both the cases. The time step for those two cases are $dt = (0.001/m_{10}, 0.001/m_{0.1})$. The maximum (comoving) momenta that can be possibly excited during the broad parametric resonance in this case will be (4.21)

$$k_{max}^2 \sim \mathcal{Q}^{1/2} m^2. \tag{4.27}$$

Now for a $N^3$ lattice with lattice spacing $L$, the minimum and the maximum (discrete) momenta that can be captured in a lattice simulation are $(2\pi)/L$ and $(\sqrt{3N}\pi)/L$ respectively. Thus in order to capture the correct UV physics, we must ensure that the minimum momenta range above must be well below the value of $k_{max}$. Also, to capture the IR physics for sufficient long time we must also ensure that the maximum momenta is large enough(which call for simulation with large lattice points). We can readily verify that these lattice parameters are adequate to capture both the IR and UV physics for a sufficient time of simulation. The

Table 4.1: Fractions of energy components at $z = z_{br}$ for $n = 2$

| $\phi_*(M_p)$ | $\frac{E^K_\phi}{E_T}$ | $\frac{E^P_\phi}{E_T}$ | $\frac{E^K_\chi}{E_T}$ | $\frac{E^I_{\phi\leftrightarrow\chi}}{E_T}$ | $\frac{E^T_\phi}{E_T}$ | $\frac{E^T_\chi}{E_T}$ |
|---|---|---|---|---|---|---|
| 10 | 48.0% | 44.0% | 3.0% | 2.0% | 95.0% | 5.0% |
| 0.1 | 48.0% | 46.3% | 2.7% | 2.1% | 95.0% | 5.0% |

Table 4.2: Fractions of energy components at $z = z_{dec}$ for $n = 2$

| $\phi_*(M_p)$ | $\frac{E^K_\phi}{E_T}$ | $\frac{E^P_\phi}{E_T}$ | $\frac{E^G_\phi}{E_T}$ | $\frac{E^K_\chi}{E_T}$ | $\frac{E^G_\chi}{E_T}$ | $\frac{E^I_{\phi\leftrightarrow\chi}}{E_T}$ | $\frac{E^T_\phi}{E_T}$ | $\frac{E^T_\chi}{E_T}$ |
|---|---|---|---|---|---|---|---|---|
| 10 | 24.5% | 5.5% | 14.6% | 27.6% | 23.4% | 4.1% | 47.0% | 53.0% |
| 0.1 | 29.4% | 15.4% | 11.0% | 22.2% | 19.1% | 3.1% | 57.2% | 42.7% |

evolution of the comomving inflaton field for two values of $\phi_*$ has been shown in fig(4.3). The back-reaction of the $\chi$ field starts to play role within $\Delta N_{br} \sim (2.7,\ 1)$ for $\phi_* = (10M_p,\ 0.1M_p)$. It is evident that the duration of parametric resonance phase decreases with decreasing $\phi_*$. In fig(4.4), the left two panel describes the evolution of every individual energy components of the inflaton and the reheating field with respect to $z$. Where as in the right panels it is their oscillation average. In order to have a quantitative understanding, the fractions of different energy components have been tabulated. From tab.(4.1), we can clearly see that during the initial phase when particle production is mainly due to parametric resonance, irrespective of $\phi_*$ value, only 5% of the total energy component is getting transferred into the reheating field. However most efficient transfer of energy occurs after the onset of back-reaction until the stationary phase is achieved with complete thermalization at around $\Delta N_{dec} \sim (3.5,\ 1.5)$ for the two values of $\phi_*$. After the end of this back-reaction dominated phase at $z = z_{dec}$, all individual energy component freezes out to a constant value given in the table(4.2). At this point let us bring to our reader's notice an important characteristic feature in the non-linear regime of thermalization is that during this phase the inhomogeneities start to grow rapidly for both the field and then reach a stationary phase. It would be interesting to understand the fact that as we decrease $\phi_*$ the growth of inhomogeneities are less. Therefore, for smaller value of $\phi_*$ or in other words for small scale inflation, local inhomogeneity during reheating will be suppressed and it can have interesting effect after the end of reheating. We will see in our subsequent discussions that this behavior of inhomogeneous evolution depending upon $\phi_*$ will be similar for other models such as $n = 4, 6$. Analytic understanding of this phenomena could interesting. As has been mentioned before, irrespective of the value of $\phi_*$, only nearly 50% of the inflation energy density has been transferred to the reheating $\chi$ field before non-perturbative production being completely stopped. Therefore, in order to complete the decay we need to perform perturbative decay separately to obtain the reheating temperature, that we will discuss in the end. For this process three leg interaction $\phi\chi^2$ may be dominant. In our future publication we will consider both four and three leg interactions to examine decay process and thermalization.

In any case for $n = 2$, we should emphasize that our numerical simulation does not give the condition of equal energy distribution among the inflaton and daughter particle in the stationary phase. As mentioned earlier the equation of state of both the field does not become that of the radiation as opposed to other models $n = 4, 6$ that will be discussed in the subsequent sections.

#### 4.4.1.2 $n = 4$

For $n = 4$ model we define the following dimensionless quantities that will be used for simulation

$$\varphi \equiv \frac{\phi}{\phi_0} a^{-1}, \quad X \equiv \frac{\chi}{\phi_0} a^{-1}, \quad z \equiv \phi_0 \sqrt{\lambda}\, t, \quad \vec{z} \equiv \phi_0 \sqrt{\lambda}\, \vec{x}, \tag{4.28}$$

where $x^\mu \equiv (t, \vec{x})$ is the cosmic time and comoving coordinate. The field equations described in Eqs.(4.4) and (4.5) reduces to

$$\varphi'' - \nabla^2 \varphi - \frac{a''}{a}\varphi + \mathcal{Q}\varphi X^2 + \frac{\partial}{\partial \varphi} V(\varphi) = 0 \tag{4.29}$$

$$X'' - \nabla^2 X - \frac{a''}{a} X + \mathcal{Q}\varphi^2 X = 0. \tag{4.30}$$

The resonance parameter is defined as

$$\mathcal{Q} \equiv \frac{g^2}{\lambda}$$

For this case too, we chose two values of $\phi_* = (10M_p, 0.1M_p)$. From PLANCK normalization the value of the dimensionless parameter $\lambda$ turned out to be $(4.2 \times 10^{-13},\ 4.7 \times 10^{-8})$. At the end of inflation the field values assumes $(0.342\mathrm{m_p},\ 0.0177\mathrm{m_p})$. The coupling parameter for both the run is chosen to be $g^2 = 2.3 \times 10^{-5}$. We have used a $256^3$ lattice with a comomving edge size $L = (10/\mathcal{B}_{10}, 180/\mathcal{B}_{0.1})$. The grid spacing in these case are $\mathrm{d}x \sim (0.04/\mathcal{B}_{10}, 0.7/\mathcal{B}_{0.1})$. The time step we chose in these cases are $dt = (0.0001/m_{10}, 0.001/m_{0.1})$. Using (4.21), the maximum (comoving) momenta that could be excited here is found to be

$$k^2_{max} \sim \mathcal{Q}^{1/2}\phi_0^2\lambda, \tag{4.31}$$

Following the discussion of the $n = 2$ case, we can verify that these parameters will capture the necessary momentum ranges for a sufficient time. As we mentioned and also clearly seen from various plots, the qualitative behavior of decaying inflaton for this case is similar to that of $n = 2$ model. From the figs.4.5 we see with the decreasing $\phi_*$, the decay of inflaton become efficient. After the initial linear regime, for this case the back-reaction sets in at around $\Delta N_{br} = (3.2,\ 0.9)$ e-folding number while the subsequent stationary phase is achieved at $\Delta N_{dec} = (4.7,\ 2.2)$. The qualitative behavior of this model will be the same as $n = 2$ case. However, from the table(4.4) it is important to see that in the stationary phase the total energy becomes equally distributed between the inflaton and the daughter field.

#### 4.4.1.3 $n = 6$

For this model the re-scaled variables are defined as

$$\varphi \equiv \frac{\phi}{\phi_0} a^{\frac{3}{4}}, \quad X \equiv \frac{\chi}{\phi_0} a^{\frac{3}{4}}, \quad z \equiv \frac{\phi_0^2}{m} t, \quad \vec{z} \equiv \frac{\phi_0^2}{m} \vec{x}. \tag{4.32}$$

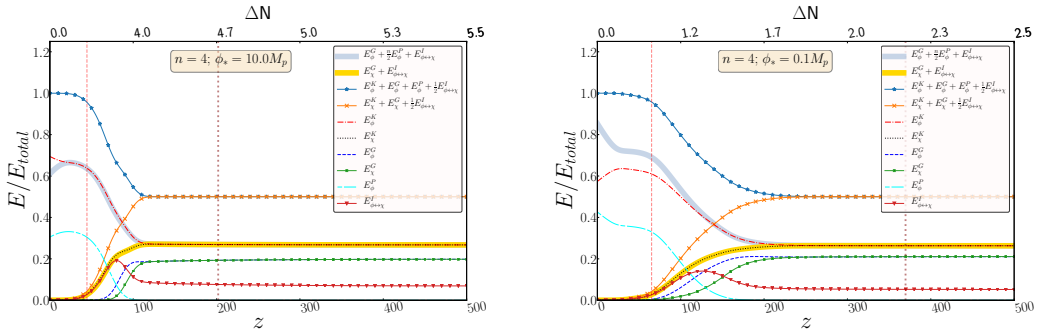


FIGURE 4.5: The variation of energy components with time and the efolding number is shown.

Table 4.3: Fractions of energy components at $z = z_{br}$ for model $n = 4$

| $\phi_*(M_p)$ | $\frac{E^K_\phi}{E_T}$ | $\frac{E^P_\phi}{E_T}$ | $\frac{E^K_\chi}{E_T}$ | $\frac{E^I_{\phi\leftrightarrow\chi}}{E_T}$ | $\frac{E^T_\phi}{E_T}$ | $\frac{E^T_\chi}{E_T}$ |
|---|---|---|---|---|---|---|
| 10 | 62.6% | 29.2% | 4.5% | 3.9% | 93.8% | 6.2% |
| 0.1 | 63.7% | 30.4% | 3.0% | 2.8% | 95.0% | 5% |

Table 4.4: Fractions of energy components at $z = z_{dec}$ for model $n = 4$

| $\phi_*(M_p)$ | $\frac{E^K_\phi}{E_T}$ | $\frac{E^P_\phi}{E_T}$ | $\frac{E^G_\phi}{E_T}$ | $\frac{E^K_\chi}{E_T}$ | $\frac{E^G_\chi}{E_T}$ | $\frac{E^I_{\phi\leftrightarrow\chi}}{E_T}$ | $\frac{E^T_\phi}{E_T}$ | $\frac{E^T_\chi}{E_T}$ |
|---|---|---|---|---|---|---|---|---|
| 10 | 26.9% | – | 19.3% | 27.0% | 19.3% | 7.6% | 50.0% | 50.0% |
| 0.1 | 26.3% | 0.2% | 21.0% | 26.3% | 21.0% | 5.2% | 50.0% | 50.0% |

The field equations described in Eqs.(4.4) and (4.5) for $n = 6$ reduces to

$$\varphi'' - a\nabla^2\varphi - \left[\frac{3}{4}\frac{a''}{a} - \frac{3}{16}\left(\frac{a'}{a}\right)^2\right]\varphi + \mathcal{Q}a^{\frac{3}{2}}\varphi X^2 + \frac{\partial}{\partial\varphi}V(\varphi) = 0 \tag{4.33}$$

$$X'' - a\nabla^2 X - \left[\frac{3}{4}\frac{a''}{a} - \frac{3}{16}\left(\frac{a'}{a}\right)^2\right]\varphi + \mathcal{Q}a^{\frac{3}{2}}\varphi^2 X = 0. \tag{4.34}$$

Where the resonance parameter turned out as

$$\mathcal{Q} \equiv \frac{g^2m^2}{\phi_0^2}$$

As opposed to the other two models $n = 2, 4$, for the this case we have to chose $\phi_* = (1M_p, 0.5M_p)$ to make the lattice input parameters $g^2m^2 = (200,\ 9)$ within the reach of simulation with a practical time step(with our current computational resource). It has been found that the model with $n = 6$ takes the longer time for simulation which further increases

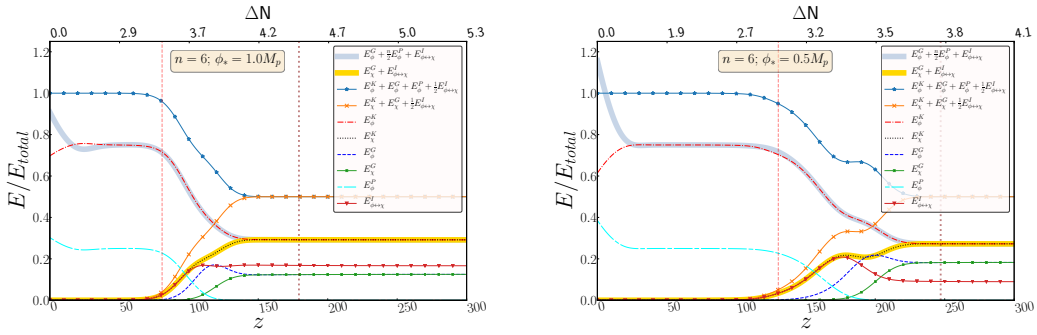


Figure 4.6: Evolution of various energy components for $n = 6$ model.

with increasing value of the coupling parameter $g^2$. With our present computational resource as well as for optimum run time, we are able to simulate for the values of the input parameter $g^2m^2 < 1000$. The value of the scale $m$ from WMAP normalization becomes $(2.7\times10^4,\ 5.6\times10^3)$ in unit of $\mathrm{m_p}$ that will be our one set of input parameters. After the end of inflation the initial field values are taken to be $(0.226\mathrm{m_p},\ 0.138\mathrm{m_p})$ and the coupling parameter for both $\phi_*$ value is chosen as $g^2 = 2.8\times10^{-7}$. In this case too we have used a $256^3$ lattice with a comoving edge size $L = (250/\mathcal{B}_1, 250/\mathcal{B}_{0.5})$. The grid spacing in these case are $\mathrm{d}x \sim (0.04/\mathcal{B}_1, 0.7/\mathcal{B}_{0.5})$. The time steps for the two cases are set as $dt = (0.0001/\mathcal{B}_1, 0.0001/\mathcal{B}_{0.5})$. For this case (4.21) yields the maximum momenta to be

$$k^2_{max} \sim \mathcal{Q}^{1/2}\frac{\phi_0^4}{m^2}. \tag{4.35}$$

Due to increases complexity of the terms in the potential and its derivatives in this case, it has been found that it take longer simulation time for the same program time compared to the previous two cases. With the above lattice parameters we can check that the simulation captures the necessary UV physics. The IR physics is also captured sufficiently within simulation period. We have run the simulation for program time $z = 300$ in these cases within which the decay of inflaton is found to reach the desired stationary limit. However, for long time simulation we need larger lattice points for sufficient IR resolution. The simulation results show that the non-linear back-reaction regime starts at around $\Delta N_{br} = (3.5,\ 3.0)$ and then finally the equilibrium condition is achieved at $\Delta N_{dec} = (4.5,\ 3.8)$ for the two values of $\phi_*$. In this case too, the energy will be distributed equally to both inflaton and daughter field as opposed to $n = 2$ case as seen in table(4.6).

### 4.4.2 Equation of state

The equation of state is one of the most important parameters to study during preheating. The equation of state in this context is defined as:

$$w = \frac{p}{\rho} = \frac{\frac{1}{2}\dot{\phi}^2 + \frac{1}{2}\dot{\chi}^2 - \frac{1}{3}\frac{(\nabla\phi)^2}{2a^2} - \frac{1}{3}\frac{(\nabla\chi)^2}{2a^2} - V(\phi,\chi)}{\frac{1}{2}\dot{\phi}^2 + \frac{1}{2}\dot{\chi}^2 + \frac{(\nabla\phi)^2}{2a^2} + \frac{(\nabla\chi)^2}{2a^2} + V(\phi,\chi)} \tag{4.36}$$

For a homogeneous inflaton condensate oscillating in a potential $V(\phi) \propto \phi^n$, using the virial theorem, the equation state is given by[41, 64] $w = (n-2)/(n+2)$. The inflaton initially oscillates with this equation of state till the other components of the total energy such as

Table 4.5: Fractions of energy components at $z = z_{br}$ for model $n = 6$

| $\phi_*(M_p)$ | $\frac{E^K_\phi}{E_T}$ | $\frac{E^P_\phi}{E_T}$ | $\frac{E^K_\chi}{E_T}$ | $\frac{E^G_\chi}{E_T}$ | $\frac{E^I_{\phi\leftrightarrow\chi}}{E_T}$ | $\frac{E^T_\phi}{E_T}$ | $\frac{E^T_\chi}{E_T}$ |
|---|---|---|---|---|---|---|---|
| 1 | 71.5% | 22.8% | 2.7% | 0.3% | 2.7% | 95.0% | 5.0% |
| 0.5 | 70.3% | 22.7% | 3.4% | 0.2% | 3.4% | 95.0% | 5.0% |

Table 4.6: Fractions of energy components at $z = z_{dec}$ for model $n = 6$

| $\phi_*(M_p)$ | $\frac{E^K_\phi}{E_T}$ | $\frac{E^G_\phi}{E_T}$ | $\frac{E^K_\chi}{E_T}$ | $\frac{E^G_\chi}{E_T}$ | $\frac{E^I_{\phi\leftrightarrow\chi}}{E_T}$ | $\frac{E^T_\phi}{E_T}$ | $\frac{E^T_\chi}{E_T}$ |
|---|---|---|---|---|---|---|---|
| 1 | 29.2% | 12.4% | 29.2% | 12.4% | 16.8% | 50.0% | 50.1% |
| 0.5 | 27.3% | 18.2% | 27.3% | 18.2% | 9.0% | 50.0% | 50.0% |

gradient, interaction energy became significant and resulting in fragmentation. Ignoring the interaction energy, and using the virial relations given in eq.4.23 the definition of $w$ in 4.36 reduces to

$$w = \frac{1}{3} + \frac{(n-4)}{6}\frac{1}{\frac{n+2}{4} + \frac{\langle(\nabla\phi)^2/2a^2\rangle}{\langle V(\phi)\rangle} + \frac{\langle(\nabla\chi)^2/2a^2\rangle}{\langle V(\phi)\rangle} + \frac{3}{2}\frac{\langle V_I\rangle}{\langle V(\phi)\rangle}} \tag{4.37}$$

Using the values of average energies of different components listed in tables 4.2, 4.4 and 4.6, we found that $w \to 0.2$ for $n = 2$ and $w \to 1/3$ for $n = 4$, and 6 in the stationary phase. The results of the simulation are plotted in figs. 4.7 to 4.9. We have plotted the instantaneous equation of state(brown curves) as well as the average value over a period of one inflaton oscillation(red dashed curves). The green line shows the homogeneous Inflation equation of state. The features we note from these figures for different models are

(i) For $n = 2$ models, the equation of state make a transition from $w = 0$ to $w \sim 0.2 - 0.3$ within a few e-folding numbers. However, the equation of state never reaches the radiation like equation of state($w = 1/3$). This behavior has also been noted in [170] for the $m^2\phi^2$ model. Similar behavior is expected here as our model boils down to usual power law potential near the minimum at $\phi = 0$. We also observed that reducing the scale $\phi_*$ does not improve the scenario except reducing the duration of preheating phase. We have found that with longer simulation equation of state starts decreasing after reaching a maximum $w \sim 0.3$ and finally settles to $w \to 0.1$. The reason for this behavior is that for $n = 2$ model, which is identical to $m^2\phi^2$ around the minimum, the massive inflaton component although may remain under-abundant during preheating eventually rise up to dominate after the inflation decay ceases. It has also been found[170] that $w(t)$ depends non-monotonically on the resonance parameter $q$ (or alternatively on the coupling $g^2$) for higher value of $\phi_*$. However it can be seen that increasing $g^2$ will not help us reaching the radiation domination as depicted in figure (4.10). However, interesting observation can be made on the dependence of $\phi_*$. For sub-Planckian value of $\phi_* = 0.1\mathrm{M_p}$ the equation

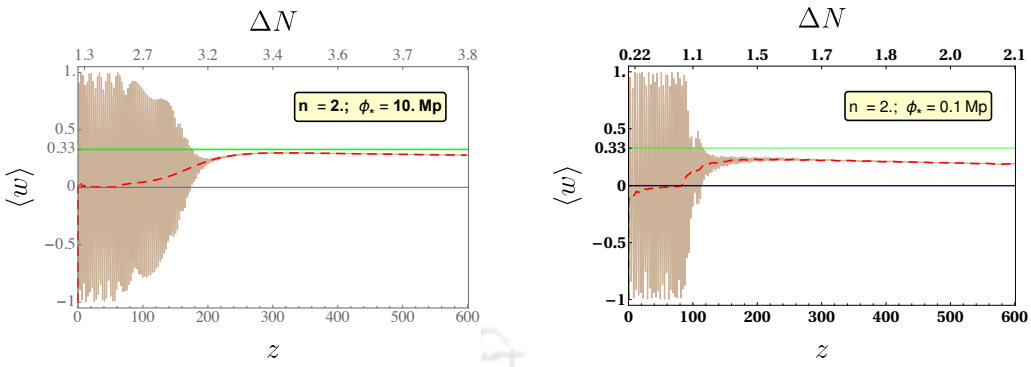


FIGURE 4.7: The variation of equation of state with time(or alternatively the e-folding number) for the two values of the scale $\phi_*$. The solid blue lines are the instantaneous value of the equation of state while the red dotted line is the averaged value over a period of inflaton oscillation. Time is measured in unit of their respective scale $m$ hence to facilitate a comparison between different models, the efolding number is shown in the upper panel.

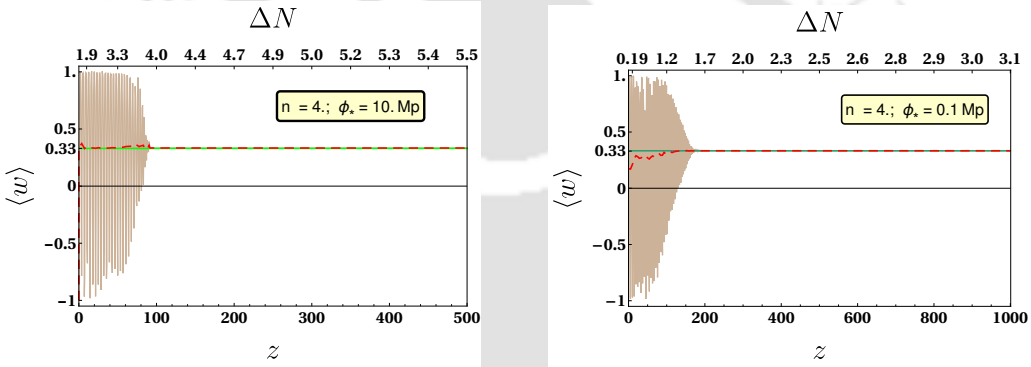


FIGURE 4.8: The variation of equation of state with time(or alternatively the e-folding number) for the two values of the scale $\phi_*$. The solid blue lines are the instantaneous value of the equation of state while the red dotted line is the averaged value over a period of inflaton oscillation.

of state $w$ changes almost instantaneously from zero to its maximum value before the system could reach the thermal equilibrium and apparently it also depends monotonically on the coupling parameter $g^2$. Therefore, lowering the value of $\phi_*$ makes the intermediate or the turbulent phase more efficient.

(ii) For $n = 4$ model, the homogeneous condensate itself oscillates with $w = 1/3$ at the onset of preheating. The simulation results shows that it retains the radiation like equation of state throughout the simulation period. Decreasing $\phi_*$ have the same qualitative behavior, with an important difference compared to $n = 2$ model is that intermediate or turbulent regime occurs for longer time. Therefore the evolution of $w(t)$ do not provide any additional information about the thermalization process in this case.

(iii) In the case of model with $n = 6$, the homogeneous condensate has equation of state $w = 1/2$. Here the equation of state makes a transition from $w = 1/2$ to $w \to 1/3$ for both values of $\phi_*$.

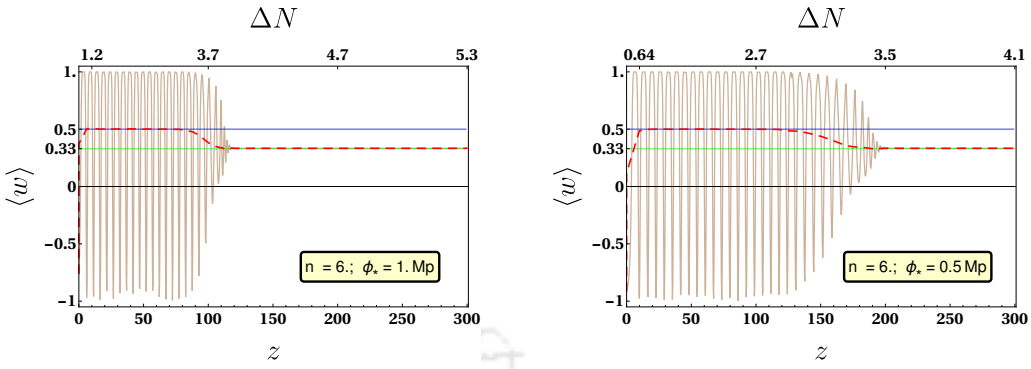


FIGURE 4.9: The variation of equation of state with time(or alternatively the e-folding number) for the two values of the scale $\phi_*$. The solid blue lines are the instantaneous value of the equation of state while the red dotted line is the averaged value over a period of inflaton oscillation.

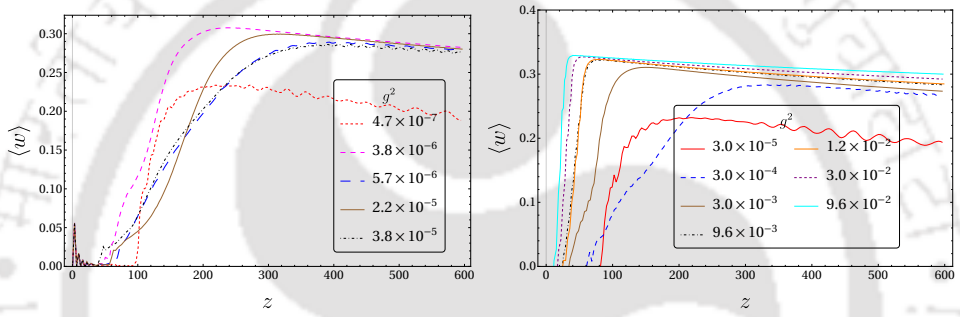


(a) (b)

FIGURE 4.10: Variation of equation of state with $g^2$ for model $n = 2$ for the two values of $\phi_*$. It is evident that indefinitely increasing $g^2$ will not bring radiation domination for $n = 2$.

### 4.4.3 Occupation Numbers

Evolution of occupation number for different modes is an another important parameter that contains important information about the microscopic mechanism of the preheating as well as the details of thermalization process. In general the occupation number will be well defined if the interaction energy is negligible. It is apparent form figs. 4.4 to 4.6 that during the whole preheating period, the interaction energy is dominated only for a very brief period of time right after the initial parametric regime where re-scattering effect is important. Therefore, the occupation number$(n_k^\phi, n_k^\chi)$ of the fields are always well defined except for this small interval. Following[43, 170], we, therefore, can understand the thermalization process across all possible modes by considering the Rayleigh-Jeans spectrum defined by the product $n_k\omega_k \simeq T$ in the large occupation number limit which is generally true during preheating. The above Rayleigh-Jeans spectrum can be easily obtained from the following bosonic distribution function defined at finite temperature $T$ as

$$n_k = \frac{1}{exp\left(\frac{\omega_k - \mu}{T}\right) - 1}, \tag{4.38}$$

in small chemical potential $\mu$ limit. This implies that rather than plotting the occupation number for a particular mode, we will get a better understanding of the thermalization process

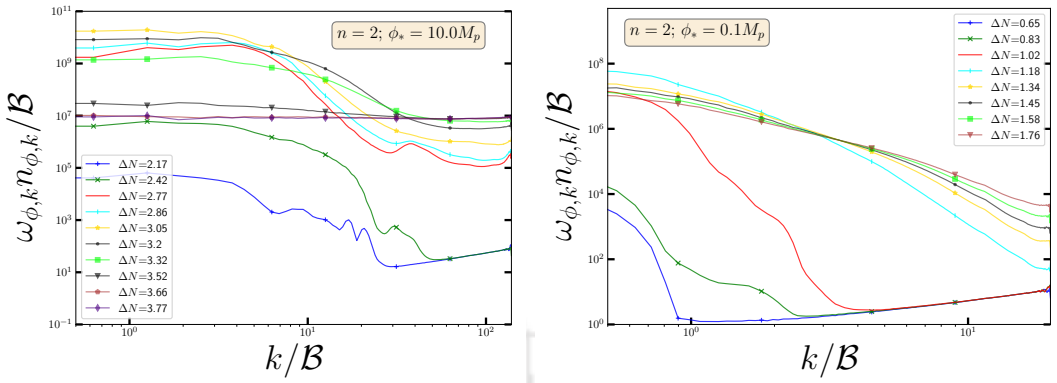


(a) $n = 2,\ \phi_* = 10M_p$ (b) $n = 2,\ \phi_* = 0.1M_p$

FIGURE 4.11: The evolution of the combination $\omega_{\phi,k}n_{\phi,k}$ as a function of momentum k at different e-folding numbers for $n = 2$ for the two values of $\phi_*$

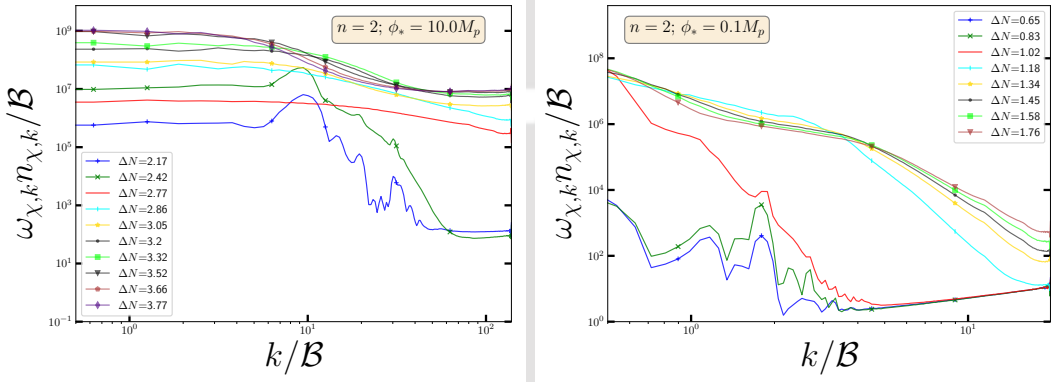


(a) $n = 2,\ \phi_* = 10M_p$ (b) $n = 2,\ \phi_* = 0.1M_p$

FIGURE 4.12: Same plot as Fig.(4.11) for the $\chi$ field.

by considering the combination $\omega_k n_k$ as a function of comoving wave number $k$ as plotted below in figs. 4.11 to 4.16 for different values $n$. We have, as usual, chosen the previous two values of the controlling scale $\phi_*$. The e-folding instants are chosen to cover all the three different stages of preheating discussed earlier. From the dynamics of occupation number over time, we clearly observes that with increasing $n$, the system thermalize faster. Therefore, it would be interesting to understand this turbulent phase more closely.

For model with $n = 2$, during the initial linear regime of parametric resonance, the (infra-red)IR modes are populated first. After the stationary phase, the IR modes shows a greater tendency for thermalization. Nevertheless the overall spectra shows that the thermalization has not been achieved. Decreasing $\phi_*$ do not improve the thermalization as we have seen earlier from the study of equation of state. For $n = 4$ the spectra after stationary phase evolve towards higher comoving momenta. But the spectra do not show thermalized behavior for $\phi_* = 10M_p$. Decreasing $\phi_*$ shows a greater tendency for thermalization. For models with $n = 6$, the spectra is mostly flat after the initial linear stage indicating the achievement of thermalization.

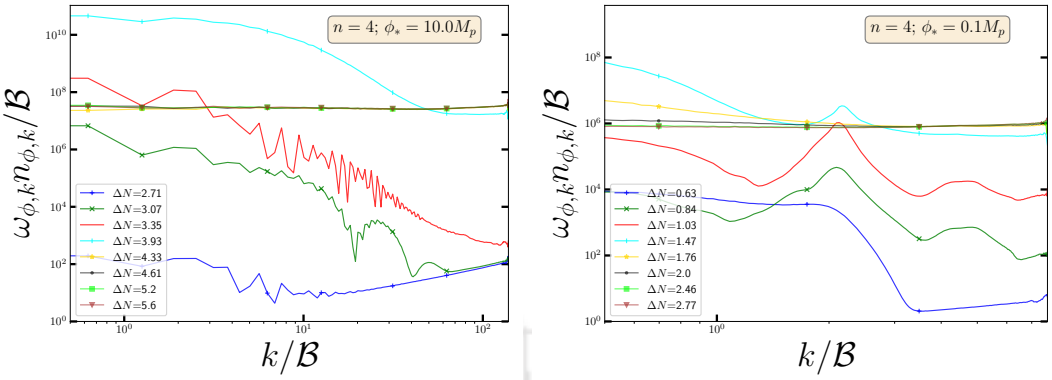


(a) $n = 4,\ \phi_* = 10M_p$ (b) $n = 4,\ \phi_* = 0.1M_p$

FIGURE 4.13: Same plot as Fig.(4.11) for the $n = 4$

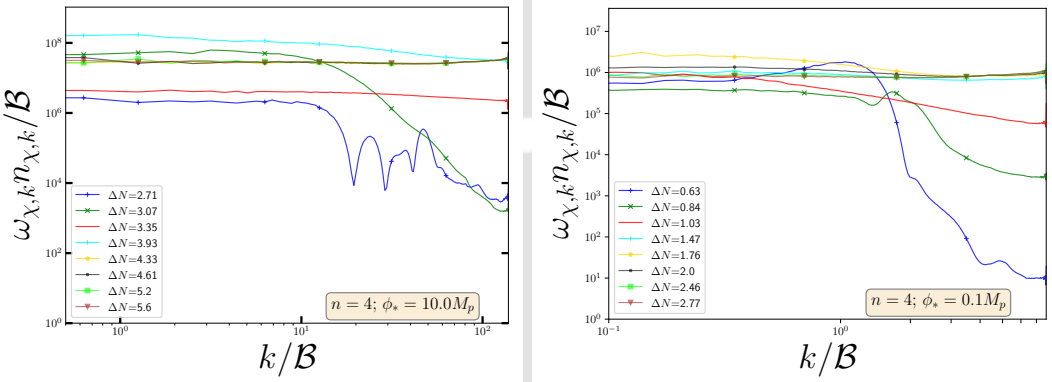


(a) $n = 4,\ \phi_* = 10M_p$ (b) $n = 4,\ \phi_* = 0.1M_p$

FIGURE 4.14: Same plot as Fig.(4.13) for the $\chi$ field

Finally, we have plotted the total number densities $n(t)$ of the two fields defined in eq. (4.12) for the models in figs. 4.17 to 4.19. Evolution of total number of particles for a particular species encodes the information about the different mechanisms responsible for changing the particle number. For example at small coupling when the particle number is small the perturbative quantum scattering process ($\phi\chi \to \phi\chi$) conserves the total particle number. This particular phase can be well described by classical wave scattering known as "weak turbulence" [171]. The weak turbulence is generally refereed to a phenomena of freely propagating energy cascade when the kinetic description is applicable, and the total particle number remain conserved which is the static phase in our ($n(t)$ *vs* $z$) curve. However, before this static phase, in the intermediate regime when the particle number is very large during preheating, despite small coupling, the higher order interactions generically dominates, and the system stays in strong turbulence regime where total particle number will not be conserved. All these phenomena has already been widely studied in the context of reheating dynamics [160, 161, 171], whose late time behavior is characterized by a turbulent and self-similar evolution of distribution functions towards equilibrium.

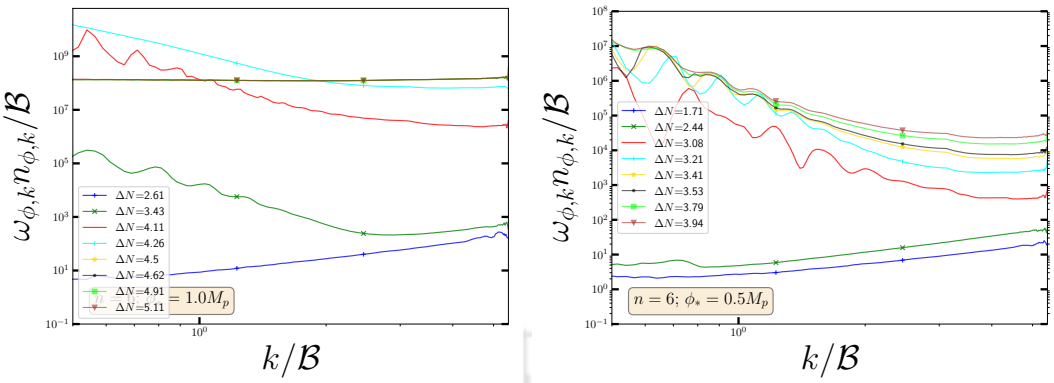


(a) $n = 6$, $\phi_* = 1M_p$ (b) $n = 6$, $\phi_* = 1M_p$

FIGURE 4.15: Same plot as Fig.(4.11) for the $n = 6$. In the inset we have zoomed in the higher values of the UV regime.

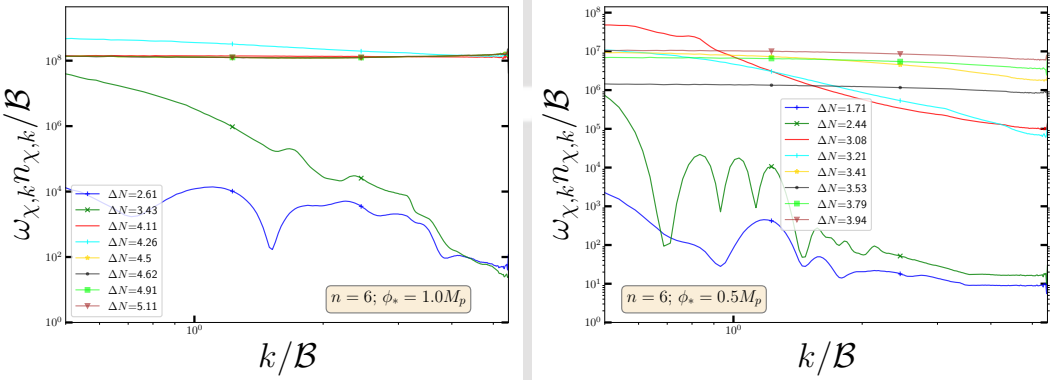


(a) $n = 6$, $\phi_* = 1M_p$ (b) $n = 6$, $\phi_* = 0.5M_p$

FIGURE 4.16: Same plot as Fig.(4.15) for the $\chi$ field

The particle numbers initially increases exponentially due to parametric resonance which is followed by a gradual decrease in the turbulent regime and finally settling to an asymptotic flat regime during the stationary phase. The gradual decrease is due to the fact that during the turbulent regime the occupation number shifts from low to higher momentum thereby decreasing the overall number. For our two non-linearly coupled system, when the same is in the non-linear regime where mode-mode coupling $XX\phi \to \int dk'dk'' X_{k'} X_{k''} \phi_{k-k'-k''}$ in the momentum space becomes non-negligible, energy flow towards UV modes should also have compensating opposite flow for $k \to k' + k''$ decay channel. [160, 161, 171]. However, as is obvious from the numerical constraints coming from the finite size 3D lattice box, such a flow towards IR modes are absent in the lattice simulation due to the finite size of the box. For, $n = 2$, the total number for the two fields do not became identical at the end of stationary phase. For, $n = 4$ decreasing $\phi_*$ make the two spectra identical. For $n = 6$ the total number for the two fields reaches the same value after the stationary phase for both the value of $\phi_*$. This feature is consistent with our previous conclusion that for $n = 2$ model, the system is not

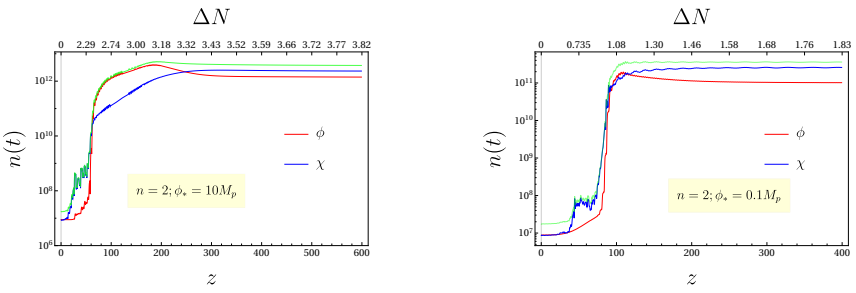


(a) (b)

FIGURE 4.17: Total number density for $n = 2$ with $\phi_* = (10M_p,\ 0.1M_p)$ Red, blue and green lines corresponds to $n_t^\phi$, $n_t^\chi$ and $(n_t^\phi + n_t^\chi)$ respectively.

fully thermalized at the end of preheating.

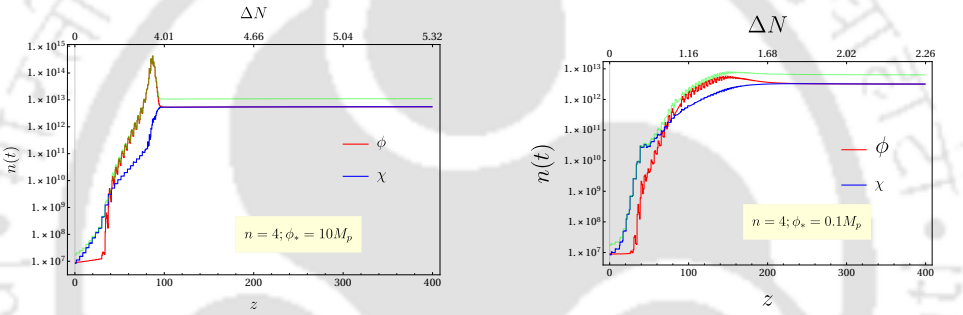


(a) (b)

FIGURE 4.18: Total number density for $n = 4$ with $\phi_* = (10M_p,\ 0.1M_p)$

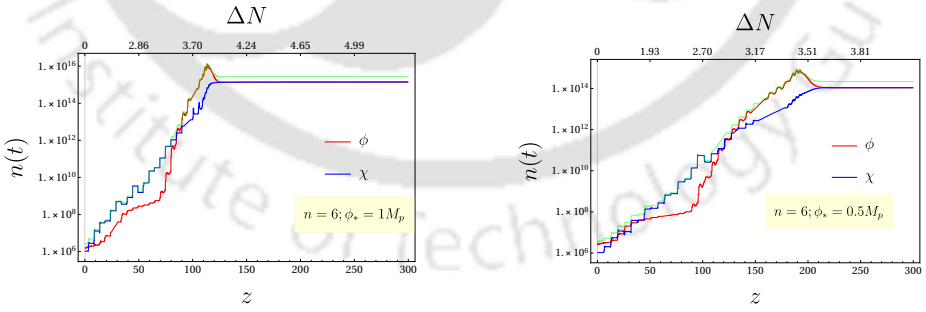


(a) (b)

FIGURE 4.19: Total number density for $n = 6$ with $\phi_* = (1M_p,\ 0.5M_p)$

### 4.4.4 Perturbative reheating and constraints from CMB

The purpose of the reheating phase is to create the right initial conditions for the standard big-bang. Therefore, after the end of reheating the final dominating energy component should

be radiation with the characteristic equation of state $w = 1/3$. As we have seen for models with $n > 2$, the preheating is sufficient to obtain the final equation of state of the system to be radiation like. However, it is important to remember that final state of preheating is a combination of two radiation like fluids with approximately 50% of it is the inflaton field itself. Therefore, even though it behaves like a radiation, in order to connect with the CMB, one needs to consider further decay of inflaton into radiation by perturbative processes. In any case for $n = 2$ models we have seen that the final equation of state is not that of radiation. For long time simulation we have seen that $w \to 0.1$ for $n = 2$ model. As we have mentioned that we need further perturbative decay of inflaton to complete the reheating and set the correct initial conditions for the big-bang. We have already mentioned before that to obtain the radiation domination, a thee-legs interaction such $\phi\chi^2$ will be important. The full numerical lattice simulation considering both the interaction term will be considered in our subsequent paper. At this point we may attempt an alternative approach that will also help us to connect the reheating phase with present CMB data. We will follow the formalism developed in our recent papers [138] generalizing the works in [60, 61] for decaying inflaton. For recent studies on CMB constraints on reheating phase see[87, 98–101, 101–103, 172, 173]. In our following analysis, we will assume that the decay of total energy density $\rho_t$ whose initial value will be identified with the value obtained after the end of preheating is via a phenomenological decay term. The perturbative reheating due to such a decay term was first considered in the initial treatments of reheating[26, 27, 29, 95]. For $n = 2$, we take the value equation of state at the onset of stationary phase which is $w_{\rm dec} \sim 0.22$. Now introducing the phenomenological decay term for total energy decay we may write

$$\begin{aligned} \dot{\rho}_t + 3H(1 + w_{\rm dec})\rho_\phi + \Gamma\rho_t = 0, \\ \dot{\rho}_R + 4H\rho_R - \Gamma\rho_t = 0, \end{aligned} \tag{4.39}$$

where $\rho_R$ is the additional radiation energy density. In terms of following dimensionless variables

$$\Phi = \frac{a^{3(1+w_{\rm dec})}\rho_t}{a_I^{3(1+w_{\rm dec})}\rho_I}; \qquad R = \frac{a^4\rho_R}{a_I^3\rho_I}, \tag{4.40}$$

the above equations for energy densities transformed into

$$\Phi'(N) + \frac{\Gamma}{\mathbb{H}}\Phi(N) = 0, \tag{4.41}$$

$$R'(N) - \frac{\Gamma}{\mathbb{H}}e^{(1-3w_{\rm dec})N}\Phi(N) = 0, \tag{4.42}$$

where "prime" is taken with respect to e-folding "N" which is obtained from the Hubble equation

$$3M_{\rm p}^2\mathbb{H}^2 = \rho_I\left[\frac{\Phi(N)}{e^{3(1+w_{\rm dec})N}} + \frac{R(N)}{e^{4N}}\right] \tag{4.43}$$

This equation could be easily solved for a given inflaton decay term. As mentioned, one of our main goal is to understand the direct constraints coming from the CMB. For a given cosmological scale $k = a_k H_k$ which exits the horizon inflation with scale factor $a_k$ and re-enters the horizon with the scale factor $a_0$ at the present time, satisfies the following relation,

$$N_k + N_{\rm pre} + N_{\rm re}^{\rm pert} + ln\left(\frac{a_0}{a_{\rm re}}\right) + ln\left(\frac{k}{a_0 H_k}\right) = 0, \tag{4.44}$$

where $(N_k, N_{\rm pre}, N_{\rm re}^{\rm pert})$ are the inflationary, preheating and perturbative reheating e-folding number respectively. $a_{re}$ is the scale factor after the end of perturbative reheating. Assuming that the entropy is preserved after reheating implies

$$g_{\rm re}T_{\rm re}^3 = \left(\frac{a_0}{a_{\rm re}}\right)^3 \left(2T_0^3 + 6\times\frac{7}{8}T_{\nu,0}^3\right), \tag{4.45}$$

where, $T_0 = 2.725K$ is the present CMB temperature, $T_{\nu,0} \sim (4/11)^{1/3}T_0$ is the present neutrino temperature and $g_{re}$ is the effective degrees of freedom at reheating. Using the usual definition of radiation temperature, $T_{\rm re} = (30/g_{re}\pi^2)^{1/4}\rho_I^{1/4}\left(R_{\rm re}/e^{4N_{\rm re}}\right)^{1/4}$ one arrives at the following relation two equation for reheating temperature $T_{re}$ and $N_{re}$ in terms of other known parameters,

$$\begin{aligned} T_{\rm re} &= \left(\frac{43}{11g_{\rm s,re}}\right)^{1/3}\left(\frac{a_0T_0}{k}\right)H_k e^{N_k}e^{N_{\rm pre}}e^{N_{\rm re}^{\rm pert}} \\ N_{\rm re}^{\rm pert} &= \ln\left(\frac{a_{\rm re}}{a_{\rm pre}}\right). \end{aligned} \tag{4.46}$$

Where, $a_{\rm pre}$ is the scale factor after the end of preheating. We will solve equation 4.42 keeping the effective decay width as free parameter. The value of the effective decay width is chosen such that $N_{\rm re}^{\rm pert}(\Gamma), T_{\rm re}(\Gamma)$ satisfies Eqs.4.46. The preheating and consequently the initial conditions for the perturbative reheating dynamics modeled by eqs.4.39 (fraction of inflaton energy density) turned out to be largely independent of the inflationary parameters $(n_s, N_k)$ for a particular model. For $n = 2$ model, this important fact fixes the value of $N_{\rm pre} \sim 1.5$ for $\phi_* = 0.1$, and $N_{\rm pre} \sim 3.5$ for $\phi_* = 10$. Therefore, subsequent dynamics will fix the value of $N_{\rm re} = N_{\rm pre} + N_{\rm re}^{\rm pert}$ supplemented by the conditions eqs.4.46. Since the reheating temperature is an exponential function of e-folding number, small change in $N_k$ or $n_s$ significantly effects the value of $(N_{\rm re}, T_{\rm re})$. In fig.4.20, we have shown the dependence of $N_{\rm re}$ and $T_{\rm re}$ on the spectral index $n_s$ for the two values of $\phi_*$. The dashed lines are the results from the conventional reheating constraint analysis in which complete dynamics of reheating phase is parameterized by an effective equation of state [60](for $n = 2$). The solid lines is the result from our calculation. We can clearly see the significant difference in $(T_{\rm re}, N_{\rm re})$ for a particular value of $n_s$. The total reheating phase is parametrized by the sum of e-folding numbers due to preheating $N_{\rm pre}$ and the perturbative reheating $N_{\rm re}^{\rm pert}$. In our case, the instantaneous reheating is thus not possible as for $N_{\rm re}^{\rm pert} \to 0$, $N_{\rm re} \to N_{\rm pre}$. Most importantly preheating dynamics restricts the value of $n_s$ within a very narrow range of $0.971 < n_s < 0.973$ for $\phi_* = 0.1\ M_p$. For $\phi_* = 10\ M_p$, the range approximately is $0.9658 < n_s < 0.9678$. For both the cases the reheating temperature can take a wide range of values with a maximum limit to be $T_{\rm re}^{\rm max} \simeq 10^{13} \sim 10^{16}$ GeV. All these constraints are based on our naive solution of Boltzmann equation. However, let us remind the reader that inflaton decay constant $\Gamma$ should not take arbitrary value. For a given interacting model it will have a theoretical constraints. Those are shown as shaded region in the $(n_s, T_{re})$ plot for the given interaction discussed below. For illustration, if we consider a particular Yukawa type interaction between the scalar components and a fermion

$$\mathcal{L}_{\rm int} \supset -h\phi\bar{\psi}\psi. \tag{4.47}$$

We may have a estimate the range of coupling when the perturbative treatment can be trusted. Although we have considered a specific interaction, the following discussions will same for

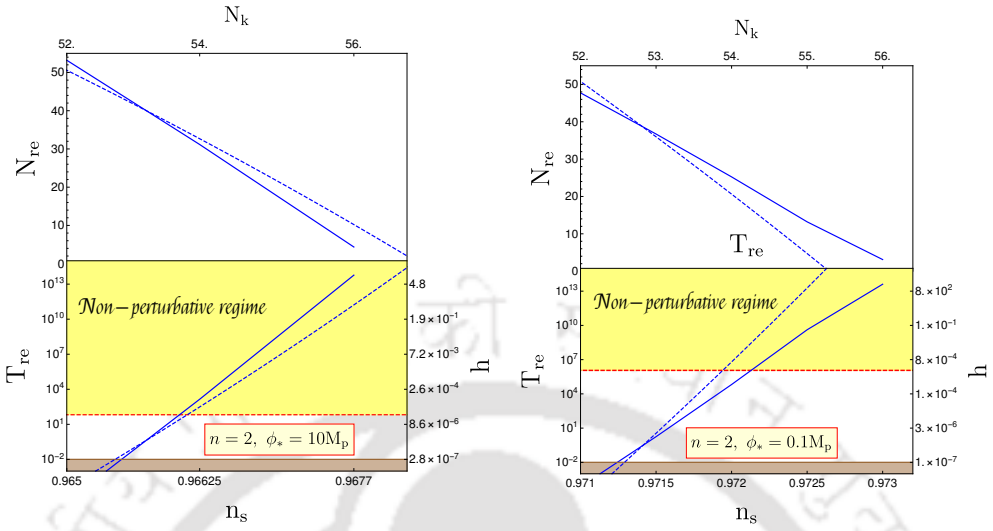


Figure 4.20: Evolution $N_{\rm re}$ and $T_{\rm re}$ with $n_s$ for $n = 2$ with two values of $\phi_*$ as before. The shaded region is the region when the value of $h$ such that the non-perturbative effects will be important. The dashed lines are the predictions from the conventional approach when the expansion during reheating phase is parameterized by an effective equation of state parameter $w_{eff} = (0.195,\ 0.251)$ for $\phi_* = (10, 0.1)M_p$. The lower brown shaded region is below 10MeV that is excluded from the constrains of big bang nucleosynthesis.

other type of three point interaction with some quantitative differences. In the present case the decay rate will be given by[30]

$$\Gamma = \frac{h^2 m_\phi}{8\pi} \tag{4.48}$$

where $m_\phi$ is the tree-level mass of $\phi$. However, in order for our discussion to be valid we need to make sure that the effect of this coupling should be insignificant during the preheating phase. For this we note that, the effect of resonance will be appreciable when the decay rate is greater than the Hubble parameter at the beginning of preheating[32, 103]. i.e.,

$$q_f^2 m_\phi \ > \ H. \tag{4.49}$$

Where $q_f$ is the resonance parameter in case of fermionic preheating analogous to the resonance parameter $q$ appeared in eq. (4.15) and for the interaction term in eq. (4.47) is given by[174]

$$q_f = \frac{h^2 \phi_0^2}{m_\phi^2} \tag{4.50}$$

Combining eq. (4.49) and eq. (4.50), we obtain the condition on the coupling $h$ when the resonance will be effective as

$$h > \left[\frac{V(\phi_0)^{\frac{1}{2}} m_\phi^3}{3^{\frac{1}{2}} \mathrm{M_P} \phi_0^4}\right]^{\frac{1}{4}} \tag{4.51}$$

This lower limit on $h$ in turn will give us a lower limit in inflaton decay constant $\Gamma$. In fig. 4.20 the red dashed line correspond to the aforementioned limit in terms of reheating temperature. Therefore, a significant part of our result that is represented by solid blue lines is in the non-perturbative region, which we may not be trusted. However, one can make progress by fitting our results (blue lines) with an effective time-independent equation of state defined during the entire reheating phase following the standard approach in[60, 61], with a simple evolution equation of total energy density $\rho = \rho_0 a^{-(1+3w_{eff})}$, and the approximate result (dotted blue lines) turned out to be $w_{\rm eff} = (0.195,\ 0.251)$ for $\phi_* = (10{\rm M_p}\ 0.1{\rm M_p})$ respectively. Now the dotted lines can be valid in the non-perturbative regime shown in the fig. 4.20 with an effective equation of state. To this end we must mention that the origin of the decay term in eq. (4.39) is phenomenological thus we are free to chose any interaction terms thereby the bound shown in fig. 4.20 can be significantly modified due to different coupling. In this regard it is also worth mentioning that a combination of perturbative and non-perturbative decay may in fact complicate the preheating scenario as considered in [169, 175] which the authors termed as *Combined Preheating*. In this work the authors considered the Higgs Inflation. They show that if the gauge bosons are coupled to fermions, they would quickly dissipate into these lighter degrees of freedom. The onset of preheating in this case is delayed(see also[136]). The analytic treatment of this mechanism has been given in [168, 169] for the case of Higgs inflation within the Standard Model. A full lattice simulation describing the limitations of the analytic study modeling the Higgs-gauge boson interactions as scalar interactions is presented in[175]. We will not consider those scenarios in this work and will take the inflation decay term is due to a phenomenological origin.

## 4.5 Conclusion and Outlook

In this work, we have studied the preheating dynamics for a specific class of plateau type inflationary potential proposed earlier by us. As we have shown previously, these type of plateau potentials fit will with the cosmological observations. The plateau potential in the present context can be thought of as a generalization of the chaotic power law potentials. Indeed the potential reduces to the form $V(\phi) \propto \phi^n$ around the minimum of the potential. However, we have a scale $\phi_*$ in our model that controls the height and width of the potential. In the present work we have explored in detail the effect of this scale on the preheating dynamics for different inflationary model parameterized by $n = (2, 4, 6)$. Lowering the value of $\phi_*$, the the system reaches its stationary stage faster. Even though qualitative behavior remains same for all the model. Some important microscopic detail changes which are worth studying in future. In order to do a comparative study, we take the same value of $g^2$ for different $\phi_*$. Below we list some of the important findings of our study,

(a) Given a particular model with fixed $(n, g^2)$, decreasing $\phi_*$ makes the energy transfer efficient by reducing the efolding number.

(b) However at the end of preheating, the total energy is distributed almost equally among the different fields taking part in the reheating dynamics. This distribution is nearly independent of the all the model parameters. Microscopic details of the dynamics will be dependent upon the parameters. For $n = 2$ this energy distribution is little asymmetric mainly due massive inflaton component.

(c) Most importantly for the models $n = 4, 6$, the final equation of state turns out to be that of radiation $w = 1/3$ independent of all the other parameters. Similar observation has been made in the recent works[165] considering the self resonance of the inflaton for similar plateau type inflationary models. For our case resonance will occur for both the fields $(\phi, \chi)$. We believe this is true for any model with $n > 2$, and for all those models the final equation of state will be that of the radiation. For $n = 2$ model, however, dynamics is little different. For this model self resonance is inefficient. The parameter $m$ plays the role of mass of the inflaton. Therefore, at the end of preheating, inflaton behave like a non-relativistic massive particle with a little asymmetric energy distribution with the relativistic $\chi$-particle. Therefore, the total equation state never reaches to that of radiation in the stationary phase.

(d) From the microscopic point of view, we found that the transition from homogeneous inflaton equation of state $w = (n-2)/(n+2)$ to that of the saturated preheating equation of state $w_{st}$ depends on $(n, \phi_*)$. For $n = 2$, with the decreasing $\phi_*$ the transition from $w = 0$ to its maximum value tend to be instantaneous. Therefore, the system must go through highly turbulent phase. This transition of equation of state occurs in the phase when transfer of energy from inflaton to reheating field is efficient. Therefore, all the interesting non-equilibrium phenomena such as chaos, turbulence, thermalization will happen in this phase. Thus, homogeneous inflaton equation of state plays very important role for those non-equilibrium processes during preheating. Detailed study of this phase will be done in future.

It is apparent that the preheating itself is not the full story of the reheating dynamics. As nearly half of the total energy density is stored in the form of inflaton, we need further mechanism to get the complete transfer of inflaton energy to radiation phase, that will set the initial condition for the standard big-bang. Since we need the complete decay of inflaton, three legs interaction[170] may be important. The effect of these interaction in the preheating has been discussed in [176–178]. A three legs interaction will also necessitate incorporating the self-interaction term such as $\lambda_\chi \chi^4$ that makes the potential bounded from below. Depending upon the value of $\lambda_\chi$, most of the energy density may or may not be converted into $\chi$ quanta before the back-reaction effect will became dominant[177] in the preheating dynamics. However, during the initial stage of preheating the four-legs interaction will be dominant over the three-legs. If both the interactions are present, we will have several interesting behavior of the system[177, 178]. We will look into those effects in a separate work. In the present work, we have considered the usual perturbative decay of inflaton with a phenomenological decay term. This helped us to connect the reheating phase with CMB. Considering $n = 2$ model, our naive analysis of Boltzmann equation limits the value of the spectral index within $0.971 < n_s < 0.973$ for $\phi_* = 0.1\ M_p$, and $0.9658 < n_s < 0.9678$ for $\phi_* = 10\ M_p$. In the above estimation, the reheating temperature is considered to be within $10\text{MeV} < T_{re} < 10^{15}\text{GeV}$. Finally we discussed qualitatively on the bound on the reheating temperature by looking at the non-perturbative limit on inflation decay constant $\Gamma$ which is assumed to be originated from the Yukawa interaction between the scalar fields and a fermion field. As we have seen that the upper limit on the Yukawa coupling below which the perturbative analysis can be carried put a maximum bound on the reheating temperature for the models under consideration. The maximum reheating temperature has been found to be $T_{\rm re} \sim 10^2\text{GeV}$ with $n_s^{\rm max} \sim 0.966$ for $\phi_* = 10\text{M}_{\rm p}$ and $T_{\rm re} = 10^6\text{GeV}$ with $n_s^{\rm max} = 0.972$ for $\phi_* = 0.1\text{M}_{\rm p}$. For higher values of

coupling Yukawa coupling $h$ when perturbative analysis can not be trusted, we can obtain the qualitative result considering the effective equation of state $w_{\rm eff}$ that can qualitatively fit our results.
However important point we should understand that there is no unified description of both the perturbative and non-perturbative reheating process. In our present analysis we have considered those as two separate phenomena connected by the initial condition for the Boltzmann equation after the end of preheating. Therefore, it would be interesting to understand those in a single framework. Another important issue we have not discussed is related to incomplete decay of inflaton for $n > 2$ models where final equation of state becomes $1/3$ after preheating. For these cases simple Boltzmann description of perturbative reheating becomes untenable for $(T_{re}, N_{re})$. Therefore for such situation how and when the actual radiation domination starts will be an important question to discuss.

Other import aspects of the non-perturbative phase is the study of production of compact structures such as oscilons or solitons. It can be seen that the potentials "open-up" when we move away from the minimum of the potential, these type of potential are found to lead copious production of oscillons[179, 180]. The self-resonance leads to an oscillon dominated phase[181] and significant production of gravitational waves[182]. We leave these interesting aspects for future study.

*"Nature seems to take advantage of the simple mathematical representations of the symmetry laws. When one pauses to consider the elegance and the beautiful perfection of the mathematical reasoning involved and contrast it with the complex and far-reaching physical consequences, a deep sense of respect for the power of the symmetry laws never fails to develop."*

*Chen Ning Yang*

## 5.1 Introduction

In all our previous chapters we have considered simple class of minimal inflationary models. In this chapter we will consider a different class of inflationary model with higher derivative term in the Lagrangian. In the standard inflationary scenario, the action consists of a canonical kinetic term and a potential which is sufficiently flat to ensure necessary amount of inflation. However, a non-canonical inflationary model with higher derivative terms in the Lagrangian has special significance from the theoretical as well as observational point of view. One such popular model is Dirac-Born-Infeld (DBI) inflation [183–185]. It has been found out that apart from usual inflationary predictions, these kind of non-canonical models have other interesting observable predictions such as large non-gaussianity, variable sound speed etc. They are constructed in such a way that the presence of higher derivative terms does not lead to any ghost degrees of freedom, which generally arises in higher derivative theory. In 1974, Gregory W Horndeski [186] first proposed a class of higher derivative single scalar field model in 4-dimension that yields second-order equations and hence free from ghosts. Long after this only recently general theory of scalar field revived again in a new disguise called Galilean [187] model. Subsequently straightforward generalization of this class of theories have been modified in the presence of gravity [188–190]. The underlying symmetry principle based on which the theory was constructed is called *'Galilean'* symmetry where the field transforms as $(\partial_\mu\phi \rightarrow \partial_\mu\phi + b_\mu)$. Where, $b_\mu$ is arbitrary constant shift vector. As our thesis is concentrated on the inflation, we will discuss about this Galilean theory of scalar field in the context of

inflation which is popularly know as G-inflation first proposed in [191]. In all those inflationary models the underlying Galilean symmetry is broken maintaining the two derivative nature of the equation of motion. However, such symmetry breaking is indeed necessary for the viability of the model specifically in the context of inflation as it naturally gives rise to graceful exit from inflationary phase and set the stage for reheating. Here we will not be talking about the symmetry breaking mechanism, rather, discuss about a specific class of inflationary models with a Galilean symmetry broken down to discrete shift symmetry.

This chapter is organized as follows. We will start by reviewing, following[191], the Galilean inflation starting with the action for most general single-field inflation in Section 5.2. In Section 5.3, we will take up a specific case of potential driven G-inflation where the potential itself too is shift symmetric. After discussing the details of inflationary predictions in this model. We conclude in Section 5.7.

## 5.2 The most General Single-Field Inflation

The study of inflation in Galilean-like higher derivative theory, dubbed as the G-inflation[192, 193] has since became an exiting field of research. The most general action for Galilean scalar field $\phi$ is

$$S = \sum_{i=2}^{5} \int d^4x\sqrt{-g}\mathcal{L}_i. \tag{5.1}$$

The different Lagrangian functions $\mathcal{L}_i$ are expressed in terms of $(\phi, X)$, where the canonical kinetic term $X \equiv -(1/2)\partial_\mu\partial^\mu\phi$.

$$\mathcal{L}_2 = K(\phi, X), \tag{5.2}$$
$$\mathcal{L}_3 = -G_3(\phi, X)\Box\phi, \tag{5.3}$$
$$\mathcal{L}_4 = G_4(\phi, X)R + G_{4X}(\phi, X)\left[(\Box\phi)^2 - (\nabla_\mu\nabla_\nu\phi)^2\right], \tag{5.4}$$
$$\mathcal{L}_5 = G_5(\phi, X)G_{\mu\nu}\nabla^\mu\nabla^\nu\phi - \frac{1}{6}G_{5X}(\phi, X)\left[(\Box\phi)^3 - 3(\Box\phi)(\nabla_\mu\nabla_\nu\phi)^2 + 2(\nabla_\mu\nabla_\nu\phi)^3\right], \tag{5.5}$$

where, $\Box\phi \equiv g^{\mu\nu}\nabla_\mu\nabla_\nu\phi$, $G_{\mu,\nu}$ is the Einstein tensor, $G_{iX} = \partial G_i/\partial X$, $(\nabla_\mu\nabla_\nu)^2 = (\nabla_\mu\nabla_\nu)(\nabla^\mu\nabla^\nu)$ and $(\nabla_\mu\nabla_\nu\phi)^3 = (\nabla_\mu\nabla_\nu\phi)(\nabla^\nu\nabla^\lambda\phi)(\nabla_\lambda\nabla^\mu\phi)$ . This is the most general single scalar field action whose equation of motion contain up to second derivative. A host of inflationary models can be derived from this action with specific choices of the functions $\{K, G_i\}$. For instance, the simplest example is by taking $K(\phi) = X - V(\phi)$, $G_4 = M_p^2/2$ and $G_3 = G_5 = 0$, one obtains a canonical scalar field action action for inflation. Before we get to our specific model, we will first describe the field equations for the above action for homogeneous background and then describe a specific model of interest and its predictions with respect to the observational data. We have two sets of equations which are essentially energy and momentum constraints originating from the general coordinate invariance,

$$\sum_{i=2}^{5}\mathcal{E}_i = 0, \quad \sum_{i=2}^{5}\mathcal{P}_i = 0, \tag{5.6}$$

where, terms in the energy constraint equations are

$$\mathcal{E}_2 = 2XK_X - K, \tag{5.7}$$
$$\mathcal{E}_3 = 6X\dot{\phi}HG_{3X} - 2XG_{3\phi}, \tag{5.8}$$
$$\mathcal{E}_4 = -6H^2G_4 + 24H^2X(G_{4X} + XG_{4XX}) - 12HX\dot{\phi}G_{4\phi X} - 6H\dot{\phi}G_{4\phi}, \tag{5.9}$$
$$\mathcal{E}_5 = 2H^3X\dot{\phi}(5G_{5X} + 2XG_{5XX}) - 6H^2X(3G_{5\phi} + 2XG_{5\phi X}). \tag{5.10}$$

The above equations only contains terms up to first order derivatives of metric and field as they are the constraint equation. The terms in the momentum constraint equations are

$$\mathcal{P}_2 = K, \tag{5.11}$$
$$\mathcal{P}_3 = -2X(G_{3\phi} + \ddot{\phi}G_{3X}), \tag{5.12}$$
$$\begin{aligned}\mathcal{P}_4 = {} & 2(3H^2 + 2\dot{H})G_4 - 12H^2XG_{4X} - 4H\dot{X}G_{4X} - 8\dot{H}XG_{4X} - 8HX\dot{X}G_{4XX} \\ & + 2(\ddot{\phi} + 2H\dot{\phi})G_{4\phi} + 4XG_{4\phi\phi} + 3X(\ddot{\phi} - 2H\dot{\phi})G_{4\phi X},\end{aligned} \tag{5.13}$$
$$\begin{aligned}\mathcal{P}_5 = {} & -2X(2H^3\dot{\phi} + 2H\dot{H}\dot{\phi} + 3H^2\ddot{\phi})G_{5X} - 4H^2X^2\ddot{\phi}G_{5XX} \\ & + 4HX(\dot{X} - HX)G_{5\phi X} + 2(2\overline{\dot{H}X} + 3H^2X)G_{5\phi} + 4HX\dot{\phi}G_{5\phi\phi}.\end{aligned} \tag{5.14}$$

This definition of the background quantity $\mathcal{E}_i$ and $\mathcal{P}_i$ are analogous to the definition of energy density and isotropic pressure in the canonical scalar field case. Finally, the variation with respect to the scalar field provide the scalar-field equation of motion:

$$\frac{1}{a^3}\frac{\mathrm{d}}{\mathrm{d}t}\left(a^3J\right) = P_\phi, \tag{5.15}$$

with the following definition of the symbols,

$$\begin{aligned}J = {} & \dot{\phi}K_X + 6HXG_{3X} - 2\dot{\phi}G_{2\phi} + 6H^2\dot{\phi}(G_{4X} + 2XG_{4XX}) - 12HXG_{4\phi X} \\ & + 2H^3X(3G_{5X} + 2XG_{5XX}) - 6H^2\dot{\phi}(G_{5\phi} + XG_{5\phi X})\end{aligned} \tag{5.16}$$

and

$$\begin{aligned}P_\phi = {} & K_\phi - 2X(G_{3\phi\phi} + \ddot{\phi}G_{3\phi X}) + 6(2H^2 + \dot{\phi})G_{4\phi} + 6H(\dot{X} + 2HX)G_{4\phi X} \\ & - 6H^2XG_{5\phi\phi} + 2H^3X\dot{\phi}G_{5\phi X}.\end{aligned} \tag{5.17}$$

In order to proceed further and discuss about the inflationary solution we will consider a particular example of G-inflation which is driven by the potential of the scalar field as in the case of usual canonical case(for kinetically driven G-inflation see [192]). It is interesting to see that the presence of the higher order terms will modify the inflationary and post inflationary dynamics. The G-inflation also provides us certain degree of freedom in choosing the functional form of $\{K,\ G_i\}$ which we will take advantage of later in our work. But before moving to a specific case let us continue our discussion with the general example of a potential driven G-inflation[194].

### 5.2.1 Potential-driven G-inflation

In case of kinetically driven G-inflation, the shift symmetry of the original Lagrangian remains intact. The shift symmetry does not allow any potential term. Therefore, to have subsequent

reheating dynamics, one needs to introduce new mechanism. Within the Galilean framework we can consider potential driven slow-roll G-inflation where the potential term manifestly breaks the shift symmetry of the Galilean model. The resulting equations are still, however, second order retaining the ghost free condition of G-inflation. As we have already mentioned the breaking is necessary for graceful exit from the inflationary phase to the reheating phase. To commence with this case let us expand the functions in terms of $X$ as

$$K(\phi, X) = -V(\phi) + \mathcal{K}(\phi)X + \cdots \tag{5.18}$$

$$G_i(\phi, X) = g_i(\phi) + h_i(\phi)X + \cdots \tag{5.19}$$

Considering the case when the inflaton field changes very slowly and neglecting all the terms containing $\dot{\phi}(t)$ in the gravitational field equations as well as assuming the usual slow-roll conditions $|\dot{H}| \ll H^2$ and $|\ddot{\phi}| \ll |H\dot{\phi}|$, we obtain the gravitational fields equations as

$$\sum_{i=2}^{5} \mathcal{P}_i \simeq -\sum_{i=2}^{5} \mathcal{E}_i \simeq -V(\phi) + 6g_4(\phi)H^2 = 0, \tag{5.20}$$

Therefore, the slow-roll Hubble-Lemaitre equation for potential driven G-inflation is given by

$$\boxed{H^2 \simeq \frac{V}{6g_4}} \tag{5.21}$$

To get the inflationary scalar field equation, we will assume the following additional conditions during the slow-roll phase

$$|\dot{J}| \ll |JH|, \quad |\dot{g}_i| \ll |g_i H|, \quad |\dot{h}_i| \ll |h_i H|, \tag{5.22}$$

Now using these conditions in Eq. (5.15) with the expansions in Eq. (5.19), the equation of motion for $\phi$ in G-inflation reads as

$$\boxed{3HJ \simeq -V_\phi + 12H^2 g_{4\phi},} \tag{5.23}$$

where,

$$J \simeq \mathcal{K}\dot{\phi} - g_{3\phi}\dot{\phi} + 6(Hh_3X + H^2h_4\dot{\phi} - H^2g_{5\phi}\dot{\phi} + H^3h_5X) \tag{5.24}$$

Here taking $\mathcal{K} = 1$ and $g_4 = M_p^2/2$ and all other coefficients to be zero, we get the canonical scalar field driven slow-roll inflation in the Einstein gravity. Different class of inflation models can obtained form the potential driven G-inflation by suitably choosing the remaining functions as listed below

$$\mathcal{K} = 1 + \kappa\phi^{2n}, \qquad \text{running kinetic inflation[195]} \tag{5.25}$$

$$h_3(\phi) = \frac{\phi}{M^4}, \qquad \text{Higgs G-inflation[193]} \tag{5.26}$$

$$g_4(\phi) = \frac{M_p^2}{2} - \frac{\xi}{2}\phi^2, \qquad \text{Higgs inflation[148, 196, 197]} \tag{5.27}$$

$$h_4(\phi) = \frac{1}{2\mu^2}, \qquad \text{new Higgs inflation[198]} \tag{5.28}$$

$$h_5(\phi) = \frac{\phi}{\mathcal{M}^6}, \qquad \text{running Einstein inflation[199]} \tag{5.29}$$

After developing the necessary equations for inflationary dynamics in G-inflation let us define power spectrum and other observational quantities in generalized G-inflation.

### 5.2.2 Perturbations in Generalized G-inflation

The power spectrum for G-inflation can be found with the methods similar to canonical inflation[191] discussed in the introduction. Decomposing the perturbations into scalar($\alpha, \beta,$ and $\xi$) and tensor perturbation ($h_{ij}$), the perturbed metric in the unitary gauge $\phi = \phi(t)$ is

$$ds^2 = -N^2\,\mathrm{d}t^2 + \gamma_{ij}(\mathrm{d}x^i + N^i\,\mathrm{d}t)(\mathrm{d}x^j + N^j\,\mathrm{d}t) \tag{5.30}$$

Where,

$$N = (1+\alpha), \quad N_i = \partial_i\beta, \quad \gamma_{ij} = a^2(t)e^{2\xi} \tag{5.31}$$

Note here that the tensor perturbation satisfies the trace-less condition viz. $h_{ii} = 0 = h_{ij,j}$. The above definition of the perturbed metric is chosen such that $\sqrt{-g}$ does not contain the perturbation $h_{ij}$ up-to second-order, and the scalar parts $\xi^2$ and $\alpha\xi$ vanish due to the background equations.

#### 5.2.2.1 Tensor Perturbations

With the above perturbed metric, the second-order action for the tensor perturbation reads as

$$S_T^{(2)} = \frac{1}{8}\int \mathrm{d}t\,\mathrm{d}^3x a^3\left[\mathcal{G}_T\dot{h}_{ij}^2 - \frac{\mathcal{F}_T}{a^2}(\nabla h_{ij})^2\right]. \tag{5.32}$$

where,

$$\mathcal{F}_T = 2\left[G_4 - X(\ddot{\phi}G_{5X} + G_{5\phi})\right], \tag{5.33}$$

$$\mathcal{G}_T = \frac{1}{2}\sum_{i=2}^{5}\frac{\partial\mathcal{P}_i}{\partial H} = 2\left[G_4 - 2XG_{4X} - X(H\dot{\phi}G_{5X} - G_{5\phi})\right], \tag{5.34}$$

we also define the effective speed of sound for the tensor perturbations as

$$c_T^2 = \frac{\mathcal{F}_T}{\mathcal{G}_T} \tag{5.35}$$

It is evident from Eq. (5.32) that the action for tensor perturbations will be free from ghost degrees of freedom and gradient instabilities if the following conditions are met

$$\mathcal{F}_T > 0, \quad \mathcal{G}_T > 0. \tag{5.36}$$

It is also important to notice that in contrast to the canonical inflationary models, the effective speed of sound is not necessarily unity. Thus the issue of super-luminous propagation of perturbations may arise in G-inflationary scenarios. The tensor power spectrum and the associated spectral tilt turn out to be

$$\mathcal{P}_T = 8\gamma_T\frac{\mathcal{G}_T^{1/2}}{\mathcal{F}_T^{3/2}}\frac{H^2}{4\pi^2}\bigg|_{-k_{y_T}=1} \quad ; \quad n_T = 3 - 2\nu_T \tag{5.37}$$

where the symbols are defined in terms of the functions as,

$$\gamma_T = 2^{2\nu_T-3}|\Gamma(\nu_T)/\Gamma(3/2)|^2(1-\epsilon-f_T/2+g_T/2), \tag{5.38}$$

$$f_T = \frac{\dot{\mathcal{F}}_T}{\mathcal{F}_T H}, \quad g_T = \frac{\dot{\mathcal{G}}_T}{\mathcal{G}_T H}, \tag{5.39}$$

$$\nu_T = \frac{3-\epsilon+g_T}{2-2\epsilon-f_T+g_T} \quad \epsilon = -\frac{\dot{H}}{H} \tag{5.40}$$

This shows that, in contrast to the canonical models, a blue spectrum $n_T > 0$ can be achieved in G-inflation.

#### 5.2.2.2 Scalar Perturbations

Now we write the action for the scalar perturbations by setting $h_{ij} = 0$, the second-order action is given by

$$\begin{aligned} S_T^{(2)} = \int \mathrm{d}t\, \mathrm{d}^3x a^3 \Big[ & -3\mathcal{G}_T\dot{\xi}^2 + \frac{\mathcal{F}_T}{a^2}(\nabla\xi)^2 + \Sigma\alpha^2 - 2\Theta\alpha\frac{\nabla^2}{a^2}\beta \\ & + 2\mathcal{G}_T\dot{\xi}\frac{\nabla^2}{a^2}\beta + 6\Theta\alpha\dot{\xi} - 2\mathcal{G}_T\alpha\frac{\nabla^2}{a^2}\xi\Big] \end{aligned} \tag{5.41}$$

where,

$$\begin{aligned} \Sigma = {} & XK_X + 2X^2K_{XX} + 12H\dot{\phi}XG_{3X} \\ & + 6H\dot{\phi}X^2G_{3XX} - 2XG_{3\phi} - 2X^2G_{3\phi} - 6H^2G_4 \\ & + 6\left[H^2(7XG_{4X} + 16X^2G_{4XX} + 4X^3G_{4XXX})\right] \\ & - H\dot{\phi}(G_{4\phi} + 5XG_{4\phi X} + 2X^2G_{4\phi XX}) \\ & + 30H^3\dot{\phi}XG_{5X} + 26H^3\dot{\phi}X^2G_{5XX} \\ & + 4H^3\dot{\phi}X^3G_{5XXX} - 6H^2X(6G_{5\phi} + 9XG_{5\phi X} + 2X^2G_{5\phi XX}), \end{aligned} \tag{5.42}$$

From this action the scalar power spectrum and the spectral tilt turns out to be

$$\mathcal{P}_S = 8\gamma_S\frac{\mathcal{G}_S^{1/2}}{\mathcal{F}_S^{3/2}}\frac{H^2}{4\pi^2}\Big|_{-k_{y_S}=1} \quad ; \quad n_s - 1 = 3 - 2\nu_S \tag{5.43}$$

with the symbols are defined as

$$\mathcal{F}_S = \frac{1}{a}\frac{\mathrm{d}\left(\frac{a}{\Theta}\mathcal{G}_T^2\right)}{\mathrm{d}t} - \mathcal{F}_T, \quad \mathcal{G}_S = \frac{\Sigma}{\Theta^2} + 3\mathcal{G}_T, \tag{5.44}$$

$$\Sigma = X\sum_{i=2}^{5}\frac{\partial\mathcal{E}_i}{\partial X} + \frac{1}{2}\sum_{i=2}^{5}\frac{\partial\mathcal{E}_i}{\partial H}, \quad \Theta = -\frac{1}{6}\sum_{i=2}^{5}\frac{\partial\mathcal{E}_i}{\partial H} \tag{5.45}$$

$$f_S = \frac{\dot{\mathcal{F}}_S}{\mathcal{F}_S H}, \quad g_S = \frac{\dot{\mathcal{G}}_S}{\mathcal{G}_S H}, \tag{5.46}$$

The squared speed of sound for scalar perturbations is given by

$$c_S^2 = \frac{\mathcal{F}_S}{\mathcal{G}_S} \tag{5.47}$$

Finally the scalar spectral index($n_s$) and the tensor-to-scalar ratio($r$) is given by

$$r = 16\frac{\mathcal{F}_S}{\mathcal{F}_T}\frac{c_S}{c_T} \tag{5.48}$$

After introduction the basics of G-inflation and its spectral quantities, we will now consider a specific model of G-inflation and look into the detail on how the presence of higher derivative terms helps us to reconcile the model predictions with observational data.

## 5.3 Potential driven G-inflation with a shift symmetric potential

We have seen that the G-inflation may reproduce a class of inflationary models depending upon the functional forms. For instance we may further simplify the Galilean model by setting $g_3 = g_5 = 0$ without loss of generality, as $g_{3\phi}$ can be absorbed into a redefinition of $\mathcal{K}$ and $g_{5\phi}$ into $h_4$, i.e.,

$$\begin{aligned}\mathcal{K} - 2g_{3\phi} &\to \mathcal{K},\\ h_4 - g_{5\phi} &\to h_4\end{aligned}$$

Setting $g_4 = M_p^2/2$ will ensure that we are in the realm of Einstein gravity. Hence let us write our action of a minimally coupled scalar field, kinetically coupled to gravity due to higher derivative kinetic terms, as

$$S = \int d^4x\sqrt{-g}\Big[\frac{M_p^2}{2}R - X - M(\phi)X\Box\phi - V(\phi)\Big] \tag{5.49}$$

where $X = \frac{1}{2}\partial\mu\phi\partial^\mu\phi$ and $\Box = \frac{1}{\sqrt{-g}}\partial_\mu(\sqrt{-g}\partial^\mu)$

This specific form of higher derivative kinetic term $G\Box\phi$ which contains a scalar-tensor kinetic coupling, of the form $G\partial g/\partial\phi$ arising due to the presence of Christoffel symbols in the covariant D'Alembertian operator is dubbed as the *kinetic gravity braiding*(KGB)[200, 201]. The effect of the kinetic braiding is that the energy-momentum tensor now no longer that of the perfect-fluid form. The effect of this departion from perfect-fluid form is studied in the context of dark energy[200, 201], however as we will see that the effect of the KGB term has important consequences in inflationary as well as post-inflationary dynamics. Now let us discuss about the potential term. We will chose a shift symmetric potential of the form

$$V(\phi) = \Lambda^4\Big[1 \pm cos\Big(\frac{\phi}{f}\Big)\Big] \tag{5.50}$$

In the context of inflationary model building it is known as the Natural Inflation[143, 144], proposed in the early 90's as an attempt to solve the so-called "*fine-tuning*" problem. As we have seen that inflation needs a flat potential for sufficient amount of inflation. It has been generally argued that the flatness of potential is subject to radiative corrections unless it is protected by a symmetry. In case of natural inflation the potential is naturally flat due to shift symmetries. This model make use of a Nambu-Goldstone bosons[202, 203] arising when a global symmetry is spontaneously broken. Though it is one of the best theoretically motivated model of inflation, it turned out to be observationally tightly constrained. Furthermore, it's predictions closest to the observations become quantum field theoretically implausible for the

super-planckian axion decay constant $f$. Nonetheless, because of its naturalness, many different modifications have been proposed to make it observationally favored and simultaneously bring down the value of $f$ to a sub-Planckian value. String inspired $\mathcal{N}$-flation [204], axion monodromy inflation[205] are the various variant of this natural inflation model where there exist multiple fields with sub-Planckian values of $f$. Multiple axionc fields are aligned in such a way that the effective axion decay constant could be sub-Planckian and make the model cosmologically viable. Recently proposed Weak-Gravity Conjecture(WGC)[206],as well as some string theory construction [207] put severe constraints on such models of alignment mechanism[208, 209]. However, considerations of covariant entropy bound seem to relax the bound[210]. Another way to keep the axion decay constant to have subplanckian value is by introducing a coupling of the Inflaton kinetic term to the Einstein tensor was introduced in [211, 212]. In this chapter, we will see that the effect of the derivative Galileon term for the axion not only we can make inflationary observables compatible with PLANCK, but also we can have sub-Planckian axion decay constant. We will derive the necessary background equations in the next section.

### 5.3.1 G-axion

Now will will describe the G-inflation for the action written in Eq. (5.49) with the shift-symmetric axion potential in Eq. (5.50) which we will call the G-axion. With the usual FLRW-background ansatz for the spacetime

$$ds^2 = -dt^2 + a(t)^2(dx^2 + dy^2 + dz^2), \tag{5.51}$$

one gets the following Einstein's equations by varying the action with respect to the metric

$$\begin{aligned} 3M_p^2H^2 &= -3H\dot{\phi}^3M(\phi) - X + 2X^2M'(\phi) + V(\phi) \\ &= -X\Big[1 + M(\phi)H\dot{\phi}(6-\alpha)\Big] + V(\phi) \end{aligned} \tag{5.52}$$

$$\begin{aligned} M_p^2\dot{H} &= -X\left(1 - 3M(\phi)H\dot{\phi} + M(\phi)\ddot{\phi} + M'(\phi)\dot{\phi}^2\right) \\ &= -X\Big[1 - M(\phi)H\dot{\phi}(3+\eta-\alpha)\Big] \end{aligned} \tag{5.53}$$

and by varying scalar field:

$$\begin{aligned} &\frac{1}{a^3}\frac{d}{dt}\left[a^3\left(1 - 3HM\dot{\phi} - 2M'X\right)\dot{\phi}\right] + \dot{\phi}\frac{d}{dt}(M'X) + \frac{\Lambda^4}{f}\sin\left(\frac{\phi}{f}\right) = 0, \\ &H\dot{\phi}\Big[3 - \eta - M(\phi)H\dot{\phi}(9 - 3\epsilon - 6\eta + 2\eta\alpha)\Big] + (1+2\beta)V'(\phi) = 0 \end{aligned} \tag{5.54}$$

where we have defined:

$$\epsilon \equiv -\frac{\dot{H}}{H^2}; \qquad \eta \equiv -\frac{\ddot{\phi}}{H\dot{\phi}}; \tag{5.55}$$

$$\alpha \equiv \frac{M'(\phi)}{M(\phi)}\frac{\dot{\phi}}{H}; \quad \beta \equiv \frac{M''(\phi)X^2}{V'(\phi)} \tag{5.56}$$

Where, $H = \dot{a}/a$ is the Hubble constant. During inflation we will assume that these parameters are small:

$$\epsilon, \quad |\eta|, \quad |\alpha|, \quad |\beta| \ll 1, \tag{5.57}$$

It is easy to identify $\epsilon$ and $\eta$ with as the Hubble slow-roll parameters as appears in the canonical inflation scenarios. We also have two extra 'slow-roll' parameters in Galileon inflation namely, the parameters $\alpha$ and $\beta$.

The above slow roll parameters in terms of the potential function, denoting $\frac{\phi}{f}$ as $\tilde{\phi}$, are

$$\begin{aligned}
\epsilon =& \frac{1}{2\mathcal{A}} \frac{\sin^{\frac{3}{2}}(\tilde{\phi})}{\sqrt{\tilde{M}(\tilde{\phi})}\left(1-\cos\left(\tilde{\phi}\right)\right)^2} \; ; \; \eta = \frac{1}{2\mathcal{A}} \frac{\sqrt{\cos\left(\tilde{\phi}\right)\cot\left(\tilde{\phi}\right)}}{\sqrt{\tilde{M}(\tilde{\phi})}\left(1-\cos\left(\tilde{\phi}\right)\right)} \\
\alpha =& \frac{2}{\sqrt{\mathcal{A}}} \frac{\tilde{M}'(\tilde{\phi})\sqrt{2\epsilon}}{\sqrt[4]{\tilde{M}(\tilde{\phi})^5 \sin\left(\tilde{\phi}\right)}} \quad ; \quad \beta = \frac{1}{36\mathcal{A}} \frac{\tilde{M}(\tilde{\phi})2\epsilon}{\sqrt{\tilde{M}(\tilde{\phi})^3 \sin\left(\tilde{\phi}\right)}}.
\end{aligned} \tag{5.58}$$

We will call $M(\phi) = \frac{1}{s^3}\tilde{M}(\tilde{\phi})$ as the KGB function and $s$ is an associated mass scale which will control the strength of the higher derivative term. We define a parameter $\mathcal{A} = \left(\frac{f^3}{s^3}\frac{\Lambda^4}{M_p^4}\right)^{1/2}$ which will greatly simplify further calculations. In case of potential driven inflation [194], the KGB function has a significant influence on the inflation dynamics. Here our aim is to identify the form of the KGB function based on the principle of constant shift symmetry and try to satisfy the experimental observation. At this point let us also define an additional parameter corresponding to the higher order slow roll parameter which is related to another measurable quantity called running of scalar spectral index,

$$\xi = M_p^4 \frac{1}{2MV'}\left(\frac{V'''V'}{V^2}\right) = -\frac{1}{\mathcal{A}^2}\frac{\sin\left(\tilde{\phi}\right)}{\tilde{M}(\tilde{\phi})\left(1-\cos\left(\tilde{\phi}\right)\right)^2}. \tag{5.59}$$

For our later convenience, we note the following relation between the KGB function and the slow roll parameter,

$$\frac{M(\phi)\dot{\phi}^3}{M_P^2 H} \simeq -\frac{2}{3}\epsilon. \tag{5.60}$$

Which tells us that, though the higher derivative term dominates the dynamics of slow-roll inflation, the standard part of the Lagrangian remains much larger than the Galileon part during inflation ($\epsilon \ll 1$) and they both became comparable only after the end of inflation ($\epsilon = 1$).

The slow-roll equation for the axion turns out to be,

$$3H\dot{\phi}\left(1 - 3M(\phi)H\dot{\phi}\right) + \frac{\Lambda^4}{f}\sin\left(\frac{\phi}{f}\right) = 0. \tag{5.61}$$

From the form of the above equation, we can consider two different ways to inflate our universe. The condition $|M(\phi)H\dot{\phi}| \ll 1$ will give the standard axion inflation scenario, while the condition

$|M(\phi)H\dot{\phi}| \gg 1$, provides alternative scenario where the higher derivative term comes into play. As emphasized in the introduction, the usual canonical axion inflation scenario is tightly constrained from the PLANCK observation. We will see for a wide range of parameter space higher derivative term will play main roll in G-axion-inflation. Solving the slow-roll equation of motion for $\dot{\phi}$ we get

$$|\dot{\phi}| \simeq M_p \left(\frac{V'}{3M(\phi)V}\right)^{1/2}. \tag{5.62}$$

Using Eq.(5.62), the condition for the KGB term to dominate the usual slow-roll term can be monitored by defining a parameter

$$\tau = M(\phi)V'(\phi) = \frac{M(\phi)\Lambda^4}{f}\sin\left(\frac{\phi}{f}\right) \gg 1. \tag{5.63}$$

### 5.3.2 Cosmological quantities: $(n_s, r, dn_s^k)$

In this section, we will note down some of the important cosmological quantities which are being measured in cosmological experiments. Following our previous discussion, the amplitude of the power spectrum of the curvature perturbation for G-axion is written as

$$P_{\mathcal{R}} = \frac{3\sqrt{6}}{64\pi^2}\frac{H^2}{M_p^2\epsilon}. \tag{5.64}$$

The spectral tilt and its running can be easily found out using the relation, $\frac{d}{d\,lnk} = \frac{\dot{\phi}}{H}\frac{d}{d\phi}$ *

$$n_s - 1 \equiv \frac{\mathrm{d}lnP_{\mathcal{R}}}{\mathrm{d}lnk} = -6\epsilon + 3\eta - \alpha, \tag{5.65}$$
$$\frac{dn_s}{\mathrm{d}lnk} \equiv dn_s^k = -3\xi + 24\epsilon\eta - 24\epsilon^2 - 3\alpha^2 - 8\alpha\epsilon + 4\alpha\eta + 3\eta^2 + 18\beta.$$

The power spectrum and the spectral index of the primordial gravitational wave are:

$$P_T = \frac{8}{M_p^2}\left(\frac{H}{2\pi}\right)^2 \tag{5.66}$$
$$n_T = -2\epsilon. \tag{5.67}$$

Another important quantity of cosmological importance is the tensor to scalar ratio

$$r = -\frac{32\sqrt{6}}{9}n_T \tag{5.68}$$

After introducing the background equations and spectral quantities, we will discuss a relation between the field excursion during inflation and the tensor-to-scalar ratio. This relation, formally known as the Lyth bound will be modified due the higher derivative term. This will help us to construct a model with detectable tensor-to-scalar ration with subplanckian field excursion.

*In case of KGB inflation,the slow-roll scalar field equation can be used to find $\frac{\dot{\phi}}{H} = -\frac{M_p^2}{V(\phi)}\left(\frac{V'(\phi)}{M(\phi)}\right)^{1/2}$

### 5.3.3 Number of e-folds and modified Lyth bound

The 'e-folding' number is given by by the following expression,

$$\mathcal{N} = \int_{t_1}^{t_2} H dt = \int_{t_1}^{t_2} \frac{H}{\dot{\phi}} d\phi = \frac{1}{M_p} \int_{\phi_{end}}^{\phi_{in}} \frac{\tau^{\frac{1}{4}}}{\sqrt{2\epsilon}} d\phi. \tag{5.69}$$

From the cosmological observation, the e-folding number is found to be $\mathcal{N} \geq 50$. It is apparent that the amount of inflation must be proportional to the amount of field excursion during the slow roll inflation. This quantity is known as Lyth bound[63](also see [213, 214]). Lyth bound is assumed to play an important role in constraining the parameter space of a model under consideration from the low energy effective field theory point of view. In the slow roll approximation, one can compute the amount of field excursion by series expansion in terms of e-folding number calculated from the onset of inflation as follows

$$\phi(\delta\mathcal{N}) = \phi_{in} + \frac{\partial\phi}{\partial\mathcal{N}}\delta\mathcal{N} + \frac{1}{2}\frac{\partial^2\phi}{\partial\mathcal{N}^2}\delta\mathcal{N}^2 + \dots. \tag{5.70}$$

Therefore, up to second order in slow roll, one can write down the general expression for the amount of field excursion $\Delta\phi$ for e-folding number $\delta\mathcal{N}$ as

$$\Delta\phi = |\phi(\delta\mathcal{N}) - \phi_{in}| = \delta\mathcal{N}\left(\frac{\partial\phi}{\partial\mathcal{N}}\right)\left[1 + \frac{\delta\mathcal{N}}{2}\left(2\epsilon - \eta + \frac{\alpha}{2}\right)\right]. \tag{5.71}$$

Therefore, by using Eq.(5.69), we get

$$\Delta\phi = \delta\mathcal{N}\left|\frac{\sqrt{2\epsilon}}{\tau(\phi)^{\frac{1}{4}}}\right|\left[1 + \delta\mathcal{N}\left(2\epsilon - \eta + \frac{\alpha}{2}\right)\right]. \tag{5.72}$$

From the above expression for the e-folding number assuming, that the slow-roll parameters and $\tau$ behave monotonously, we can write

$$\mathcal{N} \lesssim \frac{\Delta\phi}{M_p}\left|\frac{\tau(\phi)^{\frac{1}{4}}}{\sqrt{2\epsilon}}\right|_{max} = \frac{\Delta\phi}{M_p}\left|\frac{\tau_{max}^{\frac{1}{4}}}{\sqrt{2\epsilon_{min}}}\right|. \tag{5.73}$$

In deriving the above expression, we have kept only the leading order term in slow roll. However, above expression can get significant correction near the end of inflation where slow roll parameters are not small. We will do the detailed study on this issue and its consequence on the model for our future publication. Now, Eqs.(5.64-5.68) can be used to relate the field excursion during inflation with the scalar-to-tensor ratio as,

$$\Delta\phi \gtrsim (\mathcal{N}M_p)\left|\frac{\sqrt{2\epsilon_{min}}}{\tau_{max}^{\frac{1}{4}}}\right| = \frac{f}{\sqrt{\mathcal{A}}}\frac{\mathcal{N}}{\mathcal{N}_{max}}\sqrt{\frac{9r}{36\sqrt{6}}}, \tag{5.74}$$

where,

$$\mathcal{T}_{max} = (s^3 M(\tilde{\phi}_{in})\sin\tilde{\phi}_{in})^{\frac{1}{4}}.$$

As we can see there is an important difference in the above expression for Lyth Bound with usual slow-roll inflation case via the presence of the term $\tau(\phi)$ which contains the KGB

term $M(\phi)$. This feature will help us to construct a model with detectable tensor-to-scalar ratio with sub-planckian axion decay constant. Therefore, we are in a position to compare the Lyth bound between G-axion inflation and the usual canonical slow-roll inflation, which can be written in a model independent way as $\Delta\phi_{slow-roll} \sim \mathcal{N}\sqrt{\frac{r}{8}}$. For, $r = 0.08$ and $\mathcal{N} = 60$, $\Delta\phi_{slow-roll} \gtrsim 6$. Now since we have freedom in choosing $f$, the modified Lyth bound can be made very small. As an example, for $\mathcal{A} = 94$, if we choose $f = 0.5M_p$, one gets $\Delta\phi_{KGB} \gtrsim 0.59$. In the subsequent section, we will consider some simple phenomenological form of the KGB functions keeping the constant shift symmetry of the Lagrangian intact, and construct both super and sub-Planckain inflation models in compatible with PLANCK.

## 5.4 Simple choices of $M(\phi)$ and determination of cosmological parameters

As we have emphasized in the beginning, we will be considering some simple functional form of $M(\phi)$ exhibiting shift symmetry of the axion field. As we will see from our analysis, the CMB observables are not sufficient to constrain the value of the axion decay constant for the model under consideration. Therefore, the dynamics after the inflation will be important and we will indeed see the existence of a critical value of axion decay constant $f_c$ which separates super and sub-Planckian scenarios in terms of oscillation dynamics. However, in this section, we will mainly compute the inflationary observables and compare our result with the current observational bounds coming from PLANCK for some simple choices of $M(\phi)$. We consider the following forms of $M(\phi)$:

$$\text{I} : M(\phi) = \text{Constant},$$

$$\text{II} : M(\phi) = \sin(\phi/f),$$

$$\text{III} : M(\phi) = \sin^2(\phi/f),$$

$$\text{IV} : M(\phi) = \cos^2(\phi/f),$$

$$\text{V} : M(\phi) = 1 - \sin(\phi/f),$$

The CMB observables with the above choices of function have been presented in Fig. 5.1 and 5.2. For comparison, we also plotted the standard axion inflation model. From our analysis and also clear from the $(n_s, r)$ plot, we have two different categories of model based on their predictions. The best fit models are of type $(IV, V)$. One can clearly see that within $1\sigma$ region of $n_s$, natural inflation model is almost ruled out. On the other hand the our aforementioned best fit model predicts as low as $r \simeq 0.04$ within the same $n_s$ region. Other three types $(I, II, III)$ are marginally fitting with the data. All these models predict very high value of tensor to scalar ratio $r$ which can be measured in the near future CMB experiments. Particularly, for $M(\phi) = constant$, which is the best out of this group predicts, $r \simeq 0.07, n_s = 0.973$ for $N = 65$ which is within $2\sigma$ region of CMB data. Interestingly, as we will discuss in detail, those two types of models show distinct behavior after the inflation depending on the value of axion decay constant.

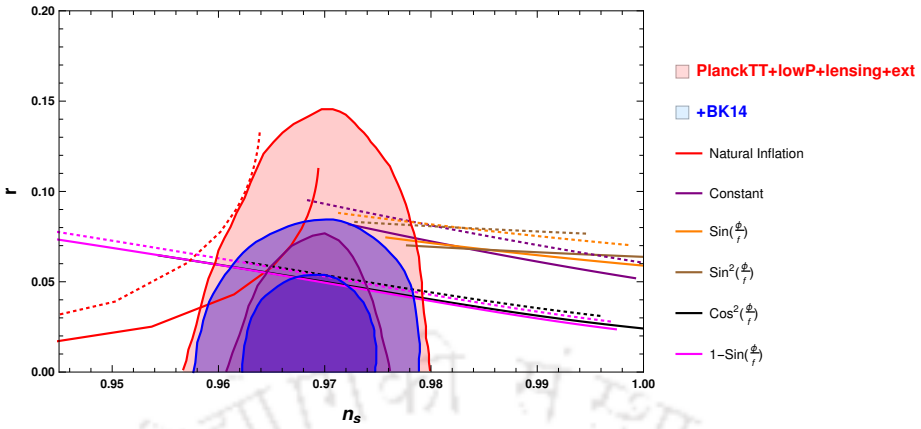


FIGURE 5.1: $n_s$ vs $r$ plot for five different forms of $M(\phi)$ for $\mathcal{N} = 55$ (dotted lines), and $\mathcal{N} = 65$ (solid lines). For comparison, red curves are plotted for usual axion inflation.

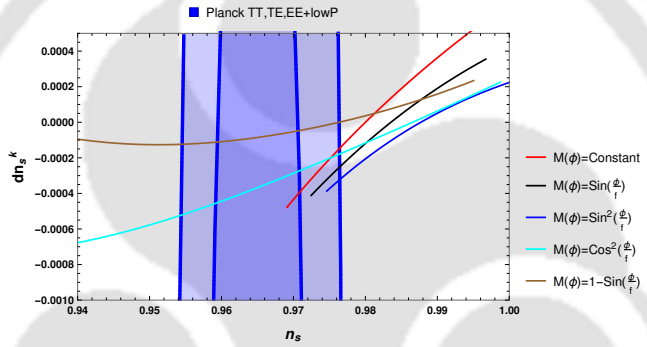


FIGURE 5.2: $dn_s^k$ vs $n_s$ plotted for five different forms of $M(\phi)$ for $\mathcal{N} = 60$ e-folding on the background of Planck TT,TE,EE+low P data ($dn_s^k = -0.003 \pm 0.007$)

## 5.5 Evolution of the scalar field: sub-Planckian $(f, s)$

Before we go for cosmological dynamics, let us first try to understand the region of stability of our G-axion system. Even though we do not have more than two time derivative in the equation of motion, higher derivative term in the Lagrangian generically gives rise to various pathological behavior for the fluctuation dynamics in a non-trivial background. Due to those behaviors, such as propagating ghost, gradient instability, superluminal speed of propagation, the effective field theory under consideration may not have conventional UV complete description. For completeness and also in order to have qualitative understanding of the aforementioned pathologies we will apply the well known method of characteristics [188–190, 215, 216]. In this method the procedure is the following. From the action given in (5.49), the axion field equation can be written as

$$P^{\mu\nu}\nabla_\mu\nabla_\nu\phi + Q^{\mu\nu\alpha\beta}(\nabla_\alpha\nabla_\beta\phi)(\nabla_\mu\nabla_\nu\phi) - 2XM''(\phi) - V'(\phi) \\ -2XM(\phi)(2X - 4X^2M(\phi)) = 0 \qquad (5.75)$$

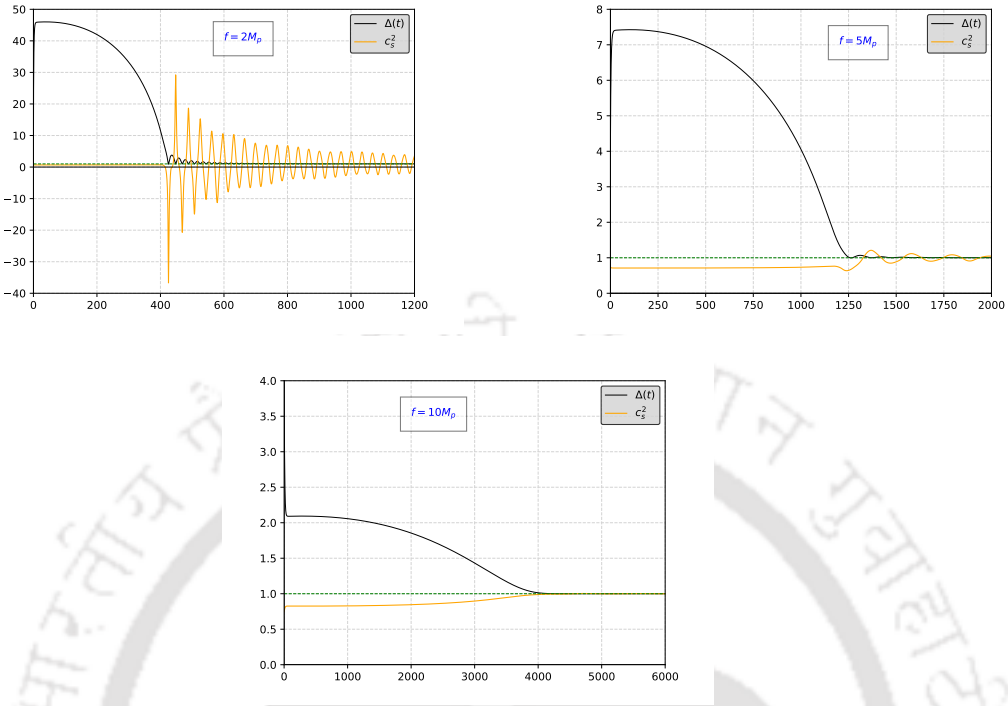


FIGURE 5.3: The evolution of $(\Delta(t), c_s^2)$ with time for three different values of the axion decay constant for $M(\phi) = Sin(\phi/f)$ when $\mathcal{A} = 92$. The value of $c_s^2$ is always smaller than unity during inflation. While the parameter $\Delta(t)$ is positive for all $f < f_c$ ensuring stability.

where, we have

$$P_{\mu\nu} = g_{\mu\nu} - 2M'(\phi)\nabla_\mu\phi\nabla_\nu\phi - 2XM(\phi)^2(Xg_{\mu\nu} - 2\nabla_\mu\phi\nabla_\nu\phi) \tag{5.76}$$

$$Q^{\mu\nu\alpha\beta} = M(\phi)g^{\mu\nu}g^{\alpha\beta} - \frac{M(\phi)}{2}\left(g^{\alpha\mu}g^{\beta\nu} + g^{\alpha\nu}g^{\beta\mu}\right) \tag{5.77}$$

Now information regarding the stability and the other aforementioned pathological behaviors of the background solutions are generically encoded in an effective metric on which the fluctuation propagates. Considering the liner order fluctuation of the above equation for the axion, one finds

$$(P^{\mu\nu} + 2Q^{\mu\nu\alpha\beta}\nabla_\alpha\nabla_\beta\phi)\nabla_\mu\nabla_\nu\delta\phi + \cdots = 0. \tag{5.78}$$

Where "$\cdots$" corresponds to all the terms which does not contain second derivative on $\delta\phi$. From the above equation for the fluctuation the aforementioned effective metric can be identified as the coefficient of $\nabla_\mu\nabla_\nu\delta\phi$, which is

$$\mathcal{G}^{\mu\nu} = (P^{\mu\nu} + 2Q^{\mu\nu\alpha\beta}\nabla_\alpha\nabla_\beta\phi). \tag{5.79}$$

This metric is calculated in a given background solution for the axion field such as inflationary background for the present case. Therefore, for any generic time dependent background, the

effective metric components take the following form,

$$\mathcal{G}^{00} = -\left(1 - 6HM(\phi)\phi' + 2\phi'^2 M'(\phi) + \frac{3}{2}M(\phi)^2\phi'^4\right) \tag{5.80}$$

$$\mathcal{G}^{ij} = \frac{\delta^{ij}}{a^2}\left(1 - 4HM(\phi)\phi' - 2M(\phi)\phi'' - \frac{1}{2}M(\phi)^2\phi'^4\right). \tag{5.81}$$

For stability of the system, following conditions has to be satisfied, $-\mathcal{G}^{00} = \Delta(t) > 0$ and the associated effective sound speed,

$$c_s^2 = \frac{\left(1 - 4HM(\phi)\phi' - 2M(\phi)\phi'' - \frac{1}{2}M(\phi)^2\phi'^4\right)}{\left(1 - 6HM(\phi)\phi' + 2\phi'^2 M'(\phi) + \frac{3}{2}M(\phi)^2\phi'^4\right)} \leq 1 \tag{5.82}$$

For illustration we have plotted those parameters $(\Delta(t), c_s^2)$ in Fig. 5.3 for a particular cosmological model with $M(\phi) = \sin(\phi/f)$. We can clearly see that depending upon the axion decay constant, before the $\Delta(t)$ parameter could cross zero, the superluminal velocity arises. If we further decrease the value of $f$, the sound speed becomes imaginary. Although for larger values of the axion decay constant these instabilities could be avoided, we are mainly interested in sub-planckian values of $f$. Hence, a further modifications to our model are necessary. Interestingly a possible resolution to these instabilities due to sound speed has been proposed recently[217] in the context of effective field theory of cosmological perturbations. Implication of these ideas could be interesting to explore further. This discussion provides us a hint for the existence of a critical value of axion decay constant below which standard evolution will not be possible after the end of inflation. In our subsequent discussion we see how the $\Delta(t)$ parameter will effect the evolution of background dynamics of $\phi$. The detail fluctuation analysis we left for our future studies. However, it is important to mention that all our models under consideration, the fluctuation are well behaved during inflation. Hence, inflationary observables will not be effected by those instability even if the value of $f$ is sub-Planckian.

It must be clear from previous discussions that the value of $(f, s)$ will be constrained from appropriate slow roll condition. For our G-axion or more generally Galileon inflation models, the nature of initial slow roll condition is dependent upon the choice of $f$ as it has to satisfy a non-trivial relation (5.63). In this section we will try to understand, qualitatively, the evolution of the scalar field depending on the initial conditions as well as our model parameters. The equation of motion for the scalar field (5.54) combined with Eq.(5.53, in unit of $M_p = 1$) can be written as

$$\Delta(t)\ddot{\phi}(t) + \Big[3H - 9M(\phi)H^2\dot{\phi} + \frac{1}{2}M''(\phi)\dot{\phi}^3 - \frac{9}{2}M^2(\phi)H^2\dot{\phi}^4 + \frac{3}{2}M(\phi)M'(\phi)\dot{\phi}^5\Big]\dot{\phi}(t) + V'(\phi) = 0 \tag{5.83}$$

From the above equation, it is evident that the solution may encounter singular behavior depending upon the initial condition when the coefficient $\Delta(t)$ becomes zero. The initial conditions in turn depend upon the parameters $(f, \Lambda, s)$. In our numerical calculation, it has been found that the scalar field does show singularity or oscillatory behavior depending on the values of the above mentioned parameters. The variation of $\Delta(t)$ and $c_s^2$ with time for three different values of $f$ has been shown in the Fig. 5.3.

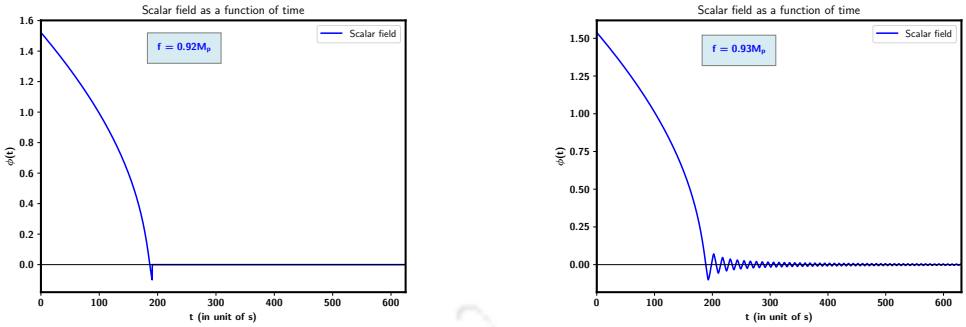


FIGURE 5.4: The evolution of the scalar field for two values of f when the solution transits from oscillatory to singular

It has been found that the minimum value of the coefficient tends to zero with decreasing $f$. The smallest value of axion decay constant which yields an oscillatory solution is when the coefficient is about to touch the zero axis. These numerical results have been confirmed in four different numerical environments. Fig. 5.4 shows an illustration of the scalar field behavior for $M(\phi) = Sin(\phi/f)$. We have shown the behavior of the scalar field solution for two adjacent values of $f$ in unit of Planck when the scalar field solution makes a transition from being singular to oscillatory. For all different functional form of $M(\phi)$, we found similar behavior for different critical values of $f$. However, it is interesting to note that models of type $(I, II, III)$, which are marginally fitting with the PLANCK observation, always complete the inflation before the field dynamics becomes singular for sub-Planckian decay constant. On the other hand best fit models of type $(IV, V)$ do not show such behavior as singularity appears well before the completion of inflation for sub-Planckian $f$. This behavior can be inferred also from the fact that for aforementioned models the slow roll condition is violated well before the inflation ends for sub-Planckian $f$. To this end we emphasize the following observation: all the models under consideration will have coherent oscillation for super-Planckian axion decay constant. Two of them can explain CMB observation for sub-Planckian $f$. From our numerical analysis, we found $f$ can even take super sub-Planckian value $\ll M_p$ without changing the properties of the solution. However, from the effective field theory point view, the value of axion decay constant should be limited to $\mathcal{O}(1) > f > \Lambda \simeq 10^{-2}$. None the less, the price we pay for those sub-Planckian model is that after inflation the inflaton field shows singular behavior, we call them non-oscillating axion models. Hence, as will be subsequently discussed, for those models we will employ the instant preheating mechanism to reheat the universe. The appreance of this type of singularity is related to the pressure singularity in KGB models. It has been shown in [200] that this pressure singularity implies infinite curvature scalar by a finite value of Hubble parameter and a divergent sound speed.

An interesting point about the solution is that there exists a minimum value of the field excursion, $\Delta\phi_c$ above which we have the oscillatory solution. This value is independent of the parameters $(f,\ \Lambda$ and, $s)$ for a particular form of $M(\phi)$. In the Table 5.1, we have shown the critical value of $f$ and the minimum field excursion when the oscillatory behavior sets in.

The PLANCK-2015 observation suggests the value of $\mathcal{A}$ should be within $40 \sim 360$, considering different models under consideration. Using the condition for dominating higher derivative term during inflation Eq.(5.63), aforementioned range of $\mathcal{A}$ constrains the value of axion decay constant to be $f \ll 6M_p \sim 18M_p$.

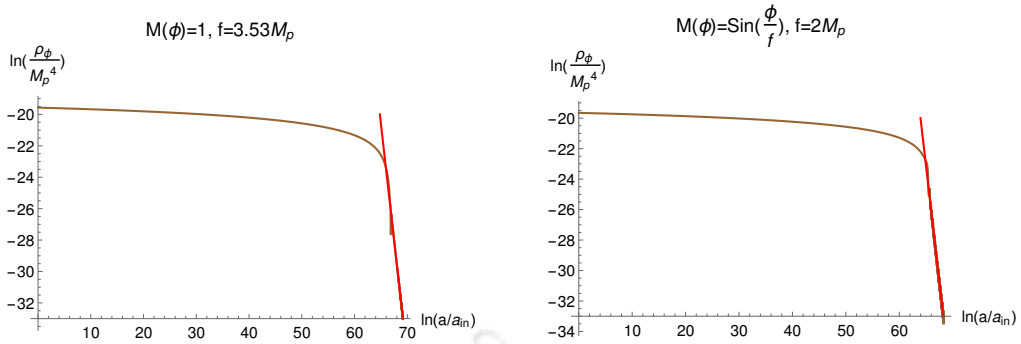


FIGURE 5.5: Evolution of energy density of the inflaton field for two different oscillating G-axion models. The fitting red line shows the behavior of $\rho_\phi \sim a^{-3}$.

| Summary of the scalar-field dynamics | | | |
|---|---|---|---|
| $M(\phi)$ | $\mathcal{A}$ | $\Delta\phi_c(=\phi_1-\phi_2)$ | $f_c/M_p$ |
| Constant | 76 | 4.85158 | 3.24 |
| | 100 | 4.86432 | 3.62 |
| $Sin(\phi/f)$ | 92 | 1.27722 | 0.93 |
| | 150 | 1.26267 | 1.1 |
| $Sin^2(\phi/f)$ | 88 | 3.30 | 2.5 |
| | 95 | 3.28 | 2.55 |

Table 5.1: $f_c$ is the minimum value of $f$ for which the oscillatory behavior set off. The values of $\mathcal{A}$ are so chosen that the predicted value of $n_s$ is the central value of PLANCK.

It is now clear that for a wide range of axion decay constant our G-axion model fits extremely well with the CMB observation. For further understanding, it is of prime importance to go beyond the inflationary dynamics. However, for the singular behavior of the inflaton field which we have been discussing in the previous sections, we need a detailed analysis considering the additional reheating field coupled with the inflaton. Thanks to the instant preheating mechanism [49], instead of considering the full dynamics, for non-oscillatory model we employ the aforementioned instant preheating mechanism which acts at the instant of the first zero crossing of the inflaton field [50, 51, 218, 219].

## 5.6 Non-oscillating axion: Instant preheating

As we have emphasized earlier, the reheating phase after the inflation is a stage when the energy stored in the inflaton field is transferred into the other field(s) which further produce all the matter we see today. As we have noted, we get two types of scalar field solution after inflation. For oscillatory solution, the standard mechanism of reheating works well in our model[220, 221]. But for the cases when the scalar field does not have coherent oscillation after the inflation, we need to invoke alternative mechanism to reheat our universe. We see that instant preheating, originally proposed as an alternative to preheating mechanism for no-oscillatory inflation models, could be important. This mechanism has been successfully implemented to reheat the universe in quintessential inflation [50, 51, 218, 219]. In the following

sections, we study instant preheating for sub-Planckian model for $f < f_c \simeq \mathcal{O}(1)M_p$. As mentioned before, we consider two types of coupling between the reheating field and the inflaton and compare their results. We will see how the higher derivative coupling term plays the important roll in our analysis.

### 5.6.1 Conventional Shift Symmetry Breaking Coupling

Let us start by considering the interaction Lagrangian as of the original work of Felder-Kofman-Linde. Where the inflation $\phi$ interacts with another scalar field $\chi$ which decays to a fermion field $\psi$. We write the interaction Lagrangian as

$$\mathcal{L}_{int} = -\frac{1}{2}g^2\phi^2\chi^2 - h\bar{\psi}\psi\chi, \tag{5.84}$$

where the couplings are supposed to be positive with $g, h < 1$ in order for the perturbation treatment to be valid. It is evident that the above Lagrangian does not respect the shift symmetry of our original Lagrangian. We will consider a special shift symmetric case in the next subsection. For simplicity, we will consider the $\chi$ particles do not have a bare mass, while its effective mass is provided by the inflation field as

$$m_\chi(\phi) = g|\phi|. \tag{5.85}$$

The production of the $\chi$ initiate as $m_\chi$ starts changing non-adiabatically after the end of inflation.

$$|\dot{m_\chi}| \gtrsim m_\chi^2 \quad or, |\dot{\phi}| \gtrsim g\phi^2 \tag{5.86}$$

In the Fig. 5.6-a, we see the region where the adiabatic condition is violated for different values of dimensionless coupling parameter $g$. Above condition implies that

$$|\phi| \lesssim |\phi_{prod}| = \left(\frac{\dot{\phi}_{end}}{g}\right)^{\frac{1}{2}} \tag{5.87}$$

Now, to estimate $\dot{\phi}$ analytically, we assume the slow-roll condition to hold till the end of the inflation. This is where the higher derivative term in our model plays the role. Using Eq.(5.60), we find that

$$|\dot{\phi}_{end}| \simeq \left(\frac{2\epsilon_{end}M_p}{3\sqrt{3}M(\phi)}\right)^{\frac{1}{3}}(V_{end})^{\frac{1}{6}} = \left(\frac{2M_p}{3\sqrt{3}M(\phi)}\right)^{\frac{1}{3}}(V_{end})^{\frac{1}{6}} \quad = P(\phi)(V_{end})^{\frac{1}{6}}, \tag{5.88}$$

where, we have denoted

$$P(\phi) = \left(\frac{2M_p}{3\sqrt{3}M(\phi)}\right)^{\frac{1}{3}}$$

It would more intuitive to express the above expression of $P(\phi)$ in terms of the derived parameter, $\mathcal{A}$ that we have defined earlier. This reads as

$$P(\phi) = 0.72\frac{1}{\mathcal{A}^{\frac{2}{3}}}\frac{f}{M_p}\left[\frac{\Lambda^4}{\tilde{M}(\tilde{\phi})}\right]^{\frac{1}{3}} \tag{5.89}$$

The production time for $\chi$ particles can be estimated as

$$\Delta t_{prod} \sim \frac{|\phi_{prod}|}{|\dot{\phi}_0|} \sim \frac{1}{\sqrt{gP(\phi)(V_{end})^{\frac{1}{6}}}} \tag{5.90}$$

where $|\dot{\phi}_0|$ is the velocity of the field near the minimum of the effective potential. Let us now make an estimate of the numerical values of the quantities involved. We can use the relation (5.64) and the observed value of the scalar power spectrum to determine the value of the inflaton potential at the end of the inflation. Taking a sample value of the KGB scale $s \sim 10^{-5}M_p$, one finds $V_{end} \sim 6 \times 10^{-6}M_p^4$. In order for the particle production to occurs within a very short period of time, we must satisfy $\Delta t_{prod}/s < 1$ which provides lower bound on $g$ as $g > 10^{-6}f_b$. Where $f_b$ is the axion decay constant in unit of $M_p$. Using these values, we find the value of $\dot{\phi}_{end} \sim 10^{-6}M_p^2$. Hence to get $\phi_{prod} < M_p$, we must choose $g > 10^{-6}$. Using uncertainty relation one can estimate the momentum $k_{prod} \simeq (\Delta t_{prod})^{-1} \sim (gP_{end})^{1/2}V_{end}^{1/12}$ of $\chi$ particles which will be be created non-adiabatically, and [32, 49], the occupation number of $\chi$ particles jumps from zero to

$$n_k \simeq exp(-\pi k^2/k_{prod}^2) \tag{5.91}$$

during the time interval $\Delta t_{prod}$. The number density can be estimated to be

$$n_\chi = \frac{1}{2\pi^2}\int_0^\infty k^2 n_k dk \simeq \frac{k_{prod}^3}{8\pi^3} \simeq \frac{(gP_{end})^{\frac{3}{2}}V_{end}^{\frac{1}{4}}}{8\pi^3} \tag{5.92}$$

and the energy density of the $\chi$ particles can be found to be

$$\rho_\chi = m_\chi n_\chi \left(\frac{a_{end}}{a}\right)^3 = \frac{(gP_{end}V^{\frac{1}{6}})^{\frac{3}{2}}}{8\pi^3} g|\phi| \left(\frac{a_{end}}{a}\right)^3 \tag{5.93}$$

where the $(a_{end}/a)^3$ term corresponds to the dilution of the energy density due to cosmic expansion.

In numerical calculation, we found that the value of $g$ as small as $\mathcal{O}(10^{-3})$ satisfy the adiabaticity condition mentioned above. And with this value of coupling constant, we can readily check that production of the $\chi$ particle is indeed instantaneous. Now, if the quanta of the $\chi$-field were to thermalized into radiation instantly, the radiation energy density would become

$$\rho_r \simeq \rho_\chi \sim \frac{(gP_{end})V^{\frac{1}{6}})^{\frac{3}{2}}}{8\pi^3} g\phi_{prod} \sim \frac{g^2P^2(\phi)V_{end}^{\frac{1}{3}}}{8\pi^3}. \tag{5.94}$$

Now the efficiency of instant preheating can be parametrized by the following ratio,

$$\frac{\rho_r}{\rho_\phi} \simeq 2 \times 10^{-3}\left(\frac{g}{\mathcal{A}^{\frac{2}{3}}}\right)^2\left(\frac{f}{M_p}\right)^2\left(\frac{1}{\tilde{M}_{end}}\right)^{\frac{2}{3}} \simeq 5 \times 10^{-6}g^2.$$

Where, in the final numerical value we considered order of magnitude values of all the parameters $\mathcal{A} \simeq 100$, $f \simeq 0.1M_p$, and $\tilde{M}_{end} \simeq 1$. To this end let us quote the above ratio of energy densities for the Quintecence inflation model where also one does not have oscillatory phase after the inflation [50]

$$\frac{\rho_r}{\rho_\phi} \simeq 10^{-2}g^2. \tag{5.95}$$

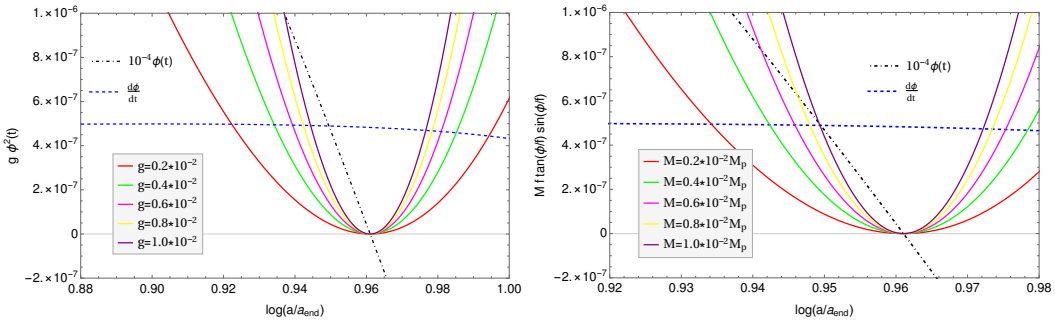


Figure 5.6: Figure shows the region where the adiabaticity condition is violated, which is evidently the region where $\phi(t)$ crosses zero (black dashed line), First figure is for the coupling $g^2\phi^2\chi^2$, while second one is for $M^2 sin^2(\phi/f)\chi^2$

This result can be proved to be generically true for conventional canonical inflation model with the aforementioned interaction Eq.(5.84) term. Therefore, comparing with the usual model, we conclude that for G-axion inflation model instant preheating will not be efficient enough as it is suppressed by the same emergent parameter $\mathcal{A}$ which played the important role in obtaining the sub-Planckian axion decay constant $f$. In addition, we also have dimensionless coupling constant $g$ which is constrained to be small to avoid strong coupling problem.

So far we have not mentioned anything about the fermionic coupling parameter $h$. Even though the particle production at the instant of first zero crossing of inflaton, does not seem efficient, for completeness let us constraint the possible value of $h$ for the instant preheating mechanism to work. The decay rate reheating field into radiation is given by $\Gamma_{\psi\bar{\psi}} = h^2 m_\chi/8\pi$, with $m_\chi = g|\phi|$. Now for instant preheating to work it must be larger than the expansion rate of the universe at instant of preheating

$$\Gamma_{\psi\bar{\psi}} \gtrsim H_{prod} \implies h^2 \gtrsim 8\pi \frac{H_{prod}}{g\phi_{prod}} \tag{5.96}$$

The order of magnitude of $h$ can be estimated for some sample value of $g$ we can have

$$\begin{aligned} h &\gtrsim 0.3 \quad \text{for} \quad g \sim 10^{-2} \\ h &\gtrsim 0.9 \quad \text{for} \quad g \sim 10^{-3} \end{aligned}$$

As we have concluded from our analysis, instant preheating mechanism turns out to be inefficient for the conventional shift symmetry breaking coupling considered above. We want to see if any other type such as shift symmetric coupling can give some enhancement in the efficiency.

### 5.6.2 Shift Symmetric Coupling

As we have started with shift symmetric theory, for completeness, we express the main result for the following shift symmetric coupling

$$\mathcal{L}_{int} = -\frac{1}{2}M^2 \; sin^2\left(\frac{\phi}{f}\right)\chi^2 - h\bar{\psi}\psi.\chi \tag{5.97}$$

Where $M$ dimensionful coupling parameter. In the Fig. 5.6-b, we plotted the region where the adiabaticity is lost. Follow the same methodology discussed before and under some reasonable

assumption and approximation, we arrived at the following ratio of produced energy density over the inflaton energy density,

$$\frac{\rho_r}{\rho_\phi} \simeq 2 \times 10^{-3} \left(\frac{M}{M_p \mathcal{A}^2}\right) \left(\frac{\Lambda}{M_p}\right)^2 \left(\frac{1}{\tilde{M}_{end}}\right) \simeq 2 \times 10^{-7} M, \tag{5.98}$$

Where again for final numerical value, we have chosen $\mathcal{A} = 100, \Lambda = 10^{-2} M_p$, and $\tilde{M}_{end} \simeq 1$. Therefore, we again see the suppression by the factor $\mathcal{A}$.

Our observation in this section is that the instant preheating mechanism seemed to be inefficient in transferring the energy from inflaton to reheating field for higher derivative driven G-axion inflation. This negative result can be attributed to the fact that the velocity of the inflaton field near the end of inflation is suppressed by the parameter $\mathcal{A}$ as opposed to the usual axion inflation scenario. Therefore, the adiabaticity violation turned out to be very weak near the zero crossing of the inflaton field. Hence, the particle production became inefficient compared to the usual canonical inflation models.

## 5.7 Conclusions

In this chapter we have studied the axion inflation model with a specific form of higher derivative kinetic term within the theory of Galileon cosmology. We call it G-axion. As we have already discussed, the usual axion inflation is now marginally consitent with PLANCK result[53, 54] and that too for superplanckian value of axion decay constant. In this chapter, we have described the modified G-axion with some simple choices of Galileon interaction term $M(\phi)X\Box\phi$. Our main motivation was to understand more on the sub-Planckian dynamics. One of the important motivations of studying such a modification, of course, is to explain the current observational data by PLANCK. However, another reason is to make the model consistent in the framework of effective field theory. With such a higher derivative modification, our model turned out to predict inflationary parameter $(n_s, r)$ within the range of Planck data for sub-Planckian values of all its parameters. However, we have found for some specific choices of functions, $M(\phi) = \{constant, \sin(\phi/f), \sin^2(\phi/f)\}$, the sub-planckian axion decay constant yields singular behavior in the scalar field dynamics specifically after the inflation. We dubbed them as non-oscillatory G-axion model. The existence of such kind of singular behavior in cosmological context has been discussed in recent studies[222, 223]. The singularity behavior emerges from the kinetic function $\Delta(t)$ when approaching towards zero. The significance of the singularity in Kinetic Gravity Braiding theories has been discussed. Exploring this property for further analysis in the context of dark energy will be interesting, and we left it for our future studies. The issues of stability and superluminal propagation speed has been briefly discussed. It has been found that there exits parameter space when such instabilities will arise. The possible resolution for this issues in the light of [217, 224, 225] could be very interesting for our future work. Nonetheless, it has been found that these sub-Planckian models provide successful inflation and right after crossing the zero in the field space it hits the singularity. Since these models give successful inflation, we employed the instant preheating mechanism to reheat our universe. However, it turned out that the mechanism under study is not efficient enough. The amount of energy transferred from inflaton to the reheating field is suppressed by the same factor $\mathcal{A}$ which helped us to make the model consistent with the PLANCK observation on inflationary observables. We have studied two different types of coupling namely, shift symmetric and conventional broken shift symmetric, to study preheating.

For both types of coupling energy transfer turned out the be inefficient. Therefore, we need further study to understand the sub-Planckian G-axion model. Interestingly, with regards to the latest observation made by PLANCK, we found out super-Planckain G-axion models for $M(\phi) = \{\cos^2(\phi), 1 - \sin(\phi)\}$ which are very well fitted as opposed to the conventional axion inflation. For those two models we have prediction of $r \simeq 0.03 \sim 0.05$ within the $1\sigma$ range of $n_s$ which could be detectable in the near future CMB experiments. For super-Planckian G-axion models, the inflaton oscillates after the end of inflation. We, therefore, have studied model independent reheating constraint analysis.

A particularly interesting point we would like to mention is the role played by the axion decay constant $f$ in the dynamics of G-axion inflation. Depending on the value of $f$, dynamics could be either usual kinetic term dominated or the galileon term dominated. Therefore, an interesting regime of $f$ exists when both terms play the role. In terms of the emergent parameter $\mathcal{A}$, the condition for inflation dominated by KGB term translated into the following approximate relation: $f \ll \mathcal{A}^{1/2}$. Although this bound on $f$ has a certain degree of dependence on the choice of $M(\phi)$. If the value of the axion decay constant violates the above bound, depending on the initial condition, our numerical computation shows that the inflaton dynamics is dominated by the higher derivative term at the initial stage and subsequently it becomes canonical kinetic term dominated around the end of inflation. This fact of two phases of inflation will certainly have interesting consequences on the observable quantities and CMB spectrum. For instance, in some models of inflation[226–228] a phase of super inflation is introduced at the initial stage of inflation to explain the power suppression in the large angular scales of the CMB. This interesting effect can be naturally explained in our model. We will be very interesting study in future.

# Conclusions 6

*"The sciences do not try to explain, they hardly even try to interpret, they mainly make models. By a model is meant a mathematical construct which, with the addition of certain verbal interpretations, describes observed phenomena. The justification of such a mathematical construct is solely and precisely that it is expected to work-that is, correctly to describe phenomena from a reasonably wide area. Furthermore, it must satisfy certain aesthetic criteria-that is, in relation to how much it describes, it must be rather simple."*

*John von Neumann in 'Method in the Physical Sciences'*

In this thesis, we have discussed the phase of inflation and reheating in the early universe driven by single scalar field. We have seen that most of the simple scalar field inflationary models, for instance the power-law chaotic models, are currently ruled out from the observation. This motivates us to look into some modifications to the standard scenario which can fit well with the observation.

We have focused on two main modifications: We have described the effects of non-polynomial modifications of power-law potentials and the effects of higher derivative kinetic term into the canonical scalar field Lagrangian. We have also generalized the exiting mechanism of constraining the inflation model via CMB anisotropy through the reheating phase, and inquired the effects of production of dark matter species during this phase. Below we summarize the main findings of the thesis.

## 6.1 Summary of chapters

- In Chapter 2, we have proposed and analyzed the predictions of a class of plateau type inflationary models from non-polynomial modifications to the chaotic power-law models. The plateau type of potentials predicting a smaller value of tensor-to-scalar ratio are now favored by observations. We have described a possible realization of these type of plateau potentials from super-gravity considering anomalous $U(1)$ symmetry superpotential. It

has also been shown that starting from simple power-law potentials in the Jordan frame in general scalar-tensor theory, we can also arrive at these potentials. The general characteristics of these potentials is an infinite plateau for large field values while they reduce to simple power-law potentials $V(\phi) \propto \phi^n$ around $\phi = 0$. In order to achieve this properties, the scale $\phi_*$ plays important role in not only controlling the shape, but also setting the inflationary energy scale. The inflaton takes the usual chaotic form after the inflation. Therefore, we have studied in detail the post-inflationary reheating dynamics within the standard setup. However, we have seen the $\phi_*$ plays again an important role during reheating.

- In Chapter 3, we have described the CMB constrains on the reheating phase by incorporating the explicit inflaton decay. This is an essential generalization of the existing works in the literature where the expansion during the reheating phase was parameterized by a time independent effective equation of the state of the system comprising inflaton and radiation. However, in this chapter we have explicitly solved the homogeneous Boltzmann equation for the decaying inflaton into radiation and radiation into dark matter, supplemented by the entropy conservation and the present dark matter abundance. Through this we were able to indirectly connect the CMB anisotropy and dark matter phenomenology. Considering the standard as well as the inflationary models discussed in the Chapter 2, we constrain the dark matter parameter space in terms of CMB power spectrum.

- In Chapter 4, we studied in detail the non-perturbative effects during (p)reheating after the minimal plateau inflation with the help of $3 + 1$ dimension lattice simulation. We have addressed the issues of equation of the state parameter during the reheating phase, the growth of non-linearity and back-reaction of the created particles and finally the termination of preheating. Our focus on these studies was to observe the effects of the controlling scale $\phi_*$ on the preheating phase. It has been found that decreasing $\phi_*$ for any inflationary model specified by the exponent $n$(as well as $m$ or $\lambda$), will result in a decrease in the e-folding number during the preheating phase. The complete decay of the inflaton energy is, however, not achieved for any of the models considered with a four-legged interaction. We, therefore, considered studying the perturbative reheating dynamics discussed in the previous chapter to complete the reheating phase.

- In Chapter 5, we have considered a different class of inflationary scenario with higher derivative derivative terms in the Lagrangian with a specific type of symmetry called the Galilean symmetry. The Galilean inflation that respects this summery are well studied in the literature in the context of dark energy and inflation. The higher derivative kinetic terms in the Galilean Lagrangian arise in such a way that the equation of motions are at most second order thereby the theory is free from any ghost degrees of freedom. The inflation in the realm of Galilean cosmology is dubbed as G-inflation. The potential we have chosen to work is the Natural inflationary potential which itself exhibits discrete shift symmetry. In natural inflation, the inflation is a pseudo Nambu Goldstone boson known as the axion in particle physics. Despite being one of the most theoretically well motivated models, the pure axion inflation is now marginally consistent and that too for the super Planckian values of the axion decay constant. In this chapter, we have constructed a viable axion inflation model called G-axion with sub-Planckian values of axion decay constant and field excursion during inflation. We have further extended

the study of G-axion in light of recent observations. We have seen that although the Galilean inflation is free from any ghost instabilities at the equation of level, however, the gradient instabilities and the issue of superluminal propagation speed may arise at the perturbation level. We addressed those issues in this chapter. It has also been found that the general oscillatory inflaton solution is absent in the case of G-axion for certain parameter space thereby rendering the particle production due to parametric resonance impossible. This motivates us to check the possibility of *instant preheating* after G-axion inflation. It has been found that the efficiency of instant preheating is not efficient enough. Therefore, further study on on the reheating is essential.

## 6.2 Future perspectives

During the course of this work, several perspectives have been found that need further study. Some of them are listed below that will be subject to future works.

- The study of CMB constrains using perturbative inflation decay has several areas that needs further refinements. For instance, explicit model building in the dark matter sector during the reheating period could be an important research direction. However, before creating model of dark matter during reheating era the proper high energy modifications must be incorporated into it.
- In the present analysis, we have only considered the homogeneous evolution. It would be very importance to analyze the evolution of perturbations of radiation and dark matter components and study their spectral properties which can give further constraints on our parameter space.
- The important fact that the full non-linear preheating never completes the reheting process itself. Therefore, the full analysis with interaction that will initiate tree-level decay and to understand how and when inflaton decay and radiation domination begins will be interesting to study.
- We have seen that the G-axion inflation provides an attractive avenue for inflationary model building due to its interesting symmetry. Even though it is free from ghost, it suffers from gradient instabilities and superluminal propagation at the perturbation level. A possible resolution to this instabilities due to sound speed has been recently proposed in[217] in the context of effective field theory of cosmological perturbations. Application of these mechanism to the case of G-axion will be interesting to explore further.
- We have also seen a particular interesting role played by the axion decay constant $f$ in the dynamics of G-axion inflation. Depending on the value of $f$, dynamics could be either usual kinetic term dominated or the galileon term dominated. Therefore, an interesting regime of $f$ exists when both terms will influence the inflationary phase. Two phases of inflation will have interesting consequences on the observable quantities and CMB spectrum. For instance, in some models of inflation[226–228] a phase of super inflation is introduced at the initial stage of inflation to explain the power suppression in the large angular scales of the CMB. Hence the G-axion inflation can naturally provide such a two phase inflation leaving distinct signature in the CMB. It will be a interesting project in the future.

# Appendices

# Background dependent unitarity for plateau potentials

In this section we briefly discuss about the issue of unitarity for the plateau potentials described in Chapter 2. As it is obvious that our model is non-renormalizable because of non-linear interaction potential. In order to be predictive, the cut off scale beyond which our model is non-unitarity should be higher than the inflationary energy scale $V^{1/4}$. For our convenience we calculated some sample numerical values of the inflation scale given in Table 1 for different $n$. From the usual effective field theory point of view, the cut off scale $\Lambda_c$ of a model can be extracted from the perturbative coefficient of the potential expanded around zero. Considering the model potential and expanding around zero, one gets,

$$V(\phi) = \lambda \frac{m^{4-n}\phi^n}{1+\left(\frac{\phi}{\phi_*}\right)^n} = \lambda \sum_{r=0}^{\infty} \frac{(-1)^r \phi^{n(1+r)}}{m^{n-4}\phi^{*nr}} = \lambda \sum_{r'} \frac{\mathcal{O}^{r'}}{\Lambda_c^{r'-4}}. \tag{1}$$

Therefore, we can identify $\Lambda_c = m^{(n-4/(n(r+1)-4))}\phi^{*(nr)/(n(r+1)-4)}$, the scale above which the unitarity will be violated. From the aforementioned expression, it is clear that as we increase the operator dimension, the cut off scale decreases. Therefore, the lowest value of the cut off scale will be exactly at $\phi^*$ for any value of $n$ in large $r$ limit. From the Table 1, we can clearly see that all the necessary scales of our model are less than the cut off scale. In addition what we found is that the inflaton field takes sub-Planckian initial value. Therefore, quantum gravity effect will be unimportant which is generically not true for usual power law inflation. The aforementioned conclusion is from the usual effective field theory point of view. However, the background value of the scalar field may effect the unitarity limit.

| $\phi_*/M_p$ | $n$ | $m/M_p$ | $\lambda$ | $H_*/M_p$ | $V_*^{1/4}/M_p$ |
|---|---|---|---|---|---|
| 0.01 | 2 | $1.2 \times 10^{-4}$ | 1 | $6.8 \times 10^{-7}$ | $1.1 \times 10^{-3}$ |
| | 4 | - | $7.3 \times 10^{-6}$ | $1.6 \times 10^{-7}$ | $5.2 \times 10^{-4}$ |
| | 6 | 8.9 | 1 | $6.5 \times 10^{-8}$ | $3.3 \times 10^{-4}$ |
| | 8 | $4.0 \times 10^{-1}$ | 1 | $3.6 \times 10^{-8}$ | $2.5 \times 10^{-4}$ |
| 1 | 2 | $1.3 \times 10^{-5}$ | 1 | $4.6 \times 10^{-6}$ | $2.8 \times 10^{-3}$ |
| | 4 | - | $3.5 \times 10^{-11}$ | $2.7 \times 10^{-6}$ | $2.1 \times 10^{-3}$ |
| | 6 | $2.8 \times 10^{5}$ | 1 | $1.7 \times 10^{-6}$ | $1.7 \times 10^{-3}$ |
| | 8 | $6.4 \times 10^{2}$ | 1 | $1.3 \times 10^{-6}$ | $1.5 \times 10^{-3}$ |

Table 1: Inflationary energy scales and the parameter $m$ and $\lambda$ for two different values of $\phi_*$

In the following discussion we analyze the aforementioned background dependent unitarity limit. In standard model of particle physics, it is known that unitarity is dependent upon the Higgs vacuum expectation value. Therefore, this should also be true during inflation. Following the argument for the Higgs inflation in [229], one can compute the background dependent cut off scale $\Lambda(\phi_0)$. The cut of scale can be read off from the coefficient of the operator of dimension higher than four. Therefore, we expand the potential $V(\phi)$ in the inflationary background $\phi_0$ taking $\phi = \phi_0 + \delta\phi$. Because of the non-trivial background, we will have all possible operators generated by the expansion. The dimension five operator turns out to be

$$\delta V^I = \mathcal{U}_c\Big[50n(-1+{\phi_0}^n)(1+{\phi_0}^n)^3 + 24(1+{\phi_0}^n)^4 + 35n^2(1+{\phi_0}^n)^2(1-4{\phi_0}^n+{\phi_0}^{2n}) + n^4(1-26{\phi_0}^n+66{\phi_0}^{2n}-26{\phi_0}^{3n}+{\phi_0}^{4n}) + 10n^3(-1+10{\phi_0}^n-10{\phi_0}^{3n}+{\phi_0}^{4n})\Big]\delta\phi^5 \tag{2}$$

where,

$$\mathcal{U}_c = \frac{\lambda m^{4-n}\phi\,{*}^{n-5}\,n{\phi_0}^{n-5}}{(120(1+{\phi_0}^n)^6)} \tag{3}$$

In the inflationary regime, inflaton usually assuems large field $\phi_0 \gg 1$ measured in unit of $\phi{*}$. In this limit, the approximate expression for the background dependent cut off turns out to be,

$$\Lambda(\phi_0) = \frac{120m^{n-4}\phi_0^{(5+n)}}{\lambda\phi\,{*}^{n-5}\,n(24+50n+35n^2+10n^3+n^4)} \tag{4}$$

In the inflationary background, one can check that above cut off scale is much larger than $\phi{*}$ for all possible values of $n$. Therefore, the observable predictions are stable against the quantum correction. However, detail analysis we will defer for our future studies.

# Boltzmann equations for out-of-equilibrium processes

In Chapter 3, we have discussed the application of Boltzmann equations for the case of particle production during the reheating phase. In this appendix, We will derive the Boltzmann equations for out-of-equilibrium processes of particle interaction.

During the earlier times of universe most of the components of the universe were in thermal equilibrium with each other and their interactions were much more frequent. As the temperature decreased due to expansion of the universe, the interactions among different species became less frequent and certain components fall out of thermal and chemical equilibrium. Depending upon their interaction strength, some species decoupled from the rest of primordial plasma. These out-of-equilibrium phenomena is studied in the realm of Boltzmann equations.

In this chapter, we will derive the Boltzmann equations[230] governing the rate of change of number densities for different components of the universe for a simple case. Let us consider the following interaction where two species 1 and 2 interacts to produce two other species 3 and 4.

$$1 + 2 \rightleftharpoons 3 + 4 \tag{5}$$

Denoting the number densities of the species as $n_i$, the rate of change of co-moving number density of component 1 is

$$\begin{aligned} a^{3(1+w_1)} \frac{\mathrm{d}}{\mathrm{d}t}\left(a^{3(1+w_1)} n_1\right) = \int \frac{d^3p_1}{2E_1(2\pi)^3} \int \frac{d^3p_2}{2E_2(2\pi)^3} \int \frac{d^3p_3}{2E_3(2\pi)^3} \int \frac{d^3p_4}{2E_4(2\pi)^3} \times \\ (2\pi)^4 \delta(E_1 + E_2 + E_3 + E_4) \delta^3(p_1 + p_2 + p_3 + p_4) \times \\ |\mathcal{M}|^2 \{f_3 f_4 (1 \pm f_1)(1 \pm f_2) - f_1 f_2 (1 \pm f_3)(1 \pm f_4)\} \end{aligned} \tag{6}$$

Where, for species "i":

$w_i$ = equation of state parameter for species 'i',

$f_i$ = The distribution function for species 'i',

$f_i$ = The distribution function for species 'i',

$p_i$ = The momentum for species 'i' and,

$E_i$ = The energy for species 'i',

The plus sign in the last line of the above equation is for bosons and the minus sign is for the fermions, thus the term $(1 \pm f_i)$ accounts for the Bose enhancements and Pauli blocking respectively.

Now in absence of any interaction, the right hand side vanishes merely reflecting the fact that the co-moving number density of the species 1 is conserved in an expanding universe. The information about the interaction is encoded into the matrix element $\mathcal{M}$ which can be easily found out once we know the interaction Lagrangian. The two Dirac delta functions in the equation signifies the appropriate energy -momentum conversations. The last line indicates the fact that the production rate of particle 1 increases with the abundance of species 3 and 4. Finally, the integral has to be evaluated over all possible momenta.

The distribution function is given by

$$f_i = \frac{1}{e^{\frac{(E_i-\mu_i)}{T}} \pm 1} \tag{7}$$

Where $\mu_i$ is the chemical potential, the minus sign in the denominator is for bosons and plus sign is for fermions. In the regime when $T \ll (E_i - \mu_i)$, the exponential term is much higher than unity and the distribution function reduces to

$$f_i \simeq e^{\mu_i/T} e^{E_i/T} \tag{8}$$

The number density will be given by

$$n_i = g_i e^{\mu_i/T} \int \frac{d^3p}{(2\pi)^3} e^{-E_i/T} \tag{9}$$

where $g_i$ is the degeneracy of the species '$i$'. The equilibrium number density can be written as

$$n_i^{(0)} = \begin{cases} g_i \frac{T^3}{\pi^2} & \text{for (relativistic),} \\ g_i \left(\frac{m_i T}{2\pi}\right) e^{-m_i/T} & \text{for (non-relativistic)} \end{cases} \tag{10}$$

Thus, the out-of-equilibrium expression for number density is expressed as

$$n_i = n_i^{(0)} e^{\mu_i/T} \tag{11}$$

with these expressions for number density and distribution, the last term in Eq.(6) can be written as

$$e^{-\frac{(E_1+E_2)}{T}} \left[\frac{n_3 n_4}{n_3^{(0)} n_4^{(0)}} - \frac{n_1 n_2}{n_1^{(0)} n_2^{(0)}}\right] \tag{12}$$

Finally defining the thermally averaged cross-section, $\langle \sigma v \rangle$, as

$$\begin{aligned} \langle \sigma v \rangle = & \frac{e^{(E_1+E_2)/T}}{n_1^{(0)} n_2^{(0)}} int \frac{d^3p_1}{2E_1(2\pi)^3} \int \frac{d^3p_2}{2E_2(2\pi)^3} \int \frac{d^3p_3}{2E_3(2\pi)^3} \int \frac{d^3p_4}{2E_4(2\pi)^3} \times \\ & |\mathcal{M}|^2 (2\pi)^4 \delta(E_1 + E_2 + E_3 + E_4) \delta^3(p_1 + p_2 - p_3 - p_4) \end{aligned} \tag{13}$$

The Boltzmann equation for the species 1 subject to the process in (5) is

$$a^{3(1+w_1)} \frac{\mathrm{d}}{\mathrm{d}t} \left(a^{3(1+w_1)} n_1\right) = n_1^{(0)} n_2^{(0)} \langle \sigma v \rangle \left[\frac{n_3 n_4}{n_3^{(0)} n_4^{(0)}} - \frac{n_1 n_2}{n_1^{(0)} n_2^{(0)}}\right] \tag{14}$$

This equation has wide applicability in different branches of physics in general and cosmology in particular, for instance, production of dark matter and radiation via perturbative inflaton decay during reheating phase can be studied with appropriate set of Boltzmann equations for a three component universe comprising the inflaton, the radiation and the dark matter particle.

# Bibliography


[1] S. G. Brush, "How Cosmology Became a Science," *Sci. Am.* **267-2** (1992) 62–71.

[2] S. Weinberg, *The First Three Minutes. A Modern View of the Origin of the Universe.* Basic Books, New York, USA, 1993. https://www.basicbooks.com/titles/steven-weinberg/the-first-three-minutes/9780465024377/.

[3] A. H. Guth, *The inflationary universe: The quest for a new theory of cosmic origins.* Addison-Wesley, Reading, USA, 1997.

[4] S. Weinberg, *Cosmology.* Oxford University Press, Oxford, UK, 2008. http://www.oup.com/uk/catalogue/?ci=9780198526827.

[5] A. H. Guth, "The Inflationary Universe: A Possible Solution to the Horizon and Flatness Problems," *Phys. Rev.* **D23** (1981) 347–356.

[6] A. A. Starobinsky, "A New Type of Isotropic Cosmological Models Without Singularity," *Phys. Lett.* **B91** (1980) 99–102. [,771(1980)].

[7] K. Sato, "First Order Phase Transition of a Vacuum and Expansion of the Universe," *Mon. Not. Roy. Astron. Soc.* **195** (1981) 467–479.

[8] A. D. Linde, "A New Inflationary Universe Scenario: A Possible Solution of the Horizon, Flatness, Homogeneity, Isotropy and Primordial Monopole Problems," *Phys. Lett.* **108B** (1982) 389–393. [Adv. Ser. Astrophys. Cosmol.3,149(1987)].

[9] A. Albrecht and P. J. Steinhardt, "Cosmology for Grand Unified Theories with Radiatively Induced Symmetry Breaking," *Phys. Rev. Lett.* **48** (1982) 1220–1223. [Adv. Ser. Astrophys. Cosmol.3,158(1987)].

[10] G. Steigman, "Primordial Nucleosynthesis in the Precision Cosmology Era," *Ann. Rev. Nucl. Part. Sci.* **57** (2007) 463–491, arXiv:0712.1100 [astro-ph].

[11] **Planck** Collaboration, P. A. R. Ade *et al.*, "Planck 2013 results. XVI. Cosmological parameters," *Astron. Astrophys.* **571** (2014) A16, arXiv:1303.5076 [astro-ph.CO].

[12] H. Kodama and M. Sasaki, "Cosmological Perturbation Theory," *Prog. Theor. Phys. Suppl.* **78** (1984) 1–166.

[13] V. F. Mukhanov, H. A. Feldman, and R. H. Brandenberger, "Theory of cosmological perturbations. Part 1. Classical perturbations. Part 2. Quantum theory of perturbations. Part 3. Extensions," *Phys. Rept.* **215** (1992) 203–333.

[14] A. Riotto, "Inflation and the theory of cosmological perturbations," *ICTP Lect. Notes Ser.* **14** (2003) 317–413, arXiv:hep-ph/0210162 [hep-ph].

[15] D. Baumann, "Inflation," in *Physics of the large and the small, TASI 09, proceedings of the Theoretical Advanced Study Institute in Elementary Particle Physics, Boulder, Colorado, USA, 1-26 June 2009*, pp. 523–686. 2011. arXiv:0907.5424 [hep-th].

[16] L. Sriramkumar, "An introduction to inflation and cosmological perturbation theory," arXiv:0904.4584 [astro-ph.CO].

[17] J. Yokoyama, "Inflation: 1980-201X," *PTEP* **2014** (2014) 06B103.

[18] J. M. Bardeen, "Gauge Invariant Cosmological Perturbations," *Phys. Rev.* **D22** (1980) 1882–1905.

[19] **Planck** Collaboration, Y. Akrami *et al.*, "Planck 2018 results. X. Constraints on inflation," arXiv:1807.06211 [astro-ph.CO].

[20] J. Martin, C. Ringeval, and V. Vennin, "Encyclopædia Inflationaris," *Phys. Dark Univ.* **5-6** (2014) 75–235, arXiv:1303.3787 [astro-ph.CO].

[21] A. D. Linde, "Chaotic Inflation," *Phys. Lett.* **129B** (1983) 177–181.

[22] A. D. Linde, "Hybrid inflation," *Phys. Rev.* **D49** (1994) 748–754, arXiv:astro-ph/9307002 [astro-ph].

[23] E. J. Copeland, A. R. Liddle, D. H. Lyth, E. D. Stewart, and D. Wands, "False vacuum inflation with Einstein gravity," *Phys. Rev.* **D49** (1994) 6410–6433, arXiv:astro-ph/9401011 [astro-ph].

[24] A. D. Linde and A. Riotto, "Hybrid inflation in supergravity," *Phys. Rev.* **D56** (1997) R1841–R1844, arXiv:hep-ph/9703209 [hep-ph].

[25] D. H. Lyth and A. Riotto, "Comments on D term inflation," *Phys. Lett.* **B412** (1997) 28–34, arXiv:hep-ph/9707273 [hep-ph].

[26] A. Albrecht, P. J. Steinhardt, M. S. Turner, and F. Wilczek, "Reheating an Inflationary Universe," *Phys. Rev. Lett.* **48** (1982) 1437.

[27] L. F. Abbott, E. Farhi, and M. B. Wise, "Particle Production in the New Inflationary Cosmology," *Phys. Lett.* **117B** (1982) 29.

[28] A. D. Dolgov and D. P. Kirilova, "ON PARTICLE CREATION BY A TIME DEPENDENT SCALAR FIELD," *Sov. J. Nucl. Phys.* **51** (1990) 172–177. [Yad. Fiz.51,273(1990)].

[29] J. H. Traschen and R. H. Brandenberger, "Particle Production During Out-of-equilibrium Phase Transitions," *Phys. Rev.* **D42** (1990) 2491–2504.

[30] M. E. Peskin and D. V. Schroeder, *An Introduction to quantum field theory*. Addison-Wesley, Reading, USA, 1995. http://www.slac.stanford.edu/~mpeskin/QFT.html.

[31] L. Kofman, A. D. Linde, and A. A. Starobinsky, "Reheating after inflation," *Phys. Rev. Lett.* **73** (1994) 3195–3198, arXiv:hep-th/9405187 [hep-th].

[32] L. Kofman, A. D. Linde, and A. A. Starobinsky, "Towards the theory of reheating after inflation," *Phys. Rev.* **D56** (1997) 3258–3295, arXiv:hep-ph/9704452 [hep-ph].

[33] Y. Shtanov, J. H. Traschen, and R. H. Brandenberger, "Universe reheating after inflation," *Phys. Rev.* **D51** (1995) 5438–5455, arXiv:hep-ph/9407247 [hep-ph].

[34] L. D. LANDAU and E. W. LIFSHITZ, *the COURSE OF THEORETICAL PHYSICS by LANDAU and LIFSHITZ*. Butterworth-Heinemann, Oxford, third edition ed., 1976. http://www.sciencedirect.com/science/article/pii/B9780080503479500010.

[35] B. A. Bassett, S. Tsujikawa, and D. Wands, "Inflation dynamics and reheating," *Rev. Mod. Phys.* **78** (2006) 537–589, arXiv:astro-ph/0507632 [astro-ph].

[36] R. Allahverdi, R. Brandenberger, F.-Y. Cyr-Racine, and A. Mazumdar, "Reheating in Inflationary Cosmology: Theory and Applications," *Ann. Rev. Nucl. Part. Sci.* **60** (2010) 27–51, arXiv:1001.2600 [hep-th].

[37] M. A. Amin, M. P. Hertzberg, D. I. Kaiser, and J. Karouby, "Nonperturbative Dynamics Of Reheating After Inflation: A Review," *Int. J. Mod. Phys.* **D24** (2014) 1530003, arXiv:1410.3808 [hep-ph].

[38] P. B. Greene, L. Kofman, A. D. Linde, and A. A. Starobinsky, "Structure of resonance in preheating after inflation," *Phys. Rev.* **D56** (1997) 6175–6192, arXiv:hep-ph/9705347 [hep-ph].

[39] N. W. McLachlan, *Theory and Application of Mathieu Functions*. Clarendon Press, Oxford, 1947. https://books.google.co.in/books?id=ZGC4AAAAIAAJ.

[40] W. Magnus and S. Winkler, *Hill's Equation*. John Wiley & Sons, New York, 1966.

[41] V. Mukhanov, *Physical Foundations of Cosmology*. Cambridge University Press, Oxford, 2005. http://www-spires.fnal.gov/spires/find/books/www?cl=QB981.M89::2005.

[42] G. N. Felder and I. Tkachev, "LATTICEEASY: A Program for lattice simulations of scalar fields in an expanding universe," *Comput. Phys. Commun.* **178** (2008) 929–932, arXiv:hep-ph/0011159 [hep-ph].

[43] G. N. Felder, "CLUSTEREASY: A program for lattice simulations of scalar fields in an expanding universe on parallel computing clusters," *Comput. Phys. Commun.* **179** (2008) 604–606, arXiv:0712.0813 [hep-ph].

[44] A. V. Frolov, "DEFROST: A New Code for Simulating Preheating after Inflation," *JCAP* **0811** (2008) 009, arXiv:0809.4904 [hep-ph].

[45] J. Sainio, "CUDAEASY - a GPU Accelerated Cosmological Lattice Program," *Comput. Phys. Commun.* **181** (2010) 906–912, arXiv:0911.5692 [astro-ph.IM].

[46] R. Easther, H. Finkel, and N. Roth, "PSpectRe: A Pseudo-Spectral Code for (P)reheating," *JCAP* **1010** (2010) 025, arXiv:1005.1921 [astro-ph.CO].

[47] Z. Huang, "The Art of Lattice and Gravity Waves from Preheating," *Phys. Rev.* **D83** (2011) 123509, arXiv:1102.0227 [astro-ph.CO].

[48] J. Sainio, "PyCOOL - a Cosmological Object-Oriented Lattice code written in Python," *JCAP* **1204** (2012) 038, arXiv:1201.5029 [astro-ph.IM].

[49] G. N. Felder, L. Kofman, and A. D. Linde, "Instant preheating," *Phys. Rev.* **D59** (1999) 123523, arXiv:hep-ph/9812289 [hep-ph].

[50] M. Sami and V. Sahni, "Quintessential inflation on the brane and the relic gravity wave background," *Phys. Rev.* **D70** (2004) 083513, arXiv:hep-th/0402086 [hep-th].

[51] S. Panda, M. Sami, and I. Thongkool, "Reheating the D-brane universe via instant preheating," *Phys. Rev.* **D81** (2010) 103506, arXiv:0905.2284 [hep-th].

[52] A. Linde, "On the problem of initial conditions for inflation," *Found. Phys.* **48** no. 10, (2018) 1246–1260, arXiv:1710.04278 [hep-th].

[53] **Planck** Collaboration, P. A. R. Ade *et al.*, "Planck 2015 results. XX. Constraints on inflation," *Astron. Astrophys.* **594** (2016) A20, arXiv:1502.02114 [astro-ph.CO].

[54] **BICEP2, Planck** Collaboration, P. A. R. Ade *et al.*, "Joint Analysis of BICEP2/*KeckArray* and *Planck* Data," *Phys. Rev. Lett.* **114** (2015) 101301, arXiv:1502.00612 [astro-ph.CO].

[55] R. Kallosh and A. Linde, "Universality Class in Conformal Inflation," *JCAP* **1307** (2013) 002, arXiv:1306.5220 [hep-th].

[56] S. Ferrara, R. Kallosh, A. Linde, and M. Porrati, "Minimal Supergravity Models of Inflation," *Phys. Rev.* **D88** no. 8, (2013) 085038, arXiv:1307.7696 [hep-th].

[57] R. Kallosh, A. Linde, and D. Roest, "Superconformal Inflationary $\alpha$-Attractors," *JHEP* **11** (2013) 198, arXiv:1311.0472 [hep-th].

[58] S. Cecotti and R. Kallosh, "Cosmological Attractor Models and Higher Curvature Supergravity," *JHEP* **05** (2014) 114, arXiv:1403.2932 [hep-th].

[59] D. Maity, "Minimal Higgs inflation," *Nucl. Phys.* **B919** (2017) 560–568, arXiv:1606.08179 [hep-ph].

[60] J. Martin and C. Ringeval, "First CMB Constraints on the Inflationary Reheating Temperature," *Phys. Rev.* **D82** (2010) 023511, arXiv:1004.5525 [astro-ph.CO].

[61] L. Dai, M. Kamionkowski, and J. Wang, "Reheating constraints to inflationary models," *Phys. Rev. Lett.* **113** (2014) 041302, arXiv:1404.6704 [astro-ph.CO].

[62] M. Galante, R. Kallosh, A. Linde, and D. Roest, "Unity of Cosmological Inflation Attractors," *Phys. Rev. Lett.* **114** no. 14, (2015) 141302, arXiv:1412.3797 [hep-th].

[63] D. H. Lyth, "What would we learn by detecting a gravitational wave signal in the cosmic microwave background anisotropy?," *Phys. Rev. Lett.* **78** (1997) 1861–1863, arXiv:hep-ph/9606387 [hep-ph].

[64] M. S. Turner, "Coherent Scalar Field Oscillations in an Expanding Universe," *Phys. Rev.* **D28** (1983) 1243.

[65] K. Dimopoulos, "Shaft Inflation," *Phys. Lett.* **B735** (2014) 75–78, arXiv:1403.4071 [hep-ph].

[66] K. Dimopoulos and C. Owen, "Modelling inflation with a power-law approach to the inflationary plateau," *Phys. Rev.* **D94** no. 6, (2016) 063518, arXiv:1607.02469 [hep-ph].

[67] M. Eshaghi, M. Zarei, N. Riazi, and A. Kiasatpour, "A Non-minimally Coupled Potential for Inflation and Dark Energy after Planck 2015: A Comprehensive Study," *JCAP* **1511** no. 11, (2015) 037, arXiv:1505.03556 [hep-th].

[68] B. J. Broy, D. Coone, and D. Roest, "Plateau Inflation from Random Non-Minimal Coupling," *JCAP* **1606** no. 06, (2016) 036, arXiv:1604.05326 [hep-th].

[69] T. Futamase and K.-i. Maeda, "Chaotic Inflationary Scenario in Models Having Nonminimal Coupling With Curvature," *Phys. Rev.* **D39** (1989) 399–404.

[70] D. I. Kaiser, "Primordial spectral indices from generalized Einstein theories," *Phys. Rev.* **D52** (1995) 4295–4306, arXiv:astro-ph/9408044 [astro-ph].

[71] J.-c. Hwang, "Cosmological perturbations in generalized gravity theories: Conformal transformation," *Class. Quant. Grav.* **14** (1997) 1981–1991, arXiv:gr-qc/9605024 [gr-qc].

[72] N. Deruelle and M. Sasaki, "Conformal equivalence in classical gravity: the example of 'Veiled' General Relativity," *Springer Proc. Phys.* **137** (2011) 247–260, arXiv:1007.3563 [gr-qc].

[73] M. Postma and M. Volponi, "Equivalence of the Einstein and Jordan frames," *Phys. Rev.* **D90** no. 10, (2014) 103516, arXiv:1407.6874 [astro-ph.CO].

[74] Y. Fujii and K. Maeda, *The scalar-tensor theory of gravitation*. Cambridge Monographs on Mathematical Physics. Cambridge University Press, 2007. http://www.cambridge.org/uk/catalogue/catalogue.asp?isbn=0521811597.

[75] R. Kallosh, A. Linde, and D. Roest, "Universal Attractor for Inflation at Strong Coupling," *Phys. Rev. Lett.* **112** no. 1, (2014) 011303, arXiv:1310.3950 [hep-th].

[76] A. Mazumdar and J. Rocher, "Particle physics models of inflation and curvaton scenarios," *Phys. Rept.* **497** (2011) 85–215, arXiv:1001.0993 [hep-ph].

[77] M. Yamaguchi, "Supergravity based inflation models: a review," *Class. Quant. Grav.* **28** (2011) 103001, arXiv:1101.2488 [astro-ph.CO].

[78] K. Nakayama, K. Saikawa, T. Terada, and M. Yamaguchi, "Structure of KÃd'hler potential for D-term inflationary attractor models," *JHEP* **05** (2016) 067, arXiv:1603.02557 [hep-th].

[79] A. de la Macorra and S. Lola, "Inflation in S dual superstring models," *Phys. Lett.* **B373** (1996) 299–305, arXiv:hep-ph/9511470 [hep-ph].

[80] P. Binetruy and G. R. Dvali, "D term inflation," *Phys. Lett.* **B388** (1996) 241–246, arXiv:hep-ph/9606342 [hep-ph].

[81] E. Halyo, "Hybrid inflation from supergravity D terms," *Phys. Lett.* **B387** (1996) 43–47, arXiv:hep-ph/9606423 [hep-ph].

[82] M. Dine, N. Seiberg, and E. Witten, "Fayet-Iliopoulos Terms in String Theory," *Nucl. Phys.* **B289** (1987) 589–598.

[83] J. J. Atick, L. J. Dixon, and A. Sen, "String Calculation of Fayet-Iliopoulos d Terms in Arbitrary Supersymmetric Compactifications," *Nucl. Phys.* **B292** (1987) 109–149.

[84] M. Dine, I. Ichinose, and N. Seiberg, "F Terms and d Terms in String Theory," *Nucl. Phys.* **B293** (1987) 253–265.

[85] M. B. Green and J. H. Schwarz, "Anomaly Cancellation in Supersymmetric D=10 Gauge Theory and Superstring Theory," *Phys. Lett.* **149B** (1984) 117–122.

[86] A. R. Liddle and S. M. Leach, "How long before the end of inflation were observable perturbations produced?," *Phys. Rev.* **D68** (2003) 103503, arXiv:astro-ph/0305263 [astro-ph].

[87] J. L. Cook, E. Dimastrogiovanni, D. A. Easson, and L. M. Krauss, "Reheating predictions in single field inflation," *JCAP* **1504** (2015) 047, arXiv:1502.04673 [astro-ph.CO].

[88] S. Bhattacharjee, D. Maity, and R. Mukherjee, "Constraining scalar-Gauss-Bonnet Inflation by Reheating, Unitarity and PLANCK," *Phys. Rev.* **D95** no. 2, (2017) 023514, arXiv:1606.00698 [gr-qc].

[89] **Euclid Theory Working Group** Collaboration, L. Amendola *et al.*, "Cosmology and fundamental physics with the Euclid satellite," *Living Rev. Rel.* **16** (2013) 6, arXiv:1206.1225 [astro-ph.CO].

[90] **PRISM** Collaboration, P. Andre *et al.*, "PRISM (Polarized Radiation Imaging and Spectroscopy Mission): A White Paper on the Ultimate Polarimetric Spectro-Imaging of the Microwave and Far-Infrared Sky," arXiv:1306.2259 [astro-ph.CO].

[91] L. Amendola *et al.*, "Cosmology and fundamental physics with the Euclid satellite," *Living Rev. Rel.* **21** no. 1, (2018) 2, arXiv:1606.00180 [astro-ph.CO].

[92] M. Kawasaki, K. Kohri, and N. Sugiyama, "Cosmological constraints on late time entropy production," *Phys. Rev. Lett.* **82** (1999) 4168, arXiv:astro-ph/9811437 [astro-ph].

[93] M. Kawasaki, K. Kohri, and N. Sugiyama, "MeV scale reheating temperature and thermalization of neutrino background," *Phys. Rev.* **D62** (2000) 023506, arXiv:astro-ph/0002127 [astro-ph].

[94] B. D. Fields, P. Molaro, and S. Sarkar, "Big-Bang Nucleosynthesis," *Chin. Phys.* **C38** (2014) 339–344, arXiv:1412.1408 [astro-ph.CO].

[95] A. D. Dolgov and A. D. Linde, "Baryon Asymmetry in Inflationary Universe," *Phys. Lett.* **116B** (1982) 329.

[96] P. Creminelli, D. López Nacir, M. Simonović, G. Trevisan, and M. Zaldarriaga, "$\phi^2$ Inflation at its Endpoint," *Phys. Rev.* **D90** no. 8, (2014) 083513, arXiv:1405.6264 [astro-ph.CO].

[97] J. Martin, C. Ringeval, and V. Vennin, "Observing Inflationary Reheating," *Phys. Rev. Lett.* **114** no. 8, (2015) 081303, arXiv:1410.7958 [astro-ph.CO].

[98] J. Ellis, M. A. G. Garcia, D. V. Nanopoulos, and K. A. Olive, "Calculations of Inflaton Decays and Reheating: with Applications to No-Scale Inflation Models," *JCAP* **1507** no. 07, (2015) 050, arXiv:1505.06986 [hep-ph].

[99] Y. Ueno and K. Yamamoto, "Constraints on $\alpha$-attractor inflation and reheating," *Phys. Rev.* **D93** no. 8, (2016) 083524, arXiv:1602.07427 [astro-ph.CO].

[100] M. Eshaghi, M. Zarei, N. Riazi, and A. Kiasatpour, "CMB and reheating constraints to $\alpha$-attractor inflationary models," *Phys. Rev.* **D93** no. 12, (2016) 123517, arXiv:1602.07914 [astro-ph.CO].

[101] A. Di Marco, P. Cabella, and N. Vittorio, "Constraining the general reheating phase in the $\alpha$-attractor inflationary cosmology," *Phys. Rev.* **D95** no. 10, (2017) 103502, arXiv:1705.04622 [astro-ph.CO].

[102] S. Bhattacharya, K. Dutta, and A. Maharana, "Constraints on KÃďhler moduli inflation from reheating," *Phys. Rev.* **D96** no. 8, (2017) 083522, arXiv:1707.07924 [hep-ph]. [Addendum: Phys. Rev.D96,no.10,109901(2017)].

[103] M. Drewes, J. U. Kang, and U. R. Mun, "CMB constraints on the inflaton couplings and reheating temperature in $\alpha$-attractor inflation," *JHEP* **11** (2017) 072, arXiv:1708.01197 [astro-ph.CO].

[104] D. Maity, "Constraints through decaying inflaton: maximum reheating temperature," arXiv:1709.00251 [hep-th].

[105] D. J. H. Chung, E. W. Kolb, and A. Riotto, "Production of massive particles during reheating," *Phys. Rev.* **D60** (1999) 063504, arXiv:hep-ph/9809453 [hep-ph].

[106] G. F. Giudice, E. W. Kolb, and A. Riotto, "Largest temperature of the radiation era and its cosmological implications," *Phys. Rev.* **D64** (2001) 023508, arXiv:hep-ph/0005123 [hep-ph].

[107] R. Allahverdi and M. Drees, "Production of massive stable particles in inflaton decay," *Phys. Rev. Lett.* **89** (2002) 091302, arXiv:hep-ph/0203118 [hep-ph].

[108] R. Allahverdi and M. Drees, "Thermalization after inflation and production of massive stable particles," *Phys. Rev.* **D66** (2002) 063513, arXiv:hep-ph/0205246 [hep-ph].

[109] C. Pallis, "Massive particle decay and cold dark matter abundance," *Astropart. Phys.* **21** (2004) 689–702, arXiv:hep-ph/0402033 [hep-ph].

[110] G. L. Kane, P. Kumar, B. D. Nelson, and B. Zheng, "Dark matter production mechanisms with a nonthermal cosmological history: A classification," *Phys. Rev.* **D93** no. 6, (2016) 063527, arXiv:1502.05406 [hep-ph].

[111] D. Maity and P. Saha, "Minimal inflationary cosmologies and constraints on reheating," arXiv:1610.00173 [astro-ph.CO].

[112] K. Griest and D. Seckel, "Three exceptions in the calculation of relic abundances," *Phys. Rev.* **D43** (1991) 3191–3203.

[113] J. Edsjo and P. Gondolo, "Neutralino relic density including coannihilations," *Phys. Rev.* **D56** (1997) 1879–1894, arXiv:hep-ph/9704361 [hep-ph].

[114] R. T. D'Agnolo and J. T. Ruderman, "Light Dark Matter from Forbidden Channels," *Phys. Rev. Lett.* **115** no. 6, (2015) 061301, arXiv:1505.07107 [hep-ph].

[115] S. Chang, A. Pierce, and N. Weiner, "Momentum Dependent Dark Matter Scattering," *JCAP* **1001** (2010) 006, arXiv:0908.3192 [hep-ph].

[116] J. Fan, M. Reece, and L.-T. Wang, "Non-relativistic effective theory of dark matter direct detection," *JCAP* **1011** (2010) 042, arXiv:1008.1591 [hep-ph].

[117] A. L. Fitzpatrick, W. Haxton, E. Katz, N. Lubbers, and Y. Xu, "The Effective Field Theory of Dark Matter Direct Detection," *JCAP* **1302** (2013) 004, arXiv:1203.3542 [hep-ph].

[118] M. Cirelli, M. Kadastik, M. Raidal, and A. Strumia, "Model-independent implications of the e+-, anti-proton cosmic ray spectra on properties of Dark Matter," *Nucl. Phys.* **B813** (2009) 1–21, arXiv:0809.2409 [hep-ph]. [Addendum: Nucl. Phys.B873,530(2013)].

[119] N. Arkani-Hamed, D. P. Finkbeiner, T. R. Slatyer, and N. Weiner, "A Theory of Dark Matter," *Phys. Rev.* **D79** (2009) 015014, arXiv:0810.0713 [hep-ph].

[120] M. Pospelov and A. Ritz, "Astrophysical Signatures of Secluded Dark Matter," *Phys. Lett.* **B671** (2009) 391–397, arXiv:0810.1502 [hep-ph].

[121] P. J. Fox and E. Poppitz, "Leptophilic Dark Matter," *Phys. Rev.* **D79** (2009) 083528, arXiv:0811.0399 [hep-ph].

[122] L. J. Hall, K. Jedamzik, J. March-Russell, and S. M. West, "Freeze-In Production of FIMP Dark Matter," *JHEP* **03** (2010) 080, arXiv:0911.1120 [hep-ph].

[123] T. Tenkanen, "Feebly Interacting Dark Matter Particle as the Inflaton," *JHEP* **09** (2016) 049, arXiv:1607.01379 [hep-ph].

[124] M. Heikinheimo, T. Tenkanen, K. Tuominen, and V. Vaskonen, "Observational Properties of Feebly Coupled Dark Matter," *PoS* **ICHEP2016** (2016) 825, arXiv:1611.04951 [astro-ph.CO].

[125] N. Bernal, M. Heikinheimo, T. Tenkanen, K. Tuominen, and V. Vaskonen, "The Dawn of FIMP Dark Matter: A Review of Models and Constraints," *Int. J. Mod. Phys.* **A32** no. 27, (2017) 1730023, arXiv:1706.07442 [hep-ph].

[126] S. Nurmi, T. Tenkanen, and K. Tuominen, "Inflationary Imprints on Dark Matter," *JCAP* **1511** no. 11, (2015) 001, arXiv:1506.04048 [astro-ph.CO].

[127] M. Bastero-Gil, R. Cerezo, and J. G. Rosa, "Inflaton dark matter from incomplete decay," *Phys. Rev.* **D93** no. 10, (2016) 103531, arXiv:1501.05539 [hep-ph].

[128] M. Heikinheimo, T. Tenkanen, K. Tuominen, and V. Vaskonen, "Observational Constraints on Decoupled Hidden Sectors," *Phys. Rev.* **D94** no. 6, (2016) 063506, arXiv:1604.02401 [astro-ph.CO]. [Erratum: Phys. Rev.D96,no.10,109902(2017)].

[129] K. Kainulainen, S. Nurmi, T. Tenkanen, K. Tuominen, and V. Vaskonen, "Isocurvature Constraints on Portal Couplings," *JCAP* **1606** no. 06, (2016) 022, arXiv:1601.07733 [astro-ph.CO].

[130] L. Visinelli, "(Non-)thermal production of WIMPs during kination," *Symmetry* **10** (2018) 546, arXiv:1710.11006 [astro-ph.CO].

[131] S.-L. Chen and Z. Kang, "On UltraViolet Freeze-in Dark Matter during Reheating," *JCAP* **1805** no. 05, (2018) 036, arXiv:1711.02556 [hep-ph].

[132] K. Enqvist, R. J. Hardwick, T. Tenkanen, V. Vennin, and D. Wands, "A novel way to determine the scale of inflation," *JCAP* **1802** no. 02, (2018) 006, arXiv:1711.07344 [astro-ph.CO].

[133] F. D'Eramo, N. Fernandez, and S. Profumo, "Dark Matter Freeze-in Production in Fast-Expanding Universes," *JCAP* **1802** no. 02, (2018) 046, arXiv:1712.07453 [hep-ph].

[134] K. Enqvist, T. Meriniemi, and S. Nurmi, "Generation of the Higgs Condensate and Its Decay after Inflation," *JCAP* **1310** (2013) 057, arXiv:1306.4511 [hep-ph].

[135] A. Kusenko, L. Pearce, and L. Yang, "Postinflationary Higgs relaxation and the origin of matter-antimatter asymmetry," *Phys. Rev. Lett.* **114** no. 6, (2015) 061302, arXiv:1410.0722 [hep-ph].

[136] K. Freese, E. I. Sfakianakis, P. Stengel, and L. Visinelli, "The Higgs Boson can delay Reheating after Inflation," *JCAP* **1805** no. 05, (2018) 067, arXiv:1712.03791 [hep-ph].

[137] C. Cercignani and G. Kremer, *The Relativistic Boltzmann Equation: Theory and Applications*. Progress in Mathematical Physics. Birkhäuser Basel, 2002. https://books.google.co.in/books?id=5RWajme51FkC.

[138] D. Maity and P. Saha, "Connecting CMB anisotropy and cold dark matter phenomenology via reheating," *Phys. Rev.* **D98** (2018) 103525, arXiv:1801.03059 [hep-ph].

[139] E. W. Kolb and M. S. Turner, "The Early Universe," *Perseus Books/Westview Press, New York,* **69** (1994) 1–547.

[140] P. S. Bhupal Dev, A. Mazumdar, and S. Qutub, "Constraining Non-thermal and Thermal properties of Dark Matter," *Front.in Phys.* **2** (2014) 26, arXiv:1311.5297 [hep-ph].

[141] A. L. Erickcek and K. Sigurdson, "Reheating Effects in the Matter Power Spectrum and Implications for Substructure," *Phys. Rev.* **D84** (2011) 083503, arXiv:1106.0536 [astro-ph.CO].

[142] A. L. Erickcek, "The Dark Matter Annihilation Boost from Low-Temperature Reheating," *Phys. Rev.* **D92** no. 10, (2015) 103505, arXiv:1504.03335 [astro-ph.CO].

[143] K. Freese, J. A. Frieman, and A. V. Olinto, "Natural inflation with pseudo - Nambu-Goldstone bosons," *Phys. Rev. Lett.* **65** (1990) 3233–3236.

[144] K. Freese and W. H. Kinney, "Natural Inflation: Consistency with Cosmic Microwave Background Observations of Planck and BICEP2," *JCAP* **1503** (2015) 044, arXiv:1403.5277 [astro-ph.CO].

[145] M. Gerbino, K. Freese, S. Vagnozzi, M. Lattanzi, O. Mena, E. Giusarma, and S. Ho, "Impact of neutrino properties on the estimation of inflationary parameters from current and future observations," *Phys. Rev.* **D95** no. 4, (2017) 043512, arXiv:1610.08830 [astro-ph.CO].

[146] S. Ferrara, R. Kallosh, A. Linde, and M. Porrati, "Higher Order Corrections in Minimal Supergravity Models of Inflation," *JCAP* **1311** (2013) 046, arXiv:1309.1085 [hep-th].

[147] R. Kallosh and A. Linde, "Planck, LHC, and $\alpha$-attractors," *Phys. Rev.* **D91** (2015) 083528, arXiv:1502.07733 [astro-ph.CO].

[148] F. L. Bezrukov and M. Shaposhnikov, "The Standard Model Higgs boson as the inflaton," *Phys. Lett.* **B659** (2008) 703–706, arXiv:0710.3755 [hep-th].

[149] J. Chluba and R. A. Sunyaev, "The evolution of CMB spectral distortions in the early Universe," *Mon. Not. Roy. Astron. Soc.* **419** (2012) 1294–1314, arXiv:1109.6552 [astro-ph.CO].

[150] J. Chluba, J. Hamann, and S. P. Patil, "Features and New Physical Scales in Primordial Observables: Theory and Observation," *Int. J. Mod. Phys.* **D24** no. 10, (2015) 1530023, arXiv:1505.01834 [astro-ph.CO].

[151] D. J. Fixsen, E. S. Cheng, J. M. Gales, J. C. Mather, R. A. Shafer, and E. L. Wright, "The Cosmic Microwave Background spectrum from the full COBE FIRAS data set," *Astrophys. J.* **473** (1996) 576, arXiv:astro-ph/9605054 [astro-ph].

[152] A. Kogut *et al.*, "The Primordial Inflation Explorer (PIXIE): A Nulling Polarimeter for Cosmic Microwave Background Observations," *JCAP* **1107** (2011) 025, arXiv:1105.2044 [astro-ph.CO].

[153] H. Tashiro, "CMB spectral distortions and energy release in the early universe," *PTEP* **2014** no. 6, (2014) 06B107.

[154] R. Khatri, R. A. Sunyaev, and J. Chluba, "Does Bose-Einstein condensation of CMB photons cancel $\mu$ distortions created by dissipation of sound waves in the early Universe?," *Astron. Astrophys.* **540** (2012) A124, arXiv:1110.0475 [astro-ph.CO].

[155] E. Pajer and M. Zaldarriaga, "A hydrodynamical approach to CMB $\mu$-distortion from primordial perturbations," *JCAP* **1302** (2013) 036, arXiv:1206.4479 [astro-ph.CO].

[156] R. K. Sachs and A. M. Wolfe, "Perturbations of a cosmological model and angular variations of the microwave background," *Astrophys. J.* **147** (1967) 73–90. [Gen. Rel. Grav.39,1929(2007)].

[157] J. P. Zibin, A. Moss, and D. Scott, "The Evolution of the Cosmic Microwave Background," *Phys. Rev.* **D76** (2007) 123010, arXiv:0706.4482 [astro-ph].

[158] S. Yu. Khlebnikov and I. I. Tkachev, "Classical decay of inflaton," *Phys. Rev. Lett.* **77** (1996) 219–222, arXiv:hep-ph/9603378 [hep-ph].

[159] T. Prokopec and T. G. Roos, "Lattice study of classical inflaton decay," *Phys. Rev.* **D55** (1997) 3768–3775, arXiv:hep-ph/9610400 [hep-ph].

[160] R. Micha and I. I. Tkachev, "Relativistic turbulence: A Long way from preheating to equilibrium," *Phys. Rev. Lett.* **90** (2003) 121301, arXiv:hep-ph/0210202 [hep-ph].

[161] R. Micha and I. I. Tkachev, "Turbulent thermalization," *Phys. Rev.* **D70** (2004) 043538, arXiv:hep-ph/0403101 [hep-ph].

[162] D. G. Figueroa and F. Torrenti, "Parametric resonance in the early Universe-a fitting analysis," *JCAP* **1702** no. 02, (2017) 001, arXiv:1609.05197 [astro-ph.CO].

[163] M. P. Hertzberg, J. Karouby, W. G. Spitzer, J. C. Becerra, and L. Li, "Theory of self-resonance after inflation. I. Adiabatic and isocurvature Goldstone modes," *Phys. Rev.* **D90** (2014) 123528, arXiv:1408.1396 [hep-th].

[164] M. P. Hertzberg, J. Karouby, W. G. Spitzer, J. C. Becerra, and L. Li, "Theory of self-resonance after inflation. II. Quantum mechanics and particle-antiparticle asymmetry," *Phys. Rev.* **D90** (2014) 123529, arXiv:1408.1398 [hep-th].

[165] K. D. Lozanov and M. A. Amin, "Equation of State and Duration to Radiation Domination after Inflation," *Phys. Rev. Lett.* **119** no. 6, (2017) 061301, arXiv:1608.01213 [astro-ph.CO].

[166] K. D. Lozanov and M. A. Amin, "Self-resonance after inflation: oscillons, transients and radiation domination," *Phys. Rev.* **D97** no. 2, (2018) 023533, arXiv:1710.06851 [astro-ph.CO].

[167] D. Maity and P. Saha, "Minimal plateau inflationary cosmologies and constraints from reheating," *Class. Quant. Grav.* **36** (2019) 045010, arXiv:1902.01895 [gr-qc].

[168] F. Bezrukov, D. Gorbunov, and M. Shaposhnikov, "On initial conditions for the Hot Big Bang," *JCAP* **0906** (2009) 029, arXiv:0812.3622 [hep-ph].

[169] J. Garcia-Bellido, D. G. Figueroa, and J. Rubio, "Preheating in the Standard Model with the Higgs-Inflaton coupled to gravity," *Phys. Rev.* **D79** (2009) 063531, arXiv:0812.4624 [hep-ph].

[170] D. I. Podolsky, G. N. Felder, L. Kofman, and M. Peloso, "Equation of state and beginning of thermalization after preheating," *Phys. Rev.* **D73** (2006) 023501, arXiv:hep-ph/0507096 [hep-ph].

[171] G. N. Felder and L. Kofman, "The Development of equilibrium after preheating," *Phys. Rev.* **D63** (2001) 103503, arXiv:hep-ph/0011160 [hep-ph].

[172] P. Cabella, A. Di Marco, and G. Pradisi, "Fiber inflation and reheating," *Phys. Rev.* **D95** no. 12, (2017) 123528, arXiv:1704.03209 [astro-ph.CO].

[173] A. Di Marco, G. Pradisi, and P. Cabella, "On Inflationary Scale, Reheating Scale and Pre-BBN Cosmology with Scalar Fields," arXiv:1807.05916 [astro-ph.CO].

[174] P. B. Greene and L. Kofman, "Preheating of fermions," *Phys. Lett.* **B448** (1999) 6–12, arXiv:hep-ph/9807339 [hep-ph].

[175] J. Repond and J. Rubio, "Combined Preheating on the lattice with applications to Higgs inflation," *JCAP* **1607** no. 07, (2016) 043, arXiv:1604.08238 [astro-ph.CO].

[176] N. Shuhmaher and R. Brandenberger, "Non-perturbative instabilities as a solution of the cosmological moduli problem," *Phys. Rev.* **D73** (2006) 043519, arXiv:hep-th/0507103 [hep-th].

[177] J. F. Dufaux, G. N. Felder, L. Kofman, M. Peloso, and D. Podolsky, "Preheating with trilinear interactions: Tachyonic resonance," *JCAP* **0607** (2006) 006, arXiv:hep-ph/0602144 [hep-ph].

[178] A. A. Abolhasani, H. Firouzjahi, and M. M. Sheikh-Jabbari, "Tachyonic Resonance Preheating in Expanding Universe," *Phys. Rev.* **D81** (2010) 043524, arXiv:0912.1021 [hep-th].

[179] M. A. Amin and D. Shirokoff, "Flat-top oscillons in an expanding universe," *Phys. Rev.* **D81** (2010) 085045, arXiv:1002.3380 [astro-ph.CO].

[180] S. Antusch, F. Cefala, S. Krippendorf, F. Muia, S. Orani, and F. Quevedo, "Oscillons from String Moduli," *JHEP* **01** (2018) 083, arXiv:1708.08922 [hep-th].

[181] M. A. Amin, R. Easther, H. Finkel, R. Flauger, and M. P. Hertzberg, "Oscillons After Inflation," *Phys. Rev. Lett.* **108** (2012) 241302, arXiv:1106.3335 [astro-ph.CO].

[182] S.-Y. Zhou, E. J. Copeland, R. Easther, H. Finkel, Z.-G. Mou, and P. M. Saffin, "Gravitational Waves from Oscillon Preheating," *JHEP* **10** (2013) 026, arXiv:1304.6094 [astro-ph.CO].

[183] M. Alishahiha, E. Silverstein, and D. Tong, "DBI in the sky," *Phys. Rev.* **D70** (2004) 123505, arXiv:hep-th/0404084 [hep-th].

[184] E. Silverstein and D. Tong, "Scalar speed limits and cosmology: Acceleration from D-cceleration," *Phys. Rev.* **D70** (2004) 103505, arXiv:hep-th/0310221 [hep-th].

[185] X. Chen, "Inflation from warped space," *JHEP* **08** (2005) 045, arXiv:hep-th/0501184 [hep-th].

[186] G. W. Horndeski, "Second-order scalar-tensor field equations in a four-dimensional space," *Int. J. Theor. Phys.* **10** (1974) 363–384.

[187] A. Nicolis, R. Rattazzi, and E. Trincherini, "The Galileon as a local modification of gravity," *Phys. Rev.* **D79** (2009) 064036, arXiv:0811.2197 [hep-th].

[188] C. Deffayet, G. Esposito-Farese, and A. Vikman, "Covariant Galileon," *Phys. Rev.* **D79** (2009) 084003, arXiv:0901.1314 [hep-th].

[189] C. Deffayet, S. Deser, and G. Esposito-Farese, "Generalized Galileons: All scalar models whose curved background extensions maintain second-order field equations and stress-tensors," *Phys. Rev.* **D80** (2009) 064015, arXiv:0906.1967 [gr-qc].

[190] C. Deffayet, X. Gao, D. A. Steer, and G. Zahariade, "From k-essence to generalised Galileons," *Phys. Rev.* **D84** (2011) 064039, arXiv:1103.3260 [hep-th].

[191] T. Kobayashi, M. Yamaguchi, and J. Yokoyama, "Generalized G-inflation: Inflation with the most general second-order field equations," *Prog. Theor. Phys.* **126** (2011) 511–529, arXiv:1105.5723 [hep-th].

[192] T. Kobayashi, M. Yamaguchi, and J. Yokoyama, "G-inflation: Inflation driven by the Galileon field," *Phys. Rev. Lett.* **105** (2010) 231302, arXiv:1008.0603 [hep-th].

[193] K. Kamada, T. Kobayashi, M. Yamaguchi, and J. Yokoyama, "Higgs G-inflation," *Phys. Rev.* **D83** (2011) 083515, arXiv:1012.4238 [astro-ph.CO].

[194] J. Ohashi and S. Tsujikawa, "Potential-driven Galileon inflation," *JCAP* **1210** (2012) 035, arXiv:1207.4879 [gr-qc].

[195] K. Nakayama and F. Takahashi, "Running Kinetic Inflation," *JCAP* **1011** (2010) 009, arXiv:1008.2956 [hep-ph].

[196] J. L. Cervantes-Cota and H. Dehnen, "Induced gravity inflation in the standard model of particle physics," *Nucl. Phys.* **B442** (1995) 391–412, arXiv:astro-ph/9505069 [astro-ph].

[197] A. O. Barvinsky, A. Yu. Kamenshchik, and A. A. Starobinsky, "Inflation scenario via the Standard Model Higgs boson and LHC," *JCAP* **0811** (2008) 021, arXiv:0809.2104 [hep-ph].

[198] C. Germani and A. Kehagias, "New Model of Inflation with Non-minimal Derivative Coupling of Standard Model Higgs Boson to Gravity," *Phys. Rev. Lett.* **105** (2010) 011302, arXiv:1003.2635 [hep-ph].

[199] K. Kamada, T. Kobayashi, T. Takahashi, M. Yamaguchi, and J. Yokoyama, "Generalized Higgs inflation," *Phys. Rev.* **D86** (2012) 023504, arXiv:1203.4059 [hep-ph].

[200] C. Deffayet, O. Pujolas, I. Sawicki, and A. Vikman, "Imperfect Dark Energy from Kinetic Gravity Braiding," *JCAP* **1010** (2010) 026, arXiv:1008.0048 [hep-th].

[201] O. Pujolas, I. Sawicki, and A. Vikman, "The Imperfect Fluid behind Kinetic Gravity Braiding," *JHEP* **11** (2011) 156, arXiv:1103.5360 [hep-th].

[202] R. D. Peccei and H. R. Quinn, "CP Conservation in the Presence of Instantons," *Phys. Rev. Lett.* **38** (1977) 1440–1443. [,328(1977)].

[203] R. D. Peccei and H. R. Quinn, "Constraints Imposed by CP Conservation in the Presence of Instantons," *Phys. Rev.* **D16** (1977) 1791–1797.

[204] S. Dimopoulos, S. Kachru, J. McGreevy, and J. G. Wacker, "N-flation," *JCAP* **0808** (2008) 003, arXiv:hep-th/0507205 [hep-th].

[205] E. Silverstein and A. Westphal, "Monodromy in the CMB: Gravity Waves and String Inflation," *Phys. Rev.* **D78** (2008) 106003, arXiv:0803.3085 [hep-th].

[206] C. Cheung and G. N. Remmen, "Naturalness and the Weak Gravity Conjecture," *Phys. Rev. Lett.* **113** (2014) 051601, arXiv:1402.2287 [hep-ph].

[207] T. Banks, M. Dine, P. J. Fox, and E. Gorbatov, "On the possibility of large axion decay constants," *JCAP* **0306** (2003) 001, arXiv:hep-th/0303252 [hep-th].

[208] J. Brown, W. Cottrell, G. Shiu, and P. Soler, "Fencing in the Swampland: Quantum Gravity Constraints on Large Field Inflation," *JHEP* **10** (2015) 023, arXiv:1503.04783 [hep-th].

[209] B. Heidenreich, M. Reece, and T. Rudelius, "Weak Gravity Strongly Constrains Large-Field Axion Inflation," *JHEP* **12** (2015) 108, arXiv:1506.03447 [hep-th].

[210] N. Kaloper, M. Kleban, A. Lawrence, and M. S. Sloth, "Large Field Inflation and Gravitational Entropy," *Phys. Rev.* **D93** no. 4, (2016) 043510, arXiv:1511.05119 [hep-th].

[211] C. Germani and A. Kehagias, "UV-Protected Inflation," *Phys. Rev. Lett.* **106** (2011) 161302, arXiv:1012.0853 [hep-ph].

[212] C. Germani and Y. Watanabe, "UV-protected (Natural) Inflation: Primordial Fluctuations and non-Gaussian Features," *JCAP* **1107** (2011) 031, arXiv:1106.0502 [astro-ph.CO]. [Addendum: JCAP1107,A01(2011)].

[213] R. Easther, W. H. Kinney, and B. A. Powell, "The Lyth bound and the end of inflation," *JCAP* **0608** (2006) 004, arXiv:astro-ph/0601276 [astro-ph].

[214] D. Baumann and D. Green, "A Field Range Bound for General Single-Field Inflation," *JCAP* **1205** (2012) 017, arXiv:1111.3040 [hep-th].

[215] D. A. Easson, I. Sawicki, and A. Vikman, "G-Bounce," *JCAP* **1111** (2011) 021, arXiv:1109.1047 [hep-th].

[216] D. A. Easson, I. Sawicki, and A. Vikman, "When Matter Matters," *JCAP* **1307** (2013) 014, arXiv:1304.3903 [hep-th].

[217] D. A. Easson and T. Manton, "Stable Cosmic Time Crystals," arXiv:1802.03693 [hep-th].

[218] A. H. Campos, H. C. Reis, and R. Rosenfeld, "Preheating in quintessential inflation," *Phys. Lett.* **B575** (2003) 151–156, arXiv:hep-ph/0210152 [hep-ph].

[219] H. Tashiro, T. Chiba, and M. Sasaki, "Reheating after quintessential inflation and gravitational waves," *Class. Quant. Grav.* **21** (2004) 1761–1772, arXiv:gr-qc/0307068 [gr-qc].

[220] D. Maity and P. Saha, "Modified natural inflation: A small single field model with a large tensor to scalar ratio," *Phys. Rev.* **D91** no. 2, (2015) 023504, arXiv:1407.7692 [hep-th].

[221] D. Maity, "Pre-heating in the framework of massive gravity," *Nucl. Phys.* **B910** (2016) 259–272, arXiv:1504.06300 [hep-th].

[222] J. S. Bains, M. P. Hertzberg, and F. Wilczek, "Oscillatory Attractors: A New Cosmological Phase," *JCAP* **1705** no. 05, (2017) 011, arXiv:1512.02304 [hep-th].

[223] D. A. Easson and A. Vikman, "The Phantom of the New Oscillatory Cosmological Phase," arXiv:1607.00996 [gr-qc].

[224] Y. Cai, Y. Wan, H.-G. Li, T. Qiu, and Y.-S. Piao, "The Effective Field Theory of nonsingular cosmology," *JHEP* **01** (2017) 090, arXiv:1610.03400 [gr-qc].

[225] Y. Cai and Y.-S. Piao, "A covariant Lagrangian for stable nonsingular bounce," *JHEP* **09** (2017) 027, arXiv:1705.03401 [gr-qc].

[226] L. Lello, D. Boyanovsky, and R. Holman, "Pre-slow roll initial conditions: large scale power suppression and infrared aspects during inflation," *Phys. Rev.* **D89** no. 6, (2014) 063533, arXiv:1307.4066 [astro-ph.CO].

[227] Z.-G. Liu, Z.-K. Guo, and Y.-S. Piao, "CMB anomalies from an inflationary model in string theory," *Eur. Phys. J.* **C74** no. 8, (2014) 3006, arXiv:1311.1599 [astro-ph.CO].

[228] L. Lello and D. Boyanovsky, "Tensor to scalar ratio and large scale power suppression from pre-slow roll initial conditions," *JCAP* **1405** (2014) 029, arXiv:1312.4251 [astro-ph.CO].

[229] F. Bezrukov, A. Magnin, M. Shaposhnikov, and S. Sibiryakov, "Higgs inflation: consistency and generalisations," *JHEP* **01** (2011) 016, arXiv:1008.5157 [hep-ph].

[230] S. Dodelson, *Modern Cosmology*. Academic Press, Amsterdam, 2003. http://www.slac.stanford.edu/spires/find/books/www?cl=QB981:D62:2003.